

https://dspace.org/

An exploratory model of water and solute excretion in animals

Letts, Robyn

2022

https://hdl.handle.net/10539/34976

Downloaded from a DSpace repository. https://dspace.org/

An Exploratory Model of Water and Solute Excretion in Animals



Robyn Letts

School of Electrical and Information Engineering
University of the Witwatersrand, Johannesburg

This thesis is submitted for the degree of
Doctor of Philosophy

August 2022

Declaration

I hereby declare that except where specific reference is made to the work of others, the contents of this dissertation are original and have not been submitted in whole or in part for consideration for any other degree or qualification in this, or any other university. This dissertation is my own work and contains nothing which is the outcome of work done in collaboration with others, except as specified in the text and acknowledgements.

Robyn Letts
August 2022

Acknowledgements

There are a number of institutions and people I need to thank, without whom this document would not exist.

The work is based on research supported in part by the National Research Foundation of South Africa (unique grant no. 105704). I would like to thank the NRF for funding a year-long sabbatical that allowed me to put aside my teaching load and focus on my research, definitely boosting my chances of completion.

The School of Electrical and Information Engineering (EIE) at Wits University was home for the duration; I would like to thank the various Heads of School for giving me the opportunity to complete a higher degree while working, and having faith in my juggling ability.

I owe a huge debt of gratitude to my supervisors, Profs David Rubin and Diane Hildebrandt, for their unwavering support at all hours of the day (and night!). I will never forget our weekly meetings for the comic relief they provided.

I'd like to acknowledge the help of Maths Profs Ebrahim Momoniat and Sonja Currie, when faced with solving ODEs with hypergeometric solutions.

Many others contributed to my research education, including but not limited to: collaborators at the University of Aarhus, Denmark and the University of South Africa; colleagues in EIE; masters students; and the interesting people I met while pursuing various (and many) tangents of interest.

Most importantly, none of this would have been possible without very understanding friends and family. I cannot thank my husband enough for the total support he has given me throughout this roller-coaster of a journey, my two children who have had to live with a preoccupied parent their entire lives, and my parents and brother, who steered me onto this path in the first place and always encouraged me to stay the course.

Abstract

"What goes in must go out" is the dictum of mass balance, and excretion. All animals need to take in nutrients and excrete excess and waste products; how they achieve this depends on the capacity of their individual excretory systems and their tolerance to survive in a particular environment. Avoiders seek refuge from extreme or highly fluctuating environmental conditions, conformers are able to follow the environment, while regulators keep their internal environment in terms of volume and osmolarity approximately constant.

A systems' analysis of excretion was performed across the animal spectrum. Taking inspiration from comparative biology, a bottom-up, exploratory and indeed, evolutionary approach to modelling was followed where the multiple iterations each represent an increasing level of structural complexity to meet increasing functional constraints, just as in the biology it aims to imitate. Acknowledging that results need to be considered with the high level of abstraction in mind; interest lies in modes of behaviour and signature trends rather than point prediction. Nonetheless, this has led to the emergence of a number of contributions and hypotheses in the field of renal physiology, worthy of further research.

It was found that, no matter the complexity of animal being considered, a single continuously-stirred tank satisfactorily provides the core of the model. The mean residence time of the tank alone was found to determine sensitivity of the response to disturbances in water and solute inflow, implying a need for more sophisticated excretory control in a volume- and osmo-regulating animal with a smaller mean residence time compared to that with a higher mean residence time, simply based on size relative to flow. Through similar argument, it is suggested that higher than expected infant drug sensitivity is due to reduced mean residence time when compared with older children and adults, and not necessarily organ immaturity. Simple volume or pressure feedback on the outflow of the tank was found to be sufficient in describing volume regulation at the level of cells; and pressure diuresis and natriuresis in primitive animals such as the hagfish through to long-term arterial pressure control in sophisticated mammals, emphasising its inherent utility. In addition, a possible explanation for the exponential shape of the renal urinary output or renal function curve in humans is suggested.

Unintentionally, simply considering increasing regulatory requirements of excretion and iteratively building in requisite structure on the tank outflow, led to the development of a multiple-separator, series-parallel model that has clear analogies with that of differential intrarenal blood flow and nephron heterogeneity as present in the kidneys of birds and mammals, incidentally the only animals able to elucidate concentrated urine. Interestingly, variable flow between parallel separators and distal series water reabsorption have direct renal analogues; i.e. vascular and tubular receptors for antidiuretic hormone, respectively.

Similar trends in electrolyte imbalance and volume- and osmo-dysregulation that are exhibited in the syndrome of inappropriate antidiuresis and exercise-associated-hyponatremia were achieved. In addition, a hypothesis regarding the proposed action of loop diuretics was made based on model findings; that a shunt in flow towards the diluting branch of the parallel separator arrangement causes the same trend in volume depletion and electrolyte imbalance (i.e. potassium-losing). In addition, the developed tank-separator-recycle architecture (as present in the kidneys of birds and mammals) provides a mechanism for achieving energetically "passive" urine concentration; i.e. one in which all energy is derived externally from blood pressure.

Real-time visualisation of blood flow to cortical and medullary regions of human kidneys under administration of both antidiuretic hormone and a loop diuretic with non-invasive phase-contrast MRI or ultrasound is suggested to provide falsifiability for the proposed contribution of flow redistribution to the urine concentrating mechanism in mammals.

Table of contents

List of figures **xiii**

List of tables **xxi**

Nomenclature **xxiii**

1 Introduction **1**

2 Background **3**

3 Basic design **15**
3.1 Aim 15
3.2 Design procedure 15
3.3 Assumptions 16
3.4 Constraints 20
3.5 Model formulation 20

4 Design 1: No control **25**
4.1 Model setup 25
4.2 Results and Discussion 28
4.3 Biological application 36

5 Design 2: Pressure feedback **39**
5.1 Model setup 39
5.2 Results and Discussion 41
5.3 Biological application 47

6 Design 3: Separation on outflow **51**
6.1 Model setup 51
6.1.1 Solute separation 51

6.1.2 Water separation 54
6.2 Results and Discussion 56
6.2.1 Steady-state analysis 56
6.2.2 Transient analysis 59
6.3 Biological application 72

7 Design 4: Multiple separators **75**
7.1 Parallel separators 75
7.1.1 Model setup 75
7.1.2 Results and Discussion 80
7.1.3 Biological application 86
7.2 Series separators 88
7.2.1 Model setup 88
7.2.2 Results and Discussion 92
7.2.3 Biological application 97
7.3 Series-Parallel separators 99
7.3.1 Model setup 99
7.3.2 Results and Discussion 101
7.3.3 Biological application 105

8 Design 5: Control **109**
8.1 Model setup 109
8.2 Results and Discussion 117
8.3 Biological application 121

9 Application **125**
9.1 Model setup 125
9.2 Results and Discussion 129
9.2.1 The syndrome of inappropriate antidiuresis 135
9.2.2 Exercise-associated hyponatremia 139
9.2.3 Loop diuretics 142
9.3 Biological application 145

10 Conclusion **149**

References **155**

Appendix A Analytical solutions **165**
A.1 General form of volume and solute balances 165
A.2 Inflow to the system 165
A.3 Outflow from the system 166
A.3.1 No separation on outflow (Design 1 and Design 2) 166
A.3.2 Solute separation (Design 3) 166
A.3.3 Water separation (Design 3) 166
A.3.4 Combined solute and water separation (Design 4) 167
A.3.5 Multiple solute and water separation (Application) 167
A.4 Ordinary Differential Equations (ODEs) 167
A.4.1 No separation on outflow (Design 1 and Design 2) 167
A.4.2 Solute separation (Design 3) 167
A.4.3 Water separation (Design 3) 168
A.4.4 Combined solute and water separation (Design 4) 168
A.4.5 Multiple solute and water separation (Application) 168
A.5 Solution to ODEs 169
A.5.1 No separation on outflow (Design 1, $m = 0$) 169
A.5.2 No separation on outflow (Design 2, $m \neq 0$) 170
A.5.3 Solute separation (Design 3) 172
A.5.4 Water separation (Design 3) 173
A.5.5 Combined solute and water separation (Design 4) 174
A.5.6 Multiple solute and water separation (Application) 175
A.6 Comparison of solutions 177

List of figures

2.1 Comparison of systems' level models that include renal function, part 1 of 3 10
2.2 Comparison of systems' level models that include renal function, part 2 of 3 11
2.3 Comparison of systems' level models that include renal function, part 3 of 3 12

3.1 Diagram of I/O system 16
3.2 Diagram relating approximate spatial and temporal scale of models involving the renal system in the literature (blue), highlighting the author's region of interest (red box) 17
3.3 Line diagram of a grey-box model (boundary shown with dashed line) with continuously-stirred tank and site of separator action indicated. Water, solute and concentration quantities are listed below each component of the model . 21
3.4 Level-rate diagram for basic continuously-stirred tank; boxed variables representing levels, valves representing flow rates, unboxed variables representing auxiliary variables, and (blue and grey) arrows representing information flow 22

4.1 Line diagram for Design 1: No control 26
4.2 Level-rate diagram for Design 1: No control 26
4.3 Design 1 (a) Tank volume, (b) tank concentration and (c) amount of solute in the tank versus time graphs in response to positive and negative 10 % (above a baseline of 100 ml/hr) finite-duration (10 min) water pulses at t = 10 hrs for $\frac{V}{Q} = 10\ hr$ 30
4.4 Design 1 (a) Tank volume, (b) tank concentration and (c) amount of solute in the tank versus time graphs in response to positive and negative 10 % (above a baseline of 28.1 mosm/hr) finite-duration (10 min) solute pulses at t = 10 hrs for $\frac{V}{Q} = 10\ hr$ 31
4.5 Design 1 Graph of tank concentration 95 % settling time as a function of $\frac{V}{Q}$; in response to positive 10 % (above baseline) 10 minute duration pulses in water and solute inflow 32

4.6 Design 1 Graph of relative percentage change in tank volume magnitude as a function of $\frac{V}{Q}$; in response to positive 10 % (above baseline) 10 minute duration pulses in water inflow 33
4.7 Design 1 Graph of relative percentage change in tank concentration magnitude as a function of $\frac{V}{Q}$; in response to positive 10 % (above baseline) 10 minute duration pulses in water and solute inflow 34

5.1 Line diagram for Design 2: Pressure feedback 40
5.2 Level-rate diagram for Design 2: Pressure feedback 40
5.3 Design 2 Tank volume (blue), concentration (red), amount of solute (magenta), water outflow rate (green) and solute outflow rate (cyan) versus time graphs in response to positive 10 % (above a baseline of 100 ml/hr) finite-duration (10 min) water pulses at t = 10 hrs for $\frac{V}{Q} = 10\ hr$ and a range of $m = 0.001, 0.1, 1, 10$ 42
5.4 Design 2 Tank volume (blue), concentration (red), amount of solute (magenta), water outflow rate (green) and solute outflow rate (cyan) versus time graphs in response to positive 10 % (above a baseline of 28.1 mosm/hr) finite-duration (10 min) solute pulses at t = 10 hrs for $\frac{V}{Q} = 10\ hr$, identical for $m = 0.1, 1, 10$ 43
5.5 Design 2 Comparison of settling times for volume and tank concentration versus mean residence time in the tank ($\frac{V}{Q}$), at m = 0.1, 1, 10, following positive 10% 10 minute duration pulse disturbances in water inflow 44
5.6 Design 2 Comparison of relative change in tank volume versus mean residence time in the tank ($\frac{V}{Q}$) at m = 0.1, 1, 10; following positive 10% 10 minute duration pulse disturbances in water inflow 45
5.7 Design 2 Comparison of relative change in tank concentration versus $\frac{V}{Q}$ at m = 0.1, 1, 10; following positive 10% 10 minute duration pulse disturbances in water or solute inflow 46
5.8 Typical renal function curve adapted from [1] and annotated to show gradients of tangents to the curve at extremes 48

6.1 Line diagram for Design 3: Solute separation on outflow; separator 1 is defined by either bulk flow coefficient f or mass transfer coefficient k . . . 52
6.2 Level-rate diagram for Design 3: Solute separation on outflow, with solute separator (labelled N_{s1}) and recycle stream shown, corresponding to Figure 6.1 53

6.3 Line diagram for Design 3: Water separation on outflow; separator 1 is defined by water reabsorption coefficient f_w 54
6.4 Level-rate diagram for Design 3: Water separation on outflow, with separator (labelled V_1) and recycle stream explicitly shown, corresponding to Figure 6.3 55
6.5 Design 3 Graph of steady-state concentration versus bulk-flow coefficient f, including both tank and outflow concentrations 57
6.6 Design 3 Graph of steady-state concentration versus lumped mass transfer coefficient k, including both tank and outflow concentrations 58
6.7 Design 3 Graph of steady-state concentration versus water reabsorption coefficient f_w, including both tank and outflow concentrations 59
6.8 Design 3 Graph showing volume (blue), tank concentration (red), amount of solute (magenta), water outflow rate (green) and solute outflow rate (cyan) versus time in response to a positive finite-duration solute inflow pulse of size 10 % (above a baseline of 28.1 mosm/hr) and duration 10 minutes at $t = 10$ hr for, from top to bottom, $f = 0.5, 1, 1.5$, $m = 1$ and $\frac{V}{Q} = 10\ hr$ . . . 61
6.9 Design 3 Graph showing volume (blue), tank concentration (red), amount of solute (magenta), water outflow rate (green) and solute outflow rate (cyan) versus time in response to a positive finite-duration water inflow pulse of size 10 % (above a baseline of 100 ml/hr) and duration 10 minutes at $t = 10$ hr for, from top to bottom, $f = 0.5, 1, 1.5$, $m = 1$ and $\frac{V}{Q} = 10\ hr$ 62
6.10 Design 3 Graph of tank concentration 95% settling time as a function of f in response to positive finite-duration solute and water inflow pulses of size 10 % (above a baseline of 28.1 mosm/hr and 100 ml/hr, respectively) and duration 10 minutes for $m = 1\ hr^{-1}$ and $\frac{V}{Q} = 10\ hr$ 63
6.11 Design 3 Graph of (absolute) relative change in tank concentration as a function of f in response to positive finite-duration solute and water inflow pulses of size 10 % (above a baseline of 28.1 mosm/hr and 100 ml/hr, respectively) and duration 10 minutes for $m = 1\ hr^{-1}$ and $\frac{V}{Q} = 10\ hr$ 64
6.12 Design 3 Graph showing volume (blue), tank concentration (red), amount of solute (magenta), water outflow rate (green) and solute outflow rate (cyan) versus time in response to a positive finite-duration solute inflow pulse of size 10 % (above a baseline of 28.1 mosm/hr) and duration 10 minutes at $t = 10$ hr for, from top to bottom, $fw = 0.5, 0.8, 1$, $m = 1$ and $\frac{V}{Q} = 10\ hr$ . . 67

6.13 Design 3 Graph showing volume (blue), tank concentration (red), amount of solute (magenta), water outflow rate (green) and solute outflow rate (cyan) versus time in response to a positive finite-duration water inflow pulse of size 10 % (above a baseline of 100 ml/hr) and duration 10 minutes at $t = 10$ hr for, from top to bottom, $fw = 0.5, 0.8, 1$, $m = 1$ and $\frac{V}{Q} = 10\ hr$ 68
6.14 Design 3 Subplots of 95 % settling time of (a) tank volume and (b) tank concentration as a function of f_w in response to positive finite-duration solute and water inflow pulses of size 10 % (above a baseline of 28.1 mosm/hr and 100 ml/hr, respectively) and duration 10 minutes for $m = 1\ hr^{-1}$ and $\frac{V}{Q} = 10\ hr$ 69
6.15 Design 3 Subplots of (absolute) relative change in magnitude of (a) tank volume and (b) tank concentration as a function of f_w in response to positive finite-duration solute and water inflow pulses of size 10 % (above a baseline of 28.1 mosm/hr and 100 ml/hr, respectively) and duration 10 minutes for $m = 1\ hr^{-1}$ and $\frac{V}{Q} = 10\ hr$ 70

7.1 Line diagram of tank setup for Design 4: Parallel separators; separator 1 is defined by f_1 or f_{w1} and separator 2 is defined by f_2 or f_{w2}, depending on the separator combination of choice 76
7.2 Level-rate diagram for Design 4: Parallel water and solute separators; separator V_1 is defined by f_{w1}, V_2 by f_{w2}, N_{s1} by f_1 and N_{s2} by f_2 76
7.3 Design 4 (Parallel solute separators) Overall f versus x for fixed $f_1 = 0.5$ and a range of f_2 81
7.4 Design 4 (Parallel solute separators) Tank and outflow concentrations vs x for fixed $f_1 = 0.5$ and a range of f_2 82
7.5 Design 4 (Parallel water separators) Overall f_w versus x for fixed $f_{w1} = 0.8$ and a range of $0 < f_{w2} < 1$ 83
7.6 Design 4 (Parallel water separators) Tank and outflow concentrations vs x for fixed $f_{w1} = 0.8$ and a range of $0 < f_{w2} < 1$ 84
7.7 Design 4 (Parallel water and solute separators) Transfer function $\frac{f}{f_w}$ versus x for fixed $f_1 = 0.5$ and a range of f_{w2} 86
7.8 Design 4 (Parallel water and solute separators) Tank and outflow concentrations vs x for fixed $f_1 = 0.5$ and a range of f_{w2} 87
7.9 Line diagram of tank setup for Design 4: Series separators; separator 1 is defined by f_1 or f_{w1} and separator 2 is defined by f_2 or f_{w2}, depending on the separator combination of choice 89
7.10 Level-rate diagram for Design 4: Series separators; separator V_1 is defined by f_{w1}, V_2 by f_{w2}, N_{s1} by f_1 and N_{s2} by f_2 90

7.11 Design 4 (Series solute separators) Overall f versus f_2 for a range of f_1 . . 93
7.12 Design 4 (Series solute separators) Tank and outflow concentrations vs f_2 for a range of f_1 94
7.13 Design 4 (Series water separators) Overall f_w versus f_{w2} for a range of f_{w1} . 94
7.14 Design 4 (Series water separators) Tank and outflow concentrations vs f_{w2} for a range of f_{w1} 95
7.15 Design 4 (Series water and solute separators) $\frac{f}{f_w}$ versus f_{w2} for a range of f_1 96
7.16 Design 4 (Series water and solute separators) Tank and outflow concentrations versus f_{w2} for a range of f_1 97
7.17 Line diagram of tank setup for Design 4: Series-parallel separators; separator 1 is defined by bulk flow coefficient f_1 and water reabsorption coefficient f_{w1}, separator 2 is defined by f_2 and water reabsorption coefficient f_{w2}, and separator 3 is defined by water reabsorption coefficient f_{w3} 99
7.18 Level-rate diagram for Design 4: Series-parallel separators; separator V_1 is defined by f_{w1}, V_2 by f_{w2}, V_3 by f_{w3}, N_{s1} by f_1 and N_{s2} by f_2 100
7.19 Design 4 (Series-parallel separators) Transfer function $\frac{f}{f_w}$ versus $x \in [0,1]$ for fixed $f_1 = f_2 = 0.5$, $f_{w1} = 0.6$, $f_{w2} = 0.4$, and a range of $f_{w3} \leq 1$ 103
7.20 Design 4 (Series-parallel separators) Steady-state concentration versus $x \in [0,1]$ for fixed $f_1 = f_2 = 0.5$, $f_{w1} = 0.6$, $f_{w2} = 0.4$, and a range of $f_{w3} \leq 1$; showing tank concentrations and fixed outflow concentration 104

8.1 Simplified illustration of feedback control (adapted from [2]) 110
8.2 Comparison of dx and df_{w3} components of the gradient of the overall transfer function with respect to x and f_{w3} for two cases of fixed membrane properties (a) $f_1 = 0.5$, $f_2 = 0.5$, $f_{w1} = 0.6$ and $f_{w2} = 0.4$ and (b) $f_1 = 0.9$, $f_2 = 0.2$, $f_{w1} = 0.6$ and $f_{w2} = 0.4$ 113
8.3 Level-rate diagram for Design 5: Control 115
8.4 Design 5 (Control) Simulated tank volume, tank concentration and outflow concentration time responses to positive and negative 10 % (above a baseline of 100 ml/hr) finite-duration (10 min) water pulses for $C_{in} = 0.35$ mosm/ml and (a) $K_p = 0$, (b) $K_p = 10, 100, 900$ at t = 10 hrs, $\frac{V}{Q} = 10\ hr$ and $C_{set-point} =$ 0.281 mosm/ml 119
8.5 Design 5 (Control) Simulated tank volume, tank concentration and outflow concentration time responses to positive and negative 10 % (above a baseline of 35 mosm/hr) finite-duration (10 min) solute pulses for $C_{in} = 0.35$ mosm/ml and (a) $K_p = 0$, (b) $K_p = 10, 100, 900$ at t = 10 hrs, $\frac{V}{Q} = 10\ hr$ and $C_{set-point} =$ 0.281 mosm/ml 120

9.1 Line diagram of tank setup for multiple solute implementation; separator 1 is defined by bulk flow coefficients f_{A1}, f_{B1} and water reabsorption coefficient f_{w1}, separator 2 is defined by bulk flow coefficients f_{A2}, f_{B2} and water reabsorption coefficient f_{w2}, and separator 3 is defined by water reabsorption coefficient f_{w3} 126
9.2 Level-rate diagram showing multiple solute implementation; separator V_1 is defined by f_{w1}, V_2 by f_{w2}, V_3 by f_{w3}, N_{s1} by f_1 and N_{s2} by f_2 127
9.3 Component and overall transfer functions versus fractional flow (x) for $f_{w3} = 1$ and $fr_A = 0.36$, with endpoints indicated 132
9.4 Component transfer functions versus fractional flow (x) for a range in distal series water reabsorption ($f_{w3} \leq 1$) 133
9.5 Tank and outflow concentrations at steady-state versus fractional flow (x) for (a) solute A, (b) solute B, and (c) combined solute; for $fr_A = 0.36$ over a range of distal series water reabsorption (i.e. $f_{w3} \leq 1$) 134
9.6 Comparison of individual and combined step changes in fractional flow (x) and series water reabsorption (f_{w3}) at $t = 10\ hr$ by 0.2 units each from a baseline of $x = 0.7$ and $f_{w3} = 1$ (modelling the syndrome of inappropriate antidiuresis), on (a) tank volume, (b) tank concentration and (c) outflow concentration 136
9.7 Comparison of individual and combined step changes in fractional flow (x) and series water reabsorption (f_{w3}) at $t = 10\ hr$ by 0.2 units each from a baseline of $x = 0.7$ and $f_{w3} = 1$ (modelling the syndrome of inappropriate antidiuresis), on (a) solute A and (b) solute B tank concentrations 137
9.8 Comparison of varying the height of finite-duration water inflow (Q_{in}) pulse (ranging from 0 % to 500 % above baseline in 100 % increments) while reducing baseline fractional flow (x) and series water reabsorption (f_{w3}) by 0.2 units each over a 5 hour period (modelling exercise-associated hyponatremia), on (a) tank volume, (b) tank concentration and (c) outflow concentration 140
9.9 Comparison of varying the height of finite-duration water inflow (Q_{in}) pulse (ranging from 0 % to 500 % above baseline in 100 % increments) while reducing baseline fractional flow (x) and series water reabsorption (f_{w3}) by 0.2 units each over a 5 hour period (modelling exercise-associated hyponatremia), on (a) solute A and (b) solute B tank concentrations 141

9.10 Simulation results for varying the height of positive finite-duration fractional flow (x) pulse in increments of 0.1 units from a baseline of $x = 0.7$ over a duration of 7 hr (with zero series water recycle (i.e. $f_{w3} = 1$)) (modelling the effect of a loop diuretic) on (a) tank volume and (b) tank concentration, and (c) outflow concentration 143
9.11 Simulation results for varying the height of positive finite-duration fractional flow (x) pulse in increments of 0.1 units from a baseline of $x = 0.7$ over a duration of 7 hr (with zero series water recycle (i.e. $f_{w3} = 1$)) (modelling the effect of a loop diuretic) on (a) solute A and (b) solute B tank concentrations 144

10.1 Summary of developed exploratory model of excretion 150

List of tables

4.1 Design 1 Model Parameters 28

5.1 Design 2 Model Parameters 41

6.1 Design 3 Model Parameters 56

7.1 Design 4 transfer functions (parallel separators) 79
7.2 Design 4 Model Parameters (Parallel separators) 80
7.3 Design 4 transfer functions (series separators) 91
7.4 Design 4 Model Parameters (Series) 92
7.5 Design 4 Model Parameters (Series-parallel arrangement) 101

8.1 A selection of plasma constituents and their concentration ranges in humans (adapted from [1] unless an alternative reference is provided) 110
8.2 Design 5 Model Parameters 117

9.1 Application Model Parameters 130
9.2 Application Model Parameters 131

Nomenclature

Superscripts

*	immediately after the tank
**	between separators

Subscripts

dss	desired steady-state
i	parallel branch number
in	referring to inflow
out	referring to outflow
$recycle$	referring to recycle stream
s	solute
ss	steady-state
$tank$	referring to the tank
w	water

Other Symbols

C	concentration
$\dot{N}$	mass flow rate
f	bulk flow or sieving coefficient
fr_A	fraction of solute A

fr_B fraction of solute B

f_w water reabsorption coefficient

k lumped mass transfer or diffusion coefficient

m gradient of the $Q_{out} - V$ characteristic

N amount

Q flow rate

t time

$t_{s,95\%}$ 95% settling time

$t_{s,V,95\%}$ 95% volume settling time

V volume in the tank

x fractional flow to first branch of parallel setup

Acronyms / Abbreviations

ADH Antidiuretic hormone

ATP Adenosine triphosphate

$CSTR$ Continuously-stirred Tank Reactor

EAH Exercise-associated hyponatremia

ECF Extracellular Fluid

GFR Glomerular filtration rate

ICF Intracellular Fluid

I/O Input-output

IV Intravenous

LRD Level-rate diagram

MRI Magnetic resonance imaging

ODE Ordinary Differential Equation

P Proportional control

PD Proportional plus derivative control

PI Proportional plus integral control

PID Proportional plus integral plus derivative control

$SIAD$ Syndrome of inappropriate antidiuresis

$SIADH$ Syndrome of inappropriate secretion of antidiuretic Hormone

TBW Total Body Water

U/P Urine-to-plasma ratio

Chapter 1

Introduction

All organisms face the same challenge; that of survival within their environment. From single cells to complex fauna and flora, all organisms need to take in food and water, remove waste products, and maintain their internal milieu within some tolerance band. An organism's excretory system is primarily responsible for this function. The complexity of the system depends on the organism's need to respond to a change in the environment - a conformer has a wider tolerance to change and therefore, necessarily, is not as constrained as a regulator, who aims to maintain the internal environment within strict bounds no matter the disturbance. The environment may be aquatic or terrestrial, extreme or temperate, all posing different volume- and osmoregulatory challenges to the animals that inhabit them.

Within a class of animals it is seen that different members thrive in different environments, and yet possess the same basic excretory machinery. For example, within mammals, the Australian hopping mouse (*Notomys*) can concentrate urine approximately 25 x relative to plasma [3] and can therefore live in extremely arid conditions, humans manage a maximum urine-to-plasma concentration ratio of 4 - 5 x, while beavers average 1 - 2 x, preferring (and ultimately needing) a watery home [4]. A maximum urine-to-plasma concentration ratio in birds of 5 x was measured in the Savannah sparrow (*Passerculus sandwichensis*) [5] , and anything simpler than a bird cannot elucidate concentrated urine, requiring alternative survival strategies.

Renal physiologists have been interested in the conundrum of how the kidney concentrates urine to a greater extent in some animals relative to others for decades. Some hone in on kidney microstructure for the answers, while others consider the problem at varying levels of abstraction. A systems' level of analysis provides the highest level of perspective, and it raises the question whether an exploratory approach to systems' analysis could add any value and provide evolutionary insight into efficiency of excretory function in biology? From the most rudimentary to the most sophisticated, there exists the need for the excretory system to

control mass balance across an organism and maintain homeostasis according to their level of tolerance. Separation down a gradient is easily achieved (mirrored by the fact that dilute and isosmotic urine can be produced by simpler animals) so the problem of regulation in this context is one of separating up a gradient (concentrated urine can only be produced by birds and mammals who possess more sophisticated kidneys). This needs to be managed in as efficient a manner as possible, given the evolutionary path taken.

To this end, it was decided to start the modelling process by taking the lead from comparative biology, bottom up with very simple base structure and function under the least constrained conditions and steadily build up complexity in an evolutionary manner, similar to the process it is aiming to imitate. Due to the range of organisms being considered (i.e. from single cells to sophisticated mammals), the level of abstraction is understandably high. Therefore the model is limited in its predicting power from the outset, to modes of behaviour, signature responses and informed speculation with the focus more on understanding - considered sufficient at this pioneering stage of potentially establishing a new research niche.

The structure of the thesis does not follow the traditional pattern of a scientific document but rather mirrors the evolution of the system being modelled; each incremental change providing the basis for a new chapter. The background chapter has been written to provide context to the problem at hand but does not include an exhaustive review of the literature. Instead, relevant literature has been woven throughout the document, introduced as necessary. A basic design chapter introduces the model structure. Five core design chapters are followed by an application chapter, each containing model setup, simulation results and discussion, and biological application sections. A concluding chapter rounds off the document.

If the reader wishes to achieve a quick overview of the project, before delving into the detail, it is suggested that the background, biological applications of each design and conclusion are read first. These are also the sections that may appeal more to a biological audience, while the individual model setups and results are more theoretical, adhering to strict engineering principles.

It is anticipated that this work would appeal to both biological and engineering audiences and therefore the reader, depending on their background, may find more introductory detail than they consider necessary. However, the author has purposefully attempted to strike a balance by including sufficient content to bring everyone into context as seamlessly as possible.

Chapter 2

Background

A challenge facing living organisms that is addressed in this research is that of excretion; a mass balance must be maintained by the organism, and simplistically for substances such as water, nitrogen and solutes, what goes in must go out, across the spectrum of organisms and environments that they inhabit. Assuming the formation of urine (in sophisticated animals) or the equivalent waste product (in simpler organisms) is what we are most interested in understanding in the research, it is clear that water and solute excretion both need to be managed. Although intrinsically linked, these two processes apparently evolved consecutively with the need of organisms living in freshwater to excrete excess water while conserving solutes pre-dating the need of terrestrial organisms to conserve water while excreting wastes and excess solutes [6].

In this context, an organism's "diet" consists of all nutrients that enter the organism from the environment. This may involve eating and drinking or other routes such as diffusion through the skin and respiratory surfaces [4]. The concentration of a nutrient (such as water, protein, electrolytes) may be lower or higher than that in the organism itself, posing various and different challenges to the excretory system to match outputs with inputs and therefore maintain multiple mass balances across the organism.

It should be noted that although proteins and their component amino acids form part of the diet, different nitrogenous waste products are formed in different animals during protein metabolism and involve different modes of excretion [4]. Ammonotelic animals ("most aquatic animals including aquatic invertebrates, coelostomes and teleost fish") excrete toxic and water soluble ammonia straight into the surrounding water, ureotelic animals ("larger land vertebrates such as mammals, amphibians and some reptiles") excrete less toxic and less water soluble urea that requires a minimal ("obligatory" [1]) amount of water for excretion, and uricotelic animals (generally terrestrial and water-stressed such as "insects, birds and smaller reptiles") excrete non-toxic and water-insoluble uric acid as a paste [4].

The concentration of urea in mammalian urine exceeds that in the blood plasma by more than 50 x [1], exemplifying just part of the excretory challenge. Water, sodium and potassium, among others, are generally excreted when in excess and retained when in deficit [1].

It appears that water and solute handling capacity of the excretory system determines the adaptability of a species to living in new or extreme environments [7]. The term "adaptability" is strictly defined in the field of evolutionary biology as the process of genetic frequency adjustment through natural selection but is more commonly used in looser reference to phenotypic plasticity or acclimatisation [4].

The environment an organism experiences depends on both abiotic (i.e. physical and chemical) factors and biotic (i.e. living) interactions [4]. Changes in the environment affect different organisms differently; with small organisms experiencing life on a much finer spatial and temporal scale than large ones [4]. Organisms have evolved to solve the problem of a change in environment to different degrees and therefore have differing environmental tolerance and sensitivity. Tolerance is loosely defined as the "ability of an organism to endure unfavourable environmental conditions" [8]. Sensitivity, on the other hand, is defined as a change in output relative to a change in input [9], not necessarily referring to system inflows and outflows but rather the effect a specific component has on system characteristics [10]. A more sensitive system produces a greater change in output relative to input than a less sensitive system.

Typically, organisms choose the least stressful and energy-intensive route available to them [4]. Adaptive and acclimatory strategies include avoidance, conformity and regulation (effected through combinations of behavioural, morphological, physiological and biochemical change), summarised from Willmer et al. [4] as follows. Avoidance details the removal of the organism from the source of the stress in space (e.g. by means of behaviours such as burrowing or migrating) or time (e.g. by means of hibernation or producing a resistant egg). Conformity means that the internal environment mirrors that of the external environment (within limits). This, however, requires the organisms' cells to continue functioning under potentially extreme conditions and therefore biochemical and physiological changes need to be made to ensure this. These are apparently cheap to implement but at the cost of reduced activity. Regulation or homeostasis is the most expensive approach, requiring change at all functional levels, to ensure maintenance of an approximately constant internal environment no matter the external influence (within limits).

Regarding water and solute balances, conformity and regulation need to be qualified as responses to osmotic and/or ionic variation [4]. Osmolarity is a measure of lumped concentration, contributed to by all osmotic substances [1], both organic and inorganic, while ionic concentrations depend on individual ions. The primary organ of excretion in vertebrates

is the kidney, while invertebrates have nephridia, protonephridia or rely directly on diffusion [4]. In response to osmotic and/or ionic stress, the more primitive animals (reptiles and earlier except some insects) are limited by their rudimentary excretory systems to the less energy-intensive options of opting out of exposure to the environment or conformity [4]. In comparison, more sophisticated animals (mammals, birds and some insects) are able to regulate their body fluid content through resource- and energy-intensive [4] complex excretion. Therefore the vast majority of land animals are osmo-tolerators.

Animals within the same class have adapted to living in different environments by tailoring their excretory systems appropriately. In more primitive vertebrates, such adaptations tend to be extrarenal, while in terrestrial vertebrates, the kidney is "the major organ of excretion" [11]. For example, the gills in marine teleosts are enlisted to excrete excess solutes (by means of "chloride secreting cells", first postulated by [12]) while their freshwater counterparts require the opposite function of ion uptake [13–15]. Similarly, marine birds have adapted to drinking sea water by using salt glands to excrete excess solute (sodium chloride in particular), a function not needed and therefore not available to birds that have access to a freshwater drinking source [11, 16].

The kidney is the sole organ responsible for volume- and osmo-regulation in mammals [11], although other routes of insensible loss exist (e.g. respiration, sweat, faeces) [1]. As such, it is the site of adaptation. The kidneys receive a large fraction of systemic blood flow (20 % of cardiac output in man [17], which is approximately 900 litres/day) via the renal arteries and are responsible for filtering, reabsorbing the majority of the flow (returning it to the circulation via the renal vein), and excreting wastes, foreign chemicals and excess water and solutes as approximately 1.5 litres/day of urine [1]. This is in addition to its other functions, including "arterial pressure regulation, acid-base balance regulation, hormone secretion, metabolism and excretion, and gluconeogenesis" [1].

It is generally accepted that the kidneys achieve their urine production function by means of a combination of passive and active trans-membrane transport processes, summarised from Guyton and Hall [1] as follows. Passive processes such as diffusion and convection use energy stored in gradients (e.g. pressure, chemical or electrical potential) to drive mass transfer down a gradient (i.e. no direct involvement of an "active agent" [18]). In contrast, active processes require energy (typically metabolic in origin) to perform mass transfer against a gradient. The most studied example of primary (i.e. direct) active transport is the $Na^+ - K^+$ pump, which is apparently powered by dephosphorylation of adenosine triphosphate (ATP) and moves three K^+ ions into a cell for every two Na^+ ions pumped out, both against their concentration gradients [1, 4]. Secondary active transport on the other hand, occurs when the source of energy drives the mass transfer of interest indirectly [1].

For example, sodium-glucose co-transport into the cell is against the concentration gradient of glucose but down the concentration gradient of sodium (as previously established by the $Na^+ - K^+$ pump) [1].

Considering the variation in energy-intensity involved in processes of mass transfer, it is interesting that the core process of separating blood into urine (i.e. ignoring the mechanism) is not energy intensive (requiring less than 54 mW of power of separation or 54 mJ of energy per second in humans) [19]. However, Willmer et al. warns that this is simply the minimum cost involved [4]. The heart provides double this in pressure drop across the kidney and yet the human kidneys consume 6 W of metabolic power (or 6 J of energy per second) [19]). Discounting the energy needs in order to perform other kidney functions, this suggests a very inefficient urine concentrating process, a consequence presumably, of the (necessary) evolutionary path taken.

The facts that mammals living under extremely dessicating conditions (such as desert rodents, e.g. the Australian hopping mouse (*Notomys*)) can create a far more concentrated urine (approximately 25 x, relative to plasma concentration [3]) than those living in wet conditions (such as beavers, who average 1 - 2 x and have no need to conserve water but rather to excrete excess water without losing solutes [1]), and that some mammals have greater tolerance to high fluctuation in the environment compared to others [4], have been the basis of much research aimed at elucidating the concentrating (and diluting) mechanisms that differentiate them.

Vertebrate kidneys perform their excretory function by means of microscopically small separation units called nephrons, specialised to different degrees depending on the animal [20]. In the mammal, it is a tubular microstructure that traverses the two regions of the kidney (i.e. outer-located cortex and inner-located medulla [16]) with different segments and associated blood supply present in each, suggesting structural and functional heterogeneity of the kidney [21]. The various segments perform distinct functions (referred to as intranephron heterogeneity [22]) depending on their membrane make-up. Very simply, the glomerulus is the site of ultrafiltration of the blood, the proximal and distal convoluted tubules manage reabsorption and secretion, respectively, in concert with the surrounding peritubular capillary network within the cortex, while the loop of Henle, together with the associated collecting duct and surrounding vasa recta, provide for the reabsorbtion of water and concentration of the filtrate within the medulla [1]. The nephrons of most non-mammalian vertebrates (excluding birds) do not have a loop of Henle [20].

Three types of mammalian nephron are distinguished based on the relative location of the glomerulus; superficial cortical, midcortical and juxtamedullary (located at the boundary between the cortex and medulla) [23]. The more superficial nephrons tend to have short loops

(i.e. those that turn in the outer medulla or cortex), while the deeper nephrons tend to have long loops (i.e. those that extend into the inner medulla) [23, 24]. Structural internephron heterogeneity is therefore obvious between the groups of nephrons with long and short loops [22].

It has been found that renal blood supply, including intrarenal differences between the cortex and medulla, is similar in most mammalian species [21, 24, 25]. In contrast, most non-mammalian kidneys are supplied by an additional renal venous portal system [20].

Various predictors of concentrating power in mammalian kidneys have been assessed over the years and are reviewed in [26], including, among others, papillary length (i.e. including inner and outer medullary thicknesses) [27, 28], absolute length of loop of Henle, relative medullary thickness [28], number of nephrons, percentage of long loops, and nephron heterogeneity. It turns out that the presence of the loop of Henle and relative medullary thickness are key determinants of concentrating ability [4]. Increased nephron heterogeneity is also linked to higher urine concentrating ability [26]. In addition, it has been seen that small mammals tend to have higher urine concentrating ability than bigger mammals and this may be related to higher mass-specific metabolic rates [4].

In tandem with experimental investigations, theoretical models have informed renal physiological understanding. A review of renal function modelling would necessarily be split along spatial resolution lines, as suggested by Moss and Thomas [29]. Intra-organ models are high resolution and can be divided into different levels depending on the focus. Micro-scale models look at renal tubular function at a cellular level [30], while meso-scale models consider tubule or whole nephron-level [31, 32]. Macroscopic models consider populations of nephrons and/or intrarenal blood supply [31] but tend to focus on specific kidney zones (e.g. the outer medulla in the well known countercurrent multiplication explanation for the generation of the observed osmotic gradient [33]). Functionally, antidiuresis is focused on much more than other physiological states, such as diuresis [29]. Weinstein commented in 2017 that the majority of intra-organ mathematical models published in the literature to date tended to be nephron-level models, with few organ- or kidney-level models (three, in fact) due to the confounding effect of "late events impacting early events" along the convoluted tubule [32]. Sands and Layton caution that "after more than 70 years of research, the concentrating mechanism of the outer medulla is not confidently understood" [18] while Stephenson concludes with "how the inner medulla concentrates urine is one of the major unsolved problems of renal physiology" [34].

In light of the gaps in understanding (especially in the inner medulla), a number of alternative hypotheses "based on the peristaltic contractions of the smooth muscles of the pelvic wall" [23] have been put forward by eminent physiologists [35, 36] seeking to provide

a mechanical (and therefore less energy-intensive) explanation for powering of the urine concentrating mechanism. However, Sands and Layton express concern over the technical complexity involved [23].

In order to avoid such continued difficulties and "factual, experimental and computational limitations" [29] of intra-organ modelling, much lower resolution whole organ and multi-organ modelling approaches have been developed to aid further renal understanding without being overly constrained by underlying anatomy and physiology [29]. Key models of the 1970s [37–41] laid the foundation for such a systems' level of analysis of renal function. Guyton et al. developed the "first whole body integrated mathematical model of a physiological system" [37] focusing on the cardiovascular system and including kidney dynamics and excretion as a subsystem. He defends the validity of a systems' approach by noting that systems' analysis does not require fully defined subsystems; helps in identification of control systems most contributory to overall control; and helps in "identifying inconsistencies between postulated mechanisms" [37]. Ikeda et al. produced a "large-scale multi-compartment model of body fluid regulation" including physiological subsystems, the extracellular and intra-cellular fluid [38]. The kidney was modelled in more detail than in the model by Guyton et al. [37] as Ikeda et al. were also interested in acid-base balance [38].

More recently, the initiation of the Physiome Project in 1997 [42] has incentivised laboratories to create and contribute to collaborative online platforms where models are made available to promote integrative (in terms of organ systems and multi-scale) physiological efforts, both in terms of education and research [43, 42]. A number of models have been built directly on the frameworks established in the 1970s (examples include those in [44, 45, 43, 46]), benefiting from enhanced computing capability and more experimental knowledge. The models vary in complexity (i.e. number of parameters and ordinary differential equations (ODEs)) and timescale being represented (the model of Guyton et al. offering the widest range, from $5\text{x}10^{-4}$ min for autonomic control to 10^4 min for heart hypertrophy or deterioration [37, 43]).

Unlike other approaches, Chandhoke and Saidel did not assume well-mixed compartments but rather spatially-discrete elements with mass balances over each one [41]. In addition, nephron heterogeneity and intrarenal blood flow differentiation between cortex and medulla were modelled explicitly [41], something largely ignored until Moss and Thomas' publication in 2014 [29]. Indeed, some mention has been made of possible contributions by differential intrarenal blood flow and internephron heterogeneity to the urine concentrating mechanism [47] but mostly suggestive of influence rather than demonstrative. Pallone and Cao mention "a growing body of literature supports the hypothesis that differential regulation of blood

flow to the cortex and medulla plays a mechanistic role in the regulation of salt and water excretion" [25] but do not go into more detail.

A comparison of some key features of systems' level models that include renal function is made across Tables 2.1, 2.2 and 2.3.

Author	Ref.	Year	Goal	Assumptions	Physiological scale	Advantages	Disadvantages
Guyton et al.	37	1972	Systems' analysis of circulatory regulation for the purpose of revealing the causes of hypertension	354 homogenous blocks and >400 mathematical operations based on gross functions of the parts; includes Na^+ and K^+ handling by the kidney	Systems' level; multi-organ; functional subsystems	First whole body integrated mathematical model of a physiological system; identified most important control systems in circulatory system and inconsistencies between postulated mechanisms from different laboratories	Kidney dynamics and excretion simplified due to representing only 1 of 18 major systems involved in circulatory control; confirmation of model predictions difficult; limited computing capability
Bigelow et al.	39	1973	Simulate renal response to a variety of stresses	Four well-mixed compartments; detailed simulation of ADH effects; includes gastrointestinal and arterial pressure effects	Systems' level; whole body, multi-compartment	Looked at multiple stresses; not limited to effect of ADH	Required mathematical compensation for ADH effects and hydration levels; difficulty initialising the model and experimental subjects to correspond; limited computing capability
Cameron et al.	40	1977	Simulation of overall renal function as a salt and water regulator	Based on Guyton (1972); pertains to the standard 70kg human male; considers electrolytes Na^+ and K^+; only drinking and urination considered in overall water balance	Systems' level; whole body, multi-compartment	Easier to validate than Guyton (1972); able to evaluate and suggest new hypotheses about renal regulatory mechanisms; extendable to include more kidney detail	Requires more detail to perform further studies; model validation is difficult; limited computing capability
Ikeda et al.	38	1979	Systems' approach to the diagnosis and therapy of body-fluid and acid-base disorders	Based on Guyton (1972) but simpler circulatory system and more complex renal system representations; described mathematically as a set of non-linear differential and algebraic equations of >200 variables; considered Na^+, K^+ and water excretion in particular; modelled ADH, aldosterone and pressure diuresis control signals; intranephron heterogeneity included	Systems' level; whole-body; subsystems of circulation, respiration, renal function; multi-compartment including extra- and intra-cellular fluid spaces	Good applicability to some clinical problems; provides a useful framework for physiological experimental research	Confirmation of model predictions difficult; limited computing capability

Fig. 2.1 Comparison of systems' level models that include renal function, part 1 of 3

Author	Ref.	Year	Goal	Assumptions	Physiological scale	Advantages	Disadvantages
Chandoke and Saidel	41	1981	Model of mass transport throughout the kidney: effects of nephron heterogeneity and tubulo-vascular organisation	Considers internephron heterogeneity and intrarenal blood flow differentiation; uses spatially discrete elements with mass balances over each component; considered salt, urea and non-permeable solutes	Systems' level; whole body, multi-compartment	Can model effect of changing medullary blood flow on cortico-medullary osmotic gradient and urine concentration	Model validation is difficult; some estimation of parameters needed; limited computing capability
Gyenge et al.	46	1999	Model of short-term transport of fluids and solutes for investigation of fluid shifts	Considers four well-mixed compartments; considers Na^+, K^+, Cl^-, lumped cation and anions; Na+ and K+ transport across membranes by electrodiffusion and active transport; cellular membrane freely permeable to water; dynamic behaviour based on mass balance equations (20 ODEs, 2 implicit non-linear algebraic equations and 2 explicit algebraic equations)	Systems' level; whole body, multi-compartment	Capable of predicting both experimentally measurable variables and inaccessible system variables for various types of infusions	Parameters estimated from literature
Abram et al.	44	2007	Integrative Quantitative Circulatory Physiology (QCP) model for medical education	Based on Guyton (1972) with higher detail submodels and extended to include nervous, respiratory and endocrine systems	Systems' level; multi-organ; functional subsystems	Comprehensive; provides a teaching environment that mimics clinical problems; facilitates the learning of physiology using a system analysis approach	First-year medical student focused rather than research oriented
Thomas et al.	43	2008	Systems' model for body fluid homeostasis and blood pressure regulation; providing for in silico exploration	Based on Guyton (1972) and Ikeda (1979); models reimplemented in FORTRAN, C++, Simulink and ODE solver Berkeley Madonna	Systems' level; multi-organ; functional subsystems	Flexibility in implementation; compatible with future applications in clinical setting; contribution to Physiome project (e.g. SAPHIR at human, rat, mouse and dog scale)	A work in progress

Fig. 2.2 Comparison of systems' level models that include renal function, part 2 of 3

Author	Ref.	Year	Goal	Assumptions	Physiological scale	Advantages	Disadvantages
Hester et al.	45	2011	User-friendly integrated model of human physiology (HumMod) from birth to death, male or female	Updated version of QCP (Abram (2007))	Systems' level; multi-organ; functional subsystems	Useful in understanding proposed physiological interactions that are not evident; allows for observation of higher-level emergent properties of complex physiological systems; time-dependent responses range from seconds to years; user-expandable functionality to aid research; teaching tool	A work in progress
Moss and Thomas	29	2014	A lumped-nephron model that accurately simulates regulation of renal salt and water excretion and that explicitly represents the main features of the underlying physiology, incorporating the major hormonal regulatory effects on both tubular and vascular function.	Incorporates 2 groups of nephrons (short and long loops) with intranephron differentiation along length as 6 lumped nephrons; includes salt, urea and non-permeable solutes; subject is a mild-antidiuretic rat; hormone effects adjust epithelial parameters; ADH affects distal water reabsorption	Systems' level; whole organ	First model to explicitly couple glomerulo-vascular and medullary dynamics; developed to be included in whole-body physiological models; includes diuresis and anti-diuresis studies; simulation of thiazide and amiloride (diuretics) administration	Model limited in concentrating ability at high arterial pressure; the model is only capable of producing a concentrated urine in the antidiuretic state when just one of the five juxtamedullary efferent arterioles is connected to the descending vasa recta, which violates the known physiology; does not include regulation of medullary blood flow

Fig. 2.3 Comparison of systems' level models that include renal function, part 3 of 3

The goal of this research is to contribute to understanding of excretion, especially that of urine concentration variation in response to the environment, both in terms of adaptation to extremes and managing high fluctuation. Interest lies in what the excretory system has to do rather than how it does it. Not only does the organism have to maintain multiple mass balances across it in response to its diet in a range of environments with potentially very different component concentrations, some above and some below that of the organism, it has to achieve all this with the same structural machinery. An engineer would find it very difficult to design a system within such constraints at high resolution. This suggests that a systems' level of analysis is key, and if this is performed at an even higher level than that of established whole kidney models, keeping comparative biology in mind, it may help elucidate biological functionality that is not obvious when focusing only on mammalian kidneys.

Systems' Science is the science of complex systems (made up of interacting parts) and their behaviour (or response to a stimulus, including environmental, characterised quantitatively) as a whole [48, 49]. Emergent behaviours are considered most of interest, i.e. those "not predicted based on the integration of behaviours of the individual parts of the system" [50]. Such a systems' approach has been used in analysing engineering, biological and social science systems [48], often yielding non-intuitive results [49].

A model is simply a representation of reality, "capturing interactions among important factors" [51], the results of which are only as valid as the assumptions it is based upon. In addition, prediction is only one purpose of modelling; models can also be built to aid understanding [51, 52]. Considering validation of a model, Levins prefers that it "generates good testable hypotheses relevant to important problems" than is considered "true" [53].

Different approaches to model design include top-down and bottom-up [54]. A top-down ideas-driven approach involves decomposition [50] or reduction [55], where a complicated system is deconstructed into simpler parts for the purpose of functional insight. It is generally hypothesis-driven and involves deductive reasoning [56, 55]. In contrast, a bottom-up data-driven design involves aggregation [50, 55], starting simply with well-defined system components and adding complexity as needed. The collective behaviour of the system is said to "emerge out of interactions among constituent components and between components and their environment" [54]. The approach is generally hypothesis-free (hypotheses result from the study, but do not initiate it) and involves inductive reasoning [55]. Although both approaches may be valid in terms of providing a path to achieve a complex end-product, one approach may be more appropriate for a particular application than the other [54]. Kell and Oliver argue that both modes of reasoning should be employed in an iterative cycle for the advancement of science [55].

A key area of modelling involves appropriate system identification; the process of defining a reasonable mathematical model to describe the system of interest's dynamics from input-output data [57]. The amount of detail included in a model determines whether it is considered black, i.e. path independent between inputs and outputs, white, i.e. fully described from first principles, or a shade of grey, i.e. informed by some mechanistic information [57]. The benefits of a grey-box model, especially one built up from simple building blocks, include flexibility and relevance through incorporation of some physical insight to establish transfer functions [57].

System dynamics is one of a number of methods that provides a means of quantitative systems' characterisation [50] within the discipline of Systems' Science. Developed by Forrester in 1961 to model industrial systems, [58], and since expanded to innumerable fields of application [51], only two constructs are needed for system dynamics model description. Accumulations are represented by levels (or stocks) while corresponding rates of change are represented by rates (or flows). Level-rate (or stock-flow) diagrams provide for clear visualisation of underpinning coupled first order ordinary differential equations (ODEs). Advantages of such an approach include rapid and intuitive modelling of complex, non-linear systems [51]. In contrast to the typical engineering focus on analytical tractability (following prescribed solution procedures) [59], system dynamics models are not intended to be used for point prediction [51]. Instead, the structure of the model provides for interrogation of all the component parts following numerical solving, therefore aiding system understanding and informing further research [51].

Vensim (by Ventana Systems, Inc.) is a simulation package used to produce System Dynamics models. Model development involves the drawing and populating of a level-rate diagram with appropriate variables and information arrows. The ODEs are solved in the background during simulation (a variety of numerical methods, including Euler, Runge-Kutta and Difference, are available to choose from) and results tabulated or graphed as desired.

As mentioned in the introduction, the idea behind this background chapter was simply to provide context for a disparate audience of biologists and engineers, laying the foundation for the modelling problem at hand. To reiterate, the model needs to address what functionality is needed to meet the challenges of excretion. In so doing, some insight into real excretory system function may be gleaned. Additional literature is introduced throughout the modelling process, either in motivating modelling decisions or relating the simulation results to what is known about the biology.

Chapter 3

Basic design

Considering the biological and systems' science contexts introduced in the previous chapter, it was decided that an approach to modelling that mimics certain evolutionary aspects of the excretory process in animals could yield results that may be interesting with respect to the urine concentrating process when referred back to the biology. To this end, a basic model is developed as follows.

3.1 Aim

It is of primary interest to investigate a spectrum of excretory systems through modelling with the long term goal of designing a separation system that is able to mimic the behaviour of a complex organism's excretory system (kidney). For varying inputs of water and other liquid and solid substances, such as salts and nitrogen in protein, the model should produce outputs of concentration and flowrate so as to maintain steady-state in terms of volume and osmolarity. Through such a step-wise modelling process, a secondary aim is elucidation (at a very high level) of essential structures and control strategies in existing excretory systems of organisms of different complexity, and in so doing, discern whether anything can be inferred about the biology.

3.2 Design procedure

Evolution is exploratory in nature [60] so although modelling a biological system with a constrained top-down approach may well allow for the testing of a particular hypothesis, it may also miss unexpected and unforeseen results. Therefore, a more inductive, bottom-up approach, responding to similarly steadily increasing constraints, was decided upon when

modelling the excretory system, with the hope of providing a new perspective. Other guiding principles include aiming for simplicity in design (i.e. Occam's razor), and designing for inherent stability first and only adding control later for the purpose of fine-tuning the system.

3.3 Assumptions

In such a bottom-up approach, a few key assumptions are necessary to provide the foundation for the model, after which supplementary assumptions are made as required in order for further model development.

If a boundary were to be drawn around an organism (anything from simple and unicellular to complex and multicellular) and all inputs of liquids (and solids) and outputs monitored over a particular period of time, a high-level model with the same average inputs and outputs (I/O) could be said to represent the overall function of the organism's excretory system, as illustrated in Figure 3.1, where the system referred to in the figure is the organism itself. The part of the excretory system particularly of interest is that of urine formation and therefore the model is limited to include only those inputs and outputs directly involved in urine production (in sophisticated animals) or the equivalent waste product (in simpler organisms).

It is assumed that baseline levels of water and solute enter the organism continuously (therefore modelling either a constant environment or a sufficiently averaged non-constant environment) and therefore the temporal resolution is considered relatively granular (more so in the case of small animals and less so in the case of large animals [4, 7]), contributing to the high-level assumption.

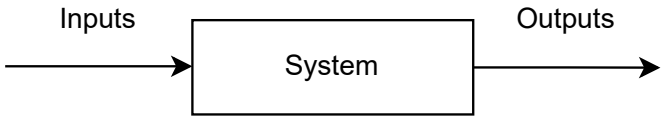


Fig. 3.1 Diagram of I/O system

The variation in spatial and temporal resolution of various published renal physiology models is graphically interpreted in Figure 3.2 to provide some additional context to the author's proposed region of interest.

Such a high level of abstraction means the model is not constrained by kidney structure (in agreement with [29]) but rather looks to emulate select excretory system function. It is assumed that limited functionality of the kidney (i.e. volume- and osmo-regulation) can be modelled independently of its other functions (i.e. those of "arterial pressure regulation, acid-base balance regulation, hormone secretion, metabolism and excretion, and gluconeogenesis"

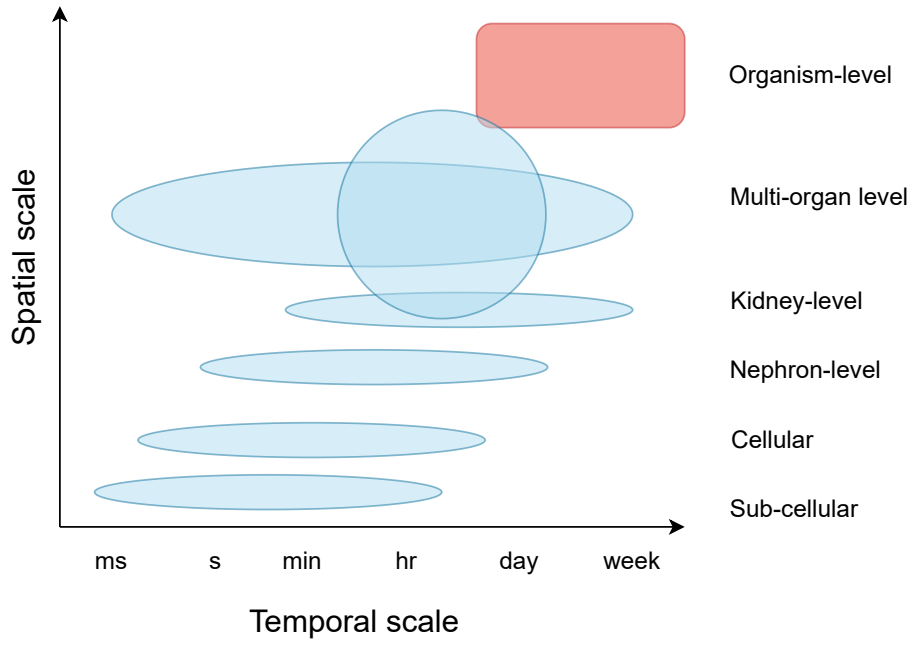


Fig. 3.2 Diagram relating approximate spatial and temporal scale of models involving the renal system in the literature (blue), highlighting the author's region of interest (red box)

[1]). This is borne out by the fact that physiological models of kidney function in literature focus on a particular function and not all (e.g. Guyton et al. consider only those functions of the kidney that contribute to circulatory system regulation [37]). A perceived weakness of such an approach, especially considering the bottom-up nature of the design, is that a different evolutionary outcome would likely be achieved if more than one kidney function were being considered from the start. However, it must be remembered that all models represent a portion of reality, depending on the boundary chosen (in this case a functional boundary, i.e. the excretory function of the kidney in isolation of other functions) and the results need to be interpreted within such. Functional signatures, trends and modes of behaviour that match qualitative description are most of interest, and obviously have implications for model validation and any conclusions drawn from the results of the model. However, reiterating the sentiment of Levins, the usefulness of a model can be quantified instead on its ability to "generate good testable hypotheses relevant to important problems" [53].

At a high level, it is assumed that a single continuously-stirred tank reactor (CSTR) can be used to model the osmotically-active solute distribution of interest in an organism. This may seem too simplified a statement but consider that, at a high-level, a single cell is simply made up of a nucleus and cytoplasmic suspension of solutes and organelles with net flux across the cell membrane ultimately dependent upon the cell environment [1], as if it were a well-stirred

tank with inflows and outflows. Now consider a multicellular organism with intercellular flux responsible for mixing and equilibration of solute distribution depending on the environment; at a high enough level, and granular enough resolution, only the net flux across the boundary of the organism is of interest, as in a well-mixed tank. Finally consider a complex animal such as a mammal that has a circulatory system responsible for rapid transport of blood gases and nutrients around the body. It is observed that the blood flow to the kidneys is high (approximately 900 litre/day or 20 % of cardiac output in humans [1]), while only a small amount of modified filtrate (i.e. urine) is extracted per pass (yielding approximately 1.5 litre/day in humans [1]). The blood flow is then recycled, yielding the same overall effect as a well-stirred tank where the tank contents represent the plasma portion of the extracellular fluid (ECF). The ECF acts as a buffer between the environment (i.e. the region immediately outside the body, and in particular, that which can enter the body, including the contents of the gastrointestinal tract) and cells (i.e. intracellular fluid (ICF)) [4], and therefore the interaction most of interest is that between the ECF and environment, especially in the case where solutes are considered lumped together. In addition, a well-mixed tank assumption is commonly used in systems' level models of the renal system, together with corresponding "spatially constant descriptive parameters, i.e., mean values for descriptive properties (e.g., transport parameters) and dependent variables (e.g., concentrations for given solutes)" [46].

The volume of the excretory system is small compared to that of the organism (for example, human average total kidney volume is 150 to 200 ml depending on gender [61], compared to a total body water (TBW) of 42 litres, an ECF of 14 litres or a plasma volume of 3 litres [1]), and therefore, tank volume is assumed to dominate over a negligible separator volume.

The net pressure driving separation is assumed to include the effects of internal hydrostatic and oncotic pressures implicitly, due to the high-level, input-output nature of the model, as noted in [40].

Since interest lies in how the excretory system maintains the mass balance and not kinetics per se, it is assumed that the rates of reaction are relatively fast relative to mass transfer rates and that the substances that need to be reacted before rejection (such as nitrogen in protein being transformed to urea and being excreted) are transformed quickly relatively to the response time of the organism to changes in its environment. This implies no need for a generation term in the mass balance [59] and that the CSTR is technically, simply a continuously-stirred tank in this context.

As a consequence of the previous assumption, it is further assumed, for simplicity, that the solutes enter the organism in their simplest form (e.g. ammonia, urea or uric acid and not protein). Although this extra layer of modelling complexity (e.g. protein metabolism)

is technically present, it is not deemed to be contributory to the application at hand; it is believed that the model is being considered at a high enough level for this to have a minimal effect.

Unlike a black box model, a grey box is built on some mechanistic information [57]. In terms of system identification, the continuously-stirred tank assumption provides a mechanism for moving from input to output (i.e. transfer function description), and therefore the physical insight necessary for grey-box modelling.

It is initially assumed that all osmotically-active solutes (e.g. sodium, potassium, chloride ions and urea, among others) can be lumped together in order to create a model based on osmolarity rather than individual solute concentrations. This follows from renowned comparative biologist Schmidt-Nielsen's statement that "it is the osmotic concentration, rather than a detailed list of all solutes, that is important in most considerations of osmotic regulation in animals" [62]. This means that the organism can be modelled by a single bulk osmolarity. There are obvious limitations involved in such an approach, such as missing the outcomes of non-intuitive inter-solute interactions [63]. However, as model development proceeds, the lumped solutes may be split into a number of species whose concentrations (and interactions) need to be taken into consideration and controlled separately. It is assumed that, together with the (negative) contribution of proteins, minor electrolytes (e.g. H^+, HCO_3^-, PO_4^{3-} etc.) neutralise the major cations (Na^+ and K^+) and anion (Cl^-, which typically follows Na^+) [1] and therefore that overall electrical neutrality is maintained at the high level being considered. A more detailed level of modelling, including the Stefan-Maxwell relations [63] and multiple electrochemical balances, would need to be pursued if lumped solute were not being considered.

It is assumed that a change in environment (causing dehydration, overhydration, solute deficiency or excess) can be modelled by superimposing a transient change in the water and / or solute input even though it may be caused through some other mechanism (e.g. dehydration through excess water loss) as the net effect on the model is considered the same. A similar decision was made by Beuchat who lumped studies involving a variety of concentrating conditions to determine maximum urine osmolality within a species [64].

Considering the fact that insensible water and solute loss (i.e. through skin, sweating, respiration and faeces) are not regulated [16] and make a sufficiently small contribution to the overall excretory process (in mammals) [1], even during exercise-heat stress ("the sweat duct does not play an important role in water conservation" [65]), it is assumed that they can effectively be ignored for the purposes of this model. This is backed up by previous high-level model implementation, where "only drinking and urination were considered in calculating changes in overall body water balance" [40].

3.4 Constraints

It was determined that such an exploratory approach to modelling is constrained both directly by data availability (or lack thereof, which in turn determined the level of abstraction and input-output nature of the model); and indirectly by the constraints on the organisms being modelled. Through comparative biology it is apparent that evolution of the kidney (and particularly the advent of terrestriality [4, 7]) represents physical realisations of an increasingly constrained system. The complexity of the excretory system depends on the organism's region of operation - a conformer has a wider internal tolerance to change and therefore, necessarily, is not as constrained as a regulator, who aims to maintain the internal environment within strict bounds no matter the disturbance. In order to mimic such step-wise development observed in the excretory systems of organisms, each step of model development needs to be similarly increasingly constrained, starting with high volume- and osmo-tolerance and steadily narrowing the internal tolerance bands. Such volume and osmolarity constraints therefore provide control objectives at each level of modelling.

3.5 Model formulation

Consider such a "single lumped composition" organism to be represented as a "grey" box, with water and solute inputs and outputs as illustrated in Figure 3.3. Inside the box, let there be a tank acted upon by a separator of negligible volume (representing the action of the excretory system). The volume of the tank may represent the total body water or a smaller compartment such as the ECF, depending on the transfer rate between compartments and site of action of the excretory system in the organism being modelled. If the tank is considered to be well mixed (which is likely considering a time-frame of days), then a simple representation could be that of a continuously-stirred tank.

V and N_s represent the volume and amount of solute in the tank, respectively, while Q and $\dot{N}_s$ are the associated flow rates, and C refers to the derived concentrations. The subscripts match the nomenclature of the continuously-stirred tank; "in" for inflow, "out" for outflow, and "tank" when referring to tank quantities.

Further assumptions needed to quantify the model include the fact that body fluids can be considered as dilute solutions [1] and therefore everything is in liquid-phase and constant density [66]; ideal mixing [66]; and isothermal conditions [67].

Any system outflow must match the inflow, on average, in order for a mass balance to be maintained. In addition, if the inflow is varied, the outflow must adjust to keep the system at steady-state. The component mass balances (i.e. water and solute) over this tank provide

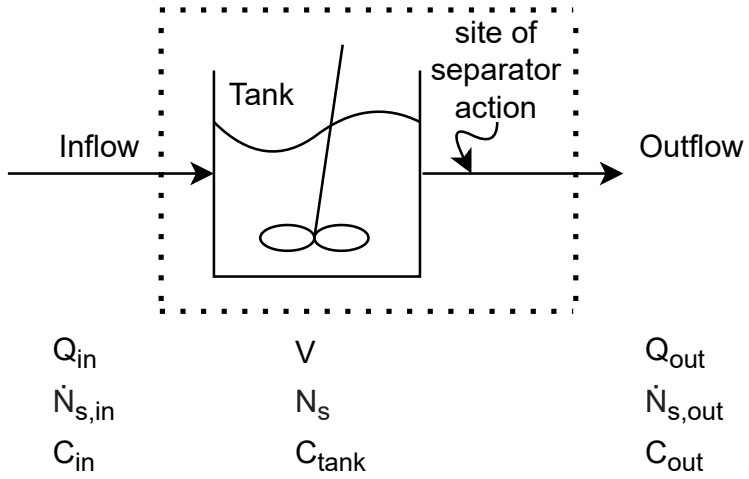


Fig. 3.3 Line diagram of a grey-box model (boundary shown with dashed line) with continuously-stirred tank and site of separator action indicated. Water, solute and concentration quantities are listed below each component of the model

two coupled first order ODEs. Equation 3.1 indicates a volume balance while Equation 3.2 a mass balance on all the osmotically-active solutes.

$$\frac{dV}{dt} = Q_{in} - Q_{out} \tag{3.1}$$

$$\frac{dN_s}{dt} = \frac{dC_{tank}V}{dt} = \dot{N}_{s,in} - \dot{N}_{s,out} \tag{3.2}$$

At steady-state, Equations 3.1 and 3.2 reduce to $Q_{out} = Q_{in}$ and $\dot{N}_{s,out} = \dot{N}_{s,in}$ such that $C_{out} = C_{in}$. In the case of no separation on the outflow, $C_{out} = C_{tank}$. At this stage, it is not the intention to solve the dynamics but rather introduce the basis of the model.

The basic continuously-stirred tank graphic can easily be converted to the level-rate diagram (LRD) (as mentioned previously, a representation typically used in the field of System Dynamics to represent the relatedness between variable accumulations and flows within a system [51]) illustrated in Figure 3.4. The mathematics behind the level-rate diagram follows directly from mass balance and therefore matches the ODEs of the continuously-stirred tank exactly but the visualisation is quite different. A major difference is the consideration of two separate levels and their associated flow rates in the level-rate diagram (more explicit) as opposed to a mixture in the continuously-stirred tank (less explicit). It must also be mentioned that flows can be bidirectional in a level-rate diagram; only the governing equation determines the ultimate direction of flow. As alluded to by the information arrows in Figure 3.4, the solute and volume remain coupled through the concentration in a single

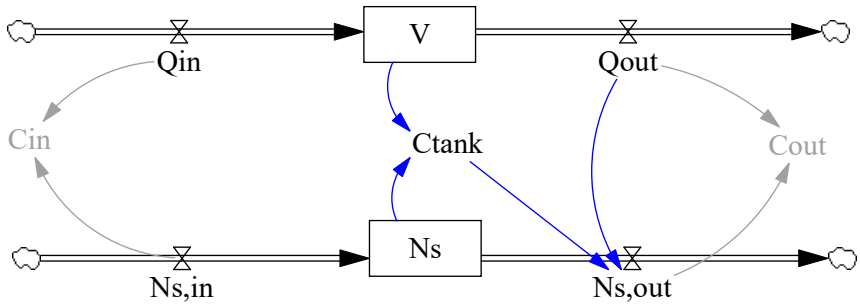


Fig. 3.4 Level-rate diagram for basic continuously-stirred tank; boxed variables representing levels, valves representing flow rates, unboxed variables representing auxiliary variables, and (blue and grey) arrows representing information flow

stream, with the solute outflow being dependent on the water outflow and tank concentration.

Let the tank quantities represent the body fluids and the outflow stream the urine (or simpler fluid). Let the inflows be constant to match daily average consumption of water and solute (which has to match daily average urine excretion by mass balance). As a starting point, let these be 100 ml/hr and 28.1 mosm/hr, respectively, yielding a steady-state inflow concentration of 0.281 mosm/ml (most vertebrates maintain the osmolarity of their extracellular fluid in the vicinity of 1/3 seawater [7], which corresponds to approximately 1000 mosm/l, and therefore this choice is not quite arbitrary but not important). This provides baseline input.

The response of a system to an impulse disturbance provides for full characterisation of the system. In biological experimentation, a short but finite duration bolus input of water (i.e. water loading) and/or solute (i.e. salt loading) is considered adequate in approximating an "impulse change" in environment or diet [68] and therefore, this is what is simulated. A rapid change in input magnitude from baseline has been chosen to represent a step disturbance while recovery of that step change within a short duration (relative to the model dynamics) has been used to approximate an impulse disturbance. The chosen size of the input disturbance is not as important (as long as it remains within biological reason) as keeping it the same

throughout the modelling procedure to provide a means of comparing the incremental designs. It should also be noted that a continuous range of water and solute input combinations is possible. In the case of a linear system, pure solute and pure water responses can simply be added together to represent the response to a mixed input, providing a means of simplifying the analysis. However, it is anticipated that a realistic model of the excretory system will incorporate non-linearities, yielding such an approach of superposition inaccurate in the long-term. If this is the case, then it is important to be aware of options going forward; either linearisation of a future non-linear model, or development of the model such that it is possible to solve such mixed input from the start. The system dynamics approach to modelling favours the latter option.

The ODEs that define the system can be solved analytically or numerically. However, as is shown in Appendix A (specifically Section A.6), the complexity introduced by a separator on the tank outflow from the third design in Chapter 6 onward, complicates the analytical solution (particularly in response to disturbances that include water).

Considering the simplifications and similarities listed under assumptions in Subsection 3.3, the single tank model provides a suitably simple base upon which to start building a model of the excretory system. Additional structure is added only as needed to improve function. In this way, the approach differs from most previous systems' level analyses of mammalian kidney function that include multiple compartments and solutes from the start [37, 38, 40, 44, 46]. It will be shown that such a high-level single well-mixed compartment with lumped solute representing the organism is in fact sufficient in providing an unchanging central element in an evolutionary model of excretion.

Chapter 4

Design 1: No control

As in evolution, the first design is the simplest. Therefore, simplifying assumptions have been made. One such assumption is the unorthodox decision (in terms of process engineering) to allow the tank volume to vary (therefore enabling the modelling of excretion in single cells and soft bodied animals that are able to contract and expand substantially). Another linked assumption involves keeping the exit flow rate constant, representing a simple excretory system with an average urine (or simpler fluid) flow rate. These assumptions may seem overly simplified, however, the chosen modelling approach remains that of starting simply and building in complexity later, only as and when needed.

4.1 Model setup

The initial design simply involves a non-constant volume continuously-stirred tank with constant water outflow (matching baseline inflow) and no explicit control mechanism. The outflow concentration matches that of the tank and no separation occurs. The corresponding tank line diagram and level-rate diagram are illustrated in Figures 4.1 and 4.2, respectively.

The defining equations remain Equations 3.1 and 3.2, repeated in Equations 4.1 and 4.2 for ease of reference. Considering the grey-box modelling structure introduced in Chapter 3, these overall input-output equations remain the same throughout all the designs.

$$\frac{dV}{dt} = Q_{in} - Q_{out} \tag{4.1}$$

$$\frac{dN_s}{dt} = \frac{dC_{tank}V}{dt} = \dot{N}_{s,in} - \dot{N}_{s,out} \tag{4.2}$$

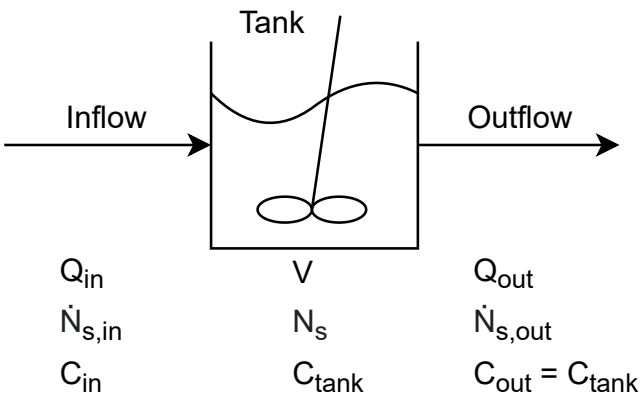


Fig. 4.1 Line diagram for Design 1: No control

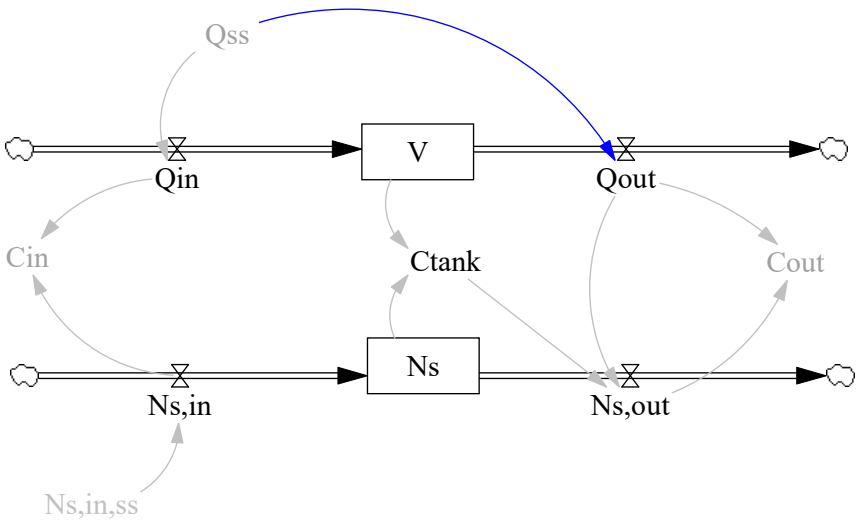


Fig. 4.2 Level-rate diagram for Design 1: No control

The water and solute inflows follow in Equations 4.3 and 4.4, respectively, and correspond to some baseline, steady-state value with or without a disturbance such as a finite-duration pulse or step function superimposed thereon.

$$Q_{in} = Q(t) = Q_{ss} + disturbance \tag{4.3}$$

$$\dot{N}_{s,in} = \dot{N}_{s,in}(t) = \dot{N}_{s,in,ss} + disturbance \tag{4.4}$$

An alternative means of modelling an impulse disturbance is to keep the inflow rate constant (i.e. at baseline or long-term steady-state) and change the initial condition on the level. This is the approach used when calculating the analytical solution in Appendix A. However, this limits the shape of disturbance to that of a perfect impulse and requires the system to be at steady-state from the start of simulation, and therefore the former approach is used for the broader numerical solution.

It should be noted that the particular solutions of interest are in response to pure water and pure solute disturbances, with the appreciation that a mixture thereof can be achieved through adding the results in appropriate proportion (as long as the system is linear).

The solute outflow depends on the water outflow and tank concentration according to Equation 4.5 and the water outflow rate is simply Equation 4.6 (in this case), where Q_{ss} is $Q_{in,\infty}$ or Q at long-term steady-state = baseline inflow.

$$\dot{N}_{s,out} = Q_{out} C_{tank} \tag{4.5}$$

$$Q_{out} = Q_{ss} \tag{4.6}$$

The inflow and outflow concentrations follow from the usual definition of concentration as amount/volume and are calculated according to Equations 4.7 and 4.8, respectively.

$$C_{in} = \frac{\dot{N}_{s,in}}{Q_{in}} \tag{4.7}$$

$$C_{out} = \frac{\dot{N}_{s,out}}{Q_{out}} \tag{4.8}$$

Through appropriate substitution, the coupled first order linear ODEs follow in Equations 4.9 and 4.10 (written in standard linear form in Appendix A.4.1). Solution depends on

the choice of disturbance.

$$\frac{dV}{dt} = Q(t) - Q_{ss} \tag{4.9}$$

$$\frac{dN_s}{dt} = \frac{dC_{tank}V}{dt} = \dot{N}_{s,in}(t) - C_{tank}(t)Q_{ss} \tag{4.10}$$

The mean residence time in the tank can be quantified by the fraction $\frac{V}{Q}$ [66], where V refers to the tank volume (i.e. total body water in a simple organism or smaller compartment in a more sophisticated organism) and Q the inflow rate to the tank (i.e. influx of water into an organism), which, by extension, can be said to match the outflow rate from the tank (i.e. efflux of water from the organism) through mass balance requirements. It is of interest to see how the tank quantities respond to changes in this ratio.

The model parameters are summarised in Table 4.1.

Table 4.1 Design 1 Model Parameters

Parameter	Value
Baseline water inflow (ml/hr)	100
Baseline solute inflow (mosm/hr)	28.1
Steady-state volume (ml)	10 - 100 000

4.2 Results and Discussion

Simulation in Vensim (by Ventana Systems, Inc.), the System Dynamics software of choice, solves the ODEs numerically using Euler integration, and has been used for generation of model output. A sampling period of 28.125 seconds (2^{-7} hr) is considered small enough to capture the dynamics of the system response, especially considering the high granularity of the model.

Figure 4.3 shows tank volume, concentration and amount of solute as a function of time in response to a positive or negative finite-duration water inflow pulse of size 10 % (above a baseline of 100 ml/hr) and duration 10 min (short when compared to a mean residence time in the tank of $\frac{V}{Q} = \frac{1000\ ml}{100\ ml/hr} = 10\ hr$). It is clear that water in the tank is retained (i.e. the volume expands by an amount equal to the area under the pulse, i.e. $(0.1)(100\ ml/hr)(\frac{10}{60}\ hr) = 1.67\ ml$) or lost (i.e. the volume contracts by the same amount) relative to an initial value of 1000 ml, respectively. Noteworthy is the linear increase or

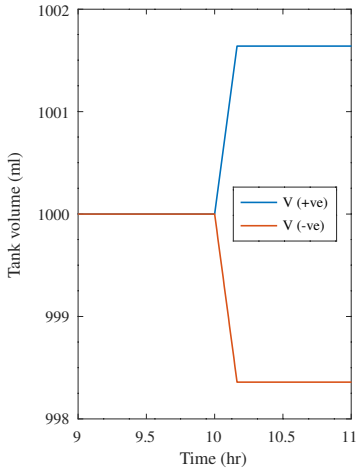
accumulation in V over the 10 minute duration of pulse application (unlike a step response in the case of an ideal impulse input). Solute accumulates or is depleted, respectively, in order for equilibrium to be re-established (a requirement for mass balance to be maintained). The tank concentration recovers back to a steady-state of 0.281 mosm/ml slowly (95 % recovery after approximately 30 hours) from being diluted or concentrated, respectively.

In comparison, Figure 4.4 shows there is no change in the tank volume of 1000 ml in response to a positive or negative finite-duration solute inflow pulse of size 10 % (above a baseline of 28.1 mosm/hr) and duration 10 min. The tank concentration returns to a steady-state of 0.281 mosm/ml slowly, as an excess of solute is washed out or a lack of solute is recovered (95 % recovery occurs after approximately 30 hours).

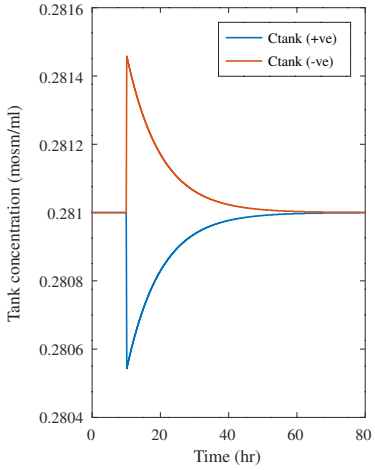
The shapes of the responses are identical whether the input disturbance is positive or negative because the model is linear. Therefore, it is considered unnecessary to simulate both cases in future investigations as long as the model remains linear. Due to linearity, the size of the input pulse is limited only by the effect it has on the volume and concentration in a biological context. Since single cells can shrink or swell substantially [1] and soft-bodied animals can withstand a change in volume of up to 80% [4], a pulse height of 10% above baseline water or solute inflow rate for a duration of 10 minutes produces a relatively small change in the tank volume and/or concentration, which remains well within the application limits. This is kept the same throughout all the designs to allow for comparison of results. The contribution of the finite-duration of the pulse to the curves is in evidence as a steep (not vertical) slope but this is considered small with respect to the dynamics of the system.

Because major concerns faced by the excretory system of any animal (be it simple or complex, conformer or regulator) are peak magnitude and settling time (of body water volume and concentration) following a water and/or solute inflow disturbance, these were chosen to parameterise the system response. It is acknowledged that such parameters do not fully describe the system response, or provide an exact fit to the volume and concentration curves, however, they do provide for curve sketching and comparison between curves. Such level of analysis has been chosen to match the level of modelling; high-level and abstract. Limitations are acknowledged but the benefits in terms of this model's development (most importantly, catering to future increased complexity and alignment with the biology) are felt to support such an approach to parameterisation of the model.

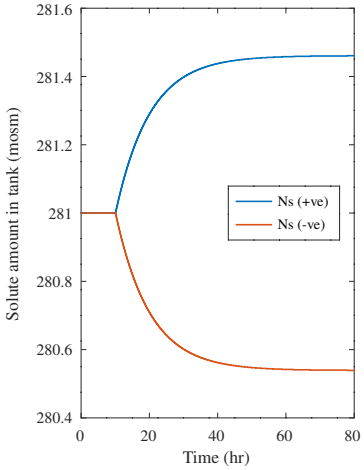
Settling time is commonly used in control engineering to quantify a time response [2]. For example, 95 % settling time or $t_{s,95\%}$ is the time taken for a response to settle to within 5 % of steady-state. Settling time is considered a broader concept than a time constant, not limited to first order responses. The settling time has been measured from the time of peak



(a) Tank volume

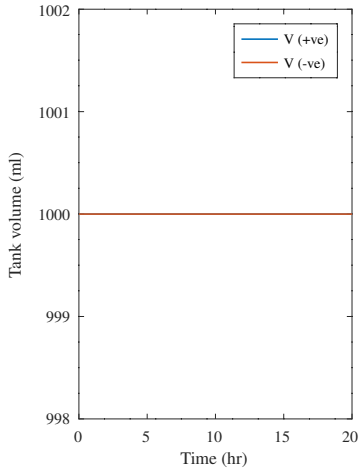


(b) Tank concentration

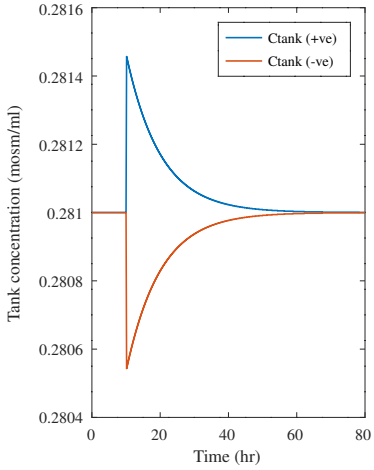


(c) Amount of solute

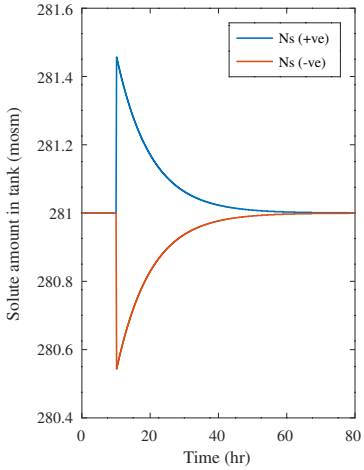
Fig. 4.3 Design 1 (a) Tank volume, (b) tank concentration and (c) amount of solute in the tank versus time graphs in response to positive and negative 10 % (above a baseline of 100 ml/hr) finite-duration (10 min) water pulses at t = 10 hrs for $\frac{V}{Q} = 10\ hr$



(a) Tank volume



(b) Tank concentration



(c) Amount of solute

Fig. 4.4 Design 1 (a) Tank volume, (b) tank concentration and (c) amount of solute in the tank versus time graphs in response to positive and negative 10 % (above a baseline of 28.1 mosm/hr) finite-duration (10 min) solute pulses at t = 10 hrs for $\frac{V}{Q} = 10\ hr$

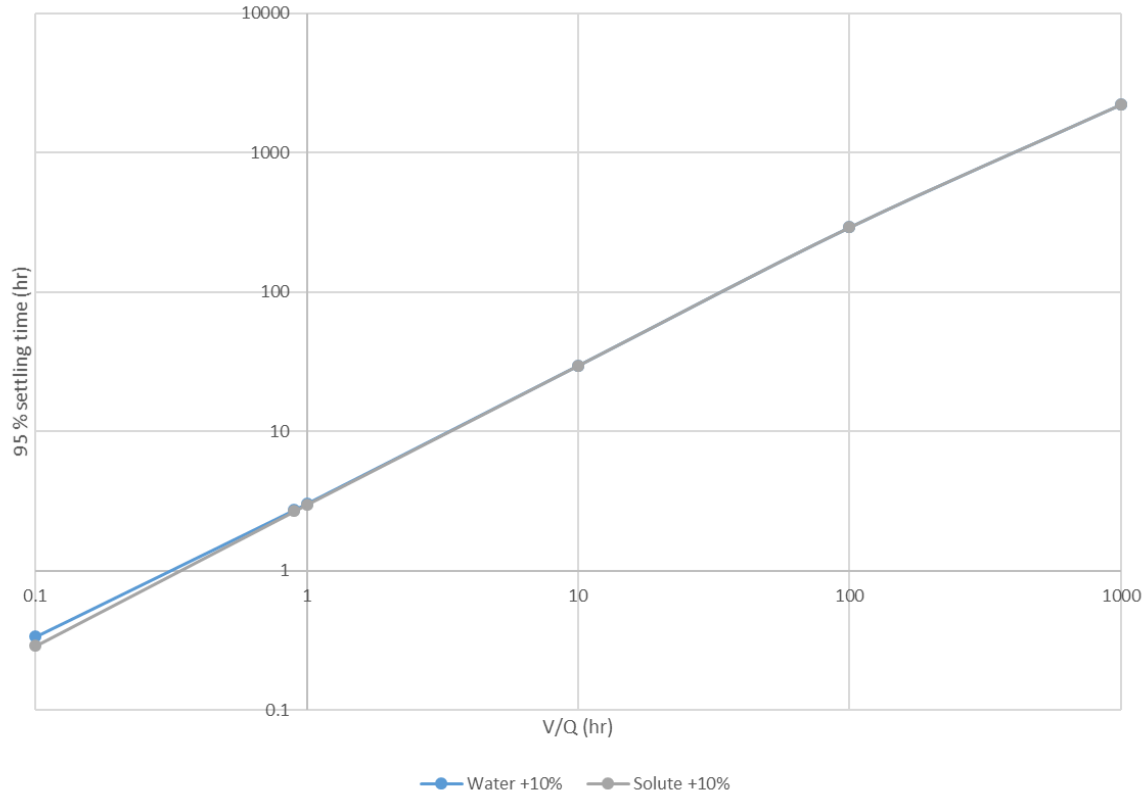


Fig. 4.5 Design 1 Graph of tank concentration 95 % settling time as a function of $\frac{V}{Q}$; in response to positive 10 % (above baseline) 10 minute duration pulses in water and solute inflow

magnitude rather than the start of the disturbance (in some cases these may coincide) but considering the long tail of the curves, these values do not differ significantly.

When simulations were run for a range of $\frac{V}{Q}$ by varying the volume from 10 ml - 100 litres and keeping inflow rate the same (baseline 100 ml/hr and 28.1 mosm/hr, with a 10 % 10 minute pulse of water or solute superimposed in the case of a water or solute disturbance, respectively), the tank concentration's 95 % settling time is seen to depend on $\frac{V}{Q}$ linearly, with a positive slope of 1, as illustrated in Figure 4.5. Deviations from the straight-line trend at small $\frac{V}{Q}$ are artefacts, introduced by the finite duration of the input pulse (i.e. 10 min = 0.167 hr) being of the same order of magnitude as $\frac{V}{Q} < 1$) and do not reflect the ideal behaviour of the system at low residence time. This illustrates an important limiting condition on the model when implemented with a finite-duration input (e.g. validity holds when $\frac{V}{Q}$ exceeds the finite-duration of the input by approximately an order of magnitude).

Instead of directly considering peak tank volume and concentration magnitude responses following water and/or solute disturbances as another modelling parameter of interest, they

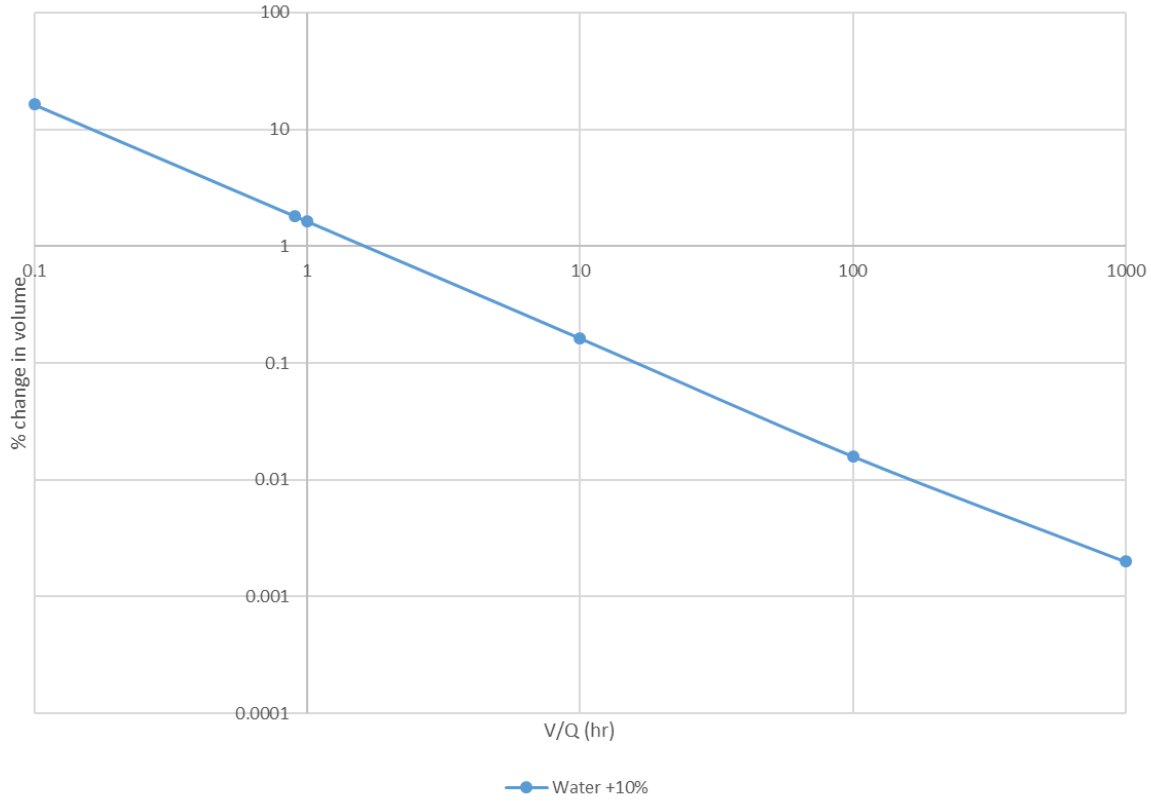


Fig. 4.6 Design 1 Graph of relative percentage change in tank volume magnitude as a function of $\frac{V}{Q}$; in response to positive 10 % (above baseline) 10 minute duration pulses in water inflow

were normalised with respect to their corresponding steady-state values to allow for easier comparison. Such relative percentage change in tank volume and concentration magnitudes following water and/or solute inflow disturbance depend on $\frac{V}{Q}$ linearly, with a slope of -1 (discounting artefacts at small $\frac{V}{Q}$), as shown in Figures 4.6 and 4.7, respectively. These observations follow directly from the fact that the water inflow rate (and therefore change in V (i.e. ΔV)) is held constant and as V increases, the relative change in V (i.e. $\frac{\Delta V}{V}$) and relative change in tank concentration (i.e. $\frac{\Delta C}{C}$) both decrease by the same relative amount.

The simulation results are obvious when the analytical solution (Appendix A.5.1) is considered. It must be emphasised that the numerical and analytical solutions were set up differently but the solutions remain the same (assuming the duration of the pulse is small compared to the dynamics of the system); instead of considering finite-duration pulses superimposed on baseline inflow as for the simulations, the inflow rates were held constant and the initial conditions changed to represent impulse disturbances analytically.

For a pure water impulse disturbance, the tank volume and concentration responses are summarised in Equations 4.11, and 4.12, respectively, where C_0 refers to the initial concen-

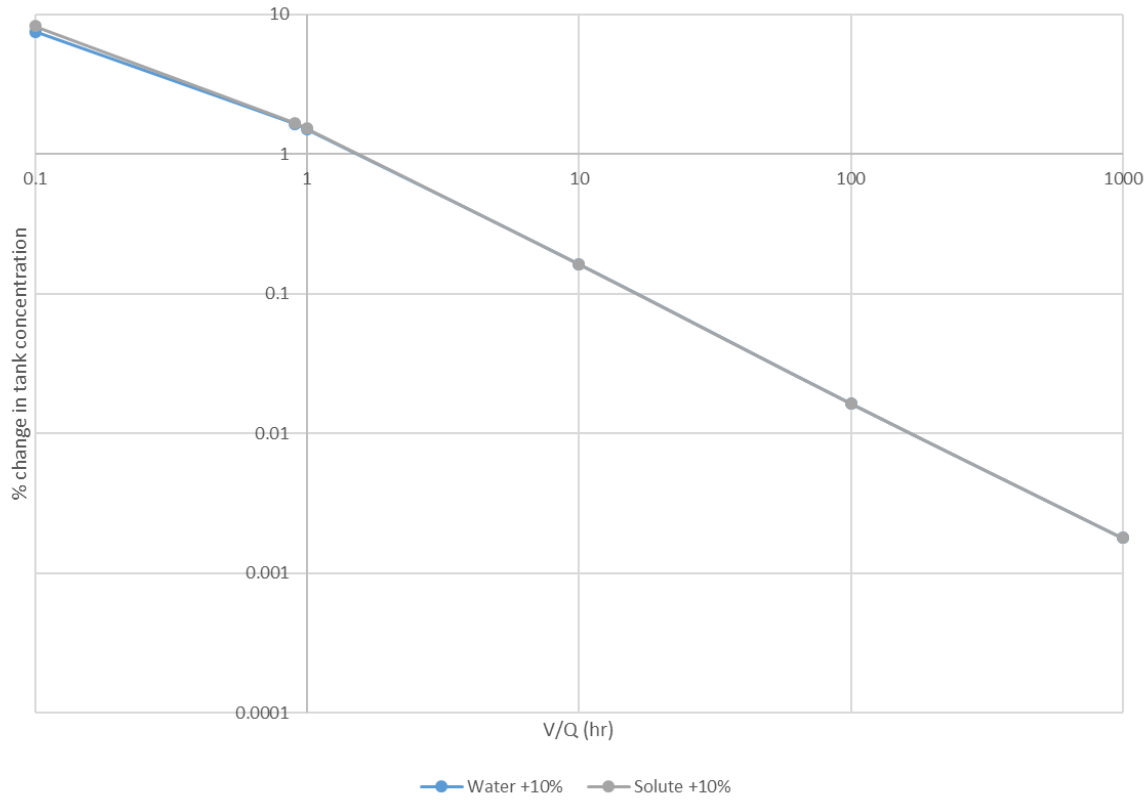


Fig. 4.7 Design 1 Graph of relative percentage change in tank concentration magnitude as a function of $\frac{V}{Q}$; in response to positive 10 % (above baseline) 10 minute duration pulses in water and solute inflow

tration in Equation 4.13, and τ represents the tank mean residence time in Equation 4.14.

$$V(t) = V_{ss} = V_{dss} + a \tag{4.11}$$

$$C(t) = C_{ss}\left[1 - \left(1 - \frac{C_0}{C_{ss}}\right)e^{\frac{-t}{\tau}}\right] \tag{4.12}$$

$$C_0 = \frac{V_{dss}}{V_{dss} + a}C_{ss} \tag{4.13}$$

$$\tau = \frac{V_{ss}}{Q_{ss}} = \frac{V_{dss} + a}{Q_{ss}} \tag{4.14}$$

It is clear that $V(t)$ remains constant at an elevated (or reduced) volume for all time, where a corresponds to the volume of water delivered (or removed in the case of a negative a) by the water pulse relative to V_{dss}, the desired steady-state (e.g. $V_{dss} = 1000$ ml in this case). $C(t)$ involves exponential recovery to steady-state at a rate dependent on $\frac{V_{ss}}{Q_{ss}}$. For a positive inflow pulse of water, $a > 0$ and $C_0 < C_{ss}$, and vice versa.

Similarly, for a pure solute impulse, the volume and concentration responses are expressed in Equations 4.15 and 4.16, where τ again represents the tank mean residence time and is detailed in Equation 4.17.

$$V(t) = V_{ss} \tag{4.15}$$

$$C(t) = C_{ss} + \frac{b}{V_{ss}}e^{\frac{-t}{\tau}} \tag{4.16}$$

$$\tau = \frac{V_{ss}}{Q_{ss}} \tag{4.17}$$

b corresponds to the amount of solute delivered (or removed in the case of a negative b) by the solute pulse. For a positive inflow pulse of solute, $b > 0$ and $C(0) > C_{ss}$, and vice versa. It is clear that $V(t)$ is not affected by a pure solute disturbance and remains constant for all time. $C(t)$ involves exponential recovery to steady-state at a rate dependent on $\frac{V_{ss}}{Q_{ss}}$.

The observed straight line relationship between 95 % settling time and $\frac{V}{Q}$ is obvious as $\frac{V}{Q}$ relates directly to the solute concentration's mean residence time in the tank (Equations 4.14

(with small a) and 4.17), and as V increases with constant Q, τ increases, where τ is related to the 95 % settling time by Equation 4.18.

$$t_{s,95\%} = 3\tau \tag{4.18}$$

Therefore, the results show that the same disturbance superimposed on baseline inflow rate has a smaller magnitude effect (tank volume or concentration) as $\frac{V}{Q}$ increases but also takes longer to recover (tank concentration in particular, as tank volume does not recover).

4.3 Biological application

In summary, the results show that the model responds differently to disturbances in water inflow rate compared to solute inflow rate. Following a pulse in the water inflow rate, the volume of water in the tank is increased by the amount delivered by the pulse, while the concentration of solute in the tank is instantaneously (for the duration of the pulse) decreased and slowly recovers back to the steady-state concentration of the feed (taking approximately 30 hours for a 95 % recovery). An impulse in the solute flow rate had no effect on the volume of water in the tank but instantaneously (for the duration of the pulse) increased the solute concentration in the tank by the amount delivered by the pulse, and slowly recovers back to the steady-state inlet concentration (95 % recovery after approximately 30 hours). In addition, the tank "mean residence time" or $\frac{V}{Q}$ is seen to affect the size of response (for tank volume and concentration), and recovery time (for tank concentration) for the same impulse disturbance.

Such a simple approach would be sufficient to describe an organism's excretory system if either the environment remains constant and there are only ever small disturbances above baseline (the case for most marine invertebrates and a few vertebrates, who are conformers but with a narrow tolerance range, i.e. stenohaline [4]), or the organism can withstand a wide range of operation (i.e. osmoconformer) and can expand or contract to accommodate more or less water volume, respectively. "Some slugs and snails, and littoral molluscs such as limpets and chitons, can tolerate 35–80% water loss, causing substantial shrinkage of the body" [4]. Such soft bodied animals have no means of protection against swelling and shrinking (unlike those with hard outer layers or exoskeletons) and are therefore more likely to favour behavioural strategies (such as avoidance of fluctuations in the environment) over acclimation in order to survive [4].

It is known that the unicellular amoeba or single cells that form part of organ systems (such as red blood cells) shrink or swell in response to a change in the tonicity of the

environment [1]. However, the presence of negative feedback helping to regulate the volume, water vacuoles and spongey cytoskeleton [69] cannot be explained by this simple model. This emphasises that even in the case of single cells, volume change is a problem and some kind of basic volume control mechanism is needed.

A disadvantage of such a simple design is that although the tank concentration does return to a steady-state value following a disturbance in inflow, the response is slow, especially at high tank mean residence time (i.e. $\frac{V}{Q}$). For example, consider urea distribution throughout 42 litres of total body water in an average 70 kg human with 100 ml/hr urine flow rate [1]. If such a simple model were valid in describing urea excretion in humans, it would imply a mean residence time of $\frac{V}{Q} = \frac{42000\ ml}{100\ ml/hr} = 420\ hr$, whereas it has been observed in normal functioning humans that, depending on the size of dose of protein, the majority is excreted within 24 to 48 hours [70]. Therefore, there exists a need for some aspect of control to be added to the model to speed it up if a faster response is required.

The design does emphasise the innate buffering capacity provided by high $\frac{V}{Q}$. A tank with a smaller volume has a shorter residence time [66] (presuming Q remains constant) and its solute concentration responds faster to the same disturbance compared to a tank of a larger volume, i.e. the smaller $\frac{V}{Q}$ is more sensitive (producing a greater change in output relative to input than a less sensitive system, as defined in Chapter 2). The implication for animals with a small $\frac{V}{Q}$ is that they have higher sensitivity to inputs and are therefore less inherently stable than animals with bigger $\frac{V}{Q}$, simply due to their relative $\frac{V}{Q}$. In simple animals whose integument is semi-permeable to the environment and therefore plays an excretory role, net inflow rate Q depends on surface area. Therefore, the decreasing sensitivity noted as $\frac{V}{Q}$ increases is related to decreasing sensitivity observed in animals with small surface area relative to volume [4]. However, the $\frac{V}{Q}$ sensitivity observation is limited to simple animals as "water use in terrestrial mammals scales allometrically with body size" (under non-extreme environmental conditions and excluding marsupials) [71]. This means that $\frac{V}{Q}$ is constant for terrestrial mammals, all of whom have adapted to living on land and possess sophisticated kidneys.

All else being equal, the $\frac{V}{Q}$ argument could be used to infer why human babies are more sensitive to changes in their environment (i.e. inputs) than adults. The Holliday-Segar method [72], commonly used in pharmacotherapy to estimate the maintenance intravenous (IV) fluid requirements in hospitalised children [73], provides a direct means of exploring the relationship between V and Q across the age spectrum of children. Very simply, the method provides a relationship between the weight of a child and the rate of IV fluid administration required to balance fluid losses [72]. For the first 10 kg, 100 ml/kg/day are to be administered, for the next 10 kg, an additional 50 ml/kg/day are to be administered, and beyond 20 kg, an

additional 20 ml/kg/day are to be administered [72]. Because the total body water makes up a large fraction of the body weight (admittedly changing a lot from birth (approximately 80 %) until the age of one year (approximately 60 %) [74], which is similar to the adult range of 50 - 60 % [74]), the three regions of steadily increasing administration rates remain valid when comparing volume (V) and flow rate (Q) rather than body weight and flow rate. Therefore, it can be seen that a newborn to 1 year old (whose body weight may vary, for example, from 3.5 kg to 10 kg) has a $\frac{V}{Q}$ between 8 and 6 days, which is less than half the 17.5 days of a 70 kg adult (assuming an average inflow rate that matches an average urine flow rate of 100 ml/hr [1] for mass balance to be maintained). This means that the same relative input will affect a baby more (i.e. they are more sensitive) because they lack the additional buffering capacity inherently provided by a bigger $\frac{V}{Q}$. And yet, drug dose in newborns is often calculated using extrapolation from adults and older children [75], an approach appreciated to be oversimplified and erroneous [76]. According to DeRose et al., "Neonates exhibit a higher variability in drug exposure, drug efficacy and toxicity than adults" [77]. As an infant ages, its V increases relative to Q, and this model suggests that the child's sensitivity to the environment (including drugs) decreases as a result (and not necessarily simply due to maturation of the kidney as suggested by [73, 76, 77]).

It is seen that such a simple continuously-stirred tank model is able to self regulate with regard to concentration (albeit slowly) but not volume, and this, therefore, provides a challenge for the second iteration in design.

Chapter 5

Design 2: Pressure feedback

5.1 Model setup

In order to address the lack of volume regulation in the previous model, pressure feedback is implemented on the water outflow such that the rate depends directly on additional or reduced volume of water in the tank compared to long-term steady-state (and volume is directly related to pressure [1]) according to Equation 5.1.

$$Q_{out} = Q_{ss} + m(V(t) - V_{ss}) \tag{5.1}$$

m is a proportionality constant and can be considered the gradient of the $Q_{out} - V$ characteristic, while V_{ss} refers to the long-term steady-state volume.

Figure 5.1 details the line diagram, which has essentially remained the same as in Figure 4.1 of previous Chapter 4, except for addition of a lid to the tank to represent the presence of some kind of feedback on the tank volume. Figure 5.2 shows the updated level-rate diagram.

The defining Equations 3.1 and 3.2, remain the same, repeated in Equations 5.2 and 5.3, respectively, with the solute outflow still depending on the water outflow and tank concentration according to Equation 4.5, repeated in Equation 5.4 for ease of reference.

$$\frac{dV}{dt} = Q_{in} - Q_{out} \tag{5.2}$$

$$\frac{dN_s}{dt} = \frac{dC_{tank}V}{dt} = \dot{N}_{s,in} - \dot{N}_{s,out} \tag{5.3}$$

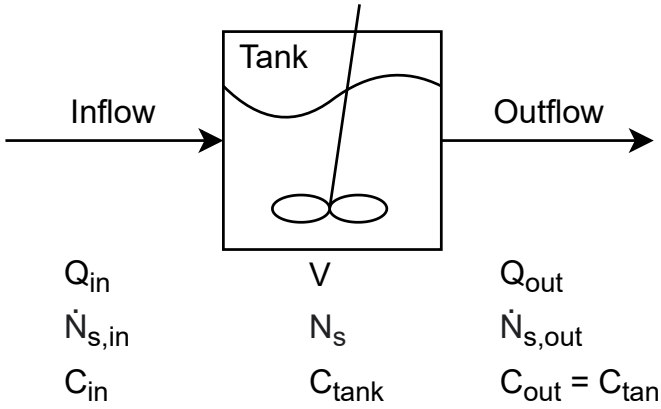


Fig. 5.1 Line diagram for Design 2: Pressure feedback

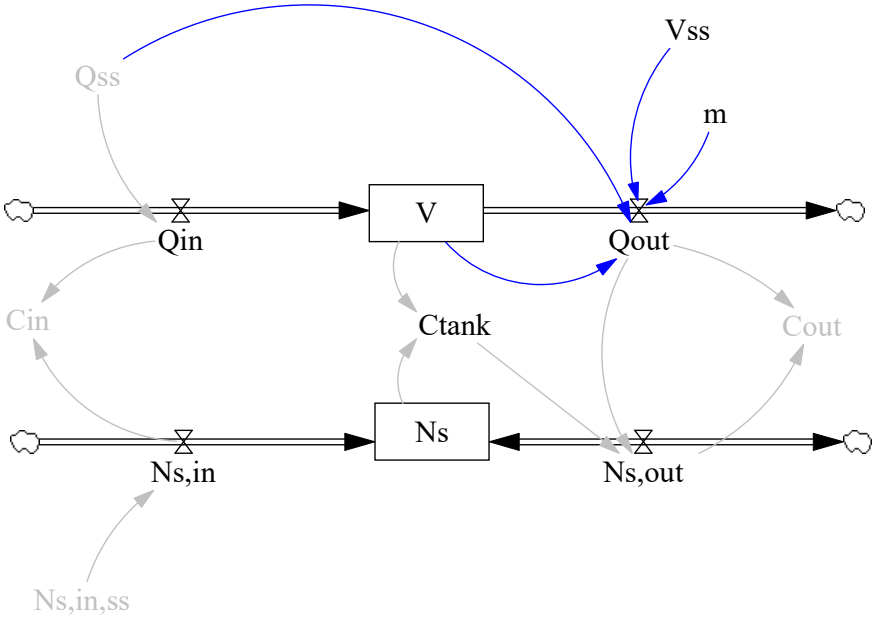


Fig. 5.2 Level-rate diagram for Design 2: Pressure feedback

$$\dot{N}_{s,out} = Q_{out} C_{tank} \tag{5.4}$$

No other changes have been made to the model. The coupled ODEs follow in Equations 5.5 and 5.6 (Appendix A.4.1).

$$\frac{dV}{dt} = Q(t) - (Q_{ss} + m(V(t) - V_{ss})) \tag{5.5}$$

$$\frac{dN_s}{dt} = \frac{dC_{tank}V}{dt} = \dot{N}_{s,in}(t) - C_{tank}(t)(Q_{ss} + m(V(t) - V_{ss}) \tag{5.6}$$

The model parameters are summarised in Table 5.1.

Table 5.1 Design 2 Model Parameters

Parameter	Value
Baseline water inflow (ml/hr)	100
Baseline solute inflow (mosm/hr)	28.1
Steady-state volume (ml)	10 - 100 000
m (1/hr)	0.1 - 10

5.2 Results and Discussion

Simulation results in response to positive finite-duration water and solute inflow rate pulses of size 10 % (above baseline) and duration 10 min (short when compared to a mean residence time in the tank of $\frac{V}{Q} = \frac{1000\ ml}{100\ ml/hr} = 10\ hr$) for a range of m are illustrated in Figures 5.3 and 5.4 for tank volume, concentration, amount of solute, water outflow rate and solute outflow rate. It is clear in Figure 5.3 that the tank volume recovers to a steady-state of 1000 ml long-term (as desired) at a rate dependent on m (i.e. the gradient of the $Q_{out} - V$ characteristic in Equation 5.1), faster for bigger m. The peak value reached by the tank volume differs slightly depending on m due to concomitant water removal while the finite-duration pulse is being applied. Such an effect is seen to worsen as m increases. The amount of solute in the tank is seen to be affected by a water pulse (except at $m = 0.1$) and the rate of recovery back to a steady-state of 28.1 mosm depends on the size on m, faster for bigger m. The tank concentration recovers back to a steady-state of 0.281 mosm/ml slowly but at the same rate no matter the size of m (95 % recovery after approximately 30 hours).

In comparison, Figure 5.4 shows that tank volume, concentration, amount of solute, water outflow rate and solute outflow rate remain the same no matter the value of m. In fact, the

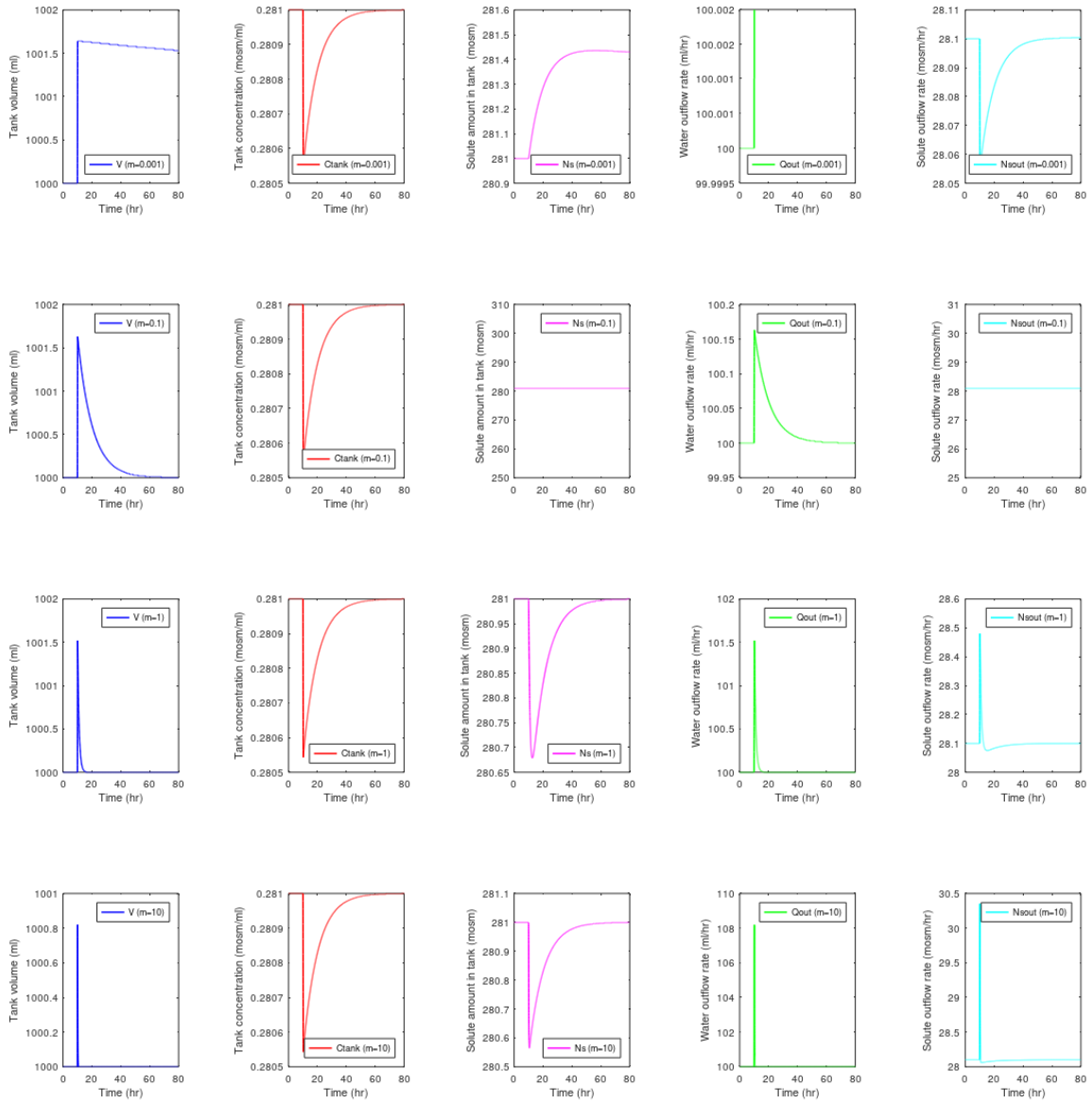


Fig. 5.3 Design 2 Tank volume (blue), concentration (red), amount of solute (magenta), water outflow rate (green) and solute outflow rate (cyan) versus time graphs in response to positive 10 % (above a baseline of 100 ml/hr) finite-duration (10 min) water pulses at t = 10 hrs for $\frac{V}{Q} = 10\ hr$ and a range of $m = 0.001, 0.1, 1, 10$

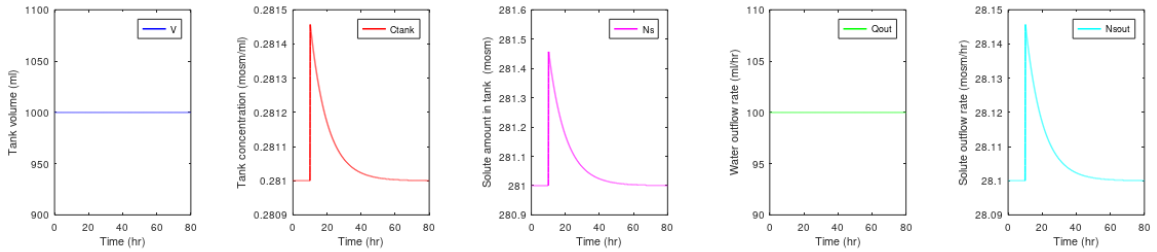


Fig. 5.4 Design 2 Tank volume (blue), concentration (red), amount of solute (magenta), water outflow rate (green) and solute outflow rate (cyan) versus time graphs in response to positive 10 % (above a baseline of 28.1 mosm/hr) finite-duration (10 min) solute pulses at t = 10 hrs for $\frac{V}{Q} = 10\ hr$, identical for $m = 0.1, 1, 10$

response to a solute pulse is observed to be independent of m and identical to that of Design 1 in Chapter 4; there is no change in the tank volume in response to a positive finite-duration solute inflow pulse no matter the value of m, and the amount of solute in the tank and tank concentration return to steady-state after approximately 30 hours.

Comparing tank volume and concentration 95 % settling times as a function of $\frac{V}{Q}$ for a variety of values for m in response to a finite-duration water inflow pulse disturbance, yields the graph in Figure 5.5. It is observed that as m increases, the tank concentration and volume curves intersect at progressively smaller $\frac{V}{Q}$. At small values of $\frac{V}{Q}$ (i.e. less than that corresponding to the point of intersection in each case of m), tank concentration settling time is faster than that of tank volume, while for greater values of $\frac{V}{Q}$, tank volume settling time remains the same (for each value of m) but tank concentration settling time is slower.

As noted in Design 1 (Section 4.2), the relative change in tank volume and concentration magnitude to pulse inflow rate disturbances (a water pulse in the case of tank volume response, and water or solute pulses in the case of tank concentration response) depend on $\frac{V}{Q}$ linearly, with a slope of -1, (illustrated in Figures 5.6 and 5.7, respectively). It is noteworthy that in Figure 5.6, it appears that m has a downward linear trend on relative change in tank volume magnitude (not present in tank concentration, Figure 5.7).

As for Design 1, the analytical solution is straightforward (Appendix A.5.2) and has been included to supplement the numerical simulation findings. Considering a pure water impulse disturbance (quantified by height a), the volume and concentration responses are expressed in Equations 5.7 and 5.8, respectively.

$$V(t) = V_{ss} + ae^{-\frac{t}{\tau_V}} \tag{5.7}$$

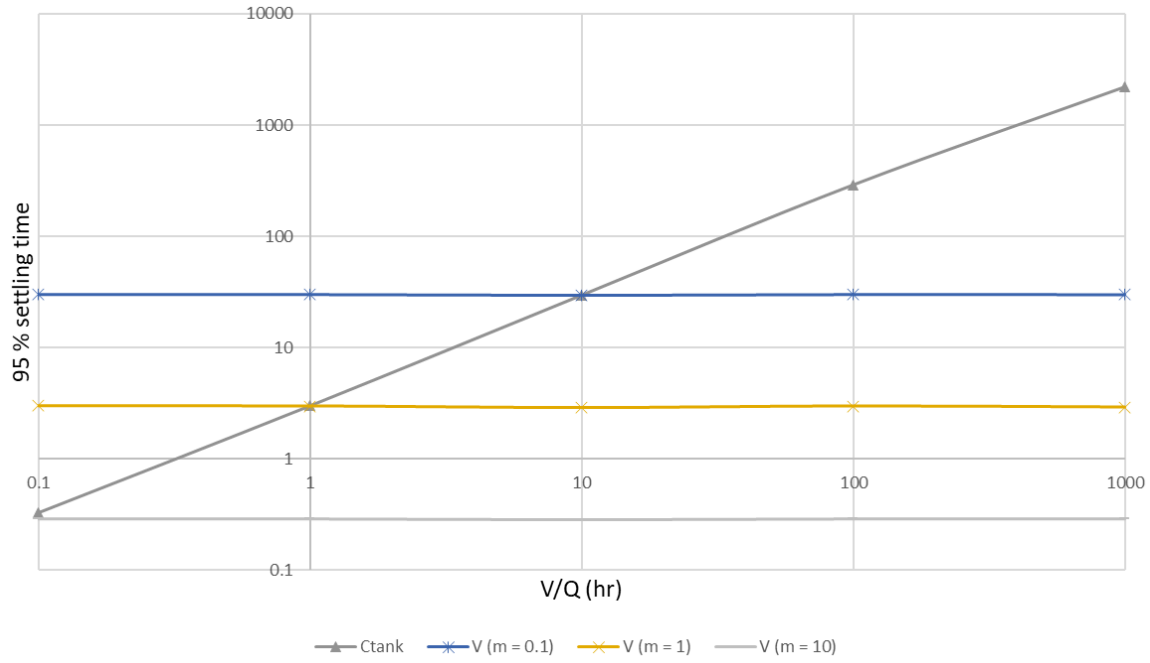


Fig. 5.5 Design 2 Comparison of settling times for volume and tank concentration versus mean residence time in the tank ($\frac{V}{Q}$), at $m = 0.1$, 1, 10, following positive 10% 10 minute duration pulse disturbances in water inflow

$$C(t) = C_{ss}\left[1 - \left(1 - \frac{C_0}{C_{ss}}\right)\left(\frac{V_{ss} + ae^{-\frac{t}{\tau_V}}}{V_{ss} + a}\right)^{-\frac{\tau_V}{\tau}} e^{\frac{-t}{\tau}}\right] \tag{5.8}$$

τ_V represents the time constant of the water outflow rate or "valve" and is related to m by Equation 5.9.

$$\tau_V = \frac{1}{m} \tag{5.9}$$

τ represents the tank mean residence time (Equation 5.10) while C_0 represents the initial tank concentration at the instant the pulse enters the system. For a positive inflow pulse of water, $a > 0$ and $C_0 < C_{ss}$, and vice versa.

$$\tau = \frac{V_{ss}}{Q_{ss}} \tag{5.10}$$

$$C_0 = \frac{V_{ss}}{V_{ss} + a} C_{ss} \tag{5.11}$$

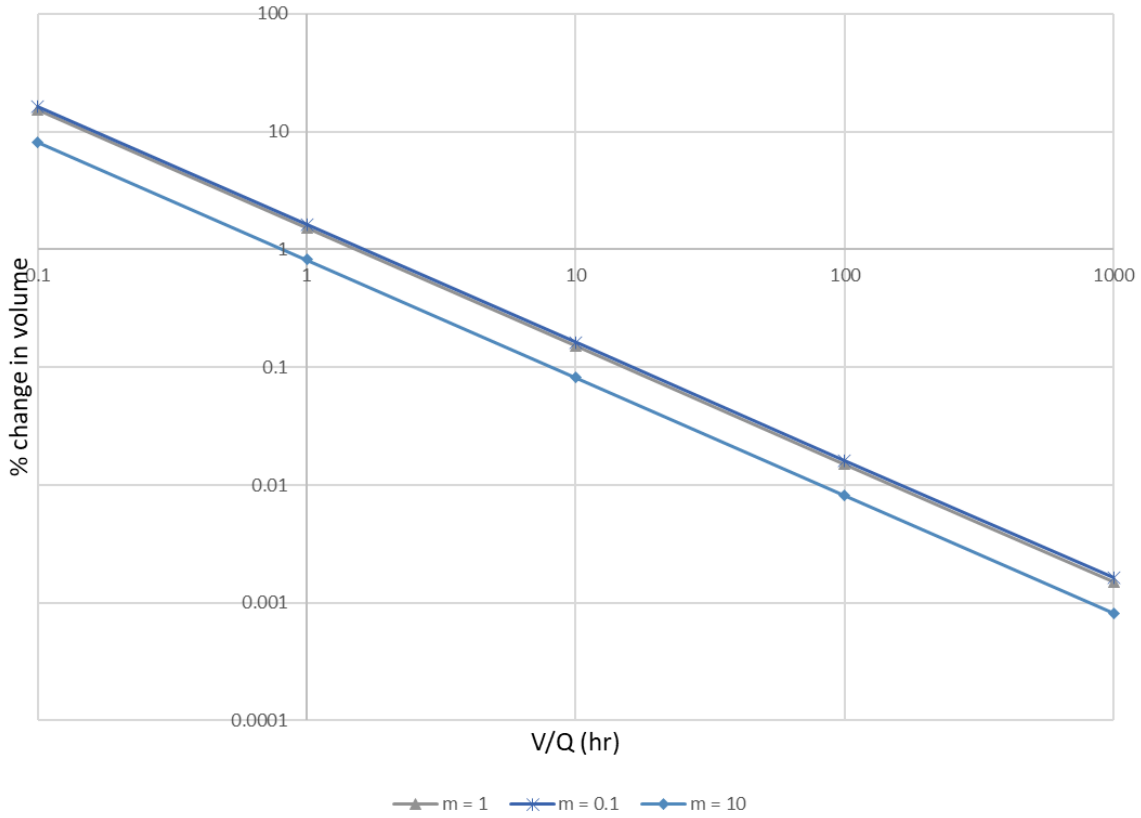


Fig. 5.6 Design 2 Comparison of relative change in tank volume versus mean residence time in the tank ($\frac{V}{Q}$) at m = 0.1, 1, 10; following positive 10% 10 minute duration pulse disturbances in water inflow

Equation 5.7 confirms that the tank volume recovers exponentially in response to a transient pulse change in water inflow and that the rate of recovery depends only on m. In the case of a first order exponential response to an impulse, τ_V is related to a more general 95 % settling time for volume, $t_{s,V,95\%}$, by Equation 5.12.

$$t_{s,V,95\%} = 3\tau_V \tag{5.12}$$

If the finite-duration of the input pulse is considered small relative to the system dynamics, then $t_{s,V,95\%} \approx 3\tau_V$ with small relative error (e.g. in response to a $+10$ % 10 min duration water pulse at $m = 1$, $t_{s,V,95\%} = 2.875$, which differs from $3_{\tau V}$ by 3.8%). Equation 5.8 details the tank concentration response as the sum of first order exponential terms; however, in this case, τ_V cancels and only τ determines the rate of concentration response. It is clear that the time constants τ and τ_V (or likewise, their related settling times) control the dynamics of the system.

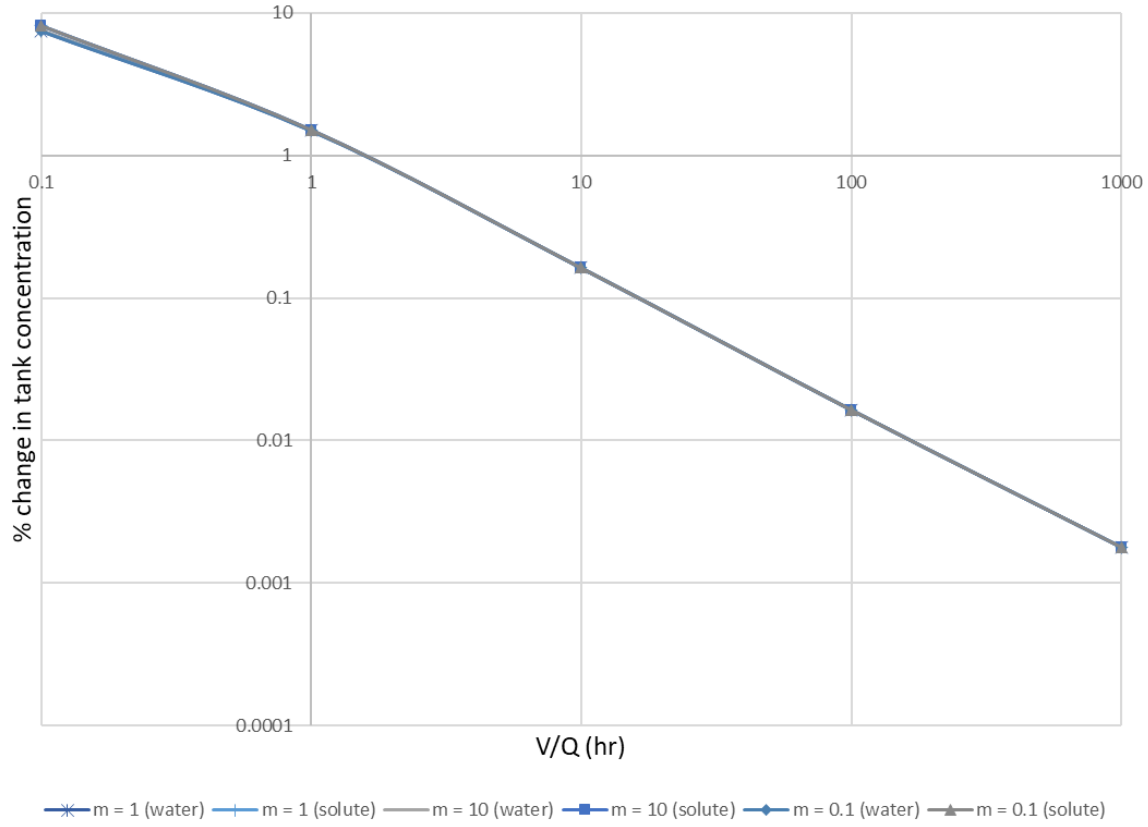


Fig. 5.7 Design 2 Comparison of relative change in tank concentration versus $\frac{V}{Q}$ at $m = 0.1$, 1, 10; following positive 10% 10 minute duration pulse disturbances in water or solute inflow

The point of intersection noted earlier in Figure 5.5, is simply a point at which the response time of the "volume adjustment" is equal to the response time of the concentration (in other words, $\tau_V = \tau$ or $m = \frac{1}{\tau} = \frac{Q_{ss}}{V_{ss}}$ in this case). At each point of intersection, $N_{s,tank}$ and $N_{s,out}$ remain constant for all time, as seen in Figure 5.3 for $\frac{V}{Q} = 10\ hr$ and $m = 0.1\ hr^{-1}$.

The downward linear trend of m on relative change in tank volume magnitude noted from simulation results in Figure 5.6, is in fact an artefact introduced at high m when correspondingly small τ_V is of the order of (or smaller than) the finite duration of the input pulse. It does however, highlight important limiting conditions related to the value of m. When the gradient of the $Q_{out} - V$ characteristic (i.e. m) is steep, $m \to \infty$, $\tau_V \to 0$, the "valve" response is so fast that the volume change is instantaneous and the volume remains constant (equatable to a constant-volume continuously-stirred tank where the inflow and outflow rates match [66]). Therefore, a high value of m can be said to result in low tank volume magnitude sensitivity to (relatively long) finite-duration inflow disturbance. In contrast, when $m \to 0$, τ_V is theoretically undefined, the valve does not respond and the volume magnitude change never recovers (as in Design 1 in Chapter 4). A small value of m does not affect tank

volume magnitude sensitivity as τ_V is long relative to a (relatively short) finite-duration inflow disturbance. There is no corresponding effect of m on relative change in tank concentration because its dynamic recovery depends on $\frac{V}{Q}$ alone (Equation 5.10 in Equations 5.8 and 5.14).

Now, considering a pure solute impulse disturbance (quantified by height b), and noting that the tank volume remains constant for all time (Equation 5.13), the tank concentration response is identical to that in Equation 4.16 of Design 1 in Chapter 4, repeated in Equation 5.14 for ease of reference, where τ represents the tank mean residence time and matches that detailed in Equation 5.10. This confirms the conclusion following simulation that the two designs respond identically to a pure solute input.

$$V(t) = V_{ss} \tag{5.13}$$

$$C(t) = C_{ss} + \frac{b}{V_{ss}} e^{\frac{-t}{\tau}} \tag{5.14}$$

5.3 Biological application

Summarising the results briefly, the current design with pressure feedback from the volume in the tank (presumed to be directly related to pressure [1]) to the water outflow rate shows that volume recovery to steady-state following an impulse change in water inflow (or short-duration pulse) is possible and controllable by choosing a particular value for m (i.e. the gradient of the outflow-volume characteristic). However, the design only provides for slow overall regulation with volume and tank concentration recovery to steady-state occurring at different rates (tank concentration recovery depends on $\frac{V}{Q}$). These differences emphasise that the two challenges, volume regulation and osmoregulation, both need to be managed and one does not necessarily follow the other.

An advantage of such a simple design is that, not only is it able to model the negative feedback involved in volume regulation at the level of cells [69] (a shortcoming of the previous design), but it is able to mimic the processes of pressure diuresis and natriuresis as present in low animals such as the hagfish [1]. An excess of water influx causes the volume (and therefore pressure [1]) to increase, which in turn causes the water outflow directly (and solute outflow indirectly) to increase, thereby relieving the excess and returning the volume (and concentration) to the original steady-state. Similarly, low volume results in less water and solute outflow relative to inflow and therefore recovery back to the original steady-state. As a similar process is known to provide the basis of long-term arterial pressure control in

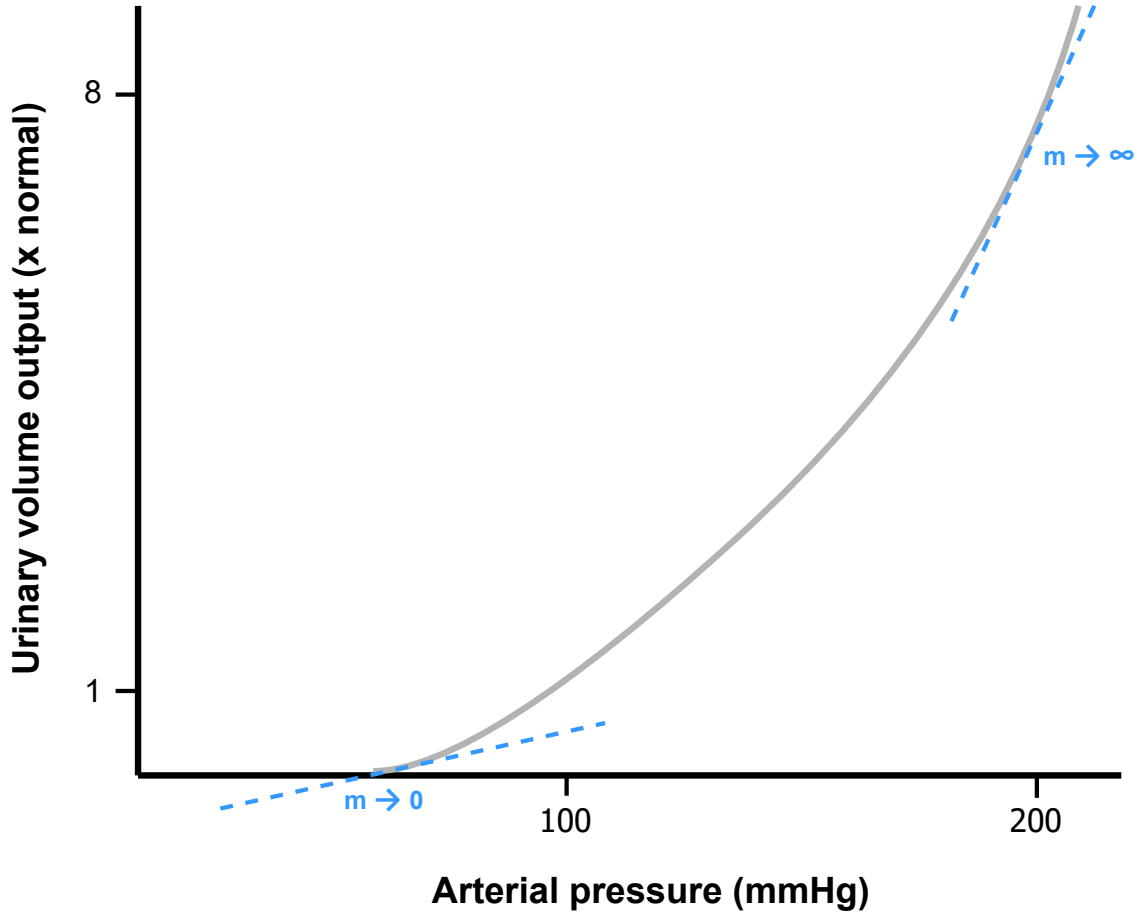


Fig. 5.8 Typical renal function curve adapted from [1] and annotated to show gradients of tangents to the curve at extremes

humans [1], at a high level, this basic negative feedback implementation is presumed to be a sound modelling foundation for volume regulation in higher order animals as well.

The model also provides a possible explanation for the exponential shape of the renal urinary output or renal function curve in humans (a graph of renal output of water and solute versus pressure, encapsulating the processes of pressure diuresis and natriuresis [1]). An example curve has been adapted from [1] and shown in Figure 5.8. The effects of the gradients of the tangents to the curve towards the extremes are considered, thereby enveloping all responses in between (the accuracy of the data [1] does not justify a more elaborate model). Performing such analysis is possible with this model by varying parameter m since it corresponds to the gradient of the $Q_{out} - V$ characteristic, and therefore, by relating volume and pressure directly [1], the renal urinary output curve. From the findings in Section 5.2, a very steep gradient (m$\rightarrow \infty$), which would occur at high pressure or volume, implies almost instantaneous tank volume recovery (and low sensitivity to the finite-duration

input) but does not affect the tank concentration (the dynamics of which depend on $\frac{V}{Q}$ alone). Conversely, a shallow gradient (m$\rightarrow$0), which would occur at low pressure or volume, implies very slow tank volume recovery to steady-state, if at all (consider Design 1 in Chapter 4), (unaffected sensitivity in the case of finite-duration input) and no effect on tank concentration (the dynamics of which are dependent on $\frac{V}{Q}$ alone). At first glance, it seems that a system that is insensitive to disturbances and responds quickly would be ideal in regulating volume and therefore a constant steep gradient is preferable. However, drawing from control theory, the physical implementation needed to achieve a fast damped response generally requires more sophisticated control [2] and energy expenditure. Therefore, implementation of a gradient that varies with the volume (or pressure [1]) exponentially (in the case of the renal function curve in humans) would provide for a more efficient solution - being steeper at occasional high volumes (or pressure) to ensure fast volume recovery to steady-state but shallower at lower volumes (or pressure) where the transient effects are presumably more withstandable.

The current design might suit those osmoconformers able to tolerate a wide ranging environment. For example, euryhaline aquatic animals living in estuaries are able to conform to an environment that constantly fluctuates between freshwater and salt water [4]. However, it must be emphasised that the model in its current form is only able to represent the urinary systems of those animals limited to producing isosmotic urine (i.e. neither dilute nor concentrated relative to blood) because the outflow concentration matches the tank concentration exactly. Therefore, the next challenge is to separate solute from water and create concentrated (or dilute) outflow relative to the tank.

Chapter 6

Design 3: Separation on outflow

Building on the previous design that achieved volume regulation, improved osmoregulation is the goal of this design step. By placing a separation device on the immediate outflow of the tank, it is possible to split the single stream into two streams that differ in the concentration of one or more species. Separation is the job of the excretory system of an animal, performed to different degrees depending on sophistication of the animal and requirement. As mentioned in the model assumptions in Chapter 3, Section 3.3, excretory organ volume is seen to be very small when compared with that of the rest of the body and therefore, it is assumed that the volume of the separator can be considered negligible for the purposes of the model.

6.1 Model setup

Outflow from the system depends on the type of separator present. There are two cases of interest; solute and water separation.

6.1.1 Solute separation

In biological systems, "solute transport occurs both through bulk fluid motion, also known as convection, and by solute diffusion due to the presence of solute concentration gradients" [78]. In addition, "the transport of small ions across the capillary membrane takes place through both convective and diffusive pathways" in a model by Gyenge et al. [46]. Therefore, two means of achieving solute separation are assumed to include convection and diffusion, where convection implies accompaniment of the solute with the bulk flow of water to different degrees depending on the membrane permeability of the separator, while diffusional flux depends on a concentration difference driving force [78] between the tank and outflow concentrations. Assuming the concentration of water can be considered to be constant (which

is reasonable because the contents of the tank are dilute), the only concentration difference driving force that needs to be considered is that of the combined osmotically-active solute.

The tank-separator structure is illustrated in Figure 6.1.

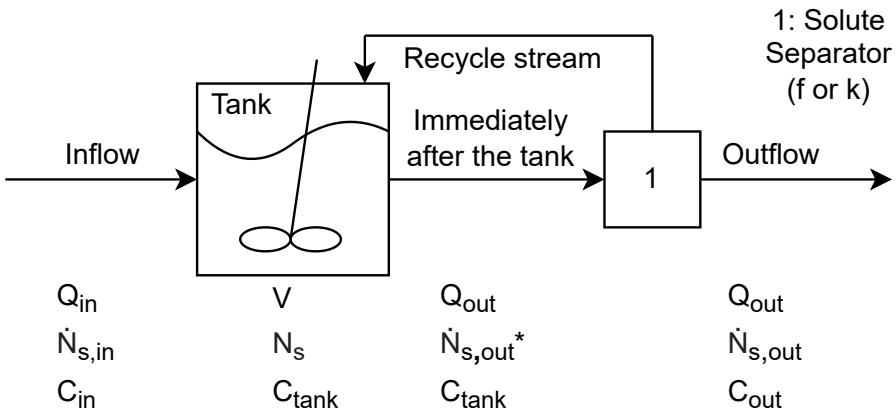


Fig. 6.1 Line diagram for Design 3: Solute separation on outflow; separator 1 is defined by either bulk flow coefficient f or mass transfer coefficient k

The solute separator (labelled as 1) is defined by either bulk flow coefficient f or lumped mass transfer coefficient k. The superscript * refers to quantities immediately after the tank, i.e. before the separator, that are affected by separation on the outflow.

The defining equations for the model remain Equation 3.1 and 3.2, repeated in Equations 6.1 and 6.2 for ease of reference.

$$\frac{dV}{dt} = Q_{in} - Q_{out} \tag{6.1}$$

$$\frac{dN_s}{dt} = \frac{dC_{tank}V}{dt} = \dot{N}_{s,in} - \dot{N}_{s,out} \tag{6.2}$$

Q_{out} follows Equation 5.1 from the previous model, repeated in Equation 6.3. $\dot{N}^*_{s,out}$ matches Equation 4.5 in Equation 6.4, while $\dot{N}_{s,out}$ accommodates convection or diffusion through Equation 6.5 or 6.6, respectively.

$$Q_{out} = Q_{ss} + m(V(t) - V_{ss}) \tag{6.3}$$

$$\dot{N}^*_{s,out} = Q_{out}C_{tank} \tag{6.4}$$

$$\dot{N}_{s,out} = f\dot{N}^*_{s,out} = fQ_{out}C_{tank} \tag{6.5}$$

$$\dot{N}_{s,out} = k(C_{tank} - C_{out}) \tag{6.6}$$

Equation 6.6 is further simplified to Equation 6.8 (using Equation 4.8, repeated in Equation 6.7), which is now independent of C_{out} and can be implemented in the corresponding level-rate diagram in Figure 6.2.

$$C_{out} = \frac{\dot{N}_{s,out}}{Q_{out}} \tag{6.7}$$

$$\dot{N}_{s,out} = \left(\frac{k}{1 + \frac{k}{Qout}} \right) C_{tank} \tag{6.8}$$

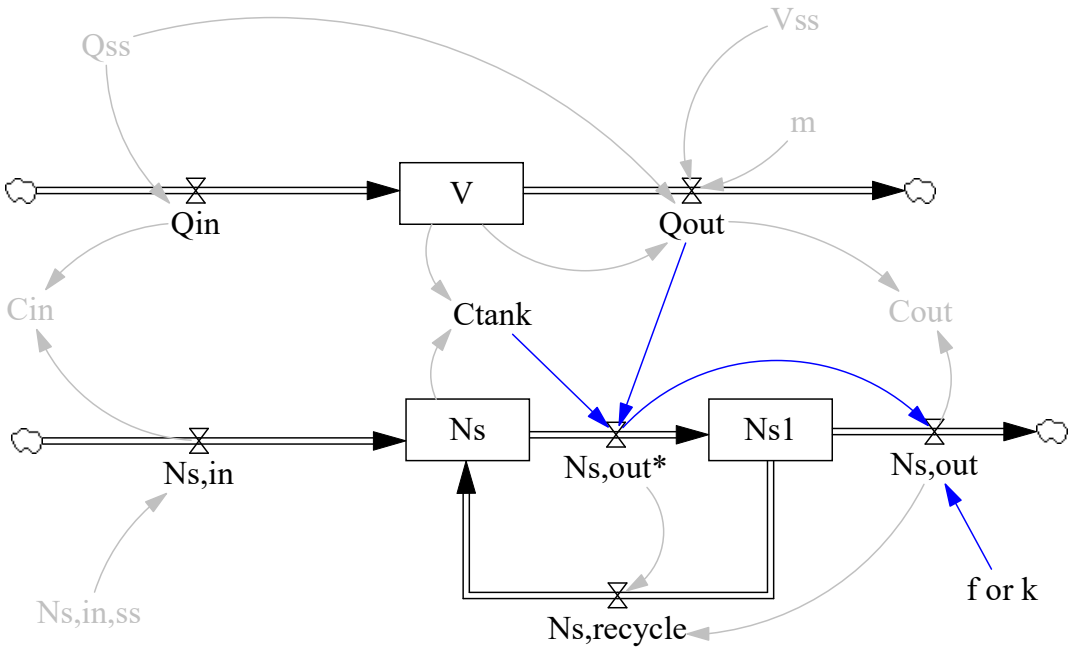


Fig. 6.2 Level-rate diagram for Design 3: Solute separation on outflow, with solute separator (labelled N_{s1}) and recycle stream shown, corresponding to Figure 6.1

f represents a dimensionless "sieving" or "bulk flow" coefficient while k corresponds to a lumped "diffusion" or "mass transfer" coefficient (that implicitly includes the area across which mass transfer occurs) (with units of ml/hr in this case). The different terminology is

used in different fields of specialisation and included here for completeness; "bulk flow" and "mass transfer" being the preferred terms in this document.

The coupled ODEs follow in Equations 6.9 and 6.10 (Appendix A.4.2) or 6.11.

$$\frac{dV}{dt} = Q(t) - (Q_{ss} + m(V(t) - V_{ss})) \tag{6.9}$$

$$\frac{dN_s}{dt} = \frac{dC_{tank}V}{dt} = \dot{N}_{s,in}(t) - fC_{tank}(t)(Q_{ss} + m(V(t) - V_{ss}) \tag{6.10}$$

$$\frac{dN_s}{dt} = \frac{dC_{tank}V}{dt} = \dot{N}_{s,in}(t) - \left(\frac{k}{1 + \frac{k}{Q_{ss}+m(V(t)-V_{ss})}}\right) C_{tank}(t)(Q_{ss} + m(V(t) - V_{ss}) \tag{6.11}$$

6.1.2 Water separation

Another separation device is that of a pure "water separator" or "water reabsorber", where a fraction (determined by the value of the water reabsorption coefficient (f_w)) of the water in the immediate tank outflow (Q^*_{out}) reaches the overall outflow from the system (Q_{out}), while the balance is recycled ($Q_{recycle}$). The tank-separator-recycle structure is illustrated in Figure 6.3 and detailed in Equations 6.12, 6.13 and 6.14.

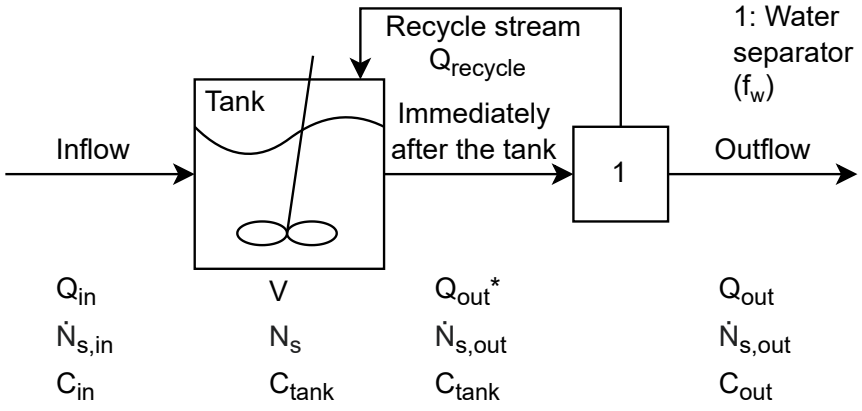


Fig. 6.3 Line diagram for Design 3: Water separation on outflow; separator 1 is defined by water reabsorption coefficient f_w

$$Q^*_{out} = \frac{Q_{ss}}{f_w} + m(V(t) - V_{ss}) \tag{6.12}$$

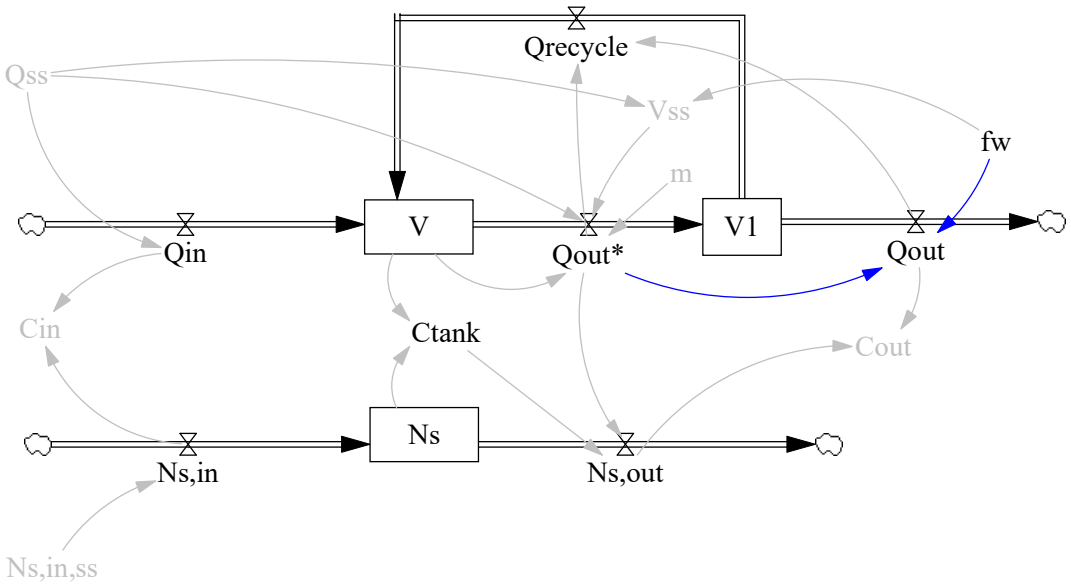


Fig. 6.4 Level-rate diagram for Design 3: Water separation on outflow, with separator (labelled V_1) and recycle stream explicitly shown, corresponding to Figure 6.3

$$Q_{out} = f_w Q^*_{out} \tag{6.13}$$

$$Q_{recycle} = Q^*_{out} - Q_{out} = Q^*_{out}(1 - f_w) \tag{6.14}$$

Unlike in solute separation, the achieved steady-state volume V_{ss} is offset from a so-called "desired" steady-state volume V_{dss} or set-point, where the quantities are related by Equation 6.15.

$$V_{ss} = V_{dss} + \frac{Q_{ss}(1 - f_w)}{f_w} \tag{6.15}$$

The level-rate diagram in Figure 6.4 emphasises the fact that only water is reabsorbed, not solute. As no solute is recycled, the final solute outflow matches that of the tank outflow, and is therefore calculated from Equation 6.16.

$$\dot{N}_{s,out} = Q^*_{out} C_{tank} \tag{6.16}$$

The coupled ODEs follow in Equations 6.17 and 6.18 (written in standard linear form in Appendix A.4.3).

$$\frac{dV}{dt} = Q(t) - (Q_{ss} + f_w m(V(t) - V_{ss})) \tag{6.17}$$

$$\frac{dN_s}{dt} = \frac{dC_{tank}V}{dt} = \dot{N}_{s,in}(t) - C_{tank}(t)\left(\frac{Q_{ss}}{f_w} + m(V(t) - V_{ss})\right) \tag{6.18}$$

In order to limit investigation to the effects of newly introduced model parameters f and f_w, m and $\frac{V}{Q}$ are held constant at 1 hr^{-1} and 10 hr, respectively. $m = 1$ corresponds to a 1:1 relationship between the volume level and the outflow rate, while $\frac{V}{Q} = \frac{1000\ ml}{100\ ml/hr} = 10\ hr$, the choices of which are arbitrary considering the high-level and non-specific nature of the model.

Model parameters are detailed in Table 6.1.

Table 6.1 Design 3 Model Parameters

Parameter	Value
Baseline water inflow (ml/hr)	100
Baseline solute inflow (mosm/hr)	28.1
Desired steady-state volume (ml)	1 000
m (1/hr)	1

6.2 Results and Discussion

6.2.1 Steady-state analysis

A steady-state analysis (i.e. as t$\rightarrow \infty$) is considered initially.

Solute separation

Firstly, considering convection and using Equation 6.7, Equation 6.5 reduces to Equation 6.19.

$$f = \frac{C_{out}}{C_{tank}} \tag{6.19}$$

Equation 6.19 emphasises the definition of the bulk flow coefficient as the ratio between the solute concentration in the outflow relative to inflow of the separator [78], and in this

way provides a transfer function across the separator. Figure 6.5 illustrates the relationship between C_{tank} and f as defined in Equation 6.19 given constant C_{out}. The outflow concentration value of 0.281 mosm/ml matches the steady-state inflow concentration, a requirement of mass balance.

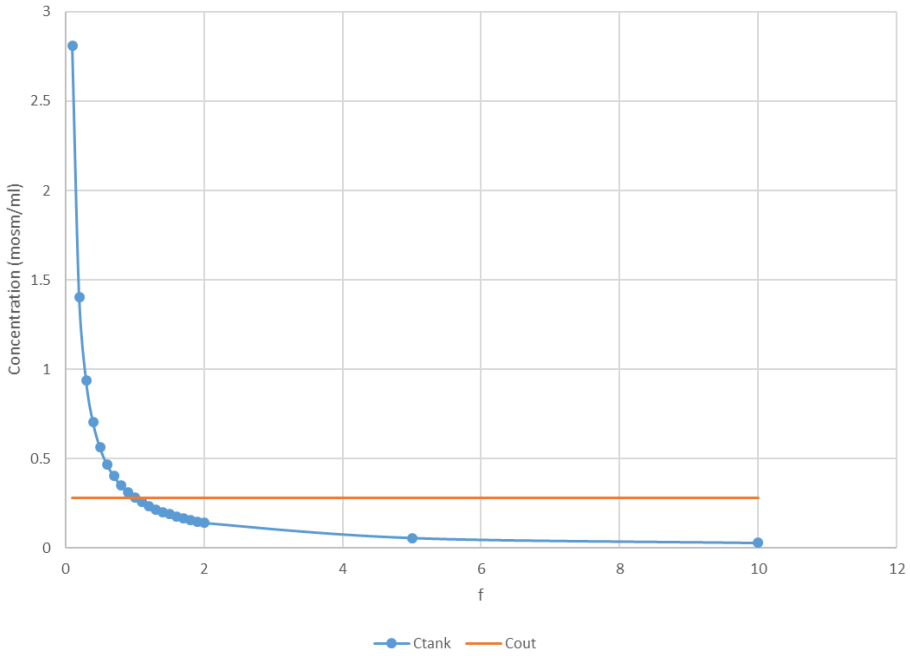


Fig. 6.5 Design 3 Graph of steady-state concentration versus bulk-flow coefficient f, including both tank and outflow concentrations

It is obvious that $f > 0$ is a requirement for steady-state to be achieved. It is also clear that a change in relationship between steady-state tank and outflow concentrations occurs at $f = 1$, the intersection of the curves; $C_{tank} > C_{out}$ for $f < 1$ while $C_{tank} < C_{out}$ for $f > 1$. This means that such a convective separator is able to adjust the tank contents to be more concentrated or dilute than that of the outflow depending on the value of f.

Now considering diffusion and using Equation 6.7, Equation 6.8 reduces to Equation 6.20.

$$k = \frac{C_{out} Q_{out}}{C_{tank} - C_{out}} \tag{6.20}$$

Equations 6.6 and 6.20 highlight the fact that the lumped mass transfer coefficient is a proportionality constant between solute flow rate and the concentration difference driving force and therefore, for a particular value of k, a constant difference between C_{out} and C_{tank} is expected. Figure 6.6 illustrates the relationship between C_{tank} and k, as defined in Equation 6.20.

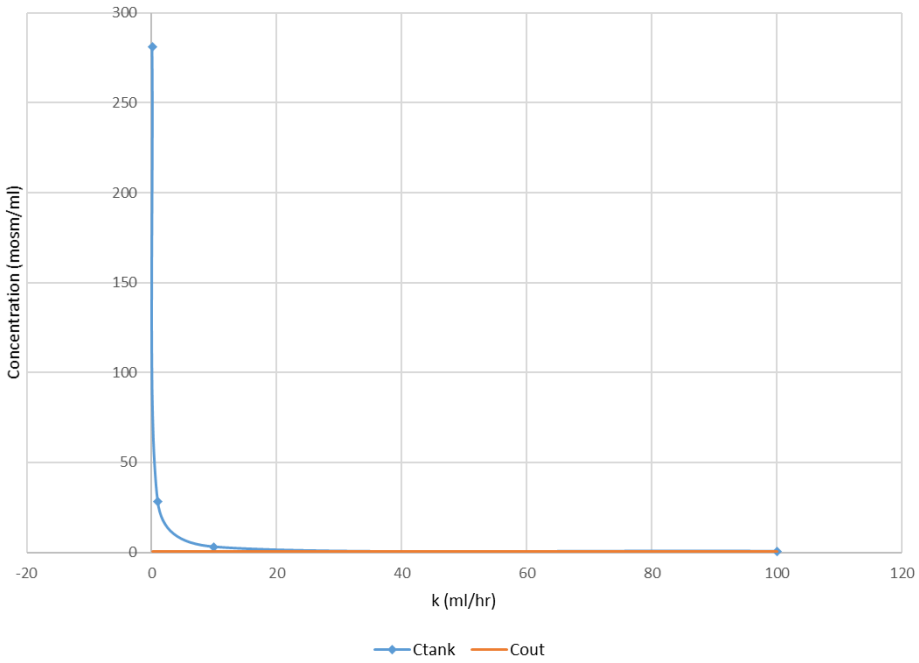


Fig. 6.6 Design 3 Graph of steady-state concentration versus lumped mass transfer coefficient k, including both tank and outflow concentrations

It is clear that for $k < 0$, steady-state is never achieved; for $k = 0$, no solute leaves the tank and, therefore, C_{out} remains zero and C_{tank} increases at a constant rate; while for $k > 0$ and increasing, tank concentration tends to the steady-state outflow value of 0.281 mosm/ml (i.e. matching the inflow concentration through mass balance). At small values for k, there is a large difference between tank and outflow concentrations at steady-state, while at large values for k, there is a small concentration difference at steady-state. It is also clear that for all $k > 0$, at steady-state, $C_{tank} > C_{out}$. This implies that no matter the disturbance, such a diffusive separator can only cause the tank to be more concentrated than the outflow.

Water separation

The outflow concentration (C_{out}) depends on the solute and water outflows such that, by substituting in Equations 6.16 and 6.13, Equation 6.21 results.

$$C_{out} = \frac{\dot{N}_{s,out}}{Q_{out}} = \frac{Q^*_{out} C_{tank}}{f_w Q^*_{out}} = \frac{1}{f_w} C_{tank} \tag{6.21}$$

If Equation 6.21 is written in terms of the ratio $\frac{C_{out}}{C_{tank}}$, then Equation 6.22 yields the transfer function for the water separator.

$$\frac{C_{out}}{C_{tank}} = \frac{1}{f_w} \tag{6.22}$$

Although not mathematically necessary, limiting f_w to the range $0 < f_w \leq 1$ means that the direction of water recycle is from the outflow to the tank and not vice versa, which matches the function of an excretory system. $f_w = 1$ implies zero water recycled, while $f_w = 0$ is mathematically undefined and, in any case, considered physically impossible as some minimum flow of water is needed to continue removing excess solute from a biological perspective.

Figure 6.7 illustrates the relationship between C_{tank} and f_w as defined in Equation 6.22 given constant C_{out} and m. It is clear that for all $f_w < 1$, $C_{tank} < C_{out}$, and therefore, that such a water separator can only cause the tank to be more dilute than the outflow.

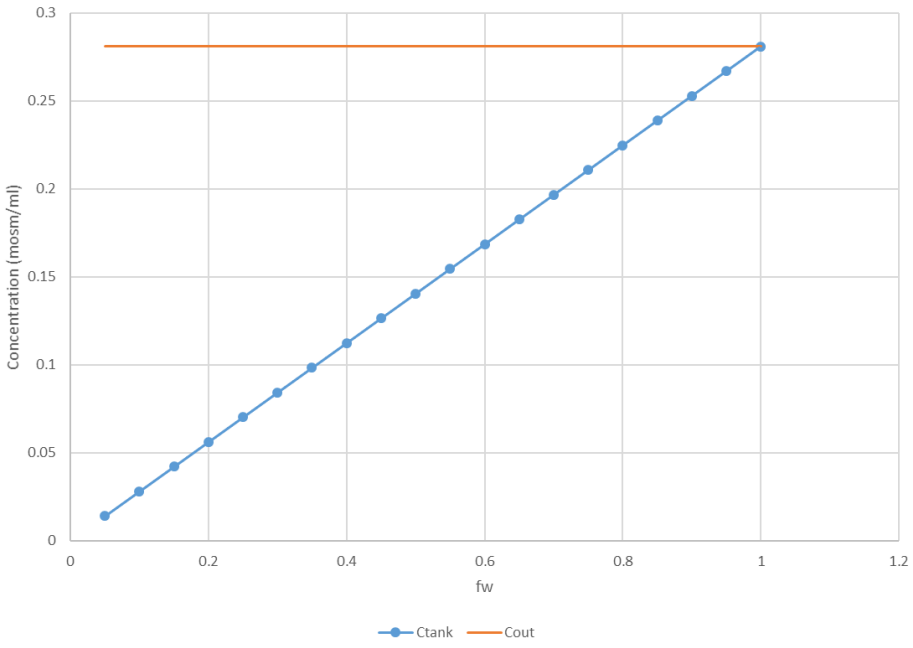


Fig. 6.7 Design 3 Graph of steady-state concentration versus water reabsorption coefficient f_w, including both tank and outflow concentrations

6.2.2 Transient analysis

Solute separation

At this stage in model development, it was decided that convective separators, capable of both concentrating and diluting the tank relative to the outflow (unlike diffusive separators),

were more useful modelling constructs and therefore became the focus of transient analysis and further model development.

Simulations were run for both solute and water inflow disturbances (only the positive cases are considered due to linearity) over a range of f ($f = 0.5, 1, 1.5$ while $m = 1\ hr^{-1}$ and $\frac{V}{Q} = \frac{1000\ ml}{100\ ml/hr} = 10\ hr$ were held constant). The results are shown in Figures 6.8 and 6.9.

As expected from no water disturbance to the inflow of the tank, the tank volume is not affected by a pure solute disturbance (Figure 6.8), while for a water disturbance (Figure 6.9), the tank volume is affected identically no matter the value of f. It is seen in both Figures 6.8 and 6.9 that the amount of solute and tank concentration at steady-state depend inversely on f, as expected from Equation 6.19.

In both Figures 6.8 and 6.9, the tank concentration recovers to steady-state faster for larger f. This is confirmed by the inverse relationship between 95 % settling time and f in Figure 6.10. However, the shape of response differs in response to a finite-duration water pulse (Figure 6.9) depending on f, and this causes the discrepancy in 95 % settling time responses seen at small f in Figure 6.10.

The (absolute) relative change in magnitude of tank concentration response also differs depending on f and the type of disturbance as seen in Figure 6.11 for $m = 1\ hr^{-1}$ and $\frac{V}{Q} = 10\ hr$. The solute response is linearly dependent on f, while the water response is approximately constant for $f < 1$ and linearly increasing for $f > 1$. Interestingly, the water response is greater in relative magnitude than the solute response for $f < 1$ and smaller for $f > 1$, an observed distinction in response to water and solute disturbances that depends on the value of f. The significance of $f = 1$ in the analysis is related to the decision to keep $m = 1$ from Design 3 onwards.

Unlike the previous two designs in Chapters 4 and 5, the analytical solution for a design that includes a solute separator is not as straightforward. The details are included in Appendices A.5.3 and A.6 and summarised here.

At the pure solute disturbance extreme, the ODEs in Equations 6.9 and 6.10 (written in standard linear form in Appendix A.4.2) are effectively decoupled and fully solvable in terms of regular functions. Considering a pure solute impulse disturbance (quantified by height b), the tank volume and concentration responses are expressed in Equations 6.23 and 6.24, respectively, where steady-state concentration is quantified by Equation 6.25 and the mean residence time in the tank is given by Equation 6.26.

$$V(t) = V_{ss} \tag{6.23}$$

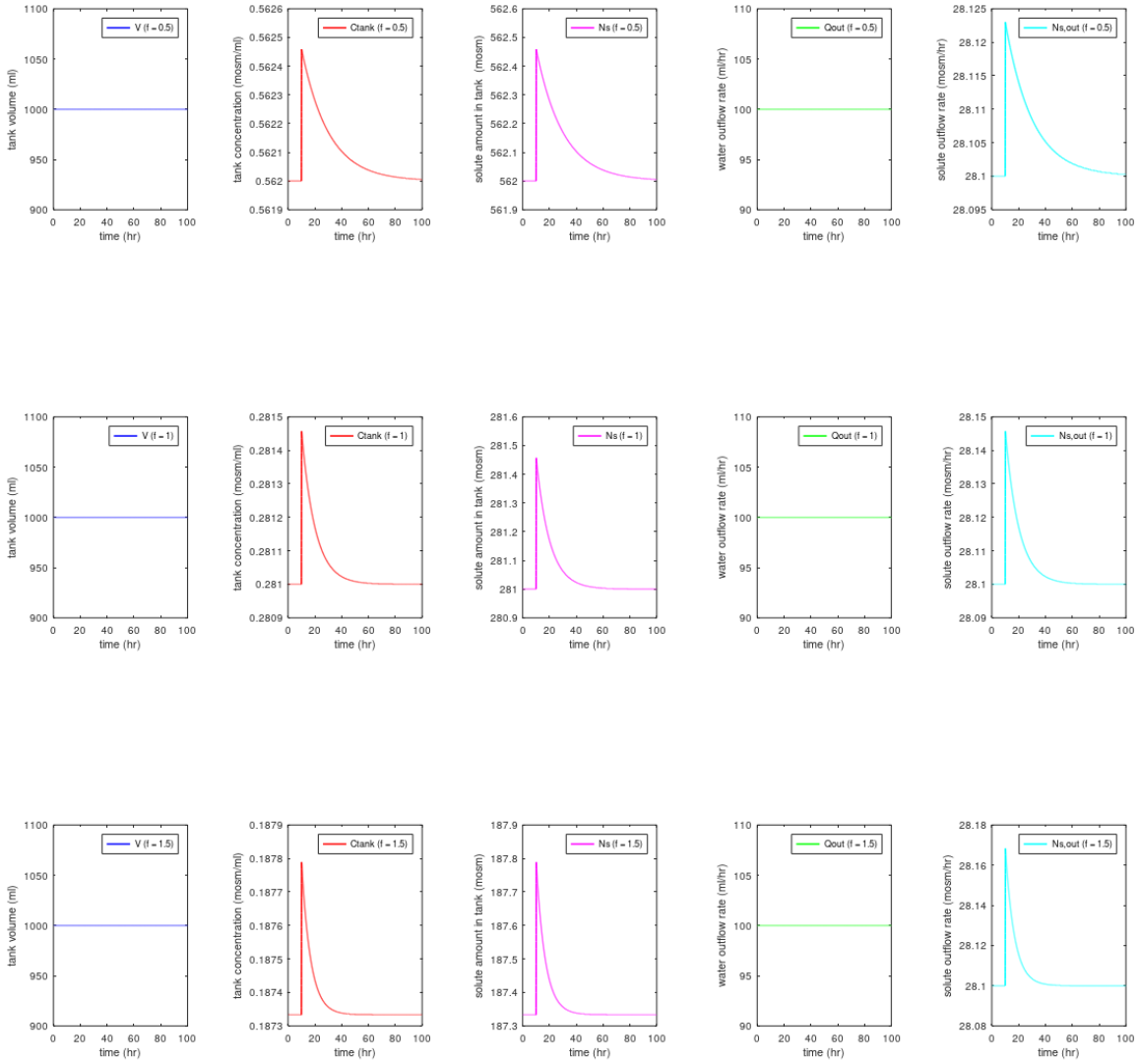


Fig. 6.8 Design 3 Graph showing volume (blue), tank concentration (red), amount of solute (magenta), water outflow rate (green) and solute outflow rate (cyan) versus time in response to a positive finite-duration solute inflow pulse of size 10 % (above a baseline of 28.1 mosm/hr) and duration 10 minutes at $t = 10$ hr for, from top to bottom, $f = 0.5, 1, 1.5$, $m = 1$ and $\frac{V}{Q} = 10\ hr$

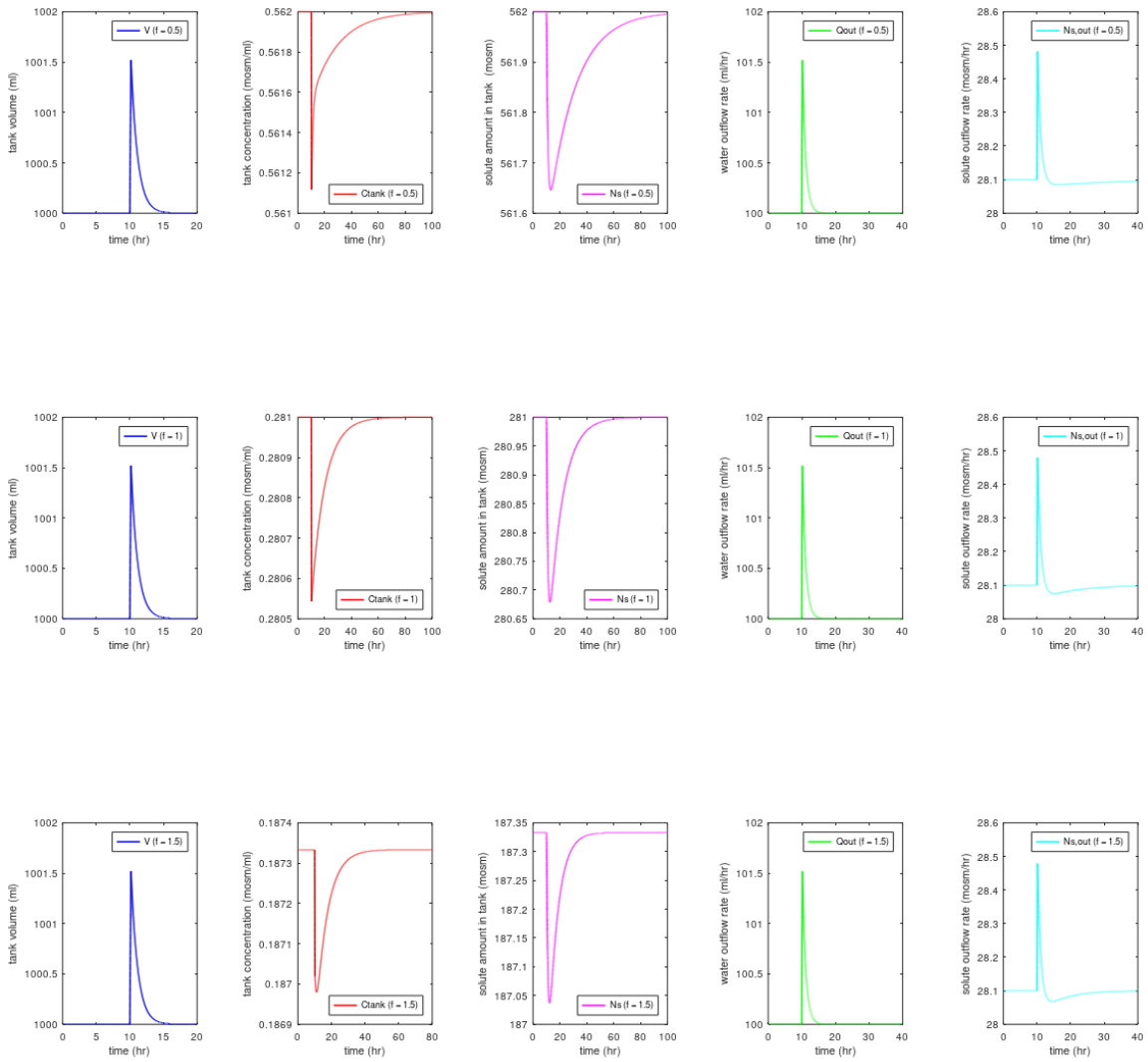


Fig. 6.9 Design 3 Graph showing volume (blue), tank concentration (red), amount of solute (magenta), water outflow rate (green) and solute outflow rate (cyan) versus time in response to a positive finite-duration water inflow pulse of size 10 % (above a baseline of 100 ml/hr) and duration 10 minutes at $t = 10$ hr for, from top to bottom, $f = 0.5, 1, 1.5$, $m = 1$ and $\frac{V}{Q} = 10\ hr$

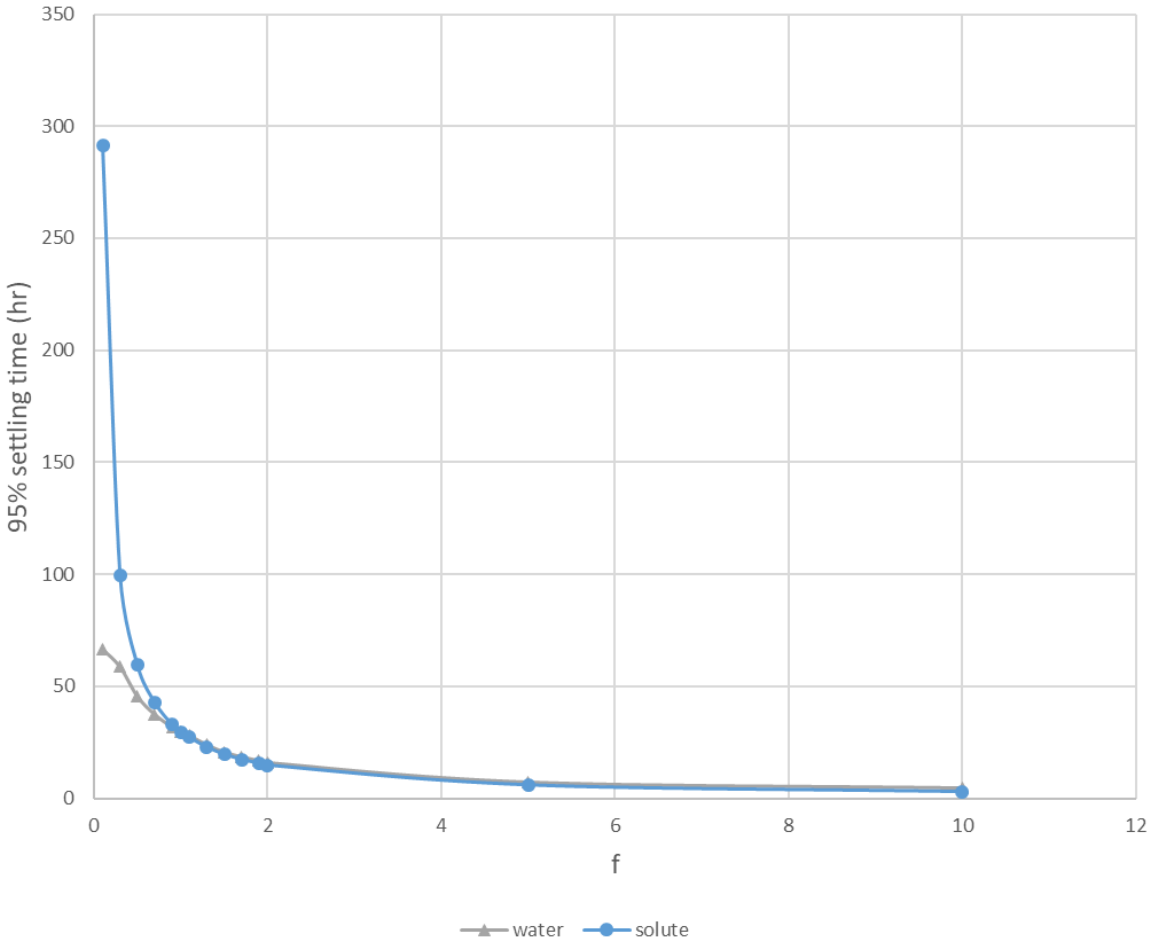


Fig. 6.10 Design 3 Graph of tank concentration 95% settling time as a function of f in response to positive finite-duration solute and water inflow pulses of size 10 % (above a baseline of 28.1 mosm/hr and 100 ml/hr, respectively) and duration 10 minutes for $m = 1\ hr^{-1}$ and $\frac{V}{Q} = 10\ hr$

$$C(t) = C_{ss} + \frac{b}{V_{ss}} e^{\frac{-t}{\tau}} \tag{6.24}$$

$$C_{ss} = \frac{1}{f} \frac{\dot{N}_{s,in,ss}}{Q_{ss}} \tag{6.25}$$

$$\tau = \frac{1}{f} \frac{V_{ss}}{Q_{ss}} \tag{6.26}$$

If $f = 1$, the solution reduces to that of Design 2, as expected.

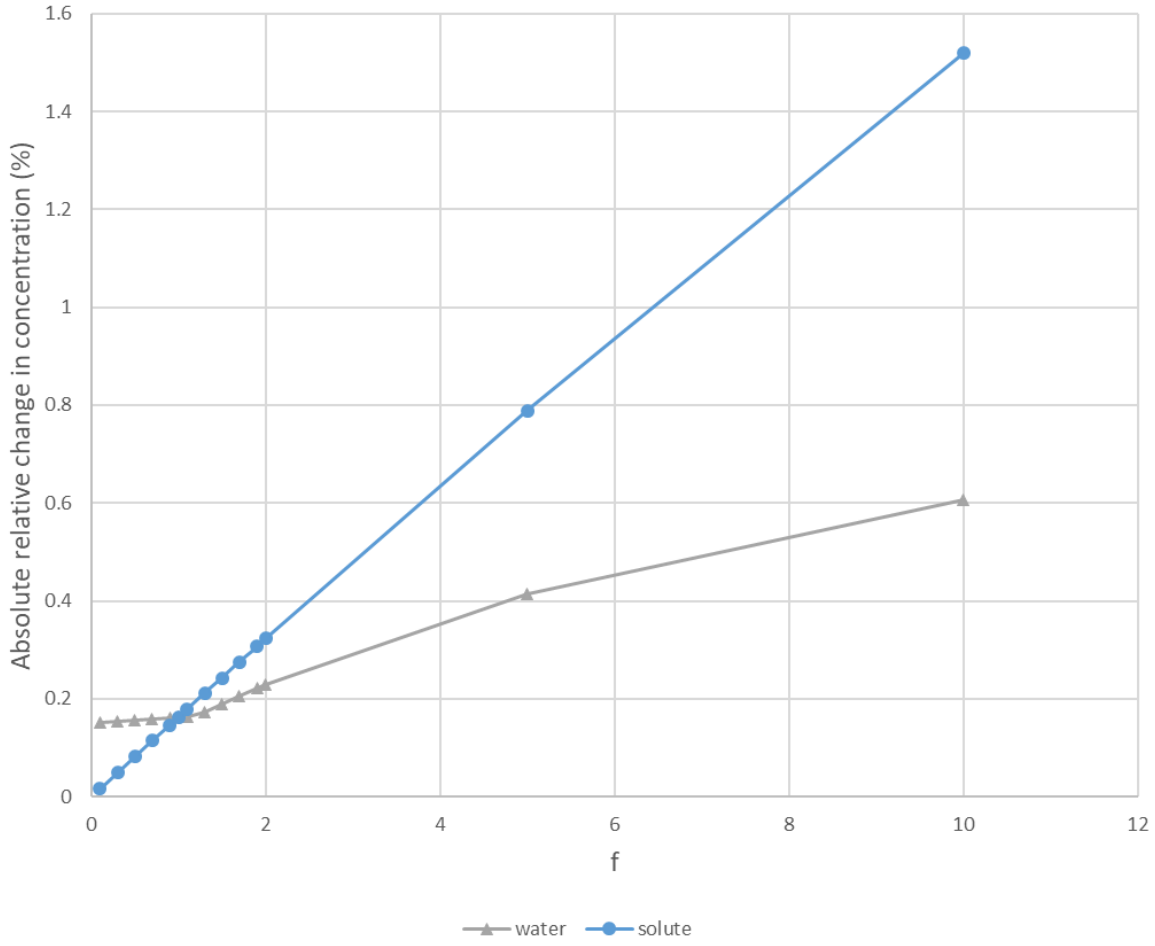


Fig. 6.11 Design 3 Graph of (absolute) relative change in tank concentration as a function of f in response to positive finite-duration solute and water inflow pulses of size 10 % (above a baseline of 28.1 mosm/hr and 100 ml/hr, respectively) and duration 10 minutes for $m = 1\ hr^{-1}$ and $\frac{V}{Q} = 10\ hr$

The analytical solution confirms and provides quantification for the earlier findings based on simulation output; constant tank volume for a pure solute input disturbance (Equation 6.23), tank concentration steady-state offset from the outflow concentration by a factor of f (Equation 6.25) and inverse dependence of 95 % tank concentration settling time (which is directly related to τ through $t_{s,95\%} = 3\tau$) on f (Equation 6.26).

The analytical solution is not as straightforward for disturbances that involve water since the system of ODEs (Equations 6.9 and 6.10 or Appendix A.4.2) remains coupled. Considering a pure water impulse (quantified by height a), the volume response is expressed in Equation 6.27, where the "valve" response time τ_V depends on m alone, according to Equation 6.28.

$$V(t) = V_{ss} + ae^{-\frac{t}{\tau_V}} \tag{6.27}$$

$$\tau_V = \frac{1}{m} \tag{6.28}$$

This fully describes the identical volume responses observed in Figure 6.9, where $m = 1$ was held constant and only f varied.

Due to the presence of f, however, terms do not cancel conveniently to aid analytical solution of the tank concentration ODE (Appendix A.4.2), and the special hypergeometric function is present (detailed in Appendices A.5.3 and A.6). In this case, the hypergeometric function represents an infinite sum of exponential terms. The weighted sum may be dominated by two exponentials (or a good fit thereof) in some particular cases, however, in order to represent reality, the model needs to be able to represent a range of animal excretory systems (and consequent model constants). Therefore, the infinite sum of exponential terms in the analytical solution may not, in general, decay at a rate such that the solution can simply be approximated as a sum of only two exponential terms. For this reason, numerical simulation and high-level parameterisation, supplemented by the analytical solution, are favoured in terms of model development and analysis.

For instance, it is possible to extract the mean residence time of the tank from the hypergeometric solution, and unsurprisingly, τ matches Equation 6.26. This explains the observation that the tank concentration recovers to steady-state following a water pulse faster for larger f (Figure 6.10). However, τ alone does not explain the observed effect at small f, for which it is appreciated that a combination of τ_V and τ (and possibly multiples thereof depending on the scenario) determine the dynamics of the tank response to a water disturbance (as was the case in Design 2 (Equation 5.8 in Chapter 5)).

Likewise, it is clear from the hypergeometric solution that the amplitude of the tank concentration response is dependent on τ_V and τ (and possibly multiples thereof depending on the scenario). Therefore, the dynamic response of the tank concentration to a solute disturbance depends on f, while that to a water disturbance depends on f and m. This helps to explain the difference in relative change in magnitude observed as a function of f between solute and water disturbances (Figure 6.11).

Water separation

As for solute separation, simulations were run for both solute and water inflow disturbances (only the positive case is considered due to linearity) over a range of $0 < f_w \leq 1$ (e.g. $f_w = 0.5, 0.8, 1$), while $m = 1\ hr^{-1}$ and $\frac{V}{Q} = 10\ hr$ were held constant, to determine the response of a water separator. The results are illustrated in Figures 6.12 and 6.13, respectively.

As expected from Equation 6.15, it is observed in the volume subplots of both Figures 6.12 and 6.13 that there is an obvious volume offset from the desired steady state $V_{dss} = 1000\ ml$, dependent on f_w. Likewise, f_w-dependent steady-state offsets are observed in the subplots for both amount of solute in the tank and tank concentration, as expected from Equation 6.21.

There is an apparent difference in shape of response between finite-duration solute and water pulse disturbances (Figures 6.12 and 6.13, respectively), with that to water disturbances depending on f_w, and that to solute disturbances, not.

Figures 6.14 and 6.15 summarise the transient responses to pure solute and water finite-duration pulses in terms of the parameters of interest, i.e. 95 % settling time and relative change in magnitude, respectively. It is clear that in response to a pure solute finite-duration pulse disturbance, the tank volume is transiently unaffected, while the tank concentration is linearly dependent on f_w in terms of 95 % settling time and inversely related to f_w in terms of relative change in magnitude. The response to a pure water finite-duration pulse disturbance is more complicated; the tank volume recovers to steady-state more slowly for smaller values of f_w, while tank concentration settling time depends differently on f_w across the domain, and the relative change in tank volume decreases as f_w decreases (due to corresponding increases in the steady-state volume) compared to the relative change in tank concentration remaining approximately constant until f_w decreases significantly (i.e. $f_w < 0.2$ in this case).

As was the case for a solute separator (Subsection 6.2.2), the analytical solution for a design that includes a water separator is not as straightforward as for the previous two designs in Chapters 4 and 5. The details are included in Appendices A.5.4 and A.6.

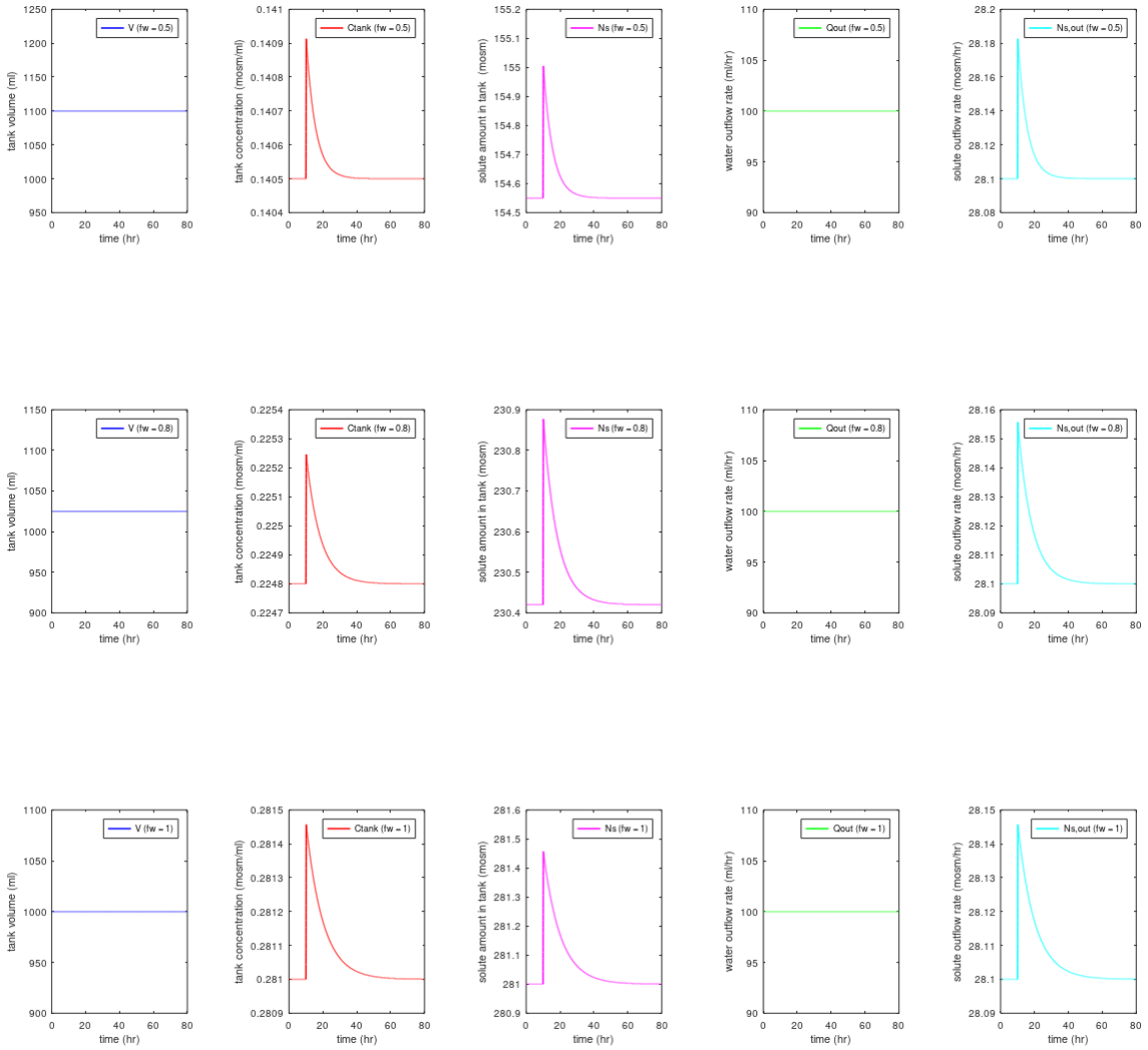


Fig. 6.12 Design 3 Graph showing volume (blue), tank concentration (red), amount of solute (magenta), water outflow rate (green) and solute outflow rate (cyan) versus time in response to a positive finite-duration solute inflow pulse of size 10 % (above a baseline of 28.1 mosm/hr) and duration 10 minutes at $t = 10$ hr for, from top to bottom, $fw = 0.5, 0.8, 1$, $m = 1$ and $\frac{V}{Q} = 10\ hr$

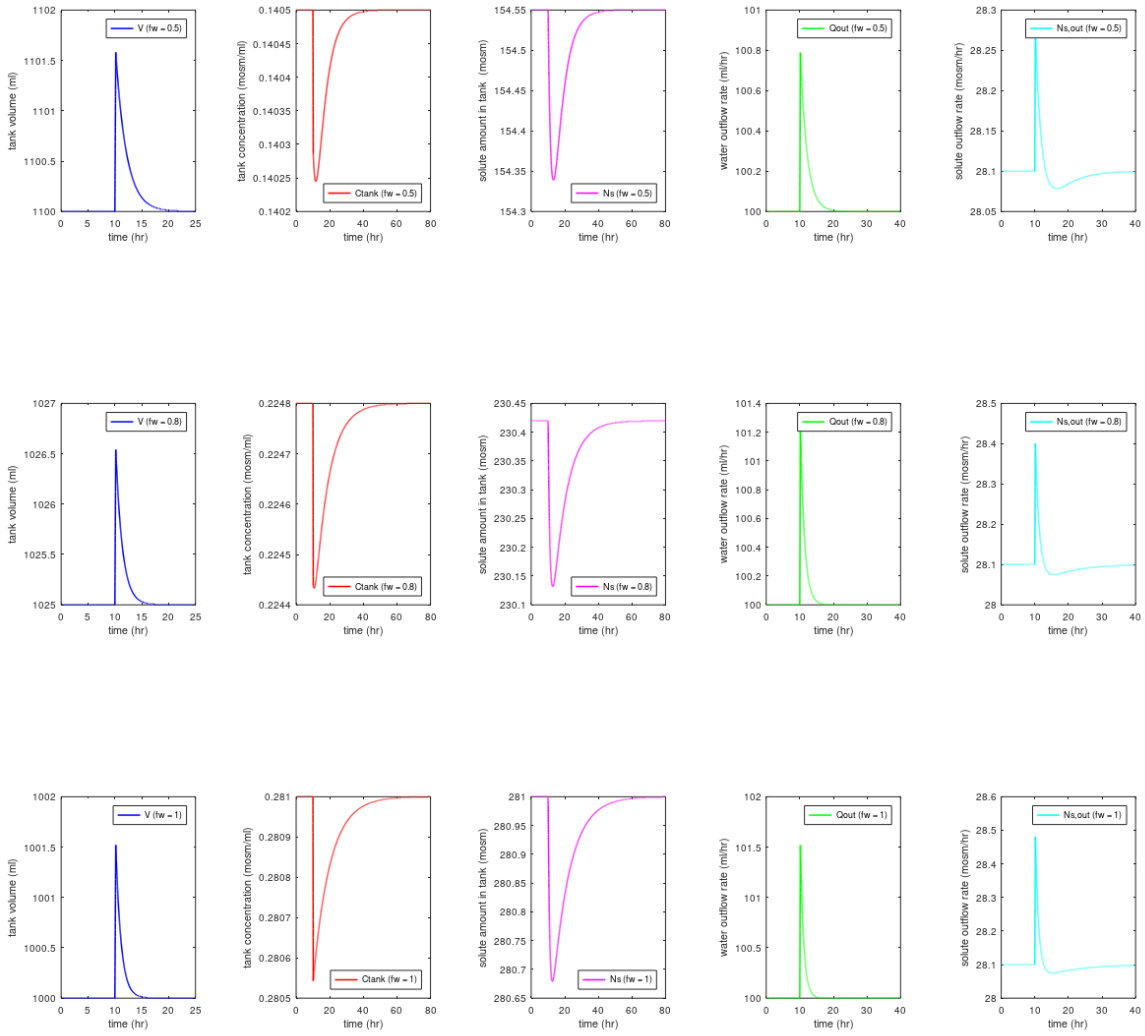
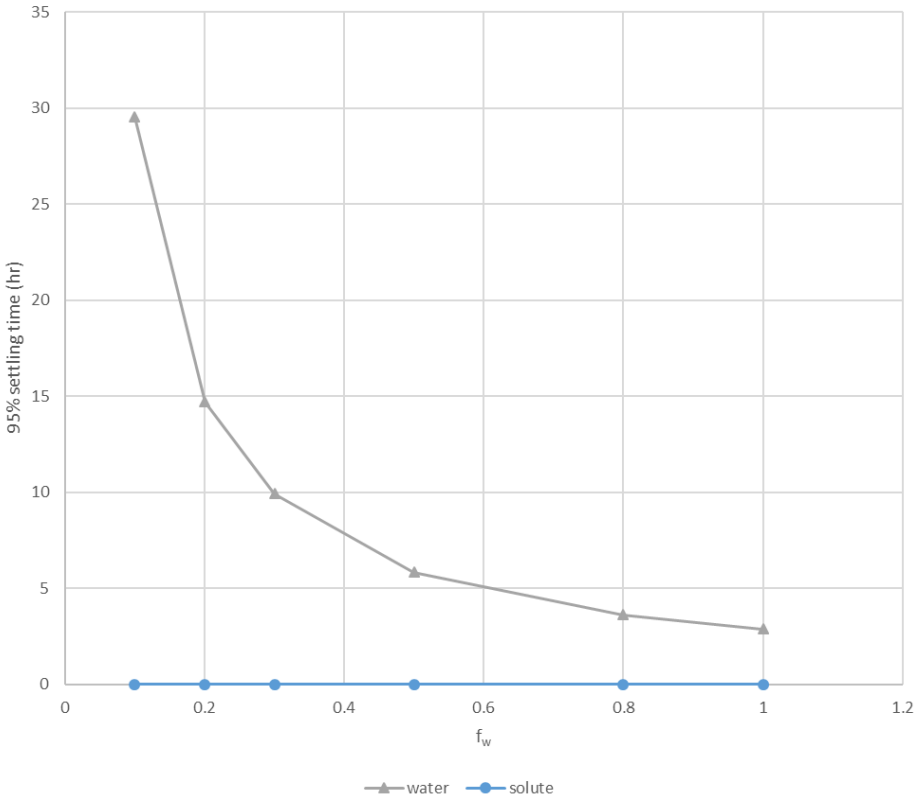
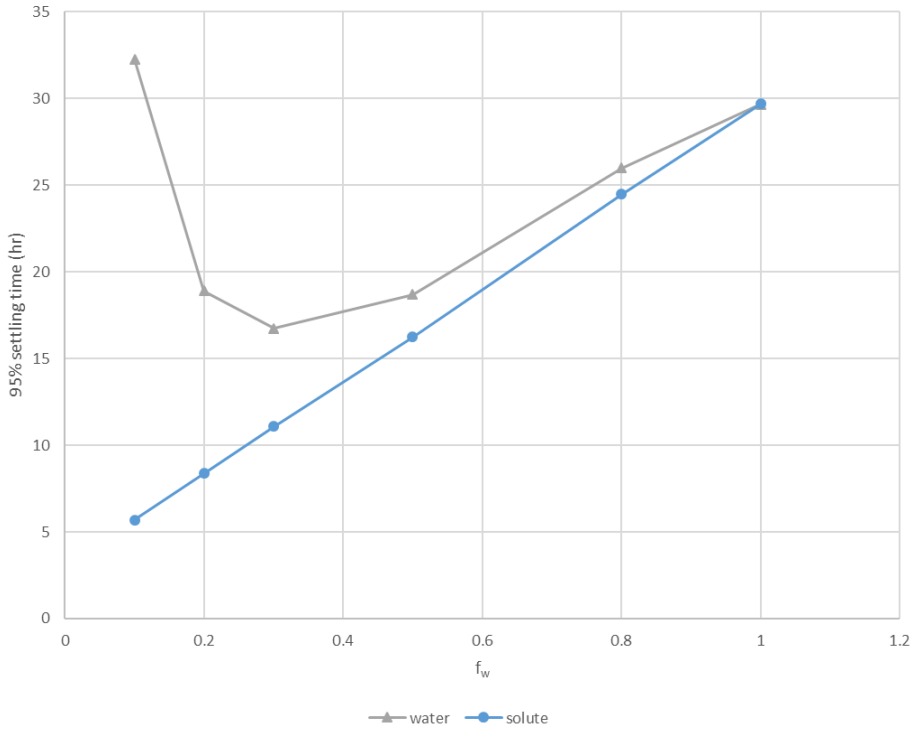


Fig. 6.13 Design 3 Graph showing volume (blue), tank concentration (red), amount of solute (magenta), water outflow rate (green) and solute outflow rate (cyan) versus time in response to a positive finite-duration water inflow pulse of size 10 % (above a baseline of 100 ml/hr) and duration 10 minutes at $t = 10$ hr for, from top to bottom, $fw = 0.5, 0.8, 1$, $m = 1$ and $\frac{V}{Q} = 10\ hr$

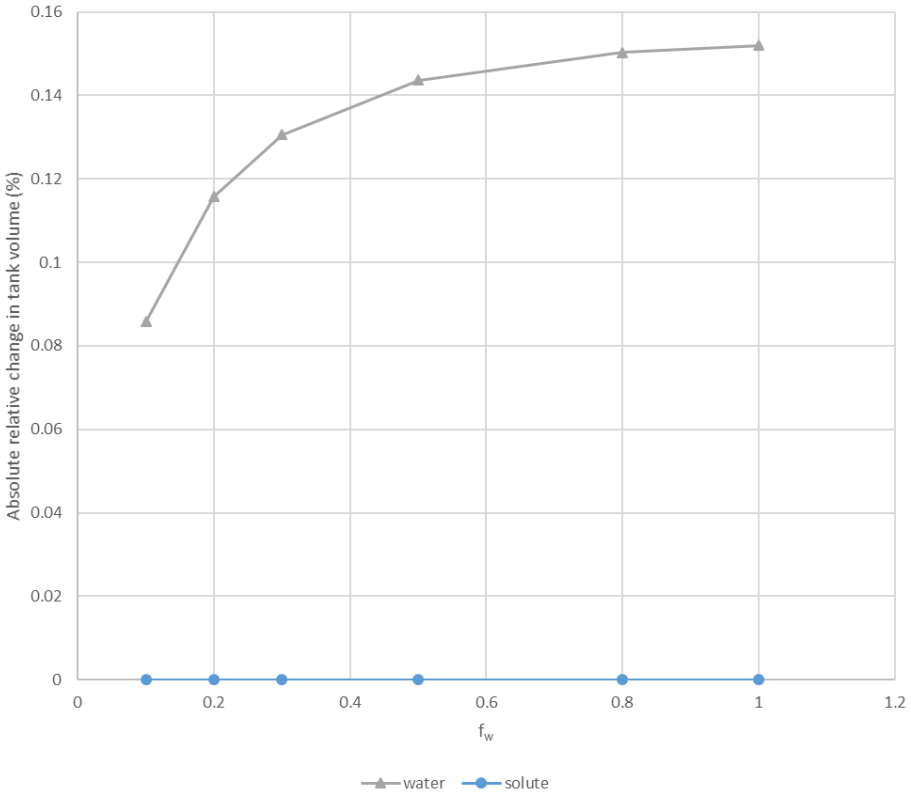


(a) Tank volume

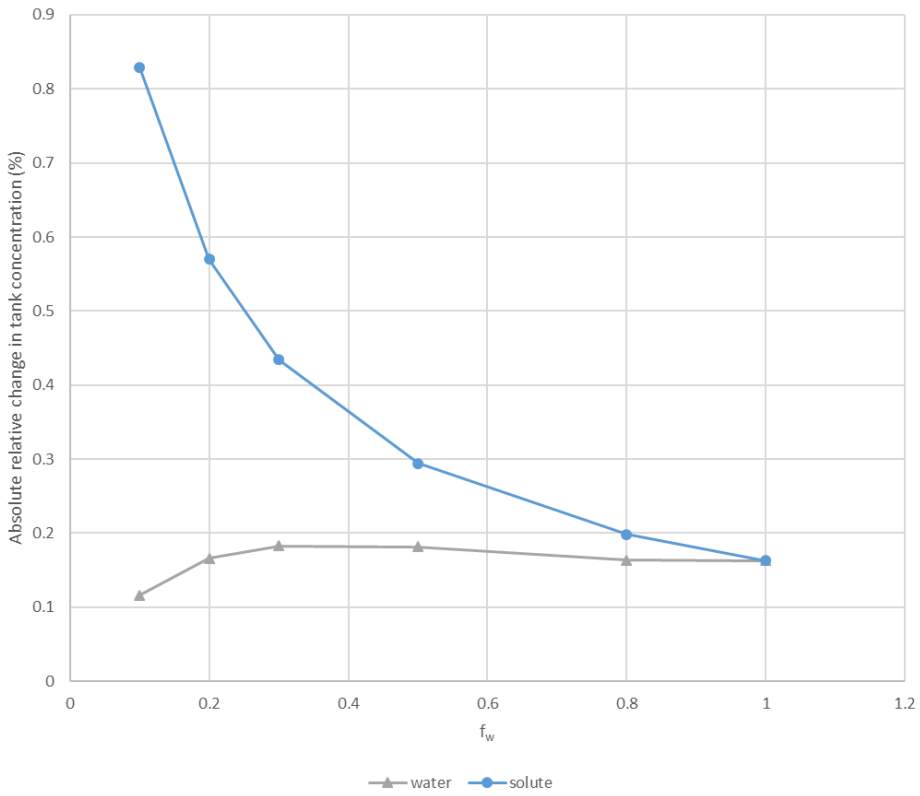


(b) Tank concentration

Fig. 6.14 Design 3 Subplots of 95 % settling time of (a) tank volume and (b) tank concentration as a function of f_w in response to positive finite-duration solute and water inflow pulses of size 10 % (above a baseline of 28.1 mosm/hr and 100 ml/hr, respectively) and duration 10 minutes for $m = 1\ hr^{-1}$ and $\frac{V}{Q} = 10\ hr$



(a) Tank volume



(b) Tank concentration

Fig. 6.15 Design 3 Subplots of (absolute) relative change in magnitude of (a) tank volume and (b) tank concentration as a function of f_w in response to positive finite-duration solute and water inflow pulses of size 10 % (above a baseline of 28.1 mosm/hr and 100 ml/hr, respectively) and duration 10 minutes for $m = 1\ hr^{-1}$ and $\frac{V}{Q} = 10\ hr$

At the pure solute disturbance extreme, the ODEs in Equations 6.17 and 6.18 (written in standard linear form in Appendix A.4.3) are effectively decoupled and fully solvable in terms of regular functions. For a pure solute impulse (quantified by height b) , the volume and concentration responses are expressed in Equations 6.29 and 6.30, respectively, where the steady-state tank concentration depends on f_w according to Equation 6.31, while the mean residence time in the tank is quantified in Equation 6.26.

$$V(t) = V_{ss} \tag{6.29}$$

$$C_{tank}(t) = C_{ss} + \frac{b}{V_{ss}} e^{\frac{-t}{\tau}} \tag{6.30}$$

where

$$C_{ss} = f_w \frac{\dot{N}_{s,in,ss}}{Q_{ss}} \tag{6.31}$$

and

$$\tau = f_w \frac{V_{ss}}{Q_{ss}} \tag{6.32}$$

If $f_w = 1$, the solution reduces to that of Design 2, as expected.

The analytical solution confirms and provides quantification for earlier findings based on simulation output; constant tank volume for a pure solute input disturbance (Figure 6.12 and Equation 6.29), tank concentration steady-state offset from the outflow concentration by a factor of f_w (Figure 6.12 and Equation 6.31), and direct dependence of 95 % tank concentration settling time (which is related to τ through $t_{s,95\%} = 3\tau$ in the case of an exponential response) on f_w (Figure 6.14a and Equation 6.32).

The analytical solution is not as straightforward for disturbances that involve water since the system of ODEs (Equations 6.17 and 6.18) remains coupled. For a pure water impulse (quantified by height a) , the volume response is expressed in Equation 6.33, where the "valve" response time τ_V depends on f_w and m, according to Equation 6.34.

$$V(t) = V_{ss} + ae^{-\frac{t}{\tau_V}} \tag{6.33}$$

where

$$\tau_V = \frac{1}{f_w m} \tag{6.34}$$

This explains the shape of the curve in Figure 6.14a since the settling time is related to τ_V, which is inversely proportional to f_w in Equation 6.34 ($m = 1\ hr^{-1}$ was held constant and only f_w varied).

As for solute separation, the special hypergeometric function is present in the tank concentration solution (detailed in Appendices A.5.4 and A.6). It is possible to extract the mean residence time of the tank from the hypergeometric solution, and τ matches Equation 6.32, proportional to f_w. This explains the observation that the tank concentration recovers to steady-state following a water pulse slower for larger f_w (Figure 6.14b). However, τ alone does not explain the observed effect at small f_w, for which it is appreciated that a combination of τ_V and τ (and possibly multiples thereof depending on the scenario) determine the dynamics of the tank response to a water disturbance (as was the case in solute separation and in Design 2 (Equation 5.8 in Chapter 5)).

It is also clear from the hypergeometric solution that the amplitude of the tank concentration response to a water disturbance is dependent on τ_V and τ (and possibly multiples thereof depending on the scenario). Therefore, the dynamic response of the tank concentration to a solute disturbance depends on f_w, while that to a water disturbance depends on f_w and m. This helps to explain the difference in relative change in tank concentration magnitude observed as a function of f_w between solute and water disturbances (Figure 6.15b).

6.3 Biological application

In summary, a single separation device on the outflow of the tank causes a shift in the tank concentration steady-state relative to the outflow (which always tends to the inflow due to mass balance requirements). Following separate implementation of convective and diffusive solute separators, it was found that only a convective separator is able to yield a tank either more dilute or more concentrated relative to outflow concentration, and therefore, knowing that in more sophisticated designs the ability to produce both these outputs would be necessary, the convective separator is the solute separator of choice. Both solute and water separators respond differently to different types of disturbances (i.e. water compared to solute). These key findings lend themselves to making specific changes in the next design to improve the osmoregulatory response.

In more detail, a steady-state offset between the tank and outflow concentrations is introduced when a single separation device is added to the outflow. Either the solute outflow has changed relative to the previous designs and now incorporates a bulk flow or diffusion term according to Equations 6.5 and 6.6, respectively, or the water outflow has changed, incorporating a water reabsorption coefficient as in Equation 6.13. However, in order for

mass balance to be maintained, the outflow always matches the inflow at steady-state and therefore, necessarily, the tank concentration needs to vary in order for this to occur.

Such a model demonstrates the capacity to produce an outflow concentration that differs from that of the tank (albeit that it is the tank concentration that differs relative to the constant outflow concentration), something that is necessary if non-isosmotic urine production is to be imitated. The current model may be sufficient in describing the excretory system of an osmoconformer such as an amphibian or reptile, for example, whose osmotic region of operation is quite wide in most cases [79, 4]. However, osmoregulation needs to be addressed in future designs if the model is to represent the urinary system of an animal such as a mammal that operates over a narrow concentration range (where it is understood that the urine concentration is varied in order to keep the blood concentration relatively constant [80]). In such a case, the tank concentration will need to be maintained within narrow limits of a desired level.

The fact that a diffusive separator has the "wrong" characteristic to yield a tank concentration more dilute than the outflow (or reciprocally, concentrated outflow relative to the tank) does not mean it is not a useful modelling construct in its own right. For example, freshwater amphibians, who are relatively tolerant to swings in osmolarity, need to remove excess water (and not solute) constantly and they achieve this by creating copious amounts of dilute urine [79]. Such a urinary system may well be sufficiently described by a diffusive separation device.

Similarly, a water reabsorber is limited in that it cannot concentrate the tank relative to the outflow. However, the tank diluting (or similarly, outflow concentrating) characteristic of a water reabsorber may still be useful in its own right in describing the excretory systems of volume- and osmoconformers living in desiccating conditions such as desert amphibians and reptiles [4]. Emphasis is placed on volume as well as osmolarity conformity because of the offset the water reabsorber causes to the volume at steady-state.

The finding that presence of a separator causes the tank concentration to respond differently to water and solute disturbances means that by implementing different separators in the model (i.e. by changing the value of f of a solute separator or f_w of a water separator), different results can be achieved. For example, a separator with small f would be able to respond to a diluting water disturbance faster (with slightly more of an effect on the tank concentration magnitude) than a separator with large f, and remove the excess water preferentially to solute. Likewise, a separator with large f would be able to respond to a concentrating solute disturbance faster (again, with more of an effect on the tank concentration magnitude), than a separator with small f, thereby removing excess solute relative to water. Similar results hold for a water separator and different values of f_w. This is due to solute handling depending on

the mean residence time in the tank alone, while water handling depends on mean residence time in the tank and the valve response time. Therefore, by combining different separators of different separating ability in future designs, it may be possible to optimise the response to a range of disturbances, and in this way, mimic the functioning of a sophisticated kidney.

Although physical realisation of the model is not required at this stage, a convective separator may simply involve some arrangement of a semi-permeable membrane able to withhold solute from (i.e. $f < 1$) or actively pump solute into (i.e. $f > 1$) the outflow stream, thereby modifying the bulk flow concentration, as detailed in Equation 6.5. Biological membranes are believed to perform both functions [1]. As for water separation, "aquaporins" or "water channels" are known to be present in the cell membranes of a variety of biological cells [1].

Ultimately, by adding either a convective solute separator or water separator to the outflow of the tank, the outflow and tank concentrations no longer match and it is possible to change the tank relative to the outflow. However, it must be emphasised that the tank concentration at steady-state is linked and offset from the outflow (which is set by the inflow through mass balance) by an amount depending on the separator of choice and it is concluded that a fixed single separator is not useful to describe the excretory system of an organism that operates over a narrow concentration range. Such a design does, however, show that it is possible to speed up concentration recovery and differentiate water and solute responses, and, together with the observed steady-state offset, this provides a basis for changing the architecture in the next design.

Chapter 7

Design 4: Multiple separators

Following the findings of the previous design, it was decided that various arrangements of multiple and different separators on the outflow should be considered with the goal of improving osmoregulation by achieving different tank concentrating ability relative to the outflow (and in some cases, opposite) when compared with a single separator. In addition, it makes sense to take advantage of the differentiation between water and solute responses of the different separators (as concluded in the previous design), to provide efficient concentrating and diluting disturbance handling going forward. Many arrangements are possible; however, only a few fundamental arrangements were considered. These include parallel, series and a combination thereof. As for the single separator design in Chapter 6, it is assumed that there is no accumulation in the separators, and that the separators act linearly. Model setup, results and discussion, and biological application sections are included for each arrangement.

7.1 Parallel separators

7.1.1 Model setup

In a parallel arrangement, two separators are placed on the outflow of the tank to provide a parallel path for flow, as illustrated in Figure 7.1 and included in the level-rate diagram in Figure 7.2. Necessarily, there is a split in flow between the two separators such that the total water and solute outflows match the sum of the individual outflows, as in Equations 7.1 and 7.2.

$$Q_{out} = Q_{out,1} + Q_{out,2} \tag{7.1}$$

$$\dot{N}_{s,out} = \dot{N}_{s,out,1} + \dot{N}_{s,out,2} \tag{7.2}$$

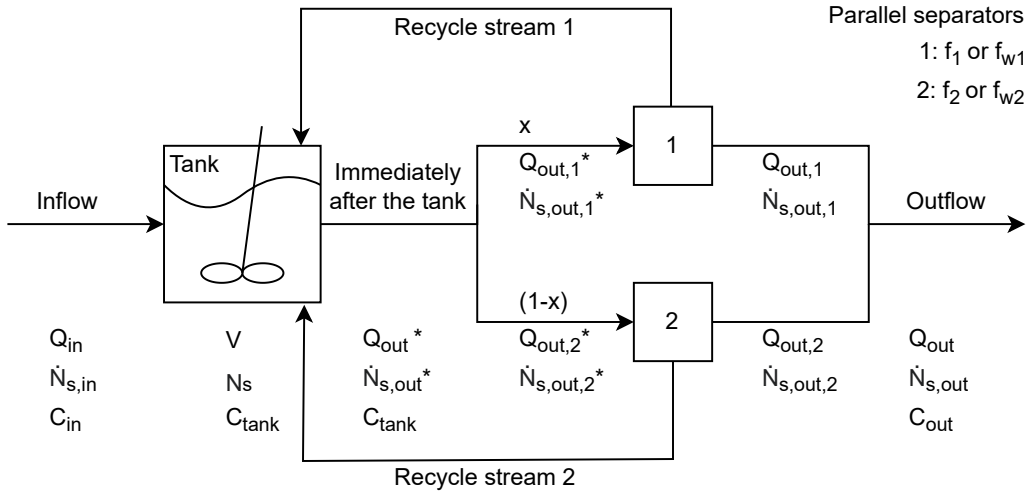


Fig. 7.1 Line diagram of tank setup for Design 4: Parallel separators; separator 1 is defined by f_1 or f_{w1} and separator 2 is defined by f_2 or f_{w2}, depending on the separator combination of choice

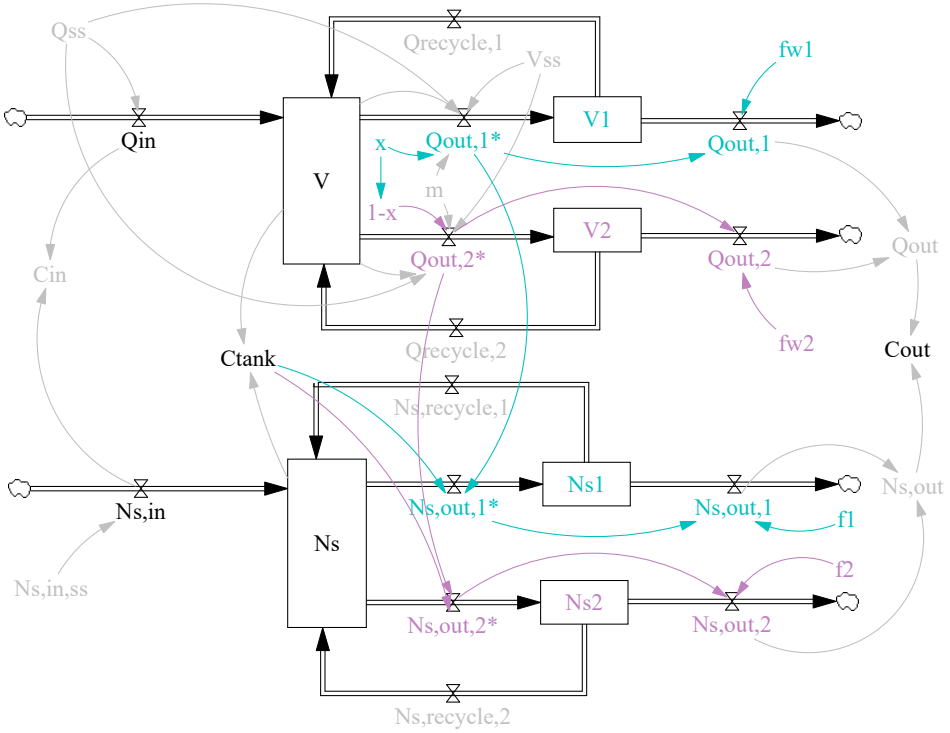


Fig. 7.2 Level-rate diagram for Design 4: Parallel water and solute separators; separator V_1 is defined by f_{w1}, V_2 by f_{w2}, N_{s1} by f_1 and N_{s2} by f_2

The total outflow concentration depends on both water and solute outflows according to Equation 7.3.

$$C_{out} = \frac{\dot{N}_{s,out}}{Q_{out}} = \frac{\dot{N}_{s,out,1} + \dot{N}_{s,out,2}}{Q_{out,1} + Q_{out,2}} \tag{7.3}$$

Solute separators

If the separators are both solute separators, then $f_{w1} = f_{w2} = 1$ in Figures 7.1 and 7.2, and the two individual water outflows are defined in Equations 7.4 and 7.5, where x represents the fractional flow to the first separator and $(1-x)$ the remaining fractional flow to the second separator. By definition, $x \in [0,1]$.

$$Q_{out,1} = Q^*_{out,1} = xQ_{out} \tag{7.4}$$

$$Q_{out,2} = Q^*_{out,2} = (1-x)Q_{out} \tag{7.5}$$

The corresponding solute outflows are defined in Equations 7.6 and 7.7, where f_1 and f_2 represent different bulk flow coefficients, emphasising different convective properties of the solute separators.

$$\dot{N}_{s,out,1} = f_1 \dot{N}^*_{s,out,1} = f_1 x Q_{out} C_{tank} \tag{7.6}$$

$$\dot{N}_{s,out,2} = f_2 \dot{N}^*_{s,out,2} = f_2 (1-x) Q_{out} C_{tank} \tag{7.7}$$

Therefore, the outflow concentration in Equation 7.3 can be expanded and simplified in Equation 7.8.

$$C_{out} = C_{tank}\left(f_1 x + f_2(1-x)\right) \tag{7.8}$$

If it is remembered that $f = \frac{C_{out}}{C_{tank}}$ from Equation 6.19 in Chapter 6, then it is possible to write Equation 7.9.

$$f = \frac{C_{out}}{C_{tank}} = f_1 x + f_2(1-x) \tag{7.9}$$

f can therefore be considered an effective or overall bulk flow coefficient for a "lumped" convective solute separator, and in this case, a transfer function across the system.

Water separators

If the separators are both water separators, then $f_1 = f_2 = 1$ in Figures 7.1 and 7.2, and the two individual water outflows are defined in Equations 7.10 and 7.11, where f_{w1} and f_{w2} represent different water reabsorption coefficients, emphasising different reabsorptive

properties of the water separators.

$$Q_{out,1} = f_{w1} Q^*_{out,1} = f_{w1} x Q^*_{out} \tag{7.10}$$

$$Q_{out,2} = f_{w2} Q^*_{out,2} = f_{w2} (1-x) Q^*_{out} \tag{7.11}$$

The corresponding solute outflows are defined in Equations 7.12 and 7.13.

$$\dot{N}_{s,out,1} = \dot{N}^*_{s,out,1} = x Q^*_{out} C_{tank} \tag{7.12}$$

$$\dot{N}_{s,out,2} = \dot{N}^*_{s,out,2} = (1-x) Q^*_{out} C_{tank} \tag{7.13}$$

Therefore, the outflow concentration in Equation 7.3 can be expanded and simplified in Equation 7.14.

$$C_{out} = C_{tank} \left(\frac{1}{f_{w1} x + f_{w2} (1-x)} \right) \tag{7.14}$$

If it is remembered that $\frac{1}{f_w} = \frac{C_{out}}{C_{tank}}$ from Equation 6.22 in Chapter 6, then it is possible to write Equation 7.15.

$$f_w = f_{w1} x + f_{w2} (1-x) \tag{7.15}$$

f_w can therefore be considered an effective or overall water reabsorption coefficient for a "lumped" water separator. Equation 7.16 details the transfer function across the system.

$$\frac{1}{f_w} = \frac{C_{out}}{C_{tank}} = \frac{1}{f_{w1} x + f_{w2} (1-x)} \tag{7.16}$$

Water and solute separators

If one of the separators is a solute separator and the other is a water separator, then $f_{w1} = 1$ and $f_2 = 1$ in Figures 7.1 and 7.2, and the two individual water outflows are defined in Equations 7.4 and 7.11 (repeated in Equations 7.17 and 7.18), where f_1 and f_{w2} quantify the different separation properties of the two separators, respectively.

$$Q_{out,1} = Q^*_{out,1} = x Q^*_{out} \tag{7.17}$$

$$Q_{out,2} = f_{w2} Q^*_{out,2} = f_{w2} (1-x) Q^*_{out} \tag{7.18}$$

The corresponding solute outflows are defined in Equations 7.6 and 7.13 (repeated in Equations 7.19 and 7.20).

$$\dot{N}_{s,out,1} = f_1 \dot{N}^*_{s,out,1} = f_1 x Q^*_{out} C_{tank} \tag{7.19}$$

$$\dot{N}_{s,out,2} = \dot{N}^*_{s,out,2} = (1-x)Q^*_{out}C_{tank} \tag{7.20}$$

Therefore, the outflow concentration in Equation 7.3 can be expanded and simplified in Equation 7.21, with transfer function in Equation 7.22.

$$C_{out} = C_{tank}\left(\frac{f_1 x + (1-x)}{x + f_{w2}(1-x)}\right) \tag{7.21}$$

$$\frac{f}{f_w} = \frac{C_{out}}{C_{tank}} = \frac{f_1 x + (1-x)}{x + f_{w2}(1-x)} \tag{7.22}$$

f_{w1} and f_2 could similarly have been chosen to quantify the different separation properties of the parallel separators, in which case $f_1 = 1$ and $f_{w2} = 1$ in Figures 7.1 and 7.2, and the transfer function in Equation 7.23 would have held.

$$\frac{f}{f_w} = \frac{C_{out}}{C_{tank}} = \frac{x + f_2(1-x)}{f_{w1}x + (1-x)} \tag{7.23}$$

In summary, Table 7.1 shows the transfer functions for the three parallel arrangements.

Table 7.1 Design 4 transfer functions (parallel separators)

Separators	Transfer function	Reference
Solute	$f = f_1 x + f_2(1-x)$	Equation 7.9
Water	$\frac{1}{f_w} = \frac{1}{f_{w1}x + f_{w2}(1-x)}$	Equation 7.16
Water and solute	$\frac{f}{f_w} = \frac{f_1 x + (1-x)}{x + f_{w2}(1-x)}$	Equation 7.22
	or $\frac{f}{f_w} = \frac{x + f_2(1-x)}{f_{w1}x + (1-x)}$	Equation 7.23

When water separators are involved, the immediate outflow of the tank, Q^*_{out}, is given by Equation 7.24 (as introduced for a water separator in Section 6.1.2 in Chapter 6).

$$Q^*_{out} = \frac{Q_{ss}}{f_w} + m(V(t) - V_{ss}) \tag{7.24}$$

The coupled ODEs for all three scenarios (substituting in appropriate f and f_w) follow in Equations 7.25 and 7.26 (written in standard linear form in Appendix A.4.4).

$$\frac{dV}{dt} = Q(t) - (Q_{ss} + f_w m(V(t) - V_{ss})) \tag{7.25}$$

$$\frac{dN_s}{dt} = \frac{dC_{tank}V}{dt} = \dot{N}_{s,in}(t) - fC_{tank}(t)(\frac{1}{f_w}Q_{ss} + mV(t) - V_{ss}) \tag{7.26}$$

Table 7.2 Design 4 Model Parameters (Parallel separators)

Parameter	Value
Baseline water inflow (ml/hr)	100
Baseline solute inflow (mosm/hr)	28.1
Desired steady-state volume (ml)	1 000
m (1/hr)	1
f_1	> 0
f_2	> 0
f_{w1}	0 - 1
f_{w2}	0 - 1
x	0 - 1

The model parameters are included in Table 7.2.

7.1.2 Results and Discussion

It is clear from Equations 7.25 and 7.26 and Appendix A.4.4 that adding multiple linear and negligible volume solute and water separators in parallel on the outflow of the tank has no effect on the system of ODEs that governs overall model behaviour. The different combinations of separators simply change the values of the overall bulk flow and water reabsorption coefficients (f and f_w, respectively). This means that a model with multiple separators is over-parameterised because many combinations of model parameters can yield the same results. It is only through comparison with biological excretory system structure and function that such a level of model development makes sense.

Solute separators

If $f_w = 1$ in Equations 7.25 and 7.26, the ODEs match those of solute separation in Design 3 (i.e. Equations 6.9 and 6.10 in Section 6.1.1). Therefore, when considering parallel solute separators, the same solutions (both numerically-simulated and analytically-derived) hold for the tank quantities as in Design 3 (solute separation) in Section 6.2.2, and it is unnecessary to repeat the transient analysis. It is, however, interesting to see how the presence of a second, parallel solute separator (f_2) changes the steady-state behaviour of the system depending on flow split x compared to the previous Design 3 (Section 6.2.2 in Chapter 6) (assuming the single solute separator is described by f_1).

Focusing on Equation 7.9, it is possible to analyse the effects of x, f_1 and f_2 on f. When $x = 0$, $f = f_2$, and when $x = 1$, $f = f_1$, such that $f \in [f_1, f_2]$ when $x \in [0, 1]$. This is illustrated

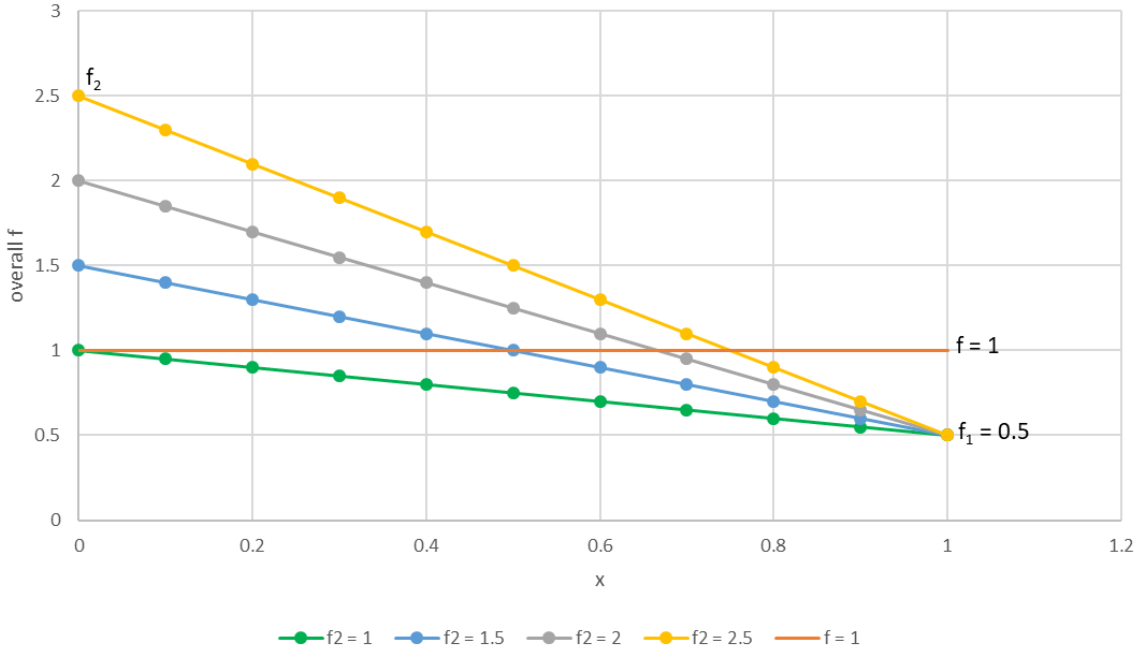


Fig. 7.3 Design 4 (Parallel solute separators) Overall f versus x for fixed $f_1 = 0.5$ and a range of f_2

in Figure 7.3 for fixed $f_1 = 0.5$ and a range of $f_2 > 1$. It is noteworthy that this is simply an example; the values of f_1 and f_2 are theoretically positive but unlimited (i.e. $f_1 > 0$ and $f_2 > 0$) and only restricted through the particular modelling application, as motivated below.

Considering the same Equation 7.9, Figure 7.4 shows the corresponding effect on the relationship between C_{tank} and C_{out} at steady-state (remembering that C_{out} is fixed by C_{in}, which has been arbitrarily chosen to be 0.281 mosm/ml).

It is clear that the values of f_1 and f_2 determine the extremes of overall f and consequently, the concentrating limits available to the parallel setup. For overall tank concentrating and diluting relative to the outflow to be possible, one branch of the parallel setup needs to have a bulk flow coefficient such that $C_{tank} > C_{out}$ (e.g. $f_1 < 1$ in this case) and the other such that $C_{tank} < C_{out}$ (e.g. $f_2 > 1$ in this case). If f_1 and f_2 are chosen to be close together in value, the gradient of the overall f versus x curve is shallower and the concentrating/diluting ability is limited, while if f_1 and f_2 are chosen to be far apart, the concentrating/diluting ability is more pronounced. The intersection at $C_{tank} = C_{out}$ (i.e. $f = 1$ in this case) indicates where the tank concentration changes from concentrated to dilute (or vice versa) relative to the fixed outflow concentration, and this differs with x depending on the choices of f_1 and f_2. Another way of looking at this is that the bigger the difference between f_1 and f_2, the more sensitive overall f is to x, and consequently, the smaller the change in x (both from 1 and in

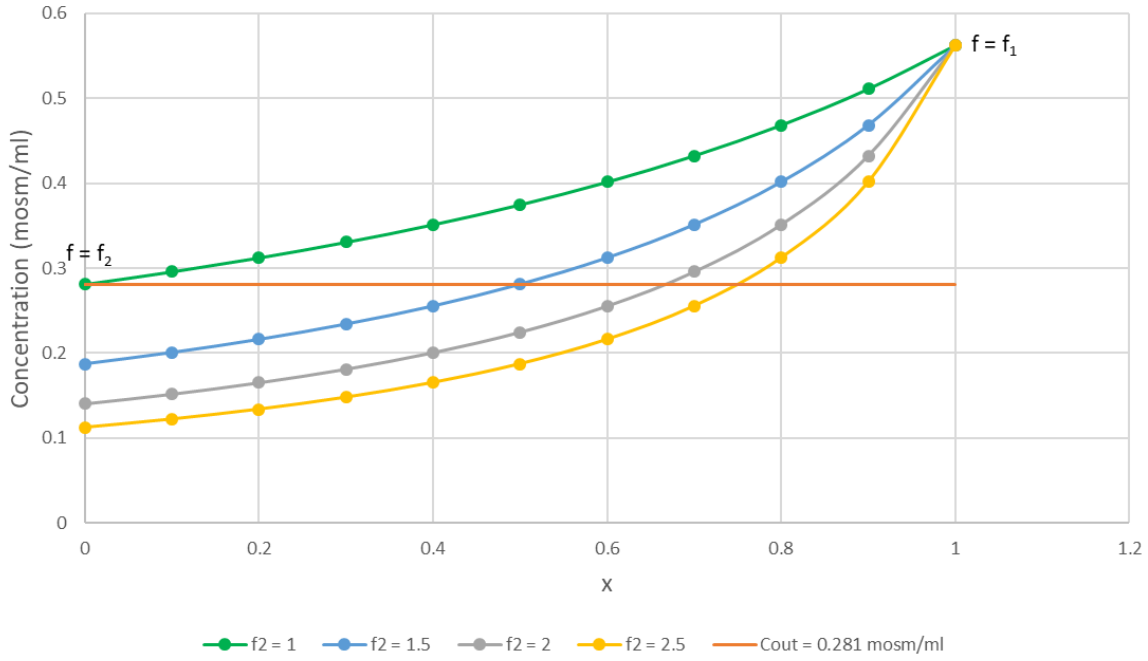


Fig. 7.4 Design 4 (Parallel solute separators) Tank and outflow concentrations vs x for fixed $f_1 = 0.5$ and a range of f_2

the region around $f = 1$ in this case) required to change the concentrating behaviour of the tank relative to the outflow. This has the added benefit of providing preferential paths for transient diluting- and concentrating-disturbance handling.

Water separators

If $f = 1$ in Equations 7.25 and 7.26, the ODEs match those of water separation in Design 3 (i.e. Equations 6.17 and 6.18 in Section 6.1.2). Therefore, when considering parallel water separators, the same solutions (both numerically-simulated and analytically-derived) hold for the tank quantities as in Design 3 (water separation) in Section 6.2.2, and it is unnecessary to repeat the transient analysis. It is, however, interesting to see how the presence of a second, parallel water separator (f_{w2}) changes the steady-state behaviour of the system depending on flow split x compared to previous Design 3 (assuming the single solute separator is described by f_{w1}).

Focusing on Equation 7.15, it is possible to analyse the effects of x, f_{w1} and f_{w2} on f_w. When $x = 0$, $f_w = f_{w2}$, and when $x = 1$, $f_w = f_{w1}$, such that $f_w \in [f_{w1}, f_{w2}]$ when $x \in [0, 1]$. This is illustrated in Figure 7.5 for fixed $f_{w1} = 0.8$ and a range of $f_{w2} < 1$.

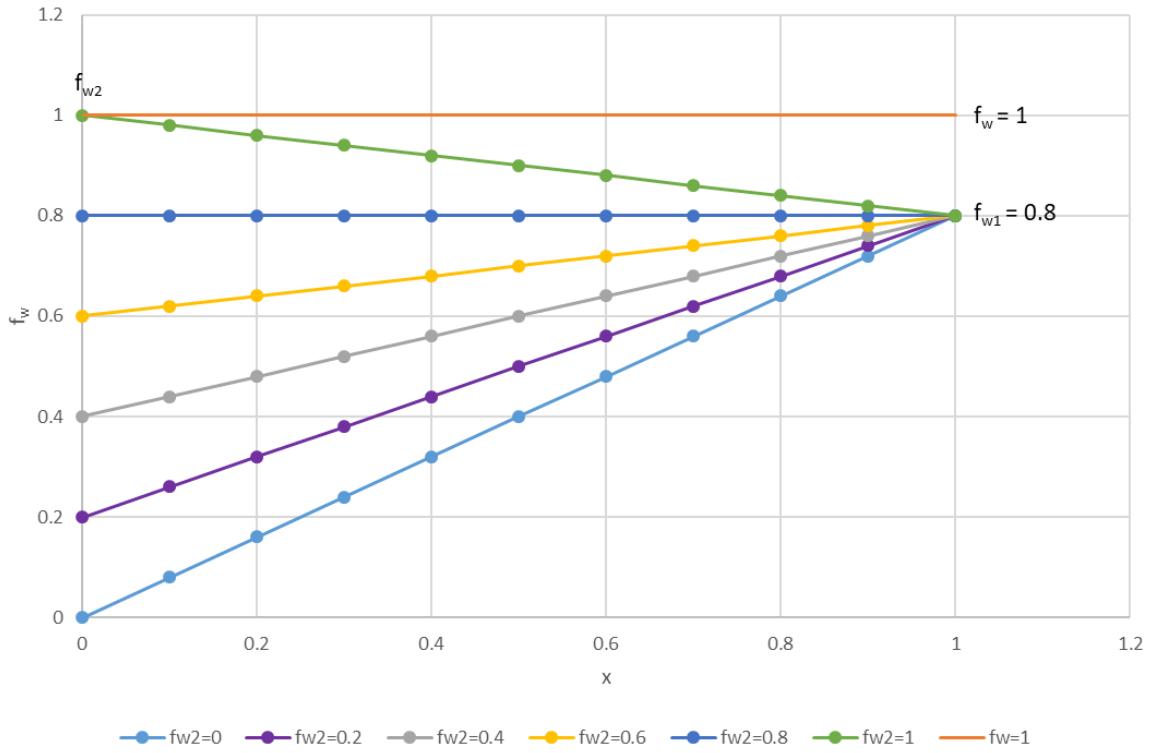


Fig. 7.5 Design 4 (Parallel water separators) Overall f_w versus x for fixed $f_{w1} = 0.8$ and a range of $0 < f_{w2} < 1$

Considering Equation 7.14, Figure 7.6 shows the corresponding effect on the relationship between C_{tank} and C_{out} at steady-state (remembering that C_{out} is fixed by C_{in}, which has been arbitrarily chosen to be 0.281 mosm/ml).

It is clear that the values of f_{w1} and f_{w2} determine the extremes of overall f_w and consequently, the concentrating limits available to the parallel setup. As x is changed, f_w accommodates an x-weighted contribution from f_{w1} and $(1-x)$-weighted contribution from f_{w2}. Unlike the inverse relationship in solute separation, the tank concentration depends linearly on x (due to the relationship in Equation 7.14). It is obvious that employing water separators alone always yields a tank diluting setup relative to the outflow (i.e. $C_{tank} < C_{out}$) since $f_w \leq 1$.

Water and solute separators

A combination of water and solute separation on the outflow of the tank has not been considered until this point in the design. However, it is clear from the system ODEs in Equations 7.25 and 7.26 (written in standard linear form in Appendix A.4.4), that aspects of both water separation and solute separation are simply combined and it is therefore

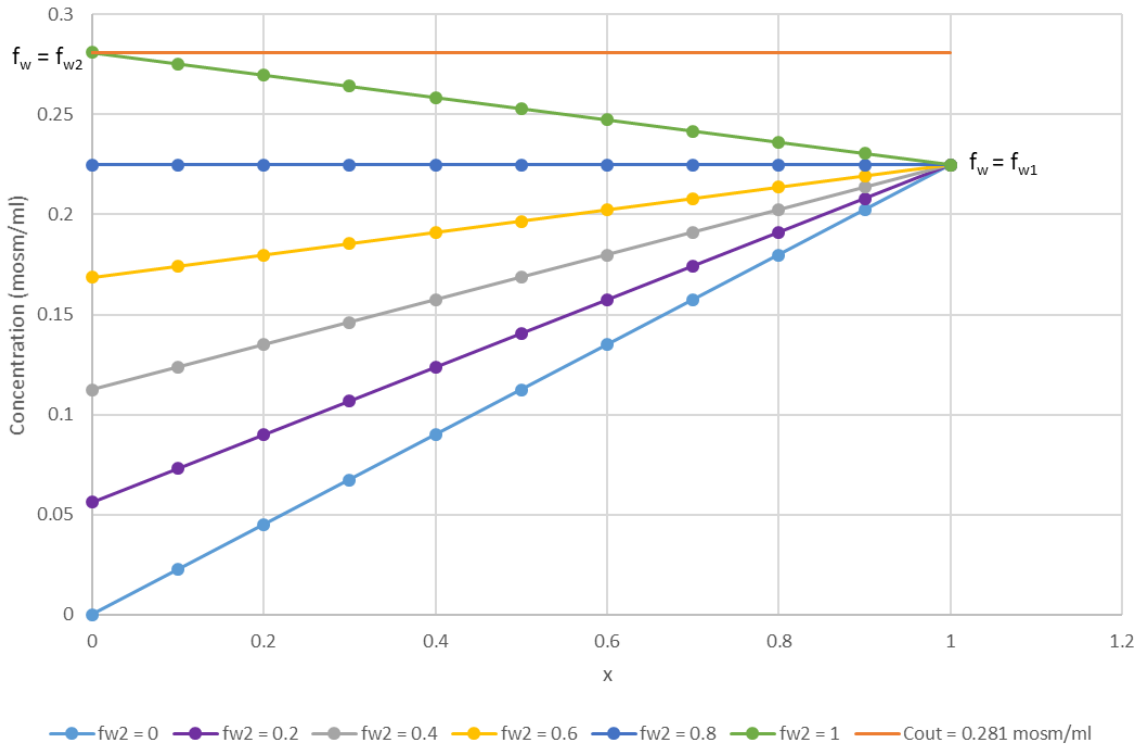


Fig. 7.6 Design 4 (Parallel water separators) Tank and outflow concentrations vs x for fixed $f_{w1} = 0.8$ and a range of $0 < f_{w2} < 1$

unnecessary to perform exhaustive numerical simulation and analysis. The general analytical solution of Appendix A.5.5 is summarised here.

The tank volume response follows that of simple water separation in Section 6.2.2 in Chapter 6, through Equation 7.27, where V_0 depends on the type of disturbance (water or solute), and steady-state volume and valve response time Equations 7.28 and 7.29, respectively. The tank concentration response has mean residence time τ in Equation 7.30, dependent on both f_w and f.

$$V(t) = V_{ss} + (V_0 - V_{ss})e^{-\frac{t}{\tau_V}} \tag{7.27}$$

$$V_{ss} = V_{dss} + \frac{Q_{ss}(1-f_w)}{f_w} \tag{7.28}$$

$$\tau_V = \frac{1}{f_w m} \tag{7.29}$$

$$\tau = \frac{f_w}{f}\frac{V_{ss}}{Q_{ss}} \tag{7.30}$$

As for previous designs, the particular analytical solutions in Appendix A.5.5 show that the dynamic response of the tank concentration to a solute impulse disturbance depends on τ, while that to a water impulse disturbance depends on τ and τ_V.

Considering the steady-state response and focusing on Equation 7.22, it is possible to analyse the effects of x, f_1 and f_{w2} on transfer function $\frac{f}{f_w}$. When $x = 0$, $\frac{f}{f_w} = \frac{1}{f_{w2}}$, and when $x = 1$, $\frac{f}{f_w} = f_1$, such that $\frac{f}{f_w} \in [f_1, f_{w2}]$ when $x \in [0,1]$. This is illustrated in Figure 7.7 for $f_1 = 0.5$ and a range of $f_{w2} < 1$.

Figure 7.8 shows the corresponding effect of varying x on the relationship between C_{tank} and C_{out} at steady-state (remembering that C_{out} is fixed by C_{in}, which has been arbitrarily chosen to be 0.281 mosm/ml).

It is clear that the values of f_1 and $\frac{1}{f_{w2}}$ determine the extremes of transfer function $\frac{f}{f_w}$ and consequently, the tank concentrating limits available to the parallel setup. The combination clearly allows for tank dilution and concentration relative to the outflow depending on the value of x (but only if $f_1 < 1$ in the first place).

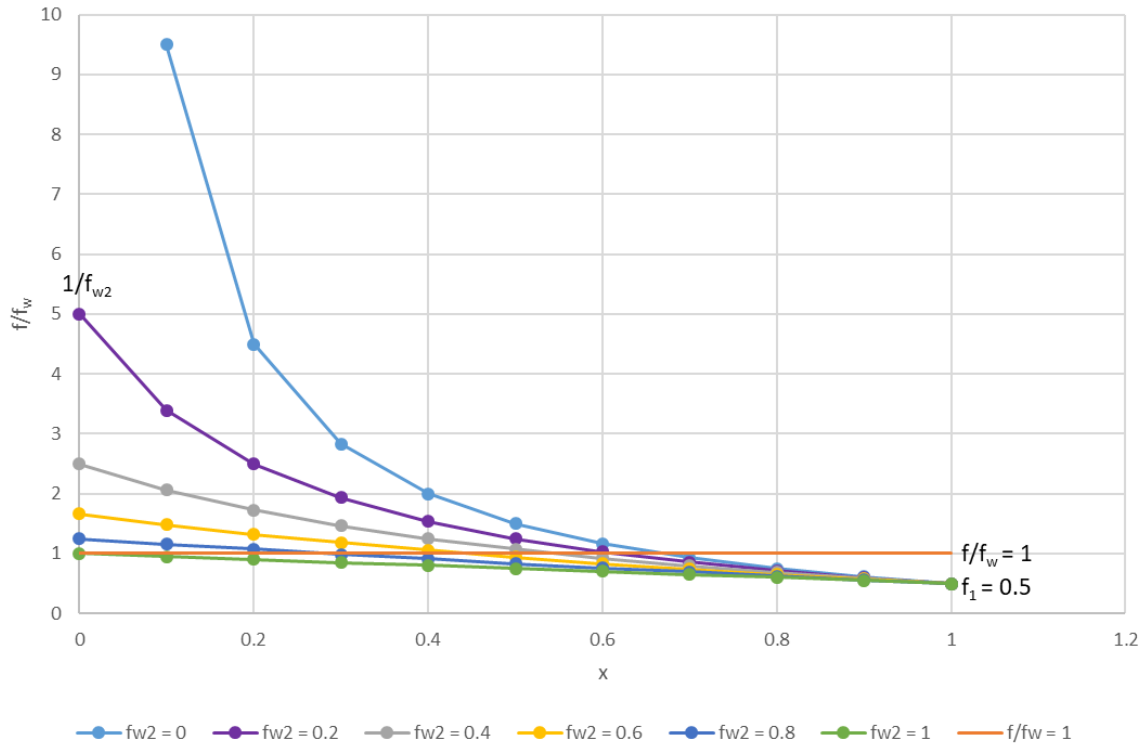


Fig. 7.7 Design 4 (Parallel water and solute separators) Transfer function $\frac{f}{f_w}$ versus x for fixed $f_1 = 0.5$ and a range of f_{w2}

7.1.3 Biological application

A new overall bulk flow or water reabsorption coefficient is established when separators are placed in parallel with flow split between them. The new arrangement may have very different behaviour when compared with the original single separator, depending on the values of the individual bulk flow or water reabsorption coefficients. Considering parallel solute separators, it is possible to change a diluting setup to a concentrating one and vice versa, depending on the choice of bulk flow coefficients and relative flow. In comparison, parallel water separators can only dilute the tank relative to the outflow. However, at this stage, the new behaviour is fixed.

The values of the individual bulk flow or water reabsorption coefficients f_1 and f_2 or f_{w1} and f_{w2}, respectively, set the theoretical diluting and concentrating limits of the parallel setup since the flow between them is conserved. If a solute separator is chosen to cause a concentrating effect on the tank relative to the outflow (i.e. $f_1 < 1$) and a parallel solute or parallel water separator is chosen to cause a diluting effect (i.e. $f_2 > 1$ or $f_{w2} < 1$, respectively), then, not only can all concentration combinations in between be achieved but according to model results, paths for preferential transient water and solute handling,

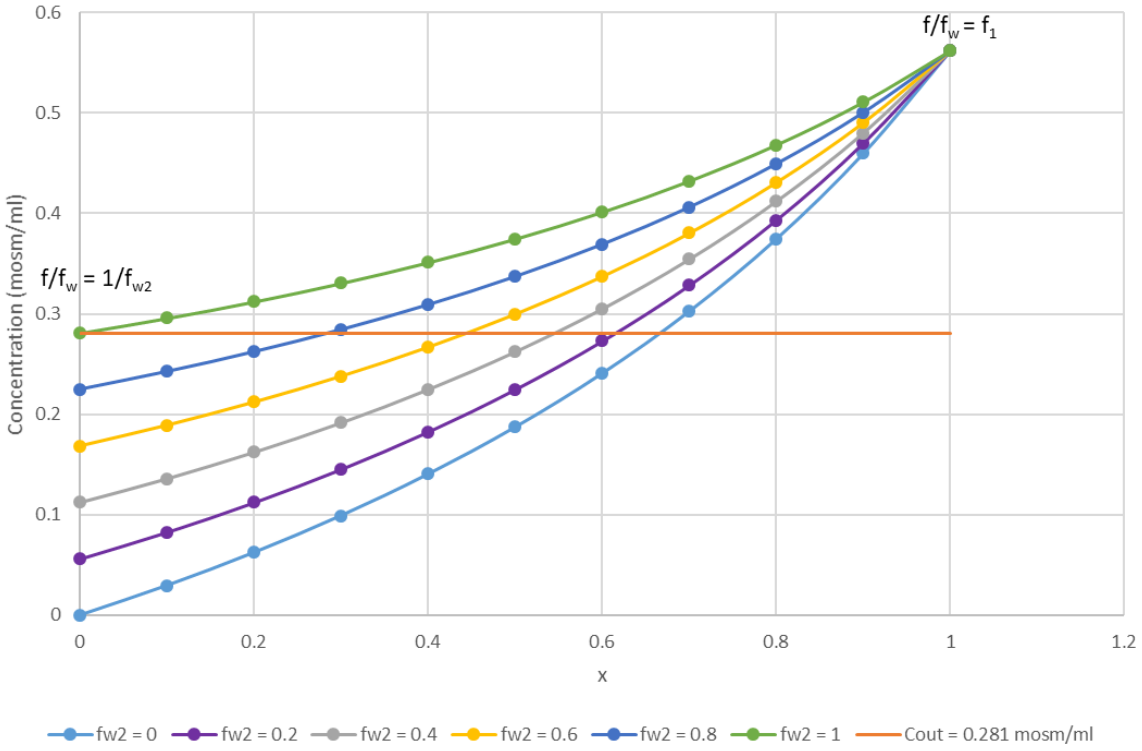


Fig. 7.8 Design 4 (Parallel water and solute separators) Tank and outflow concentrations vs x for fixed $f_1 = 0.5$ and a range of f_{w2}

respectively, will have been provided that depend on the choice of relative flow between separators.

Birds, the only kind of animal other than mammals that is able to produce concentrated urine [16], are known to have two distinct populations of nephrons in their kidneys (reptilian-type and mammalian-type[81]), with the looped mammalian-type nephrons deep to the loopless reptilian-type nephrons [81]. During times of dehydration, reptilian-type nephrons are essentially turned off (receiving significantly diminished flow) while mammalian-type nephrons remain on and concentrated urine is produced, compared to times of over-hydration, when the majority of flow passes through the reptilian-type non-concentrating nephrons and dilute urine results [81, 20]. Ignoring the obvious need for control of the variable flow between nephron populations for now, it is interesting to note the similarities between bird kidneys and the parallel separator arrangement with $f_1 < 1$ and $f_2 > 1$ or $f_{w2} < 1$ - both providing two extremes of concentrating ability; i.e. dilute and concentrated, depending on which population of nephrons (or separator) is "turned on".

7.2 Series separators

7.2.1 Model setup

In a series arrangement, two separators are placed on a single outflow from the tank as illustrated in Figure 7.9 and modelled in the level-rate diagram in Figure 7.10. The order of separation is not important because the system is linear. The superscript ** refers to quantities between the separators.

Solute separators

If the separators are both solute separators defined by f_1 and f_2 (i.e. $f_{w1} = f_{w2}$), the water outflow is defined in Equation 7.31, and the solute outflow in Equation 7.32.

$$Q_{out} = Q^{**}_{out} = Q^{*}_{out} \tag{7.31}$$

$$\dot{N}_{s,out} = f_2 \dot{N}^{**}_{s,out} = f_2 f_1 \dot{N}^{*}_{s,out} = f_1 f_2 C_{tank} Q^{*}_{out} \tag{7.32}$$

The outflow concentration is therefore given by Equation 7.33, which can be rewritten as a an effective or overall bulk flow coefficient for a "lumped" solute separator (and in this case,

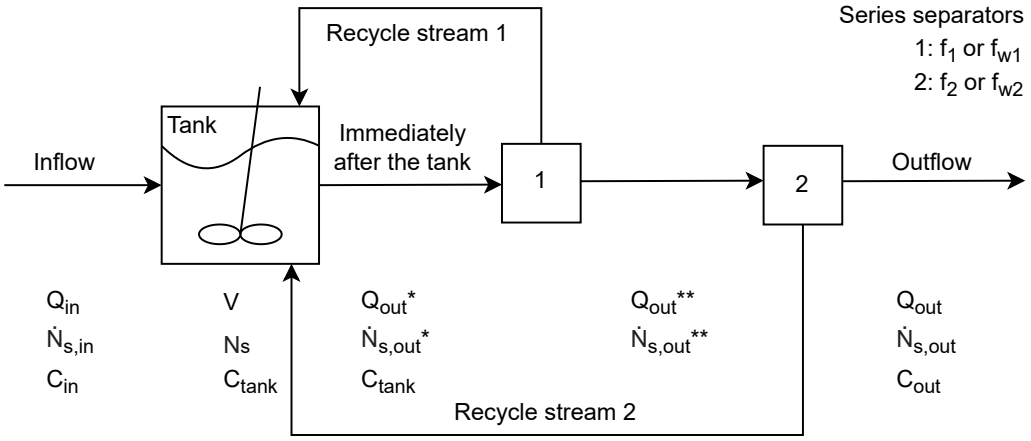


Fig. 7.9 Line diagram of tank setup for Design 4: Series separators; separator 1 is defined by f_1 or f_{w1} and separator 2 is defined by f_2 or f_{w2}, depending on the separator combination of choice

transfer function across the system) in Equation 7.34.

$$C_{out} = \frac{\dot{N}_{s,out}}{Q_{out}} = f_1 f_2 C_{tank} \tag{7.33}$$

$$f = \frac{C_{out}}{C_{tank}} = f_1 f_2 \tag{7.34}$$

Water separators

If the separators are both water separators defined by f_{w1} and f_{w2} (i.e. $f_1 = f_2 = 1$), the water outflow is defined in Equation 7.35, and the solute outflow in Equation 7.36.

$$Q_{out} = f_{w2} Q^{**}_{out} = f_{w2} f_{w1} Q^{*}_{out} \tag{7.35}$$

$$\dot{N}_{s,out} = \dot{N}^{**}_{s,out} = \dot{N}^{*}_{s,out} = C_{tank} Q^{*}_{out} \tag{7.36}$$

The outflow concentration is therefore given by Equation 7.37, where the effective water reabsorption coefficient describing a "lumped" water separator is given by Equation 7.38.

$$C_{out} = \frac{\dot{N}_{s,out}}{Q_{out}} = \frac{C_{tank}}{f_{w1} f_{w2}} \tag{7.37}$$

$$f_w = f_{w1} f_{w2} \tag{7.38}$$

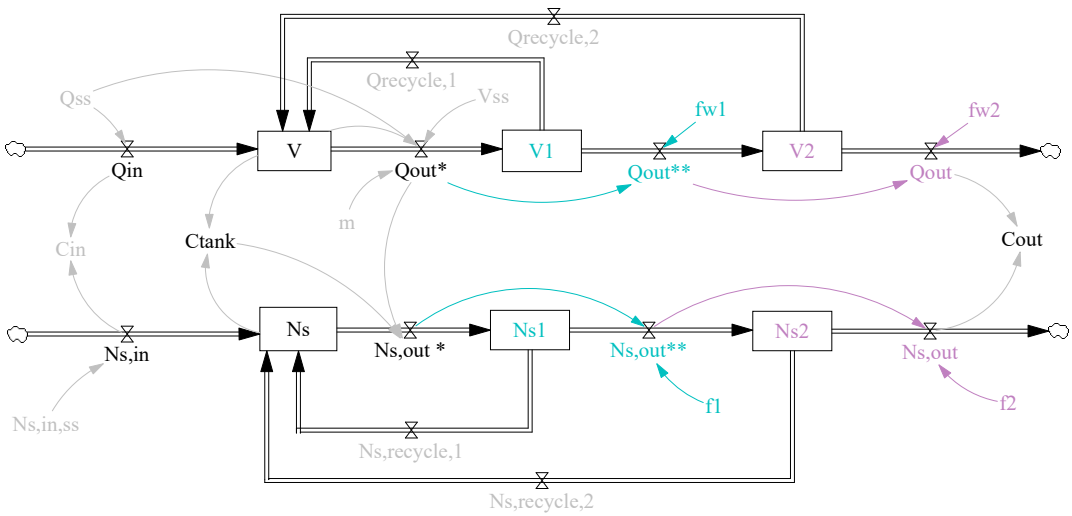


Fig. 7.10 Level-rate diagram for Design 4: Series separators; separator V_1 is defined by f_{w1}, V_2 by f_{w2}, N_{s1} by f_1 and N_{s2} by f_2

The transfer function across the system is given by Equation 7.39.

$$\frac{1}{f_w} = \frac{C_{out}}{C_{tank}} = \frac{1}{f_{w1} f_{w2}} \tag{7.39}$$

Water and solute separators

If one of the separators is a solute separator defined by f_1 and the other is a water separator defined by f_{w2} (i.e. $f_2 = f_{w1} = 1$), the water outflow is defined in Equation 7.40, and the solute outflow in Equation 7.41.

$$Q_{out} = f_{w2} Q^{**}_{out} = f_{w2} Q^{*}_{out} \tag{7.40}$$

$$\dot{N}_{s,out} = \dot{N}^{**}_{s,out} = f_1 \dot{N}^{*}_{s,out} = f_1 C_{tank} Q^{*}_{out} \tag{7.41}$$

The outflow concentration is therefore given by Equation 7.42, which can be rewritten in Equation 7.43 as a transfer function across the separators, in terms of the constituent separator

parameters.

$$C_{out} = \frac{\dot{N}_{s,out}}{Q_{out}} = \frac{f_1}{f_{w2}} C_{tank} \tag{7.42}$$

$$\frac{f}{f_w} = \frac{C_{out}}{C_{tank}} = \frac{f_1}{f_{w2}} \tag{7.43}$$

f_2 and f_{w1} could similarly have been chosen to quantify the different separation properties of the series separators (i.e. $f_1 = f_{w2} = 1$), in which case, the transfer function in Equation 7.44 would have held.

$$\frac{f}{f_w} = \frac{C_{out}}{C_{tank}} = \frac{f_2}{f_{w1}} \tag{7.44}$$

Noteworthy is the fact that the order of the separators is not important due to linearity of the system, and the fact that the separators are working on the same outflow stream.

In summary, Table 7.3 shows the transfer functions for the three series arrangements.

Table 7.3 Design 4 transfer functions (series separators)

Separators	Transfer function	Reference
Solute	$f = f_1 f_2$	Equation 7.34
Water	$\frac{1}{f_w} = \frac{1}{f_{w1} f_{w2}}$	Equation 7.39
Water and solute	$\frac{f}{f_w} = \frac{f_1}{f_{w2}}$	Equation 7.43

When water separators are involved, the immediate outflow of the tank, Q^*_{out}, is given by Equation 7.45 (as introduced for a water separator in Section 6.1.2 in Chapter 6).

$$Q^*_{out} = \frac{Q_{ss}}{f_w} + m(V(t) - V_{ss}) \tag{7.45}$$

The coupled ODEs for all three scenarios (substituting in appropriate f and f_w) follow in Equations 7.46 and 7.47 (written in standard linear form in Appendix A.4.4).

$$\frac{dV}{dt} = Q(t) - (Q_{ss} + f_w m(V(t) - V_{ss})) \tag{7.46}$$

$$\frac{dN_s}{dt} = \frac{dC_{tank}V}{dt} = \dot{N}_{s,in}(t) - fC_{tank}(t)(\frac{1}{f_w} Q_{ss} + mV(t) - V_{ss}) \tag{7.47}$$

The model parameters are included in Table 7.4.

Table 7.4 Design 4 Model Parameters (Series)

Parameter	Value
Baseline water inflow (ml/hr)	100
Baseline solute inflow (mosm/hr)	28.1
Steady-state volume (ml)	1 000
m (1/hr)	1
f_1	> 0
f_2	> 0
f_{w1}	0 - 1
f_{w2}	0 - 1

7.2.2 Results and Discussion

As for parallel separators, it is clear from Equations 7.46 and 7.47 and Appendix A.4.4 that adding multiple linear and negligible volume solute and water separators in series on the outflow of the tank has no effect on the system of ODEs that governs overall model behaviour. The different combinations of separators simply change the values of the overall bulk flow and water reabsorption coefficients (f and f_w, respectively). Such a series model is over-parameterised and it is only through comparison with biological excretory system structure and function that such a level of model development makes sense.

Solute separators

If $f_w = 1$ in Equations 7.46 and 7.47, the ODEs match those of solute separation in Design 3 (i.e. Equations 6.9 and 6.10 in Section 6.1.1).

Therefore, when considering series solute separators, the same solutions to the ODEs in Equations 7.46 and 7.47 (both numerically-simulated and analytically-derived) hold for the tank quantities as in Design 3 (solute separation) in Section 6.2.2, and it is unnecessary to repeat the transient analysis.

It is, however, necessary to comment on how the presence of a second, series solute separator (f_2) changes the steady-state behaviour of the system compared to the previous Design 3 (Section 6.2.2 in Chapter 6) (assuming the single solute separator is described by f_1). To this end, Equation 7.34 shows that the overall bulk flow coefficient f in series solute separation is the product of f_1 and f_2.

Figure 7.11 illustrates the relationship between f and f_2 for a range of f_1. Since there is no restriction on the value of a bulk flow coefficient (other than $f > 0$), the presence of f_2 can increase or decrease overall f linearly relative to that of Design 3 (a special case of Design 4 where $f_2 = 1$ and $f = f_1$), depending on the value of f_2.

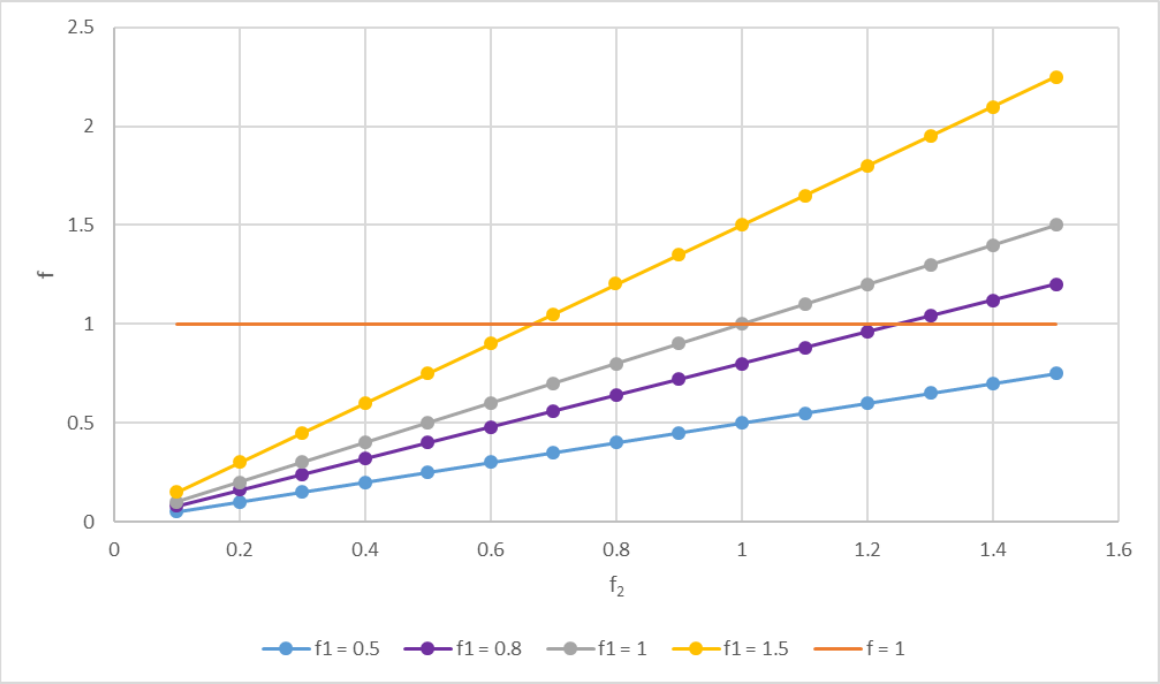


Fig. 7.11 Design 4 (Series solute separators) Overall f versus f_2 for a range of f_1

Figure 7.12 shows the corresponding effect on C_{tank} for constant C_{out}. It is therefore possible to counteract the separating effect of f_1 with f_2 (anywhere the curves intersect with the $f = 1$ line). It is important to remember that f_2 is static and f cannot be adjusted dynamically in a series setup.

Water separators

If $f = 1$ in Equations 7.46 and 7.47, the ODEs match those of water separation in Design 3 (i.e. Equations 6.17 and 6.18 in Section 6.1.2). Therefore, when considering series water separators, the same solutions (both numerically-simulated and analytically-derived) hold for the tank quantities as in Design 3 (water separation) in Section 6.2.2, and it is unnecessary to repeat the transient analysis.

It is, however, necessary to comment on how the presence of a second, series water separator (f_{w2}) changes the steady-state behaviour of the system compared to the previous Design 3 (Section 6.2.2 in Chapter 6) (assuming the single water separator is described by f_{w1}). To this end, Equation 7.38 shows that the overall water reabsorption coefficient f_w in series water separation is the product of f_{w1} and f_{w2}.

This is illustrated in Figure 7.13. Since water reabsorption coefficients are restricted to $0 < f_w < 1$, the presence of $f_{w2} < 1$ can only decrease overall f_w relative to that of Design 3

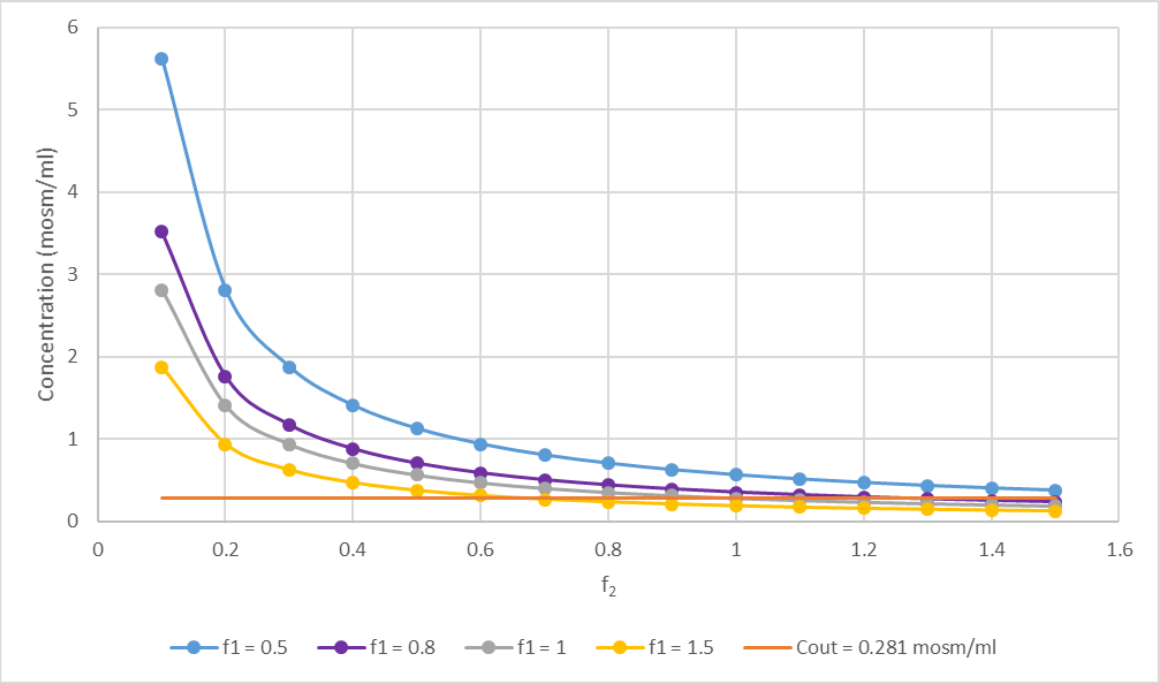


Fig. 7.12 Design 4 (Series solute separators) Tank and outflow concentrations vs f_2 for a range of f_1

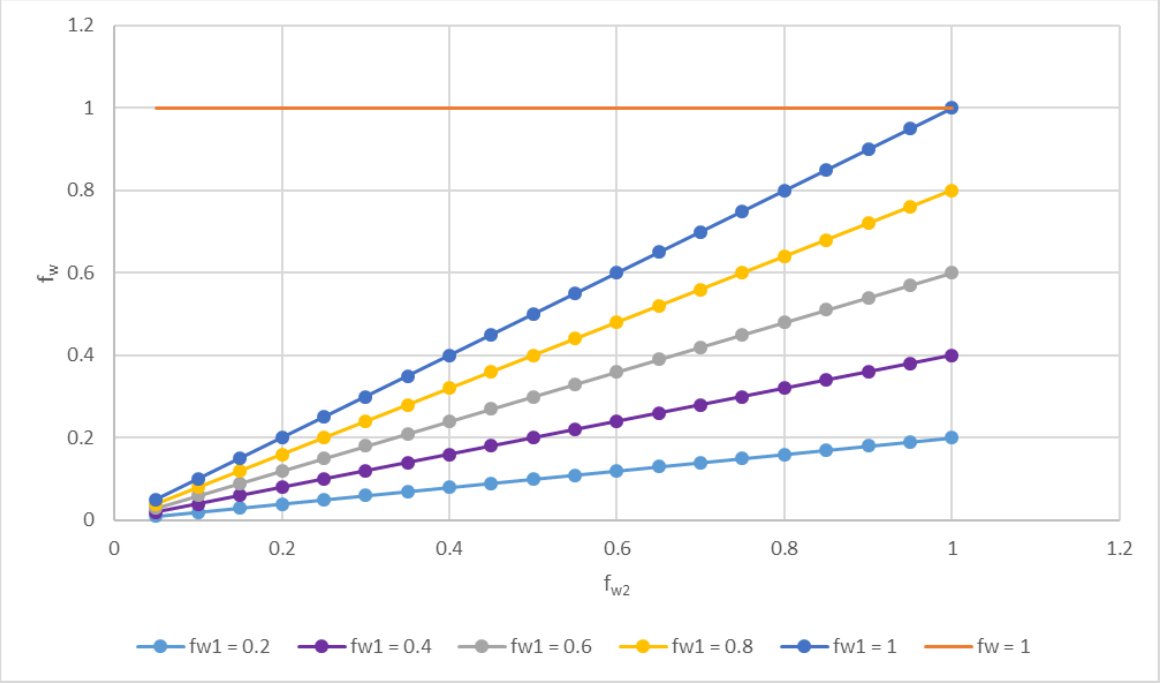


Fig. 7.13 Design 4 (Series water separators) Overall f_w versus f_{w2} for a range of f_{w1}

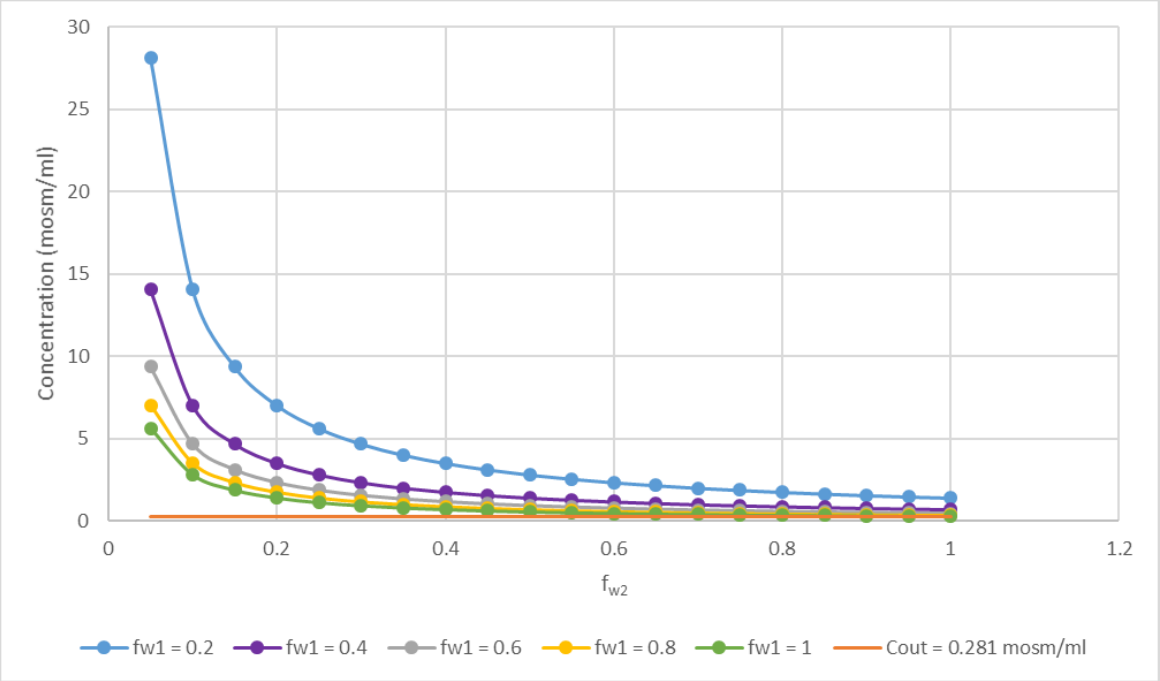


Fig. 7.14 Design 4 (Series water separators) Tank and outflow concentrations vs f_{w2} for a range of f_{w1}

(a special case of Design 4 where $f_{w2} = 1$ and $f_w = f_{w1}$). This is seen to concentrate the tank further relative to the outflow in all cases in Figure 7.14. It remains important to comment that f_{w2} is static and f_w cannot be adjusted dynamically in a series setup.

Water and solute separators

Combining water and solute separators in series on the outflow of the tank results in the system of ODEs in Equations 7.25 and 7.26 (written in standard linear form in Appendix A.4.4); the same as for the parallel combination in Section 7.1.1. This is not surprising as the only difference between the parallel and series water-and-solute separator setups is how f and f_w are made up. The general analytical solutions are identical (Appendix A.5.5 and Section 7.1.2) and repeated here. The tank volume response follows that of water separation in Section 6.2.2 in Chapter 6, through Equations 7.48, 7.49 and 7.50, while the tank concentration response has mean residence time τ in Equation 7.51, dependent on both f_w and f.

$$V(t) = V_{ss} + (V_0 - V_{ss})e^{-\frac{t}{\tau_V}} \tag{7.48}$$

$$V_{ss} = V_{dss} + \frac{Q_{ss}(1 - f_w)}{f_w} \tag{7.49}$$

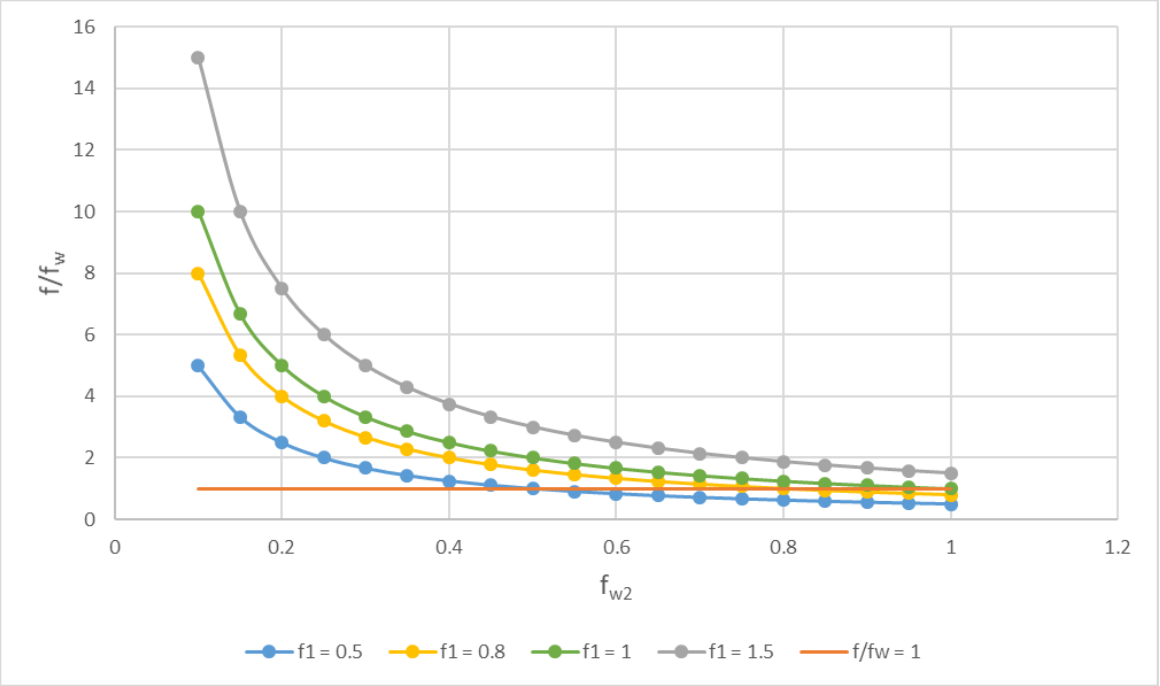


Fig. 7.15 Design 4 (Series water and solute separators) $\frac{f}{f_w}$ versus f_{w2} for a range of f_1

$$\tau_V = \frac{1}{f_w m} \tag{7.50}$$

$$\tau = \frac{f_w}{f}\frac{V_{ss}}{Q_{ss}} \tag{7.51}$$

As for previous designs, the particular analytical solutions in Appendix A.5.5 show that the dynamic response of the tank concentration to a solute impulse disturbance depends on τ, while that to a water impulse disturbance depends on τ and τ_V.

Considering the steady-state response and focusing on Equation 7.43 (which is simply the product of the individual separator transfer functions), it is possible to analyse the effects of f_1 and f_{w2} on transfer function $\frac{f}{f_w}$. This is illustrated in Figure 7.15 for a range of $f_1 > 0$ and $0 < f_{w2} < 1$.

Figure 7.16 shows the corresponding effect on C_{tank} for constant C_{out}. It is seen that the contribution of $f_{w2} < 1$ is to dilute the tank relative to that of Design 3 (solute separation) where $f_{w2} = 1$ and $\frac{f}{f_w} = f_1$. If f_{w2} is chosen carefully (i.e. smaller than $\frac{1}{f_1}$) and if $f_1 < 1$ (i.e. $C_{tank} > C_{out}$), a transition from the tank being more concentrated to being less concentrated than the outflow, can be made. It is clear from Figure 7.16 that the value of $f_1 < 1$ determines how easy it is to transition from the tank being more concentrated to being less concentrated

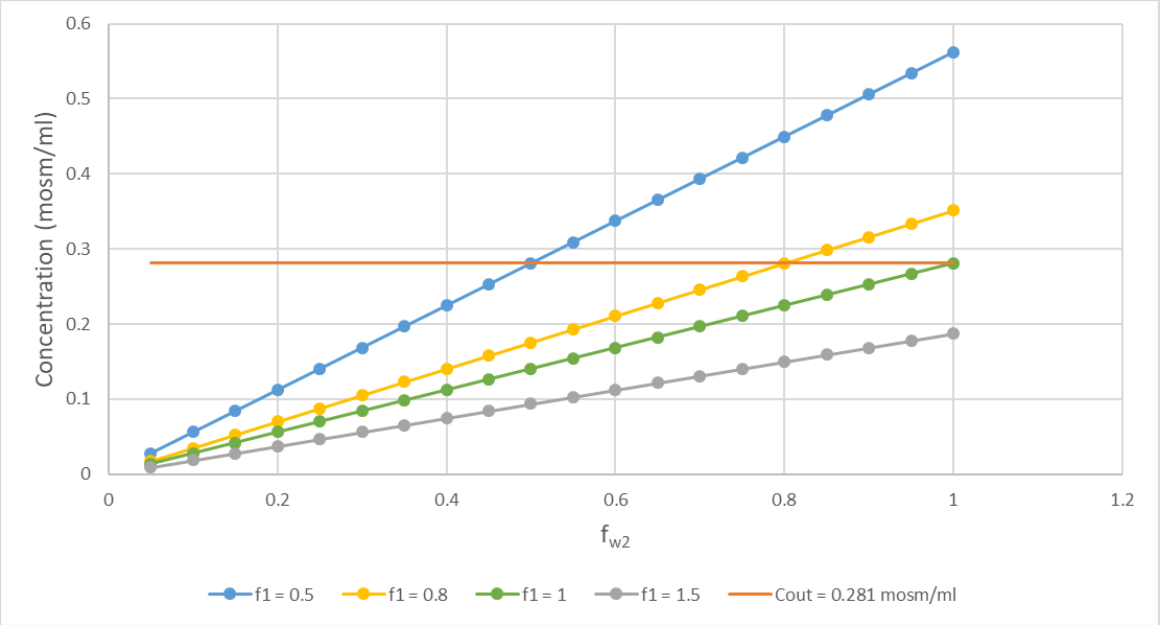


Fig. 7.16 Design 4 (Series water and solute separators) Tank and outflow concentrations versus f_{w2} for a range of f_1

than the outflow. If $f_1 << 1$ to cater to diluting disturbances effectively, it is more difficult for the water reabsorber (quantified by f_{w2}) to counteract this in response to concentrating disturbances than if $f_1 \to 1$. At this stage of development, however, there is no means of changing model parameters f_1 and f_{w2} once set.

7.2.3 Biological application

A new overall bulk flow or water reabsorption coefficient is established when separators are placed in series. The transfer function across the separator arrangement is in fact the product of the component transfer functions. The new arrangement may have very different behaviour when compared with the original single separator, depending on the values of the individual bulk flow or water reabsorption coefficients. For example, when solute separators are placed in series, it is possible to change a diluting setup to a concentrating one and vice versa. In the same way, however, it is possible to counteract the separating effect of one with the other. In comparison, series water separators can only dilute the tank relative to the outflow.

It is appreciated that a series water separator behaves in the same way as the collecting duct in sophisticated kidneys (i.e. those of reptiles, birds and mammals [16]) in terms of being able to selectively reabsorb water from the outflow stream. Reptiles and birds lack the countercurrent collecting duct arrangement of mammals since their loopless nephrons

(all in the case of reptiles and the majority in the case of birds) connect to their associated collecting ducts perpendicularly [16]. This severely limits concentrating ability; reptiles cannot concentrate their urine while birds can elucidate urine approximately 2 - 2.5 x their plasma osmolality [16] (the urine-to-plasma ratio of the Savanna sparrow (*Passerculus sandwichensis*), approximately 5 [5], is uncommon), with the caveat that their plasma osmolality is relatively labile, tending to increase with water deprivation [16]. Mammals, on the other hand, have collecting ducts, although continuous, arranged in parallel with the long loops of Henle and surrounding descending and ascending vasa recta in the medulla, contributing to establishment of the corticomedullary osmotic gradient [1], yielding a much more efficient water reabsorber. However, much water reabsorption is still required to counteract the diluting effect of the preceeding section if a concentrated outflow is desired. Different mammals are able to concentrate urine to different degrees, for example, the Australian hopping mouse (*Notomys*) can concentrate urine approximately 25 x relative to plasma [3], cats and dogs average a urine-to-plasma ratio of 10.8 and 8.7 [16], respectively, humans manage a maximum urine-to-plasma concentration ratio of 4 - 5 x, while beavers average 1 - 2 x, preferring (and ultimately needing) a watery home [4].

A trade-off is noted between series solute-and-water separators in managing transitions in response to diluting and concentrating disturbances; either $f_1 << 1$ to cater to diluting disturbances effectively but then difficult for the water reabsorber to counteract this in response to concentrating disturbances, or $f_1 \rightarrow 1^-$ to ensure concentrating the tank relative to the outflow is at least possible in response to diluting disturbances but then diluting the tank by means of the water reabsorber in response to concentrating disturbances is limited (reference is made to Figure 7.16). The facts that reptiles cannot elucidate urine hyperosmotic to blood plasma and that their kidneys consist of a single population of loopless nephrons followed by a collecting duct system oriented perpendicularly [16], suggest they have adopted the former strategy and outsourced desiccation-avoidance to extrarenal mechanisms (such as lower gastro-intestinal tract involvement, salt glands and uricotelic nitrogen excretion [16]).

A limitation of the series setup is that, unlike the parallel setup, it is not possible to concentrate the tank relative to the outflow if a solute separator with individual $f < 1$ is not present. Additionally, it must be remembered that once the model parameters have been set, there is no means of adjusting them, yet.

7.3 Series-Parallel separators

7.3.1 Model setup

Keeping the goals of the fourth design step in mind (including improving osmoregulation compared to the previous design and introducing capacity for efficient disturbance handling), and considering possible biological excretory system applications of simple series and parallel combinations of water and solute separators as mentioned in Sections 7.1.3 and 7.2.3, a composite series-parallel structure is suggested. A parallel section with series solute-and-water separators defined by $\frac{f_1}{f_{w1}} < 1$, and $\frac{f}{f_{w2}} > 1$ provides two paths, each specific for processing diluting or concentrating disturbances, respectively, followed by series water reabsorption defined by f_{w3}, responsible for adjusting the water content of the outflow.

Such a setup is illustrated in Figure 7.17. The associated level-rate diagram is included in Figure 7.18.

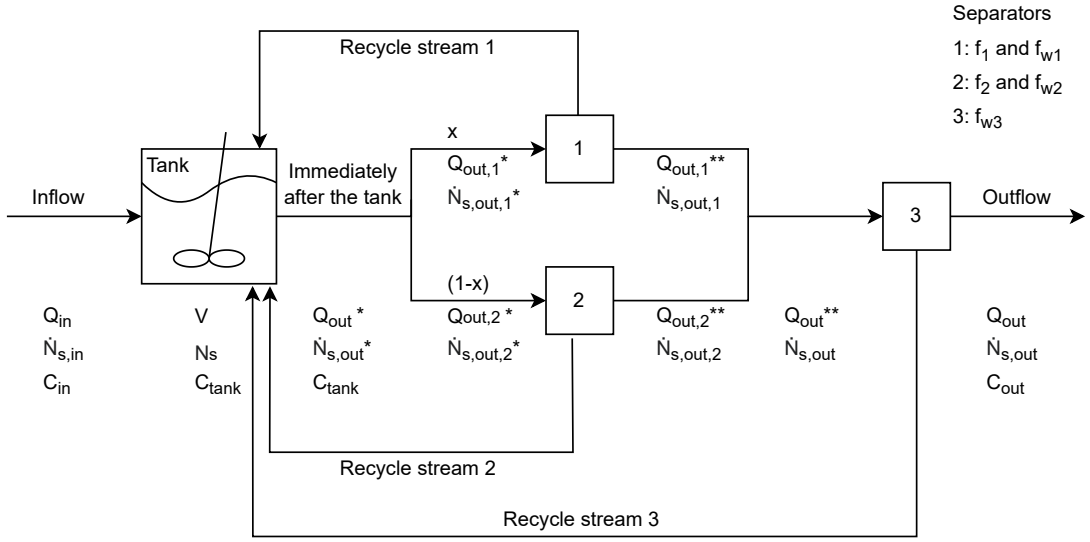


Fig. 7.17 Line diagram of tank setup for Design 4: Series-parallel separators; separator 1 is defined by bulk flow coefficient f_1 and water reabsorption coefficient f_{w1}, separator 2 is defined by f_2 and water reabsorption coefficient f_{w2}, and separator 3 is defined by water reabsorption coefficient f_{w3}

From the previous sections on parallel and series separators (Sections 7.1.1 and 7.2.1, respectively), the transfer function across the series-parallel setup in Equation 7.52 is simply a combination of individual separator transfer functions.

$$\frac{f}{f_w} = \frac{C_{out}}{C_{tank}} = \frac{f_1 x + f_2(1-x)}{f_{w3}(f_{w1}x + f_{w2}(1-x))} \tag{7.52}$$

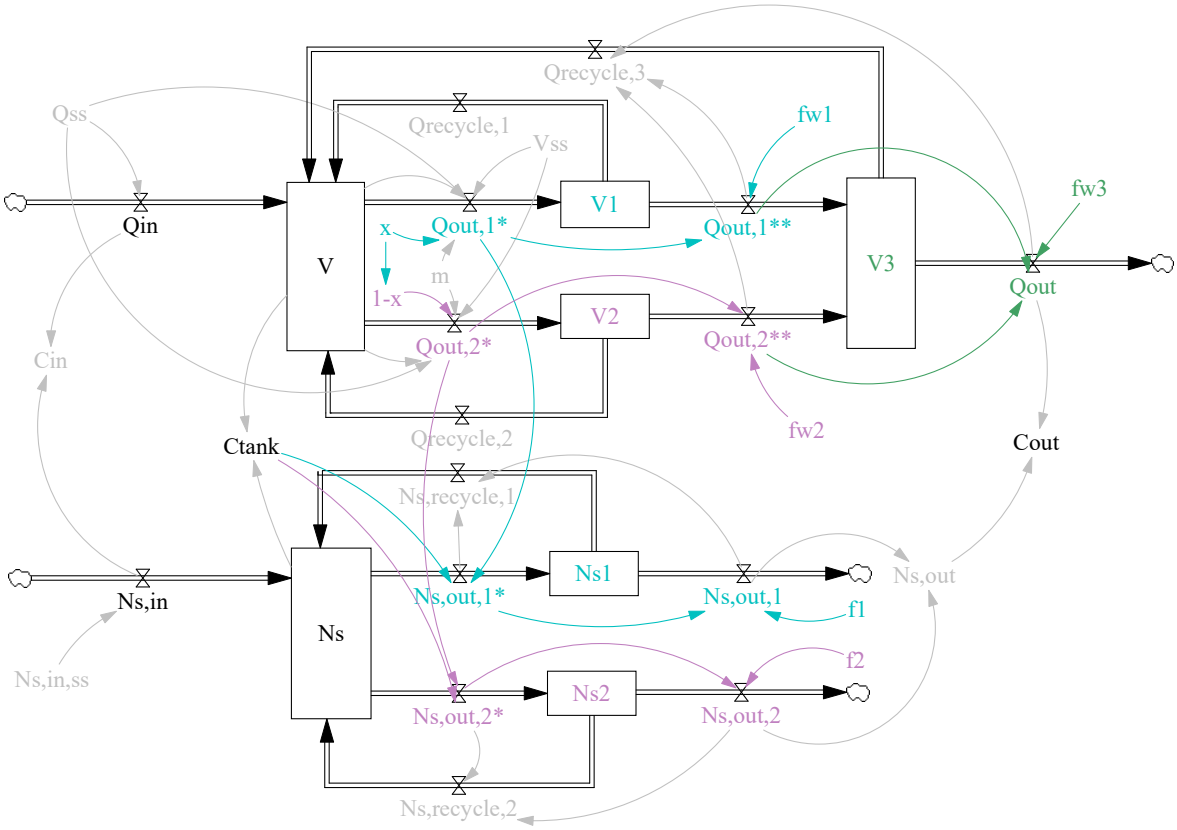


Fig. 7.18 Level-rate diagram for Design 4: Series-parallel separators; separator V_1 is defined by f_{w1}, V_2 by f_{w2}, V_3 by f_{w3}, N_{s1} by f_1 and N_{s2} by f_2

Table 7.5 Design 4 Model Parameters (Series-parallel arrangement)

Parameter	Value
Baseline water inflow (ml/hr)	100
Baseline solute inflow (mosm/hr)	28.1
Steady-state volume (ml)	1 000
m (1/hr)	1
f_1	0 - 1
f_2	0 - 1
f_{w1}	0 - 1
f_{w2}	0 - 1
f_{w3}	0 - 1
x	0 - 1

Such composition is possible due to the linearity of the system. Presumably, this can be extended to an infinite number of parallel branches and series separators.

When water separators are involved, the immediate outflow of the tank, Q^*_{out}, is given by Equation 7.53 where the steady-state volume V_{ss} depends on the desired steady-state volume V_{dss} according to Equation 7.54 (as introduced for a water separator in Section 6.1.2 in Chapter 6).

$$Q^*_{out} = \frac{Q_{ss}}{f_w} + m(V(t) - V_{ss}) \tag{7.53}$$

$$V_{ss} = V_{dss} + \frac{Q_{ss}(1 - f_w)}{f_w} \tag{7.54}$$

The coupled ODEs follow in Equations 7.55 and 7.56 (written in standard linear form in Appendix A.4.4).

$$\frac{dV}{dt} = Q(t) - (Q_{ss} + f_w m(V(t) - V_{ss})) \tag{7.55}$$

$$\frac{dN_s}{dt} = \frac{dC_{tank}V}{dt} = \dot{N}_{s,in}(t) - fC_{tank}(t)(\frac{1}{f_w}Q_{ss} + mV(t) - V_{ss}) \tag{7.56}$$

The model parameters are included in Table 7.5.

7.3.2 Results and Discussion

It is clear from Equations 7.55 and 7.56, and Appendix A.4.4, that combining multiple linear and negligible volume solute and water separators in series and parallel on the outflow

of the tank has no effect on the system of ODEs that governs overall model behaviour. The different combinations of separators simply change the values of the overall bulk flow and water reabsorption coefficients (f and f_w, respectively). As mentioned previously, it is acknowledged that a model with multiple separators is over-parameterised since many combinations of model parameters can yield the same results.

The general analytical solutions are identical to those for parallel and series water-and-solute separator combinations (Appendix A.5.5 and Sections 7.1.2 and 7.2.2, respectively) and repeated here. The tank volume response follows that of water separation in Section 6.2.2 in Chapter 6, through Equations 7.57, 7.58 and 7.59, while the tank concentration response has mean residence time τ in Equation 7.60, dependent on both f_w and f.

$$V(t) = V_{ss} + (V_0 - V_{ss})e^{-\frac{t}{\tau_V}} \tag{7.57}$$

$$V_{ss} = V_{dss} + \frac{Q_{ss}(1-f_w)}{f_w} \tag{7.58}$$

$$\tau_V = \frac{1}{f_w m} \tag{7.59}$$

$$\tau = \frac{f_w}{f}\frac{V_{ss}}{Q_{ss}} \tag{7.60}$$

As for previous designs that include water and solute separators, the particular analytical solutions in Appendix A.5.5 show that the dynamic response of the tank concentration to a solute impulse disturbance depends on τ, while that to a water impulse disturbance depends on τ and τ_V. A mixed input (which includes both water and solute) would therefore depend on both τ and τ_V as well.

Considering the steady-state response and focusing on Equation 7.52, if $\frac{f_1}{f_{w1}} < 1$ and $\frac{f_2}{f_{w2}} > 1$ are fixed and both x and f_w are varied, Figures 7.19 and 7.20 illustrate the effect on the overall transfer function and steady-state tank concentration relative to the fixed outflow (presuming that the baseline inflow concentration remains at 0.281 mosm/ml), respectively. The ratios $\frac{f_1}{f_{w1}} < 1$ and $\frac{f}{f_{w2}} > 1$ can be achieved in many ways but by setting both $f_1 < 1$ and $f_2 < 1$ and setting $f_{w1} > f_1$ and $f_{w2} < f_2$, the desired overall effect can be achieved in a passive manner, i.e. one in which active pumping of solute against a concentration gradient is not necessary. Figures 7.19 and 7.20 have been drawn with $f_1 = f_2 = 0.5$, $f_{w1} = 0.6$ and $f_{w2} = 0.4$ for illustrative purposes.

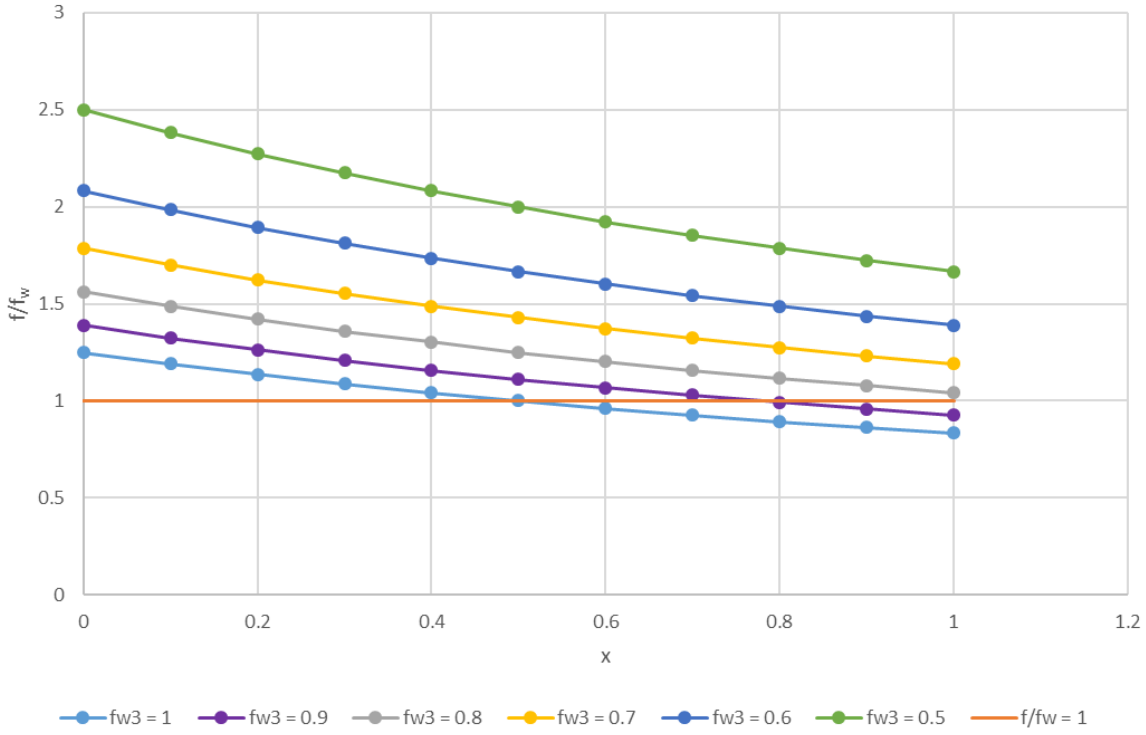


Fig. 7.19 Design 4 (Series-parallel separators) Transfer function $\frac{f}{f_w}$ versus $x \in [0,1]$ for fixed $f_1 = f_2 = 0.5$, $f_{w1} = 0.6$, $f_{w2} = 0.4$, and a range of $f_{w3} \leq 1$

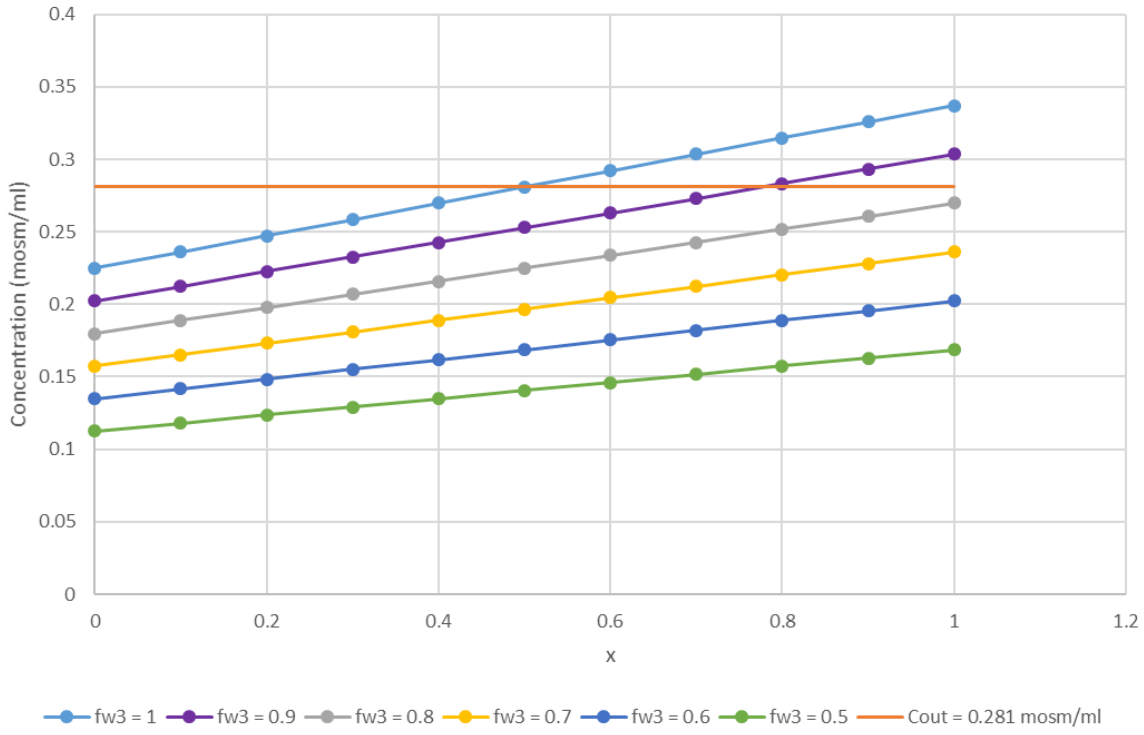


Fig. 7.20 Design 4 (Series-parallel separators) Steady-state concentration versus $x \in [0,1]$ for fixed $f_1 = f_2 = 0.5$, $f_{w1} = 0.6$, $f_{w2} = 0.4$, and a range of $f_{w3} \leq 1$; showing tank concentrations and fixed outflow concentration

It is clear that at $x = 1$ and $f_{w3} = 1$, all flow is directed through the series combination of $f_1 = 0.5$ and $f_{w1} = 0.6$ in the first parallel branch, yielding transfer function $\frac{f_1}{f_{w1}} = 0.83 < 1$ and the tank concentrated with respect to the outflow. Similarly, at $x = 0$ and and $f_{w3} = 1$, all flow passes through the series combination of $f_2 = 0.5$ and $f_{w2} = 0.4$ in the second parallel branch, yielding transfer function $\frac{f_2}{f_{w2}} = 1.2 > 1$ and the tank diluted with respect to the outflow. Between these two points, all combinations of flow exist. At $x = 0.5$ and $f_{w3} = 1$, $\frac{f}{f_w} = 1$ and the tank concentration matches the outflow concentration. The same point, $\frac{f}{f_w} = 1$, can be reached if more flow is directed through the first parallel branch with $x = 0.8$ and the series water separator is turned on with $f_{w3} = 0.9$ (there are many other combinations of x and f_{w3} for which this is true but this is the one illustrated). It can be seen that as f_{w3} is decreased, the transfer function curve moves up and the tank concentration curve moves down, crossing the constant $\frac{f}{f_w} = 1$ and C_{out} lines, respectively, at increasing values of x, if at all. Obviously the end-points of the figures change if model constants f_1, f_2, f_{w1} and f_{w2} are changed. However, it must be reiterated that once the model constants have been set, they cannot be changed in the current configuration.

More generally, a change in x alone implies movement along the horizontal axis between $x = 0$ and $x = 1$ extremes, and has the ability to cross the concentrating/diluting behaviour boundary as long as said boundary lies within the range of $x = 0$ and $x = 1$ (i.e. $\frac{f_1}{f_{w1}} < 1$ and $\frac{f_2}{f_{w2}} > 1$). In addition, a change in f_{w3} alone implies movement along the vertical axis, and can cause the concentrating/diluting behaviour boundary to be crossed but the same condition must hold, (i.e. $\frac{f_1}{f_{w1}} < 1$ and $\frac{f_2}{f_{w2}} > 1$). Adjusting both x and f_{w3} simultaneously has the greatest effect, as the responses of the linear separators are added.

Something that may seem obvious but worth noting is that not all series-parallel combinations are able to concentrate the tank relative to the outflow. For example, if the majority of flow is directed through the branch with transfer function $\frac{f_2}{f_{w2}} > 1$, then the tank concentration will never be more concentrated than the tank. This would also be the case if both branches had concentrating characteristics (i.e. $\frac{f_1}{f_{w1}} > 1$ and $\frac{f_2}{f_{w2}} > 1$).

Importantly, the benefits of the series-parallel setup over simpler setups include passive implementation of $\frac{f}{f_w} > 1$ and the potential for future flexibility afforded by the parallel section, especially in terms of diluting and concentrating the tank relative to the outflow.

7.3.3 Biological application

All combinations of water-and-solute (be they series or parallel) separators are described by a transfer function that includes two parameters; overall bulk flow and water reabsorption coefficients. Therefore, the model remains exactly the same mathematically as in previous

designs, the increased number of dependent parameters and their associated geometry only making sense when considered in line with the biological excretory system application.

Continuing the previous analogies (where the parallel solute separators in Section 7.1 were shown to have similarities with the internephron heterogeneity and differential intrarenal blood supply of bird kidneys, and the series water separator (in Section 7.2) was shown to behave in the same way as the collecting duct in the kidneys of sophisticated animals such as reptiles, birds and mammals), the series-parallel setup is structured as a combination of the two; i.e. internephron heterogeneity and differential intrarenal blood supply followed by a distal water reabsorption system. In addition, the series water separators in each parallel branch together represent the automatic reabsorption of the majority of filtered water (85 %) by the proximal tubule and loop of Henle of the nephrons [1], prior to the distal series water separator, which represents approximately 15 % of water reabsorption in the collecting duct. The parallel water separators provide for differential water recycling between the parallel branches, something that occurs within sophisticated kidneys, where only long-looped nephrons penetrate deep into the high osmolarity inner medulla [24], providing for efficient water reabsorption compared to short-looped nephrons that remain in the outer medulla and cortex [24]. It is known that approximately 20 % of water is reabsorbed in the loop of Henle [1], presumably predominantly via the long-looped nephrons. Thus, differential water (and solute) recycle in the parallel setup of the model reflects another aspect of internephron heterogeneity in sophisticated kidneys.

Such a composite series-parallel structure is evident in both bird and mammalian kidneys, although the internephron heterogeneity is less extreme in mammals where all nephrons exhibit loops, just different lengths [16]. Having said that, within mammals, "an increase in nephron heterogeneity is linked to an improvement in urine concentrating ability" [26] and such a model structure speaks to this finding. As a limited number of published whole-kidney models consider internephron heterogeneity and differential intrarenal blood supply (examples being [41, 29]), it is suggested that both experimental and theoretical physiologists consider this avenue of research further.

In addition, it has been suggested that "with some exceptions, the superficial cortical nephrons tend to be considerably shorter than the juxtamedullary nephrons. This structural difference may have a functional correlate in the overall renal processing of sodium and water" [16]. This is something that is definitely evident in the model findings, looking at responses to lumped solute (including sodium) and water disturbances. In the parallel part of the setup, the $\frac{f_1}{f_{w1}} < 1$ branch (ostensibly analogous to short looped nephrons in mammalian kidneys) has the capacity to manage diluting disturbances preferentially while the $\frac{f_2}{f_{w2}} > 1$

branch (analogous to long-looped nephrons) handles concentrating disturbances better, by design.

Importantly, the recycle paths within the tank-separator-recycle structure provide a means of implementing water and solute excretion "passively" (i.e. relying simply on pressure and no additional metabolically-derived "active" transport) down a concentration gradient, no matter the solute concentration in the outflow relative to the tank.

Unlike mammals, who are strict omoregulators, the blood osmolality of reptiles (and birds to a lesser extent) is labile, tending to increase with concentrating disturbances [16] and therefore conforming to their environment (at least over some range in blood osmolality; birds, for example, apparently increase their blood and urine osmolality in line with water deprivation or salt loading from approximately 300 to 450 mosm/ml and only then start regulating through reduction in urine production and salt gland activation [16]). The current static model provides for such an osmoconforming response - the tank concentration compensating to ensure the outflow concentration matches the inflow concentration at steady-state and mass balance is maintained. Although limited to representing animals with fixed excretory systems, an advantage of the current design over the previous (i.e. Chapter 6) is the provision for manipulation of the overall transfer function and therefore a future means of controlling the response.

In order to address the inflexible nature of the current design (and therefore improve volume- and osmo-regulation further), some form of dynamic control needs to be incorporated.

Chapter 8

Design 5: Control

Until now, the open-loop response of the model with static parameters has been stable and reaches steady-state; sufficient in describing the response of a conformer or regulator with wide tolerance. All that is required to describe such an animal's response is the right choice of model parameters to meet the animal's criteria. However, tight osmo-regulation is not possible; the tank concentration cannot be maintained at desired levels. This is because, in order to maintain mass balance across an organism, the tank concentration is integrally linked to the outflow concentration via the overall transfer function and compensates to ensure the outflow concentration matches the inflow concentration at steady-state. Therefore, for the first time, closed-loop control is investigated and implemented on the separation system.

8.1 Model setup

Context is provided by way of example. Table 8.1 has been adapted from [1] and shows normal and short-term non-lethal plasma concentration ranges in humans for a selection of solutes that contributes to overall plasma osmolarity. The normal range is seen to be relatively narrow in each case, with values beyond the normal range usually associated with illness. The wider non-lethal range provides an absolute limit beyond which death may occur. For example, potassium ion concentration less than 1.5 mmol/l causes paralysis, while above 9.0 mmol/l causes heart muscle depression [1].

In addition, Jimenez et al. determined that plasma volume in humans is "dramatically decreased (11.4 %) during and after heat exposure, while it is better maintained during and after exercise (4.2 %) although hyperosmolality is similar" [83]. This implies tighter osmoregulation than volume-regulation in humans in response to dehydration pressures. This is backed up by Bankir who notes that both volume and plasma osmolarity are regulated in mammals, however, osmoregulation is favoured over volume-regulation [84].

Table 8.1 A selection of plasma constituents and their concentration ranges in humans (adapted from [1] unless an alternative reference is provided)

Constituent	Unit	Normal range	Short-term non-lethal range
Sodium ion	mmol/l	138 - 146	115 - 175
Potassium ion	mmol/l	3.8 - 5.0	1.5 - 9.0
Calcium ion	mmol/l	1.0 - 1.4	0.5 - 2.0
Chloride ion	mmol/l	103 - 112	70 - 130
Bicarbonate ion	mmol/l	24 - 32	8 - 45
Urea	mmol/l	2.5 - 7.8	> 15.3 [82]
Glucose	mg/dl	75 - 95	20 - 1500

Taking a step back from the example pertaining to humans, and considering relevance to the developed abstract model of excretion, and if it is assumed that osmoregulation is more critical than volume regulation, the control objective of tight regulation (as achieved in mammals) involves maintenance of the tank's concentration in particular within some narrow tolerance band of that desired, under a wide variety of input conditions, including shifts in baseline and transient disturbance.

Such an objective calls for negative feedback set-point control on the tank concentration (as illustrated in Figure 8.1), as this will decouple the tank and outflow concentrations (and therefore ensure the tank concentration tends to a desired level no matter the inflow concentration). This is not normally considered possible since the amount of solute and volume in the tank will be automatically coupled but findings in Chapter 7 for Design 4 show that solute-and-water separator combinations (that have biological application) can be used not only to concentrate the tank relative to the outflow (i.e. $\frac{f}{f_w} < 1$) but also to dilute the tank relative to the outflow (i.e. $\frac{f}{f_w} > 1$). In addition, an appropriately tuned controller that reduces the "error magnitude" and shortens the "transient period" [2], both of which are control performance indicators [59], will help keep the response within tolerated bounds.

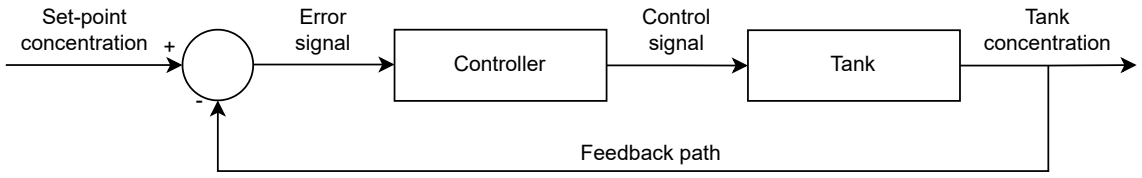


Fig. 8.1 Simplified illustration of feedback control (adapted from [2])

From a control engineering perspective [2], the current tank concentration (output value of interest and therefore "controlled variable" [59]) needs to be continuously compared with the desired tank concentration (or set-point value) and any difference between the two (i.e.

error signal) passed to a controller that generates a control signal to drive the tank (via some "manipulated variable" [59]) until its concentration equals the set-point (or falls within an acceptable range).

According to [59], the manipulated variable of choice should have the following properties: causally related to the control variable with a "dynamic response that is monotonic and fast with little dead time or inverse response", externally and independently adjustable, "have sufficient range to achieve the desired set-points and compensate for expected disturbances", and have "little effect on plant performance". These properties need to be taken into account when choosing manipulated variables to drive the tank to its desired volume and concentration without overly affecting the tank (i.e. the plant of interest) itself.

A variety of control strategies are available but a simple implementation is that of a controller that changes the overall transfer function properties (or potential "manipulated variables" [59]) temporarily in a negative feedback arrangement until the tank concentration reaches the desired level. There are a few means of changing the overall transfer function for the series-parallel setup (i.e. the design to be controlled, detailed in Section 7.3 Equation 7.52 and repeated in Equation 8.1 for ease of reference), including changing the membrane properties of the parallel solute and water separators (i.e. f_1, f_2, and f_{w1}, f_{w2}, respectively), changing the relative flow between the parallel branches (i.e. x) to change f and f_w, and adjusting f_w via the distal series water separator f_{w3}).

$$\frac{f}{f_w} = \frac{C_{out}}{C_{tank}} = \frac{f_1 x + f_2(1-x)}{f_{w3}(f_{w1}x + f_{w2}(1-x))} \tag{8.1}$$

Since interest lies in how changing flow patterns can affect separation and provide for certain behaviours, let the manipulated variables be x and f_{w3} and keep membrane properties (i.e. f_1, f_2, f_{w1} and f_{w2}) fixed.

The gradient of the overall transfer function of Equation 8.1 with respect to x and f_{w3} (and fixed f_1, f_2, f_{w1} and f_{w2}) in Equation 8.2, with components expanded in Equations 8.3 and 8.4, provides a means of comparing the sensitivity of the overall transfer function (and therefore tank concentration) to changes in x and f_{w3}.

$$\nabla\left(\frac{f}{f_w}\right) = \left(\frac{\delta\left(\frac{f}{f_w}\right)}{\delta x}, \frac{\delta\left(\frac{f}{f_w}\right)}{\delta\, f_{w3}}\right) \tag{8.2}$$

$$\frac{\delta\left(\frac{f}{f_w}\right)}{\delta x} = \frac{(f_1 - f_2)(f_{w1}x + f_{w2}(1-x)) - (f_{w1} - f_{w2})(f_1 x + f_2(1-x))}{f_{w3}(f_{w1}x + f_{w2}(1-x))^2} \tag{8.3}$$

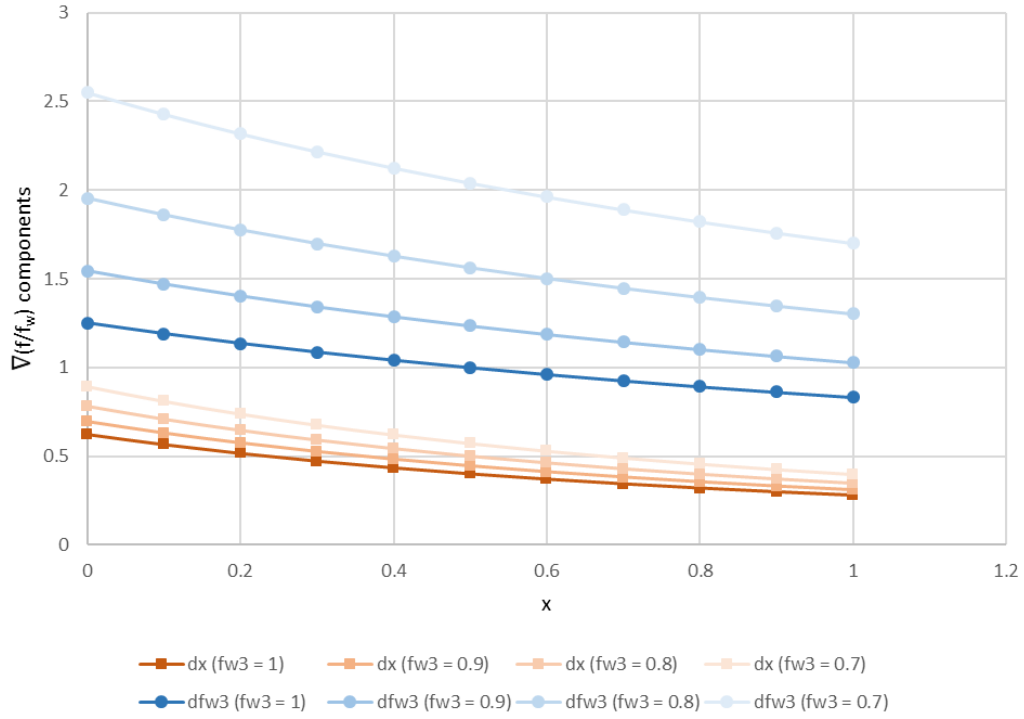
$$\frac{\delta\left(\frac{f}{f_w}\right)}{\delta\, f_{w3}} = \frac{-(f_1 x + f_2(1-x))}{{f_{w3}}^2(f_{w1}x + f_{w2}(1-x))} \tag{8.4}$$

It is clear that each component of the gradient depends on the fixed membrane properties f_1, f_2, f_{w1} and f_{w2}. Consider the example in Figure 8.2, where two cases of membrane properties that provide for $\frac{f_1}{f_{w1}} < 1$ and $\frac{f_2}{f_{w2}} > 1$ are shown; Figure 8.2a where the choice of $f_1 = 0.5$, $f_2 = 0.5$, $f_{w1} = 0.6$ and $f_{w2} = 0.4$ causes the absolute value of the df_{w3} component to exceed that of the dx component for all $x \in [0,1]$ and $f_{w3} < 1$, and Figure 8.2b where the choice of $f_1 = 0.9$, $f_2 = 0.2$, $f_{w1} = 0.6$ and $f_{w2} = 0.4$ causes the absolute value of the dx component to exceed that of the df_{w3} component for all $x \in [0,1]$ while $0.8 \leq f_{w3} \leq 1$. What this means is that manipulation of x and f_{w3} each provides for coarse or fine control (involving incremental changes that are best brought about by large or small changes in output per unit change in input, respectively) of the tank concentration, depending on the values of the fixed membrane properties, which can be chosen to meet a particular animal's criteria.

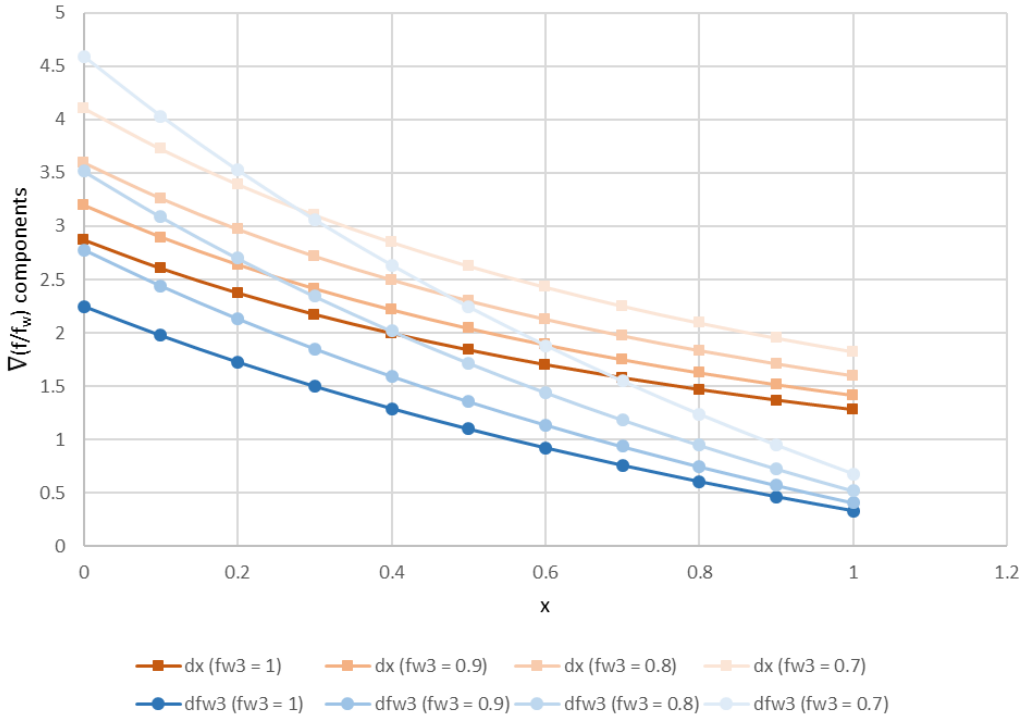
The simplest and cheapest automated control strategy is that of on-off or bang-bang control [59, 2], where, in response to an error signal between the controlled variable and its set-point value, the control signal would cause a drastic change to the plant (such as switching flow completely between separators or turning water reabsorption either "on" or "off") in a direction so as to minimise the error signal. However, this form of control tends to suffer from oscillation [59] and only works well when there is a wide tolerance band around the set-point [59, 2]. When accuracy is favoured over cost (in terms of energy expenditure), tighter automated control can be achieved with a continuous strategy [59] such as Proportional (P) control.

In P-control, the control signal (and subsequent changes to the plant via the manipulated variables) is proportional to the error signal and therefore causes a continuous change in the controlled variable in a direction to minimise the error [2]. However, such a simple scheme has the unavoidable drawback of steady-state error between the controlled variable and its set-point value and the potential for instability in higher order plants [2]. If necessary, Proportional plus Integral (PI) and Proportional plus Derivative (PD) control can improve the P-control response by removing steady-state error and improving stability, respectively [2] but it is acknowledged that some catabolic penalty is involved in increasing the sophistication of the controller.

Of the "thousands of homeostatic control mechanisms in the human body" [1], proportional control is a common characteristic, sometimes augmented with additional complexity [1] such as integral- and derivative-control. PD-control does not appear to be as common as PI-control. PI control is present at all levels, from cellular to whole organism to ecosystem



(a) Example of coarse control by f_{w3}, fine control by x



(b) Example of coarse control by x, fine control by f_{w3}

Fig. 8.2 Comparison of dx and df_{w3} components of the gradient of the overall transfer function with respect to x and f_{w3} for two cases of fixed membrane properties (a) $f_1 = 0.5$, $f_2 = 0.5$, $f_{w1} = 0.6$ and $f_{w2} = 0.4$ and (b) $f_1 = 0.9$, $f_2 = 0.2$, $f_{w1} = 0.6$ and $f_{w2} = 0.4$

homeostasis [85], "regardless of their particular mechanics" [86]. It can be used to describe "the regulation of hormone secretion in humans" [87]. For example, a PI-controlled model of glucose homeostasis in humans is motivated by "an instantaneous (glucagon and insulin hormone) response in proportion to the deviation of the glucose level from the set point" and the presence of "memory in the system due to the finite time it takes the body to excrete or metabolize the hormones involved" [86]. An example of PD control, on the other hand, is in the photoreceptors of the retina where "proportional and derivative action is generated by a combination of cones and horizontal cells; the cones are the primary receptors stimulated by light, which in turn stimulate the horizontal cells, and the horizontal cells give inhibitory (negative) feedback to the cones" [88]. The more complex scheme of Proportional plus Integral plus Derivative (PID) control (which is used more in process control than any other control algorithm [59, 89]) does not appear to be commonly implemented in biology. An example could be in a model of the secretion of insulin by β-cells of the pancreas [90] but Veen et al. believe validation of the work is needed "under more realistic circumstances" [86].

Considering the established model of the excretory system (Section 7.3) and the requirement for relatively tight osmoregulation in particular [84], a trade-off is necessary between simple, less energy-intensive P-control that has disadvantages in terms of steady-state offset; and the more complex and energy-intensive but physiologically-likely and steady-state offset-removing approach of PI-control. Since the focus throughout the design process has been on step-wise improvement, it was decided that P-control should be investigated initially, and depending on the findings, extended to PI-control only if necessary. The level-rate diagram in Figure 8.3 shows P-control implementation on previous Design 4, where red has been used to indicate the controller.

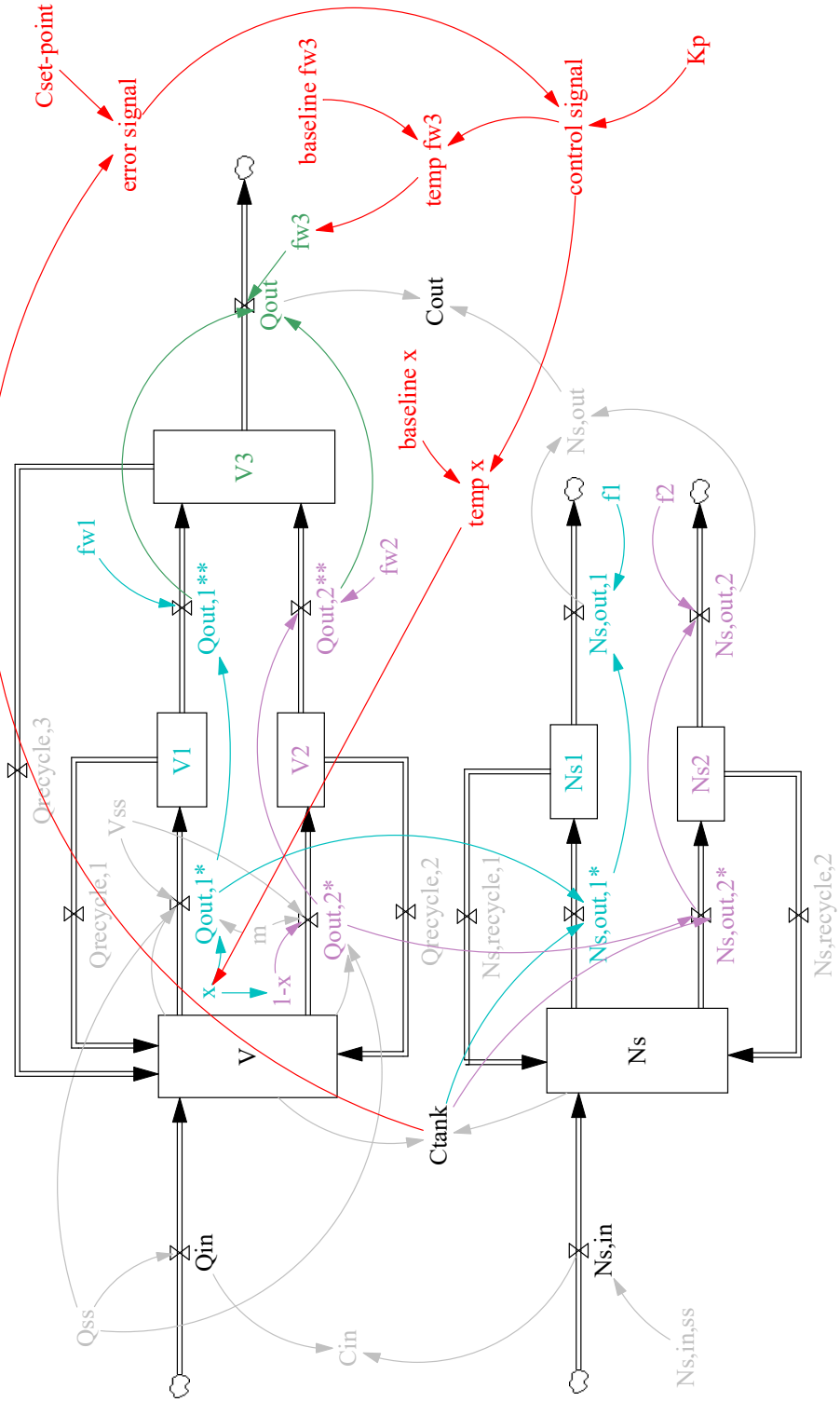


Fig. 8.3 Level-rate diagram for Design 5: Control

Depending on the tank concentration relative to set-point concentration (i.e. the "error signal"), the split in flow to the different solute separators (i.e. via x) is varied away from "baseline x" (which matches the fixed x of the previous design in Section 7.3) by the "control signal", affecting the concentrating contribution the different separators have on the tank concentration with the goal of reducing the error signal. In addition, the distal series water separator may be turned "on" (i.e. $f_{w3} < 1$) in response to a positive "control signal" (i.e. only in the concentrating disturbance case) or remain in the default "off" (i.e. $f_{w3} = 1$) position. If C_{tank} differs from $C_{set-point}$, the relative error signal is calculated from Equation 8.5 and multiplied by tuning constant K_p in the control signal (Equation 8.6), which adjusts the variable x according to Equation 8.7 and variable f_{w3} according to Equation 8.8. Noteworthy is that a temporary x variable ("temp x") is needed to prevent x from going out of bounds (i.e. as fractional flow, x, is limited to values between 0 and 1) while a temporary f_{w3} variable ("temp f_{w3}") is needed to limit $f_{w3} \leq 1$ and prevent water secretion from the tank to the outflow stream.

$$\text{error signal} = \frac{C_{tank} - C_{set-point}}{C_{set-point}} \tag{8.5}$$

$$\text{control signal} = K_p * \text{error signal} \tag{8.6}$$

$$\text{temp } x = \text{baseline } x - \text{control signal} * \text{baseline } x \tag{8.7}$$

$$\text{temp } f_{w3} = \text{baseline } f_{w3} - \text{control signal} * \text{baseline } f_{w3} \tag{8.8}$$

If x is increased (in response to a decrease in C_{tank} relative to $C_{set-point}$), relatively more solution will flow through the parallel branch with transfer coefficient $\frac{f_1}{f_{w1}}$ (typically chosen to be less than 1, which promotes tank concentration relative to the outflow). On the other hand, if x is decreased (in response to a decrease in C_{tank} relative to $C_{set-point}$), relatively more solution will flow through the parallel branch with transfer coefficient $\frac{f_2}{f_{w2}}$ (typically chosen to be greater than 1, which promotes tank dilution relative to the outflow). In contrast, the same control signal causes f_{w3} to change from its steady-state value only in response to a decrease in C_{tank} relative to $C_{set-point}$, facilitating water reabsorption and dilution of the tank relative to the outflow.

Changes made to the model of the previous design (Chapter 7, Section 7.3) include fixing the values of f_1, f_2, f_{w1} and f_{w2} so that $\frac{f_1}{f_{w1}} < 1$ and $\frac{f_2}{f_{w2}} > 1$; providing baseline x and f_{w3}; and differentiating the inflow concentration from the tank set-point concentration.

The model parameters are included in Table 8.2.

Table 8.2 Design 5 Model Parameters

Parameter	Value
Baseline water inflow (ml/hr)	100
Baseline solute inflow (mosm/hr)	35
Desired steady-state volume (ml)	1 000
m (1/hr)	1
f_1	0.5
f_2	0.5
f_{w1}	0.6
f_{w2}	0.4
Tank set-point concentration (mosm/ml)	0.281
Baseline x	0.5
Baseline f_{w3}	1

8.2 Results and Discussion

If the inflow concentration is lower than the tank set-point concentration, this means that the outflow concentration is lower than the tank concentration at steady-state (achieved through an automatic adjustment in x since both the tank and outflow concentrations at steady-state have essentially been set by the action of the controller and mass balance considerations). In this case, the separation challenge is quite straightforward as solutes can move down a concentration gradient easily with an overall transfer function $\frac{f}{f_w} < 1$.

If, however, the inflow concentration is higher than the tank set-point concentration, this means that the tank concentration is lower than the outflow concentration at steady-state (achieved through an appropriate adjustment in x) and the separation challenge involves moving solutes up a concentration gradient, requiring an overall transfer function $\frac{f}{f_w} > 1$. This is not normally possible in a "regular" system or process. Biological systems, however, are able to concentrate up an exit stream. This is traditionally proposed to happen through active transport [1]. Passive recycling, as demonstrated in Section 7.3, can achieve concentration up a gradient without the need for additional energy expenditure. Therefore, in this section, it is assumed that passive recycling is used to concentrate up a gradient.

Simulations were performed in order to determine whether the implemented P-controller can maintain the tank's concentration within a "narrow" tolerance band of the set-point no matter a change in input conditions, including the challenging case of a positive shift in steady-state inflow concentration (relative to the tank's set-point concentration) and transient water and solute disturbances.

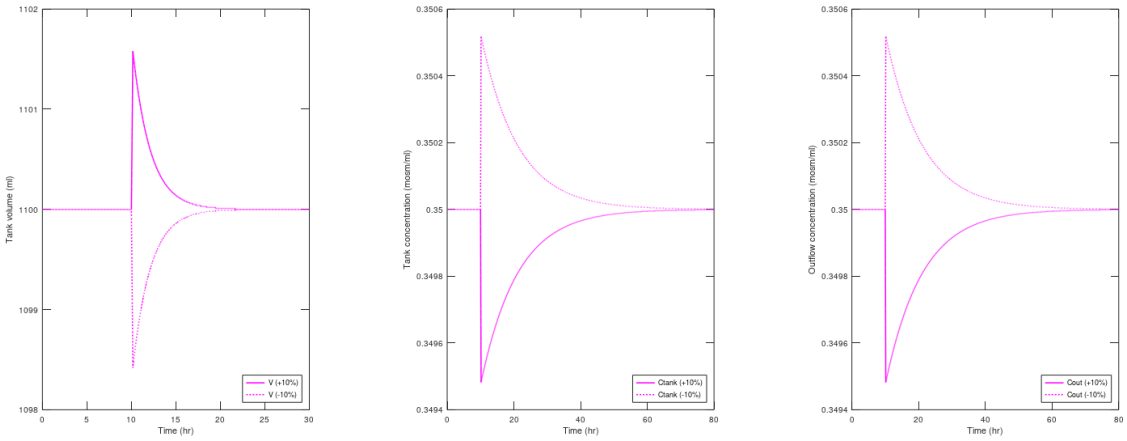
Figures 8.4 and 8.5 show the tank volume, tank concentration and outflow concentration responses to positive and negative finite-duration water and solute pulses on the inflow, respectively, for $C_{in} = 0.35$ mosm/ml and $C_{set-point} = 0.281$ mosm/ml for a range of $Kp = 0, 10, 100, 900$.

The $K_p = 0$ curves (Figures 8.4a and 8.5a) represent the response of previous Design 4 of Section 7.3 in Chapter 7, i.e. without feedback control, to positive and negative 10 % (above a baseline of 100 ml/hr and 28.1 mosm/hr, respectively) finite-duration (10 min) water and solute pulses, respectively, for $C_{in} = 0.35$ mosm/ml and $C_{set-point} = 0.281$ mosm/ml. It is immediately obvious from the $K_p = 10, 100, 900$ curves in Figures 8.4b and 8.5b that, as K_p is increased, the steady-state tank concentration approaches (but never reaches) the set-point value (0.281 mosm/ml), typical of P-control [59]. In addition, as K_p is increased, the transient response of the tank concentration becomes smaller and quicker, as desired. It is clear that the outflow concentration's steady-state remains at 0.35 mosm/ml, no matter the presence of control, set by the inflow concentration. The transient part of the outflow concentration's response increases in magnitude with K_p (with changes an order of magnitude bigger than in the tank); this is necessary to balance the changes occurring in the tank.

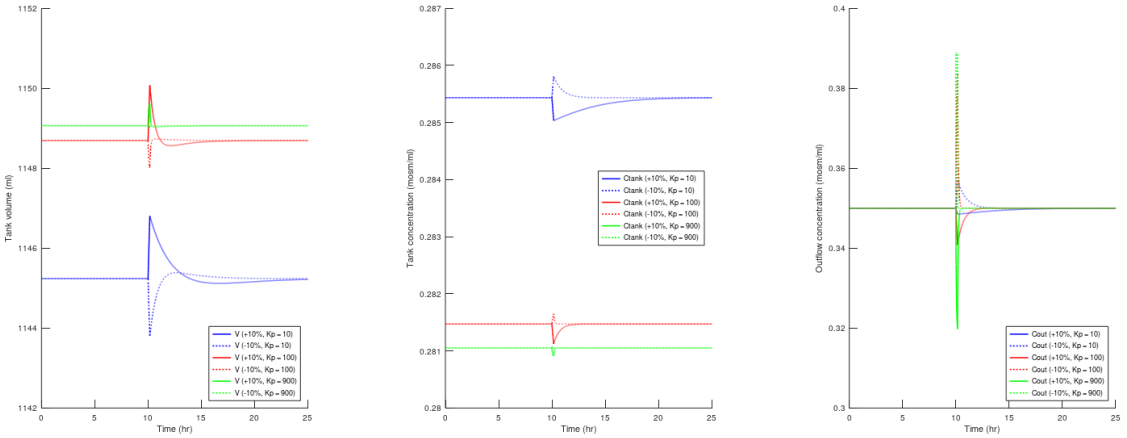
It is noteworthy that the tank concentration responses at a particular K_p in Figures 8.4b and 8.5b differ in appearance to concentrating and diluting (both water and solute) disturbances; they are not mirror-images. This implies that the system no longer behaves linearly. The responses to concentrating (i.e. negative water or positive solute) finite-duration pulses are faster and smaller in magnitude than the responses to diluting (i.e. positive water or negative solute) finite-duration pulses. This is expected from the contribution of $f_{w3} < 1$ in concentrating disturbance cases only.

Considering the volume curves in Figures 8.4 and 8.5, it is obvious that feedback control on the tank concentration comes at the cost of slightly worsening volume regulation in terms of steady-state (and transient magnitude in the solute disturbance case) since it moves further from that desired (e.g. 1000 ml, in this case) as K_p increases. However, since the model was set up on the assumption that the bounds on osmoregulation are tighter than those on volume-regulation, this is considered a necessary trade-off.

Following simulation, it was decided that the effectiveness of a P-controller (with relatively high tuning constant K_p) is sufficient in describing relatively tight osmoregulation as it exists in animals with sophisticated excretory systems, such as mammals. There is therefore, no need at this stage of model development to extend the controller to include an integrator, especially considering the concomitant increased energy expenditure this would entail.

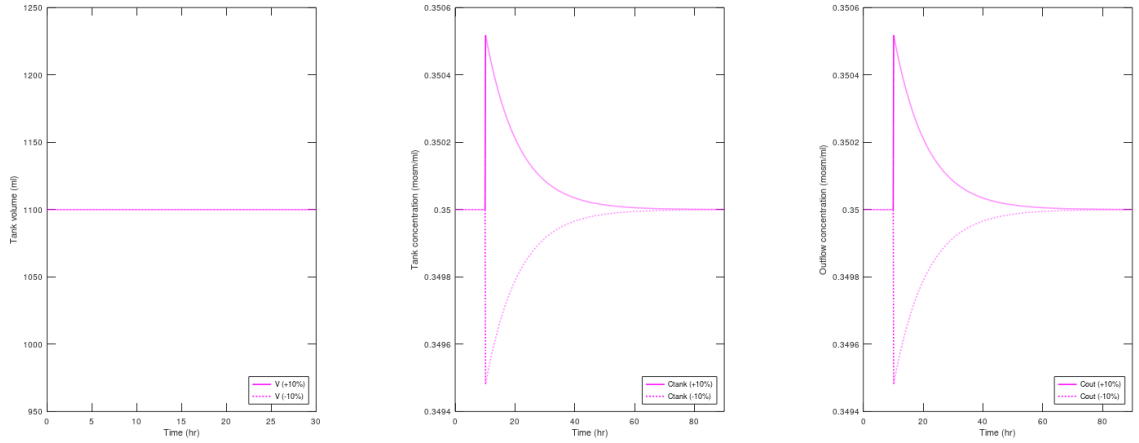


(a) $K_p = 0$

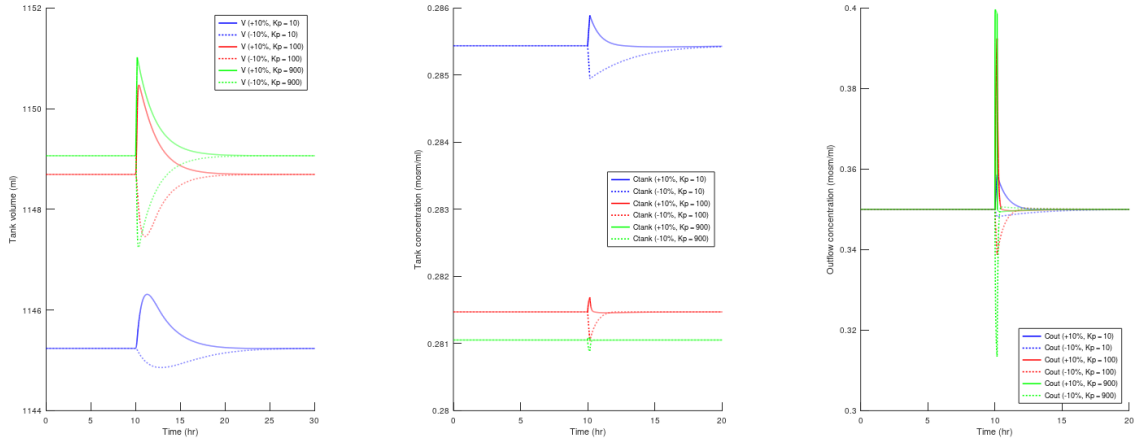


(b) $K_p = 10, 100, 900$

Fig. 8.4 Design 5 (Control) Simulated tank volume, tank concentration and outflow concentration time responses to positive and negative 10 % (above a baseline of 100 ml/hr) finite-duration (10 min) water pulses for $C_{in} = 0.35$ mosm/ml and (a) $K_p = 0$, (b) $K_p = 10, 100, 900$ at t = 10 hrs, $\frac{V}{Q} = 10\ hr$ and $C_{set-point} = 0.281$ mosm/ml



(a) $K_p = 0$



(b) $K_p = 10, 100, 900$

Fig. 8.5 Design 5 (Control) Simulated tank volume, tank concentration and outflow concentration time responses to positive and negative 10 % (above a baseline of 35 mosm/hr) finite-duration (10 min) solute pulses for $C_{in} = 0.35$ mosm/ml and (a) $K_p = 0$, (b) $K_p = 10, 100, 900$ at t = 10 hrs, $\frac{V}{Q} = 10\ hr$ and $C_{set-point} = 0.281$ mosm/ml

8.3 Biological application

For the first time in the current setup, a dynamic response to a particular disturbance is made possible through the implementation of feedback control. Up until now, all system parameters have been fixed and the ability to respond to various disturbances limited. In addition, it has not been possible to operate the tank at or around a particular set-point, independently of the output (and the input, through mass balance considerations). Therefore, it has only been possible to model the excretory systems of osmoconformers or osmoregulators with wide tolerance.

Introduction of a negative feedback architecture, however, provides a means of achieving different degrees of osmoregulation. A basic P-controller has been shown to be sufficient in achieving relatively tight set-point control. Implementation thereof demonstrates the usefulness of dynamic control; delinking the tank and outflow (and therefore, inflow) concentrations, and speeding up and reducing the magnitude of transient responses across the board.

Limitations of the P-control approach are acknowledged and, instead of determining the "right" control algorithm (if such a thing exists) or optimising the tuning constants to represent the excretory systems of particular animals of interest (both of which are possible avenues of future research), it was considered more fitting to note the signature trends introduced into the system response by implementing basic feedback control as done here, and focus instead on further insights the system structure might yield going forward.

The points of control were chosen to be relative flow (x) between the parallel branches and distal water reabsorption (f_{w3}), with membrane properties (i.e. f_1, f_2, f_{w1} and f_{w2}) kept constant. In addition to interest in how flow patterns can affect separation given the developed separation structure, x and f_{w3} are presumed to be easier to manipulate than membrane properties, if such a scheme were ever to be physically realised. Manipulation of x causes a redistribution of flow between parallel separators, shunting flow towards the separator best suited to respond to a particular disturbance; $\frac{f_1}{f_{w1}} < 1$ for diluting disturbances and $\frac{f_2}{f_{w2}} > 1$ for concentrating ones. Reducing $f_{w3} < 1$ in response to a concentrating disturbance causes water reabsorption from the outflow to the tank, diluting the tank back to set-point (or within some tolerance band).

Continuing the analogy of the previous design in Chapter 7 where the series-parallel setup was shown to have structural similarities with the kidneys of birds and mammals, by including negative feedback set-point control in the system, functional similarities become obvious too. It is known that in response to high plasma osmolality (primarily) or low pressure-volume [84], antidiuretic hormone (ADH) is released (in both birds and mammals;

details to follow) and acts to dilute the blood by reducing urine output (i.e. antidiuresis) through promoting urine concentration [1]. In the absence of such stimuli, ADH is not released and dilute urine is passed (i.e. water diuresis) in order to concentrate the blood plasma [1]. In this way, plasma osmolality, in particular, is kept within a narrow band of operation (narrower for mammals than birds, who are more labile [16]).

The implemented P-controller (with additional condition that manipulated variable $f_{w3} < 1$) provides a non-linear response (as expected by Bankir, who noted that the relationships between hyper-osmolality, ADH release and its antidiuretic effect are non-linear [84]) but is obviously an oversimplification. However, the aim was to demonstrate the principle of control, not optimise a controller. Presumably if a very simple P-control system can improve the response, any further control sophistication (if justifiable in terms of energy expenditure), would only improve the response further. The manipulated variables x and f_{w3}, have direct renal analogues, i.e. vascular and tubular receptors, sensitive to the presence of ADH that, when activated, promote water conservation.

The tubular response is well documented; arginine vasopressin (ADH in mammals) binds to V_2-type receptors in the collecting duct and initiates insertion of aquaporins (AQP_2 in particular [91]) as purported in the “membrane shuttle hypothesis” of Wade et al [92], increasing water permeability and return to the blood plasma. In the absence of ADH, the collecting duct remains impermeable to water. Likewise, arginine vasotocin (ADH in birds) has a similar effect on the collecting duct in avian kidneys (although indicated not to be as marked as in mammalian kidneys [93]). This type of ADH-mediated aquaporin response is suggested to have "evolved with terrestriality" as only mammals, birds and amphibians have been found to exhibit it [7].

The vascular response to ADH is not as thoroughly researched, especially in mammals. Braun and Dantzler studied the effect of arginine vasotocin on single-nephron glomerular filtration rates in the kidney of the desert quail, Lophortyx gambelli [94]. They found that the total-kidney glomerular filtration rate dropped, caused by a reduction in the number of filtering reptilian-type nephrons. This is similar to the effect found in reptiles [16]. In further research it was found that arginine vasotocin causes vasoconstriction of the afferent arterioles of the reptilian-type nephrons, causing them to stop filtering, but has no effect on the afferent arterioles of the mammalian-type nephrons [95]. Goldstein warns that these "landmark studies of functional heterogeneity among avian nephron populations" of the 1970s have neither been invalidated nor further rigorously tested [96]. He argues that what has been shown unequivocally is arginine vasotocin causing a reduction in whole avian kidney glomerular filtration rate (GFR) with concomitant reduction in urine flow. In addition,

he suggests that reduced filtrate means less flow, and thus improved tubular reabsorption aiding urine concentration.

In mammals, type V_{1a} receptors (to arginine vasopressin) are found in the renal vasculature, and particularly in the vascular smooth muscle cells and pericytes in the walls of descending vasa recta [97]. Stimulation has been found to reduce medullary blood flow [98–101] and in particular, inner medullary blood flow [84, 102] with no change in cortical or total renal blood flow. Such reduction in flow to the inner medulla is said to prevent a washout of the corticomedullary osmotic gradient [84], promoting tubular reabsorption, and thereby enhancing urine concentration.

Hura and Stein suggest that changes in blood flow to individual glomeruli (through relative changes in afferent and efferent arteriolar resistances) could affect SNGFR [47], a mechanism similar to that suggested in the model. However, according to them, a lack of consistent and accurate measurements of regional renal blood flow in mammals by renal scientists at the micro-level required has so far prevented the determination of whether this suggestion is true or not [47].

From a comparative biological point of view, Pang looked at the ADH response in a range of vertebrates and hypothesised that there has been an evolutionary shift in "relative predominance" from vascular (in more primitive species) to tubular (in more sophisticated and terrestrial species) [103]. This is not to say the vascular response is not contributory in mammals; in fact, it raises the question whether the vascular response provides ubiquitous background coarse control while the tubular response provides fine-tuning, but as shown in Section 8.1, this depends on the specific numerical values in the implementation. Bankir hypothesises dual interplay between the two mechanisms (i.e. vascular and tubular) dependent on the level of circulating ADH [84], modulated by prostaglandin secretion [104], something easily incorporated into the model by changing the relative contributions of the two control signals. As mentioned in Chapter 2, few high-level computational models of renal function in the literature incorporate nephron heterogeneity and intrarenal blood flow, those by Chandhoke and Saidel [41] and Moss and Thomas [29] standing out. The fact that such structure and function has essentially emerged from a bottom-up exploratory approach to modelling animal excretion suggests that this is definitely an avenue of research worthy of further investigation.

Fitting the model to specific data or hypotheses has not been the focus of this research; rather an investigation into the system structure needed to respond to increasingly constrained excretory requirements. To this end, progressively more complex structures have been realised, starting with a conformer's basic yet static structure and leading to a regulator's more complex and dynamic setup. A necessary investigation remains how splitting the

lumped solutes into constituents (and therefore more closely representing a mixed diet) will be managed by the developed system structure.

Chapter 9

Application

Now that the model structure is able to represent the excretory system of a volume- and osmo-regulator, albeit at a high-level, it is interesting (and necessary) to see whether the model is able to mimic a number of more life-like scenarios. Therefore, the original assumption of lumping all solutes together was relaxed, providing the mechanistic information necessary for mathematically describing mammalian excretion in more depth. In other words, such a change is responsible for lightening the shade of the grey box model, and in so doing, representing slightly more of reality.

9.1 Model setup

The decision was made to perform the following analysis on the pre-control design of Section 7.3 in Chapter 7 and not the controlled design of Chapter 8, since the open-loop response is stable and returns to steady-state, therefore emphasising the contribution of the innate structure of the design (and not the extra layer of feedback control) to its excretory function.

Instead of lumping all solutes together, consider two groups of solutes with different osmotic behaviour, say A and B. The corresponding extension to the model is illustrated in the tank setup in Figure 9.1 and level-rate diagram in Figure 9.2.

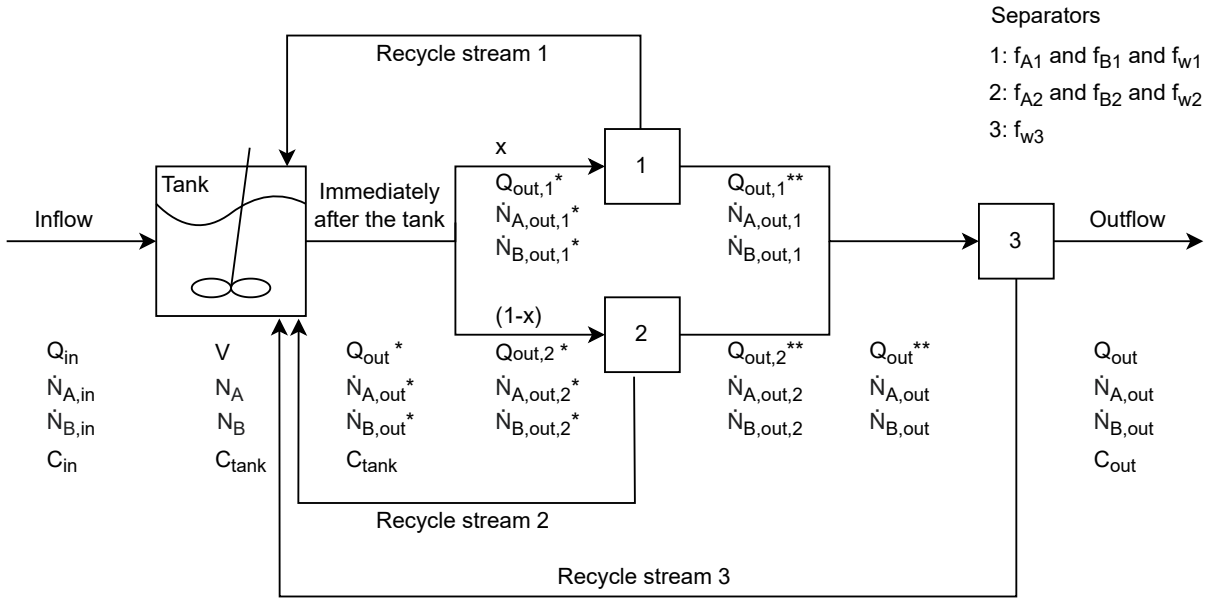


Fig. 9.1 Line diagram of tank setup for multiple solute implementation; separator 1 is defined by bulk flow coefficients f_{A1}, f_{B1} and water reabsorption coefficient f_{w1}, separator 2 is defined by bulk flow coefficients f_{A2}, f_{B2} and water reabsorption coefficient f_{w2}, and separator 3 is defined by water reabsorption coefficient f_{w3}

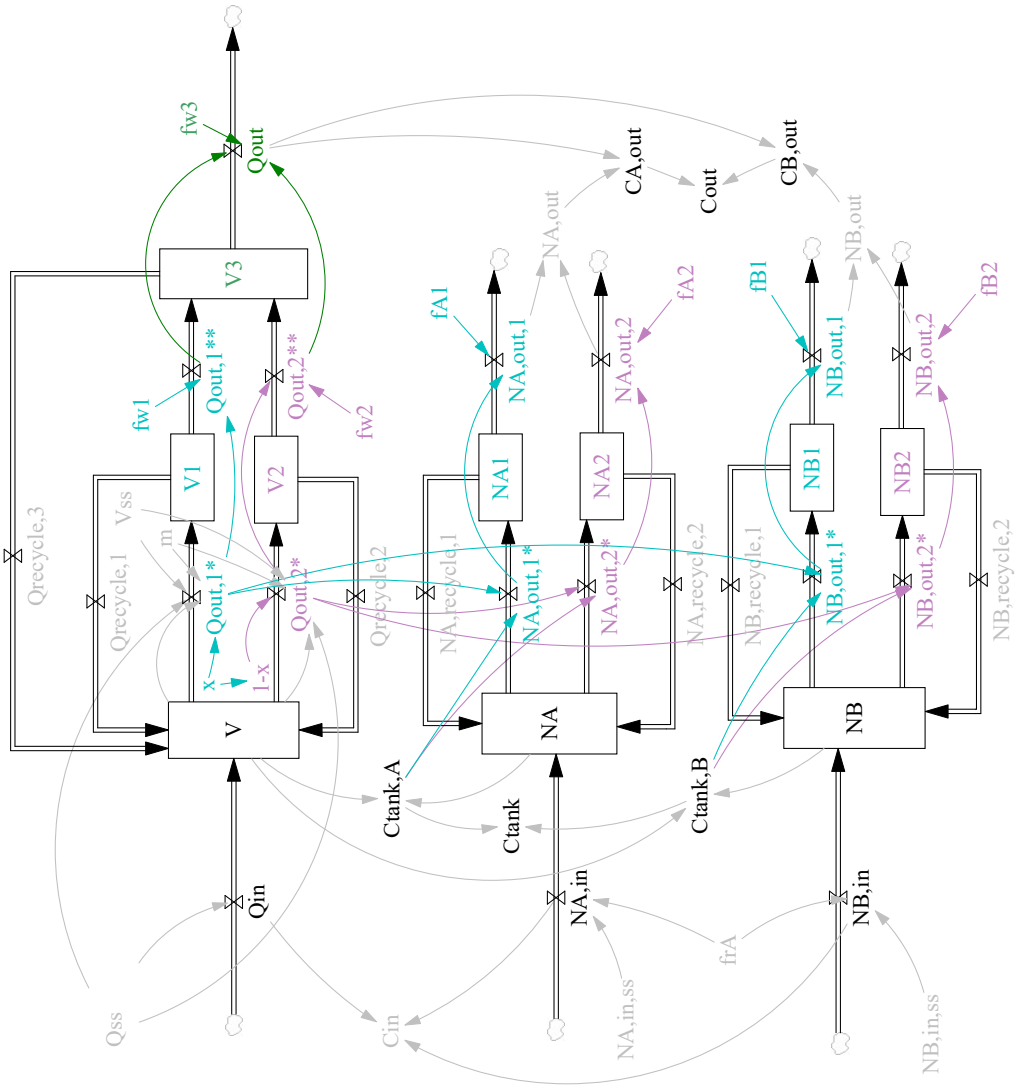


Fig. 9.2 Level-rate diagram showing multiple solute implementation; separator V_1 is defined by f_{w1}, V_2 by f_{w2}, V_3 by f_{w3}, N_{s1} by f_1 and N_{s2} by f_2

It is assumed that the two groups of solutes can be considered separately, mathematically (and therefore graphically as two levels with their associated rates in Figure 9.2), even though they are well-mixed in the tank and their overall behaviour is determined by their combined osmolarity (assuming the same osmotic contribution per mole for each of them).

Due to the independence of the solutes and system linearity, the individual overall solute transfer functions match Equation 7.52 in Section 7.3, Chapter 7 and are rewritten in terms of solute s (referring specifically to A or B in this chapter) in Equation 9.1.

$$\frac{f_s}{f_w} = \frac{C_{s,out}}{C_{s,tank}} = \frac{f_{s1}x + f_{s2}(1-x)}{f_{w3}(f_{w1}x + f_{w2}(1-x))} \tag{9.1}$$

Across separators 1 and 2, the individual solute transfer functions are defined in Equation 9.2.

$$\frac{f_{si}}{f_{wi}} = \frac{C_{s,out,i}}{C_{s,tank}} \tag{9.2}$$

Let "A" represent those solutes that are present at a lower concentration outside the organism than inside such that $\frac{f_A}{f_w} = \frac{C_{A,out}}{C_{A,tank}} < 1$ (an example of such a solute would be sodium (Na^+), which has a urine-to-plasma ratio (U/P) of 0.7 in humans [1]) and are easier to eliminate down a concentration gradient than "B", those solutes that are present at a higher concentration outside the organism compared to inside with $\frac{f_B}{f_w} = \frac{C_{B,out}}{C_{B,tank}} > 1$ (e.g. potassium (K^+) and urea, both with $U/P > 10$ in humans [1]) and therefore, harder to manage osmotically.

Combining the effects of solutes A and B depends on their relative fractions, calculated in Equations 9.3 and 9.4, respectively.

$$fr_A = \frac{C_{A,out}}{C_{out}} \tag{9.3}$$

$$fr_B = \frac{C_{B,out}}{C_{out}} = 1 - fr_A \tag{9.4}$$

Using Equations 9.1 to 9.4, the overall, dual-solute transfer function across the separation system can be written in Equation 9.5.

$$\frac{f}{f_w} = \frac{C_{out}}{C_{tank}} = \frac{C_{A,out} + C_{B,out}}{C_{A,tank} + C_{B,tank}} = \frac{\frac{f_A}{f_w}\frac{f_B}{f_w}}{(fr_A\frac{f_B}{f_w} + fr_B\frac{f_A}{f_w})} \tag{9.5}$$

The immediate water outflow of the tank, Q^*_{out}, is given by Equations 9.6 and 9.7 (as introduced for a water separator in Section 6.1.2 in Chapter 6).

$$Q^*_{out} = \frac{Q_{ss}}{f_w} + m(V(t) - V_{ss}) \tag{9.6}$$

$$V_{ss} = V_{dss} + \frac{Q_{ss}(1 - f_w)}{f_w} \tag{9.7}$$

The three ODEs follow in Equations 9.8, 9.9 and 9.10 (written in standard linear form in Appendix A.4.5).

$$\frac{dV}{dt} = Q(t) - (Q_{ss} + f_w m(V(t) - V_{ss})) \tag{9.8}$$

$$\frac{dN_A}{dt} = \frac{dC_{A,tank}V}{dt} = \dot{N}_{A,in}(t) - f_A C_{A,tank}(t)(\frac{1}{f_w}Q_{ss} + mV(t) - V_{ss}) \tag{9.9}$$

$$\frac{dN_B}{dt} = \frac{dC_{B,tank}V}{dt} = \dot{N}_{B,in}(t) - f_B C_{B,tank}(t)(\frac{1}{f_w}Q_{ss} + mV(t) - V_{ss}) \tag{9.10}$$

Because many conditions result in an imbalance in the electrolytes sodium and potassium [1], it is of interest to see whether such a simple, high-level model built to represent the osmotic behaviour of two such groups of solutes is able to accommodate the direction of such imbalance. This would provide some level of model validation considering the high-level implementation, adapted from the criteria used by Summers, which include qualitative directional appropriateness, quantitative stability and dynamic response [105]. As discussed in Chapter 8, it is assumed that the membrane properties remain fixed, and instead, it is through changing relative flow x between the solute separators, water reabsorption f_{w3}, solute inflow fractions fr_A and fr_B, and water inflow Q_{in}, that the model is interrogated.

The model parameters are included in Table 9.1.

9.2 Results and Discussion

It is clear from Equations 9.8, 9.9, 9.10, and Appendix A.4.5, that separating solutes into two groups simply increases the number of ODEs that govern overall model behaviour by one. Due to system linearity, the structure of the two solute ODEs, and therefore their response, is the same; they differ only in overall bulk flow coefficient (f_s) and therefore, mean residence time (τ_s).

Table 9.1 Application Model Parameters

Parameter	Value
Baseline water inflow (ml/hr)	100
Baseline solute inflow (mosm/hr)	28.1
Desired steady-state volume (ml)	1 000
m (1/hr)	1
fr_A	0 - 1
f_{wi}	0 - 1
f_{si}	0 - 1
x	0 - 1
f_{w3}	0 - 1

The general analytical solutions for each solute are identical to those for the series-parallel setup in Section 7.3.2 and repeated here. The tank volume response follows that of water separation in Section 6.2.2 in Chapter 6, through Equations 9.11, 9.12 and 9.13, while each component tank concentration response has mean residence time τ_s in Equation 9.14, dependent on both f_w and f_s.

$$V(t) = V_{ss} + (V_0 - V_{ss})e^{-\frac{t}{\tau_V}} \tag{9.11}$$

$$V_{ss} = V_{dss} + \frac{Q_{ss}(1-f_w)}{f_w} \tag{9.12}$$

$$\tau_V = \frac{1}{f_w m} \tag{9.13}$$

$$\tau_s = \frac{f_w}{f_s}\frac{V_{ss}}{Q_{ss}} \tag{9.14}$$

As for previous designs that include water-and-solute separators, the particular analytical solutions in Appendix A.5.6 show that the dynamic response of each component tank concentration to an impulse disturbance in solute s depends on τ_s, while that to a water impulse disturbance depends on τ_s and τ_V. A mixed input (which includes both water and potentially both solutes) would therefore depend on each τ_s and τ_V as well.

Referring to the steady-state analysis in Section 7.3.2 of Chapter 7, the choice of parameters f_{s1}, f_{s2}, f_{w1} and f_{w2} determines the extremes of the component and overall transfer functions over $x \in [0,1]$. In order to mimic the opposing osmotic behaviour of the solutes

Table 9.2 Application Model Parameters

Parameter	Value
f_{w1}	0.6
f_{w2}	0.4
f_{A1}	0.5
f_{A2}	0.5
f_{B1}	0.9
f_{B2}	0.2

being modelled (i.e. sodium with $\frac{U}{P} \approx 0.7 < 1$ and potassium or urea with $\frac{U}{P} \approx 10 > 1$), $\frac{f_A}{f_w} < 1$ and $\frac{f_B}{f_w} > 1$ must coincide over a region of x. And in order to achieve this passively, the values of f_{si} and f_{wi} are limited to the range $[0,1]$. The values in Table 9.2 provide one such example. Although many sets of different parameters will yield the same results, a passive implementation is considered key in this model's development.

Figure 9.3 shows how the component and overall transfer functions vary with x (assuming $f_{w3} = 1$ and $fr_A = 0.36$, arbitrarily); $\frac{f_A}{f_w} = \frac{C_{A,out}}{C_{A,tank}}$ decreasing and $\frac{f_B}{f_w} = \frac{C_{B,out}}{C_{B,tank}}$ increasing over the domain of x, providing an envelope in which overall $\frac{f}{f_w} = \frac{C_{out}}{C_{tank}}$ varies with the inflow ratio of A:B. The endpoints of the component transfer functions are fixed by $\frac{f_{s2}}{f_{w2}}$ at $x = 0$ (i.e. $\frac{f_{A2}}{f_{w2}}$ for solute A and $\frac{f_{B2}}{f_{w2}}$ for solute B) and by $\frac{f_{s1}}{f_{w1}}$ at $x = 1$ (i.e. $\frac{f_{A1}}{f_{w1}}$ for solute A and $\frac{f_{B1}}{f_{w1}}$ for solute B). The intersections of the curves with the "Transfer function = 1" line create regions of steady-state osmotic behaviour; Region 1 where $\frac{f_A}{f_w} > 1$ and $\frac{f_B}{f_w} < 1$, Region 2 where $\frac{f_A}{f_w} > 1$ and $\frac{f_B}{f_w} > 1$, and Region 3 where $\frac{f_A}{f_w} < 1$ and $\frac{f_B}{f_w} > 1$. Region 3 is obviously the region of choice for appropriate sodium and potassium or urea behaviour, and this is the case where $x \in [0.5, 1]$.

In Figure 9.4 it is seen that as f_{w3} decreases, the endpoints increase in proportion to $\frac{1}{f_{w3}}$ (as expected from Equation 9.1). In addition, the intersections of the curves with the horizontal line through 1 change; those of solute A occurring at greater values of x while those of solute B occurring at smaller values of x, ultimately changing the regions of osmotic behaviour.

A particular choice of $x = 0.7$ and $f_{w3} = 1$ for baseline conditions ensures desired Region 3 osmotic behaviour (as would many other choices). The steady-state effect of changing x and f_{w3} from baseline can be deduced from Figure 9.5, where component and combined steady-state concentrations in the tank and outflow are shown as a function of x for a range in $f_{w3} \leq 1$ (at $fr_A = 0.36$ in particular). An increase in x from baseline causes the tank concentration of solute A to increase (Figure 9.5a) and B to decrease (Figure 9.5b) with very little change in tank concentration overall (Figure 9.5c). A decrease in x from baseline

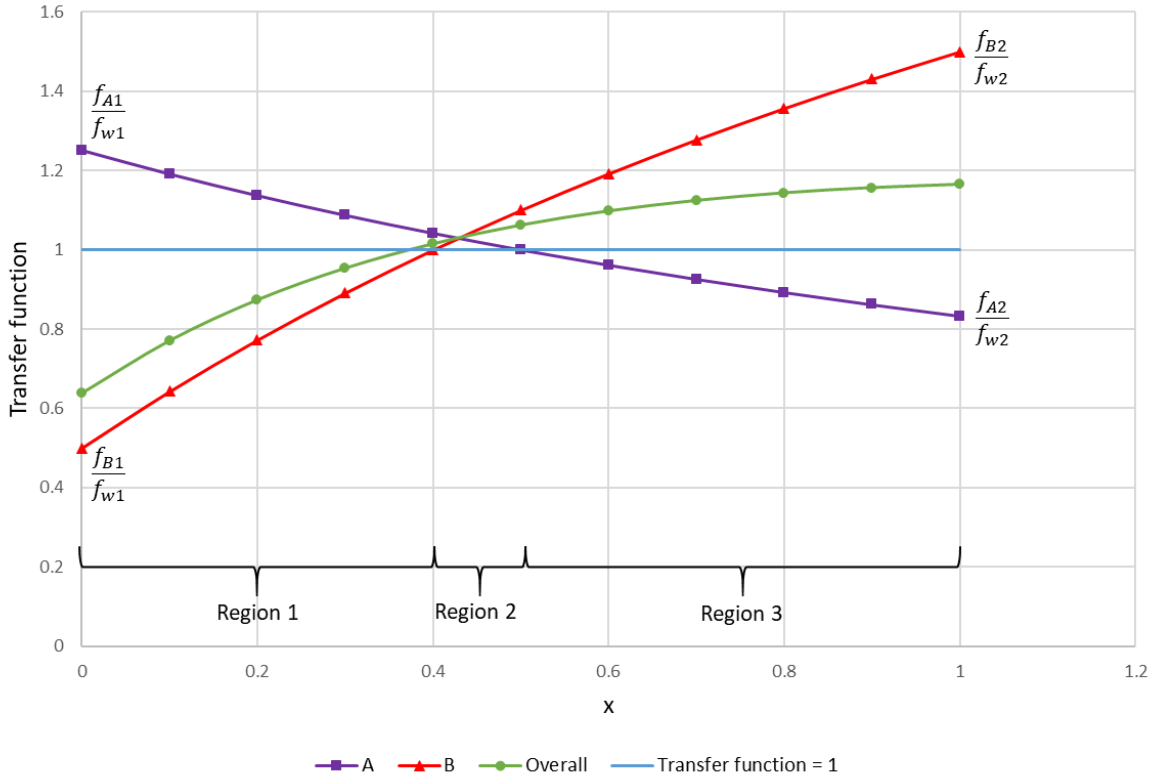


Fig. 9.3 Component and overall transfer functions versus fractional flow (x) for $f_{w3} = 1$ and $fr_A = 0.36$, with endpoints indicated

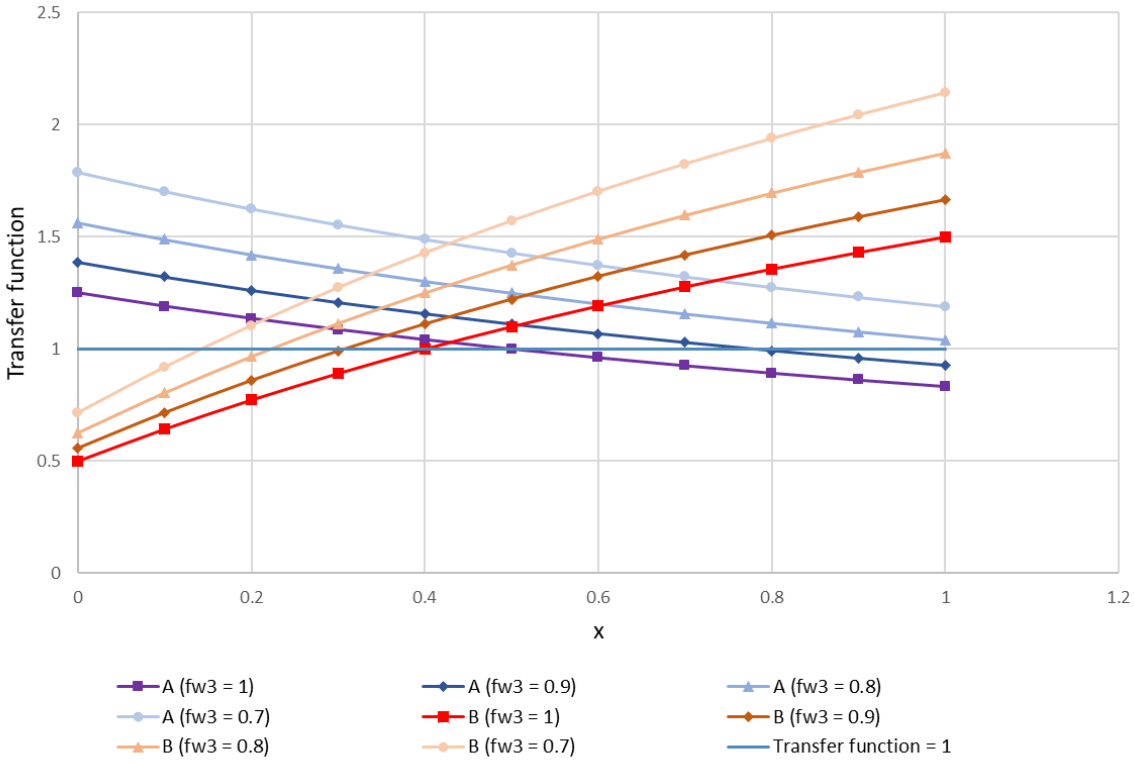
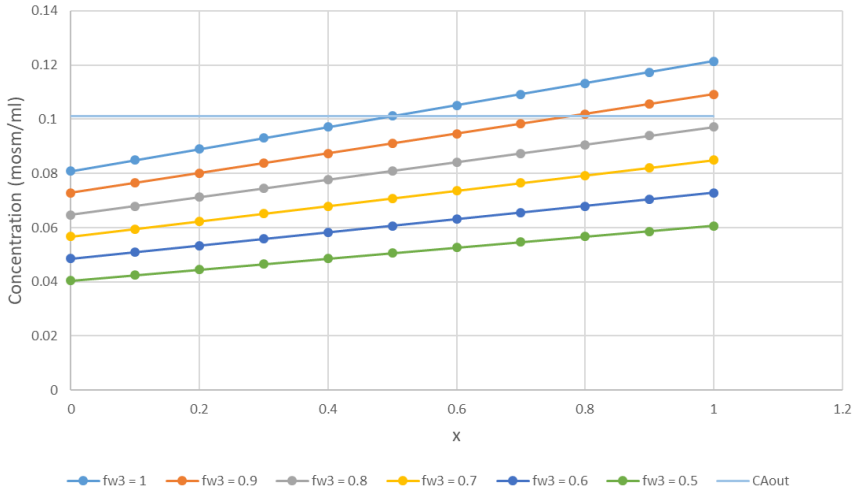
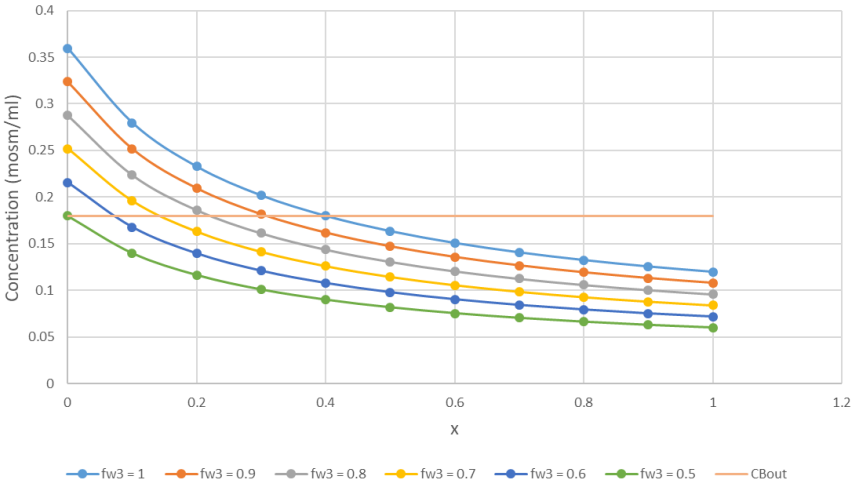


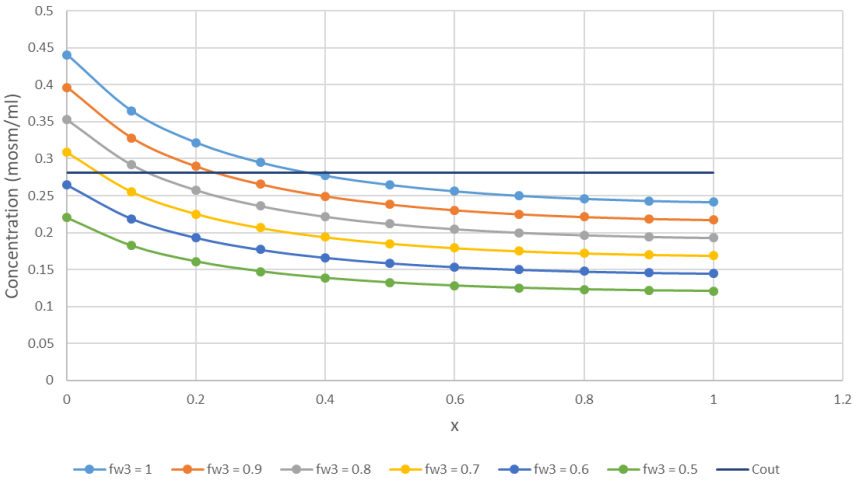
Fig. 9.4 Component transfer functions versus fractional flow (x) for a range in distal series water reabsorption ($f_{w3} \leq 1$)



(a) Solute A



(b) Solute B



(c) Combined solute

Fig. 9.5 Tank and outflow concentrations at steady-state versus fractional flow (x) for (a) solute A, (b) solute B, and (c) combined solute; for $fr_A = 0.36$ over a range of distal series water reabsorption (i.e. $f_{w3} \leq 1$)

on the other hand causes a decrease in A (Figure 9.5a) and an increase in B (Figure 9.5b) with a shallow increase in overall tank concentration (Figure 9.5c) that becomes more pronounced as $x \to 0$. As f_{w3} is reduced from baseline (i.e. more water is reabsorbed), component and overall tank concentrations maintain approximately the same shape or relationship with x but are shifted downwards, i.e. occurring at lower concentrations throughout, with no change in the corresponding outflow concentrations (set by the inflow through mass balance requirements).

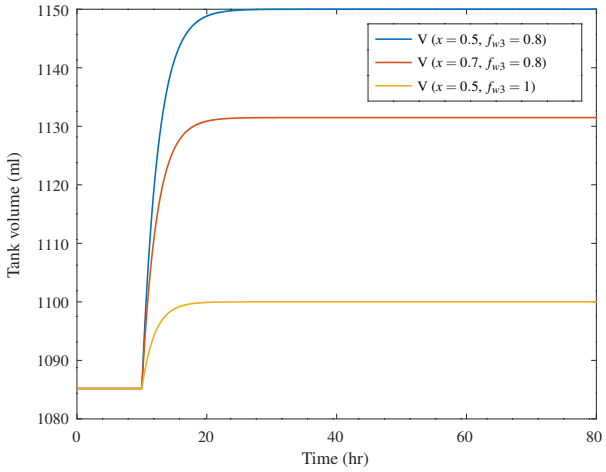
Transient (and steady-state) effects of changes to x and f_{w3} can be viewed in the time domain through simulation. If simulations are repeated in a systematic study of parameter combinations, some insight may be gained as to what the model structure is capable of through a process of discovery. A limited number of conditions that exhibit imbalances in sodium and / or potassium were considered.

9.2.1 The syndrome of inappropriate antidiuresis

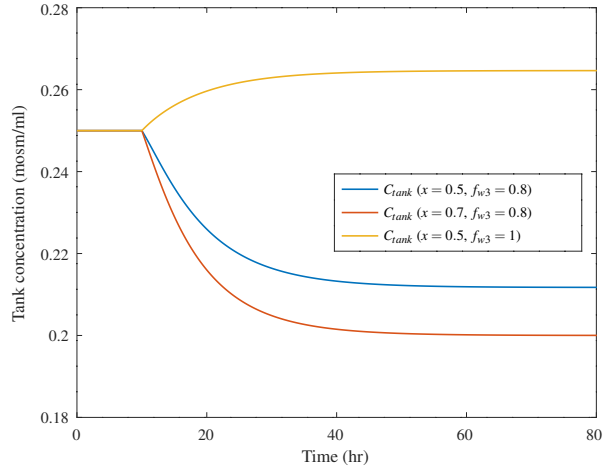
The syndrome of inappropriate antidiuresis (SIAD), previously referred to as the syndrome of inappropriate secretion of ADH (SIADH) [106], is a pathological condition in which the antidiuretic action of ADH is present in the absence of osmotic stimuli (and not simply due to excessive ADH circulation as previously thought) [107]. SIAD is said to make up approximately 35 % of all hyponatremic cases [108].

Assuming the model's response to concentrating stimuli via flow redirection and water reabsorption provides an acceptable analogy for the dual action of ADH on vascular and tubular receptors as argued in the previous chapter (Chapter 8), an abnormality in ADH secretion (such as occurs in SIAD) may be modelled as effecting the same changes but over a more sustained/indefinite period. This provides a scenario where both x and f_{w3} step down from baseline simultaneously (i.e. $x < 0.7$ and $f_{w3} < 1$).

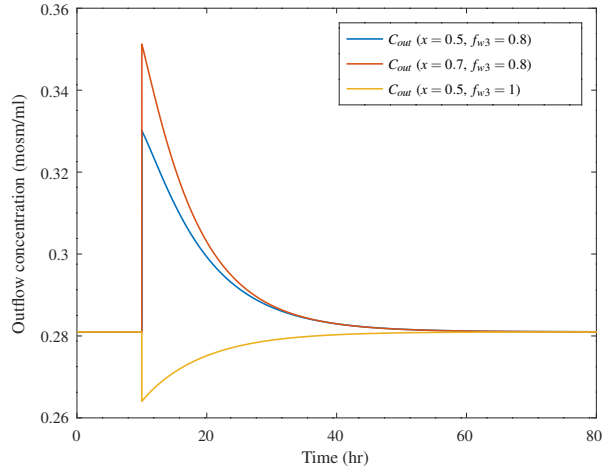
Figures 9.6 and 9.7 provide for comparison of individual and combined decreases in x and f_{w3}, simulated as negative step changes at $t = 10\ hr$ of height 0.2 units each. The yellow curve indicates a decrease in x alone, the red curve a decrease in f_{w3} alone, and the blue curve, a decrease in both x and f_{w3}. Figure 9.6 shows a long-term increase in volume in all three cases, with the combined case having the biggest effect (Figure 9.6a), a long-term change in tank concentration with f_{w3} changing alone and the combined case both decreasing and x changing alone increasing (Figure 9.6b), and an opposite transient change in outflow concentration (Figure 9.6c). Figure 9.7 shows the specific solute responses; the tank concentration of A decreasing and settling at a lower steady-state long-term for all three cases (Figure 9.7a), while B shows a relatively small decrease in steady-state long-term for the combined reduction in x and f_{w3}, a pronounced decrease for f_{w3} changing alone, and the



(a) Tank volume

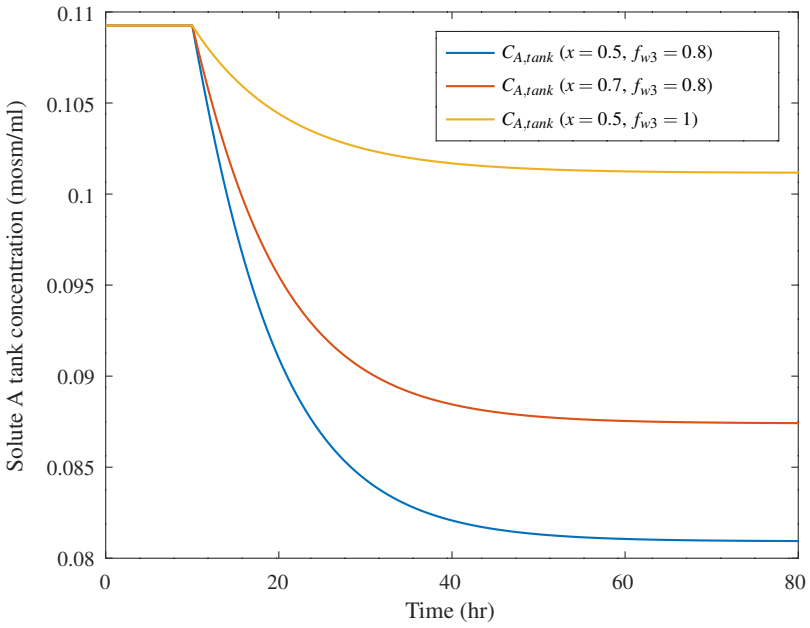


(b) Tank concentration

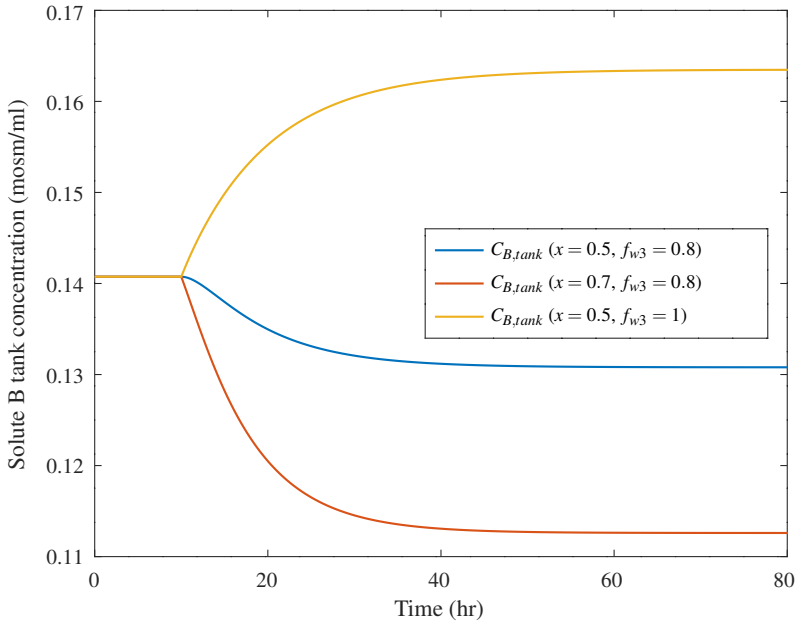


(c) Outflow concentration

Fig. 9.6 Comparison of individual and combined step changes in fractional flow (x) and series water reabsorption (f_{w3}) at $t = 10$ hr by 0.2 units each from a baseline of $x = 0.7$ and $f_{w3} = 1$ (modelling the syndrome of inappropriate antidiuresis), on (a) tank volume, (b) tank concentration and (c) outflow concentration



(a) Solute A tank concentration



(b) Solute B tank concentration

Fig. 9.7 Comparison of individual and combined step changes in fractional flow (x) and series water reabsorption (f_{w3}) at $t = 10$ hr by 0.2 units each from a baseline of $x = 0.7$ and $f_{w3} = 1$ (modelling the syndrome of inappropriate antidiuresis), on (a) solute A and (b) solute B tank concentrations

opposite for x changing alone (Figure 9.7b). Only the trends for the combined reduction in x and f_{w3} match all the characteristics of SIAD; i.e. water retention, hypo-osmolality, high urine osmolality (transiently), hyponatremia, and no typical association with a potassium imbalance [106], respectively.

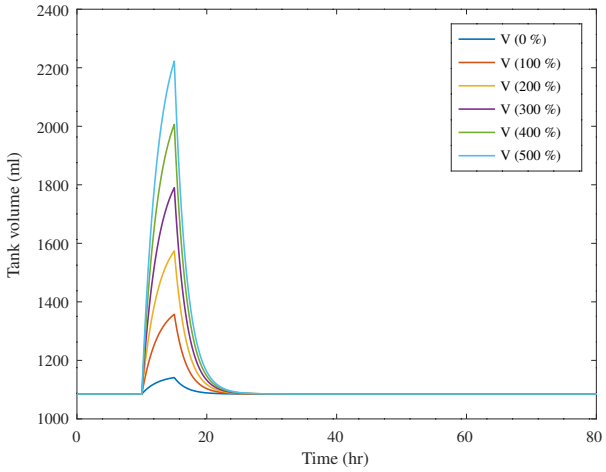
9.2.2 Exercise-associated hyponatremia

Exercise-associated hyponatremia (EAH) is defined as "hyponatremia occurring during or up to 24 hours after physical activity" [109]. It is most commonly caused by excessive fluid intake (beyond the requirement of thirst) at the same time as an unexpected exercise-induced non-osmotic ADH secretion [110, 109, 111], which reduces urine output, exacerbating fluid retention and electrolyte imbalance [112].

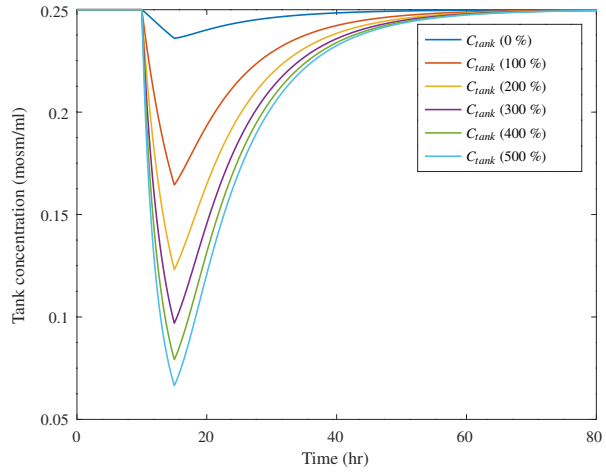
From Figure 9.5 it is expected that (following a prolonged water pulse and concurrent decreases in x and f_{w3}, modelling an antidiuretic response to excessive fluid intake) the tank concentration of solute A will decrease, that of B will increase due to a reduction in x but decrease due to a reduction in f_{w3}, and the overall tank concentration will decrease.

A temporary yet sustained increase in water inflow is modelled using a positive finite-duration water pulse of variable height (increasing in increments of 100 % to a maximum of 500 % above baseline, which would occur if the guidelines to drink 600 - 1200 ml/hour [113], replacing and exceeding sweat loss, were followed) and 5 hour duration (according to Noakes, less competitive athletes with slow marathon times of at least 5 hours who overhydrate for the duration are particularly at risk of developing EAH [114]). Concurrently, combined decreases in x and f_{w3} from baseline values of $x = 0.7$ and $f_{w3} = 1$ are modelled using negative finite-duration pulses of height 0.2 units each and 5 hour duration.

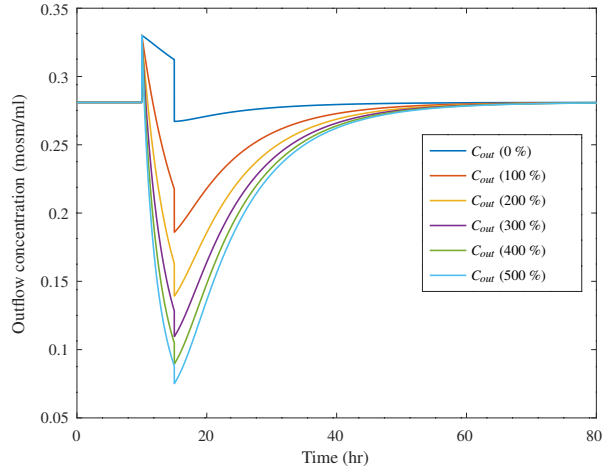
Figure 9.8 illustrates that the tank volume increases transiently (Figure 9.8a) while the tank concentration decreases transiently (Figure 9.8b), both returning to baseline steady-state once the disturbance has passed, however, at different rates (the tank volume response is quicker than the tank concentration response). This is backed up by the analytical solution in response to a water impulse disturbance (Appendix A.5.6; the tank volume response depends on τ_V (Equation 9.13) while the tank concentration response depends on τ_V, and τ_A and τ_B (Equation 9.14). The outflow concentration is seen to increase at onset of the disturbance and then decrease as the pulse is turned off, before returning to the original steady-state (Figure 9.8c). Since the tank acts as a buffer, a smooth transition back to steady state is expected; however, the unexpected discontinuous behaviour is due to the separators being simplified as having no dynamics for modelling purposes, and when x is changed, the output response is immediate. Figure 9.9 shows that solute A (Figure 9.9a) and B (Figure 9.9b) are diluted significantly but also have different recovery times, with solute A taking longer than solute B to recover back to steady-state (due to different τ_s in Equation 9.14). The significant and pro-longed decreases in solute A and overall tank concentration agree well with hypotonic hyponatremia experienced during EAH [112]. However, the severe and unpredicted decrease in solute B throughout the exercise pulse has no match in the literature and deserves further attention in the discussion.



(a) Tank volume

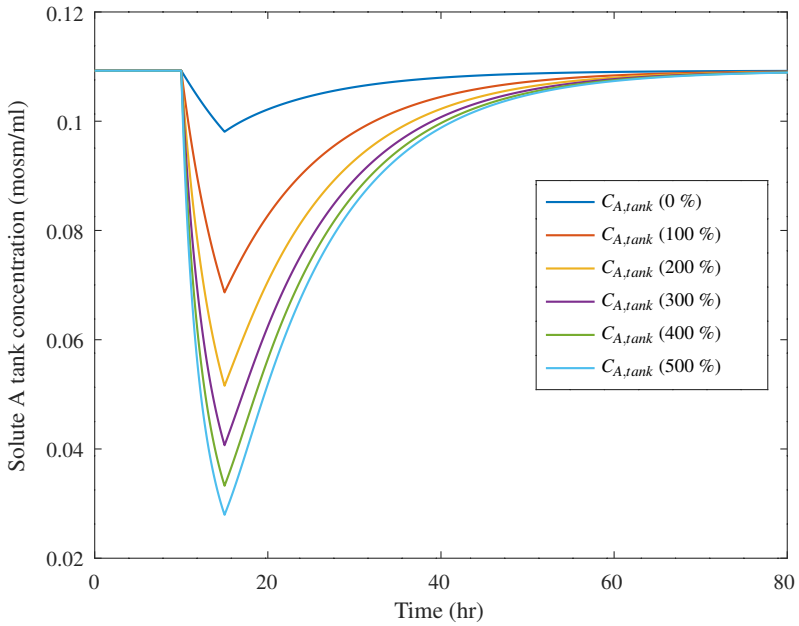


(b) Tank concentration

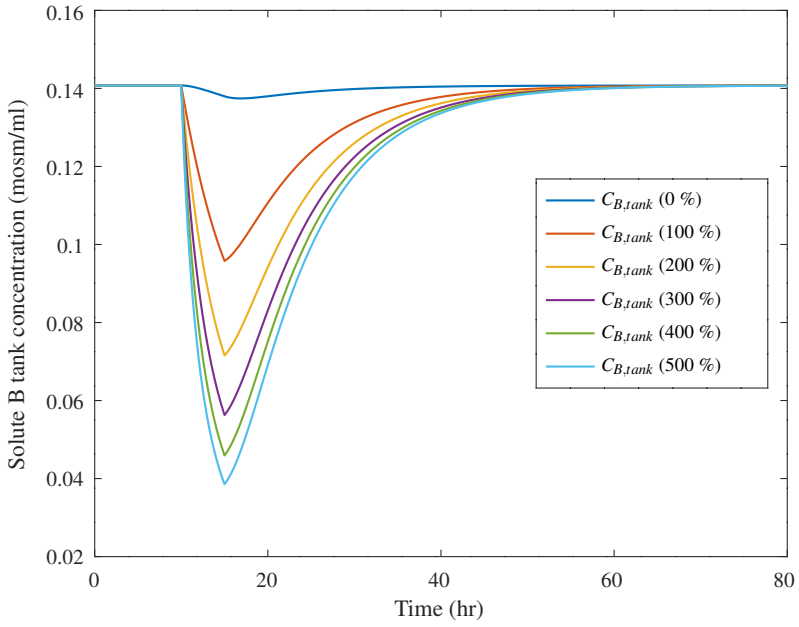


(c) Outflow concentration

Fig. 9.8 Comparison of varying the height of finite-duration water inflow (Q_{in}) pulse (ranging from 0 % to 500 % above baseline in 100 % increments) while reducing baseline fractional flow (x) and series water reabsorption (f_{w3}) by 0.2 units each over a 5 hour period (modelling exercise-associated hyponatremia), on (a) tank volume, (b) tank concentration and (c) outflow concentration



(a) Solute A tank concentration



(b) Solute B tank concentration

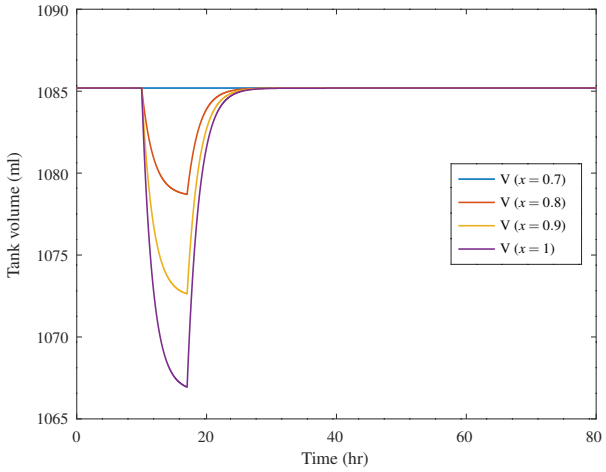
Fig. 9.9 Comparison of varying the height of finite-duration water inflow (Q_{in}) pulse (ranging from 0 % to 500 % above baseline in 100 % increments) while reducing baseline fractional flow (x) and series water reabsorption (f_{w3}) by 0.2 units each over a 5 hour period (modelling exercise-associated hyponatremia), on (a) solute A and (b) solute B tank concentrations

9.2.3 Loop diuretics

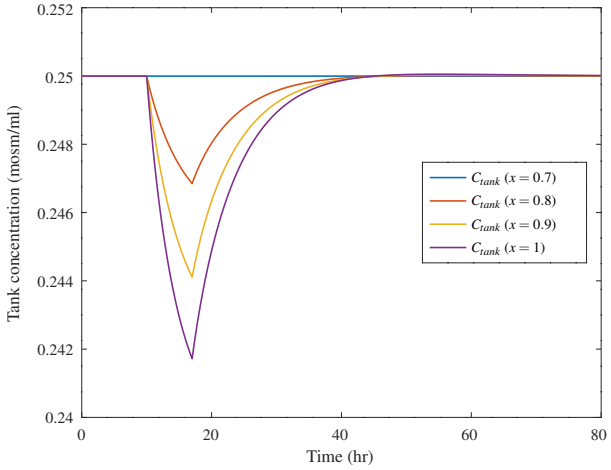
Diuretics are substances that relieve water retention through increased production of urine [1]. Different types exist depending on their mechanism of action, including but not limited to thiazide, loop and potassium-sparing [1]. Because diuretics influence electrolyte excretion in addition to water, an imbalance, and therefore electrolyte disorder, may occur as a side effect of their use [115]. The potassium-losing effect of loop diuretics [1] is most of interest here.

However, since the high-level model does not include sufficient detail to implement the generally accepted mechanism of action of loop diuretics (i.e. a decrease in active electrolyte reabsorption in the thick ascending limb of the loop of Henle and consequent water excretion [1]), another path had to be taken. It was realised that if flow were diverted (via increasing x) to the tank-concentrating first branch of the parallel setup (i.e. with less water recycle than the tank-diluting second branch), preferential water excretion would be achieved, as desired. In terms of associated solute flow, it is expected from Figure 9.5 that solute A will increase in the tank, while B will be pushed out, with no real net change in the overall tank concentration.

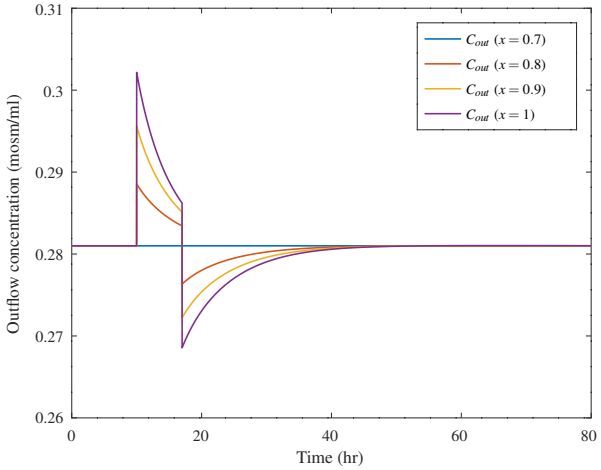
A temporary increase in x is modelled using a positive finite-duration pulse of variable height ($x \in [0.7, 1]$ in 1 unit increments) and 7 hour duration (furosemide has a therapeutic effect of 6-8 hours [116]). Figures 9.10 and 9.11 show simulation results; the tank volume decreases transiently (during application of the pulse in x) and returns quickly to the original steady-state (Figure 9.10a), while the tank concentration decreases a little during application of the water pulse, and returns (relatively) slowly back to steady-state (Figure 9.10b). The outflow concentration is seen to increase at onset of the pulse, decay exponentially during application of the pulse, decrease rapidly as the pulse is turned off, and then slowly increase back to steady-state (Figure 9.10c). Again, the rapid transitions are simply due to a lack of dynamics in the modelled separators. The direction of effect on the individual solute concentrations in the tank are opposite; solute A increasing and recovering slower (Figure 9.11a), and solute B decreasing and recovering faster (Figure 9.11b). The different mean residence times of the two solutes (Equation 9.14) determine their corresponding recovery times. Although the absolute concentration magnitudes are not relevant in themselves, the change of up to 20% in both cases is considered significant. Obviously repeated dosing (i.e. pulsing) would have more composite results. Such solute trends (an increase in solute A and decrease in solute B) tie in with signature responses to loop diuretics; i.e. hypernatremia and more importantly, hypokalemia [117].



(a) Tank volume

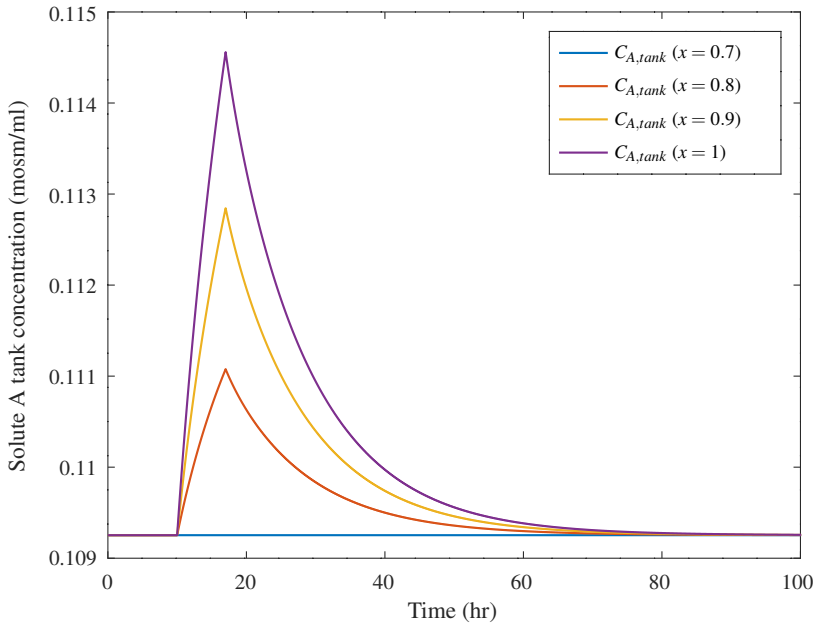


(b) Tank concentration

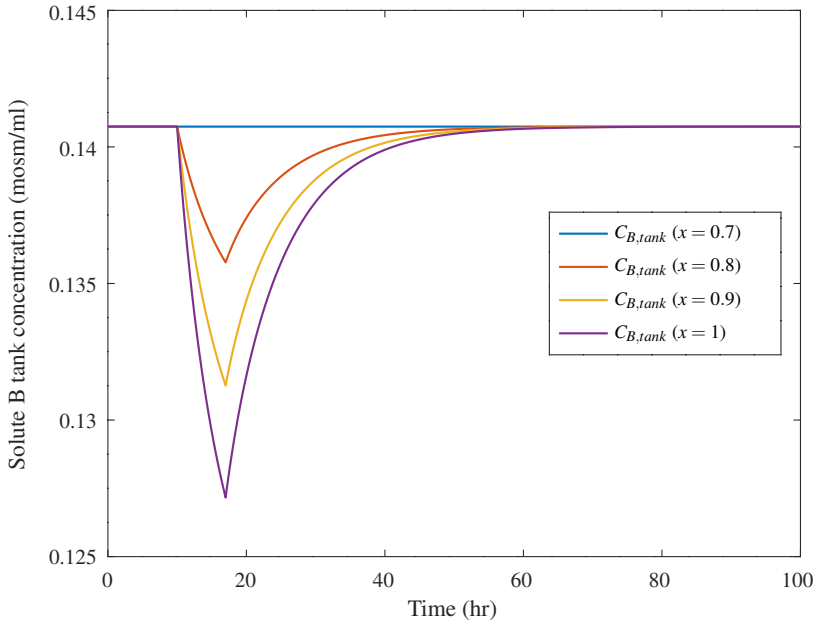


(c) Outflow concentration

Fig. 9.10 Simulation results for varying the height of positive finite-duration fractional flow (x) pulse in increments of 0.1 units from a baseline of $x = 0.7$ over a duration of 7 hr (with zero series water recycle (i.e. $f_{w3} = 1$)) (modelling the effect of a loop diuretic) on (a) tank volume and (b) tank concentration, and (c) outflow concentration



(a) Solute A tank concentration



(b) Solute B tank concentration

Fig. 9.11 Simulation results for varying the height of positive finite-duration fractional flow (x) pulse in increments of 0.1 units from a baseline of $x = 0.7$ over a duration of 7 hr (with zero series water recycle (i.e. $f_{w3} = 1$)) (modelling the effect of a loop diuretic) on (a) solute A and (b) solute B tank concentrations

9.3 Biological application

The idea behind this application chapter was to extend the model and determine whether it could be used to represent more real-life detail than had thus far been achieved. Considering the particular electrolyte imbalance scenarios of interest (i.e. SIAD, EAH and loop diuretics), the results show that the model is able to qualitatively demonstrate behaviour consistent with the known biology.

In order to achieve this, the previously lumped solute was split into two opposingly osmotically-active solutes; solute A favouring leaving the tank and solute B favouring remaining in the tank. This provided opposite osmotic challenges, which needed to be met through appropriate choice of design architecture and parameterisation. It was decided not to use the controlled version of the design (i.e. Chapter 8) in order to see what the innate structure of the design could explain without the contribution of an extra layer of control. But it must be remembered that the benefits of control, including de-linking the tank concentration from the outflow and improved transient response, would therefore be absent. Necessarily, changes were made to the pre-control open-loop version of the design (Section 7.3 in Chapter 7).

The two solutes, A and B, were chosen to represent lumped solutes of opposing osmotic behaviour (i.e. $\frac{f_A}{f_w} = \frac{C_{A,out}}{C_{A,tank}} < 1$ and $\frac{f_B}{f_w} = \frac{C_{B,out}}{C_{B,tank}} > 1$) and therefore the direction if not magnitude of the osmotic behaviour of sodium ions and potassium ions (or urea), respectively. This allowed some sort of comparison of model output to real-life observation to be possible. A next step in the modelling process could involve separating the lumped solutes into individual osmolytes (e.g. [38, 46]) but although the magnitude of response will depend on individual urine-to-plasma ratios, the direction of behaviour will be the same (a necessary component of model validation [105]). In addition, it is remembered that the abstract and high-level nature of the model makes any sort of point prediction meaningless and signature trends remain most of interest.

The particular scenarios of interest were chosen for presence of both volume and electrolyte imbalance effects, thereby essentially testing the volume- and osmo-regulatory capacity of the model (remembering the implications of lack of feedback control). Modelling an SIAD scenario through flow redistribution towards the tank-diluting second branch of the parallel setup (in terms of increased volume recycling) and promotion of series water reabsorption resulted in volume and osmolarity trends that match the observed characteristics of SIAD; i.e. water retention, hypo-osmolality and high urine osmolality [106]. These results are not surprising since analogies with ADH action had been drawn previously in the design process (Section 7.3.3). However, the development since then is achievement of the "correct"

direction of solute imbalance caused by shifting flows, especially that of hyponatremia and no typical association with a potassium imbalance [106].

Similarly, through modelling EAH with an extended finite-duration water pulse plus flow redistribution towards the tank-diluting second branch of the parallel setup and distal series water reabsorption that mimic the action of ADH (in this case, unexpected [110]), it was found that solute A and the overall tank osmolarity behave as expected during EAH (i.e. mimicking hypotonic hyponatremia [112]). However, the prediction of a decrease in solute B throughout the duration of the pulse representing the period of exercise and absence of matching documented hypokalemia in the literature highlights a limitation of the model; that of solute A and B simply representing the direction of osmotic behaviour of sodium and potassium and not relative magnitude (i.e. $\frac{C_{A,out}}{C_{A,tank}} < 1$, not ≈ 0.7 and $\frac{C_{B,out}}{C_{B,tank}} > 1$, not ≈ 10 at baseline to match U/P values [1]). The mean residence times in such a case would differ dramatically, with the much shorter mean residence time for solute B in the tank suggesting a need for a reservoir or second tank to compensate quickly for depletion (or excess) in the main tank, as is realised both in the body [1] and in high-level models thereof (examples are provided by Ikeda et al. [38] and Gyenge et al. [46]) for potassium ions through the intra-cellular fluid compartment [1]. Therefore, the current model is limited by a single compartment or tank representing a more complicated solute distribution. In lieu of an additional tank, a simple addition to the model could be a stream of solute B into the tank that turns on during exercise (and therefore similar to muscle contraction release of potassium into blood [118]) countering the observed depletion.

Although not implemented according to the generally accepted mechanism of action, similar volume and osmolarity trends to those of a loop diuretic (i.e. water diuresis accompanied by loss of potassium ions [1]) were achieved by simulating a temporary diversion of flow towards the tank-concentrating first branch of the parallel setup. As a result, in broad brush strokes, an alternative explanation for the mechanism of action of loop diuretics is hypothesised; i.e. fractional flow redistribution towards the non-concentrating cortical nephrons. To test such a claim would involve some means of assessing the relative intrarenal blood flow distribution in response to a loop diuretic. Real-time visualisation of blood flow to cortical and medullary regions of human kidneys with non-invasive phase-contrast magnetic resonance imaging (MRI) or ultrasound is suggested.

A core assumption throughout the design process has been the decision to keep membrane properties fixed (i.e. bulk flow coefficients f_{A1}, f_{A2}, f_{B1}, f_{B2} and water reabsorption coefficients f_{w1} and f_{w2}) and only change flow properties (i.e. flow distribution x and water reabsorption coefficient f_{w3}). The same mathematical results for overall f and f_w could be achieved if appropriate changes were made to the membrane permeabilities (via bulk

flow coefficients f_{A1}, f_{A2}, f_{B1}, f_{B2} and water reabsorption coefficients f_{w1} and f_{w2}) instead of x due to dependence of parameters. However, taking the biological excretory system application into consideration, it is considered interesting that it is possible to achieve an explanatory model without the need to invoke influence on membrane characteristics.

In fact, it is wondered whether the action of potassium-sparing diuretics such as the mineralocorticoid receptor antagonist Spironolactone may be modelled as affecting particular membrane permeabilities (via some or all of the bulk flow coefficients f_{A1}, f_{A2}, f_{B1} and f_{B2} and water reabsorption coefficients f_{w1} and f_{w2}), which would change the endpoints of the component transfer function curves in Figure 9.3 and therefore the dynamics of the response. In the case of Spiranolactone, water diuresis is accompanied by increased excretion of sodium and decreased excretion of potassium [1], which may be explained by an upward shift in the transfer function curve for solute A and downward shift in the transfer function curve for solute B. It must be realised that this is only one of several possible explanations, some of which may not be as physically plausible.

The implication of the tank-separator-recycle structure and fractional flow switching between parallel separators with differential water reabsorption coefficients and membrane permeabilities, and distal series water reabsorption, is that pressure energy from the heart (via 20% of cardiac output [17]) provides sufficient energy to achieve similar volume and osmotic regulation as in the sophisticated mammalian kidney. All of which are structures and functions essentially present in the actual kidney. Such a "passive" mechanism would agree with the findings of Louw et al., who calculated that the pressure drop across the kidneys alone provides for about twice as much work than that required to separate blood into urine, discounting the need for large quantities of metabolic energy [19]. Again, assessing intrarenal blood flow redistribution following volume and osmotic disturbances (employing phase-contrast MRI or ultrasound, for example) would provide falsifiability.

These findings illustrate how simulation with a simple model is able to show valid modes of behaviour and provide mechanistic suggestions despite the high-level of abstraction assumed at the start, emphasising the usefulness of such an approach.

Chapter 10

Conclusion

From a comparative biology perspective, it is considered interesting that all organisms, no matter their complexity, are faced with the same excretory challenge (i.e. taking in water and nutrients and removing excess and wastes in order to maintain some kind of internal balance), and yet manage it differently. The capacity of the excretory system seems to have evolved depending on the organism's environment (i.e. constant versus wide-ranging diet and exposure) and tolerance, with conformers more volume- and osmo-tolerant internally than regulators.

Modelling can be performed for the sole purpose of aiding understanding [51]. Both the approach taken and level considered determine the usefulness of the results to the particular application of interest. Due to limitations involved in intrarenal modelling [29], the field of whole-kidney and multi-organ modelling was established. However, whole-kidney models remain constrained by anatomy and physiology (although less so than higher resolution intrarenal models) due to the assumption that they model the complex mammalian kidney from the start. Taking the lead from evolutionary biology, an even higher systems' level analysis of excretion across the animal spectrum (but starting simply), is less constrained and consequently more flexible and potentially more exploratory.

In order to model such a system of varying sophistication, a step-wise, bottom-up and iterative approach to modelling was favoured. A high-level grey-box model was developed in stages, each characterised by a particular relationship between the outflow and tank concentrations (essentially the transfer function across the excretory system). This provided a means of quantifying the need to excrete with or against the concentration gradient between the inside and outside of the organism. Differences between successive stages represent incremental changes in structure and function, accommodating increasing constraints on the system. A strength of such an approach to modelling is that the various stages in the design are able to mimic the response of animals ranging from the unicellular to sophisticated mammals,

Goal	Key assumptions	Physiological scale	Advantages	Disadvantages
An exploratory approach to systems' analysis to add value and provide evolutionary insight into efficiency of excretory function in biology	High-level low resolution input-output grey-box series of models representing evolution of excretion from volume- and osmo-conformers through to tight regulators; single well-mixed compartment; lumped solute; volume of the excretory system is small compared to that of the organism; adjustment of relative flow between parallel separators and distal water reabsorption matches intrarenal blood flow redistribution between heterogeneous populations of nephrons and changing collecting duct permeability under the influence of ADH	Systems' level; whole organism; representing excretion in single cells to complex mammals	Simple; less constrained, flexible, exploratory approach to modelling; built based on functional requirement; passive implementation; different stages in design mimic different animal excretory responses, therefore not limited to describing mammalian excretion; includes simulations of diuretic and anti-diuretic states; shows valid modes of behaviour and provides mechanistic suggestions; (limited) exploration within physiological, pathophysiological and pharmacological contexts is possible	High level of abstraction and analysis yields point prediction impossible; overparameterised model means solutions can only be interpretted in terms of the biological application; true model validation not possible; single compartment model limited once lumped solute assumption relaxed; bottom-up evolutionary approach limited by choice to model excretion and not other kidney functions

Fig. 10.1 Summary of developed exploratory model of excretion

to volume and solute disturbances in their environment, and not limited to mammals. In addition, the iterative approach to modelling provided opportunities to propose tangential hypotheses throughout the process rather than simply at the end, emphasising the exploratory nature.

Table 10.1 provides a means of comparing the developed design with previous systems' level analyses of renal function, as summarised in Tables 2.1, 2.2 and 2.3 in Chapter 2, emphasising its uniqueness in the field. Weaknesses in the model are acknowledged, however, many of the findings would not have been possible if a higher-resolution, functionally-constrained approach had been taken.

In the first design of Chapter 4, a simple non-constant-volume continuously-stirred tank is able to mimic the behaviour of primitive cells in terms of expanding and contracting in response to diluting and concentrating disturbances, respectively.

Adding pressure feedback in the second design of Chapter 5 yields a constant-volume continuously-stirred tank, which is better able to describe volume and solute regulation evident in primitive animals such as the hagfish and even crude blood pressure control in sophisticated mammals.

Incorporating various separators on the outflow of the tank in the third design of Chapter 6 provided for comparison of solute and water separators, both able to provide for differentiation of the outflow and tank concentrations. The convective solute separator design is useful in describing the excretory systems of osmoconformers or those organisms that are relatively

osmotolerant, while the water separator, by design, can only describe organisms limited to producing concentrated outflow.

Placing additional separators on the outflow in different configurations in the fourth design of Chapter 7 provided a means of achieving different excretory behaviour, for example, providing the means to concentrate the outflow in a previously diluting setup, and vice versa. Structural analogies with bird and mammalian kidneys were drawn. However, the model remained static and the tank concentration dependent on the outflow (and therefore inflow through mass balance considerations).

Set-point control was implemented in the fifth design of Chapter 8 by means of two control points (i.e. variable flow between parallel water-and-solute separators, and variable distal water reabsorption), providing a means of delinking the tank and outflow concentrations and improving the transient response to water and solute disturbances, ultimately providing for tight volume- and osmo-regulation, as is realised by sophisticated animal kidneys (i.e. mammals and, to some extent, birds).

Initially unconstrained, the different levels of the model have been designed to describe an increasingly constrained or regulated system. In other words, the requirements of the excretory system in tolerant simple organisms are minimal when compared to sophisticated volume- and osmo-regulators, and the different levels of the model reflect this.

Through such an exploratory bottom-up approach to the design of an excretory system model able to mimic the function of a sophisticated kidney, many findings were made, the most interesting and pivotal included here.

The continuously-stirred tank assumption of Section 3.3 in Basic Design Chapter 3 is considered simple yet proved fundamental in providing the mechanistic information needed for grey-box modelling. No change was made to the single compartment model (despite other kidney-level models incorporating multiple compartments [38, 46]) over the entire range of organisms considered, incremental additions being made to the outflow only.

The need for different types and complexity of control mechanisms, e.g. those that flatten versus speed up a response, was seen to depend on the degree of osmo-tolerance and size relative to flow (i.e. mean residence time). An animal with small mean residence time is inherently more sensitive to disturbance and more prone to larger and faster responses than an animal with high mean residence time, which is less sensitive due to inherent buffering capacity, unless catered for by means of control. It is therefore suggested that an osmoregulating animal with a smaller mean residence time requires a more complex excretory system than that with a higher mean residence time. A similar argument is postulated for increased infant drug sensitivity, based simply on size relative to flow, and not necessarily organ immaturity.

The fact that simple pressure feedback in the second design (Chapter 5) onwards is sufficient in providing volume regulation at the level of cells, and pressure diuresis and natriuresis in primitive animals such as the hagfish through to long-term arterial pressure control in sophisticated animals, emphasises its inherent utility. A possible explanation for the exponential shape of the renal urinary output or renal function curve (which depicts the processes of pressure diuresis and natriuresis in humans [1]) is suggested.

Solute and water separation on the outflow, introduced in the third design of Chapter 6, provide a means of differentiating the tank's response to solute and water disturbances, a fact exploited later in the parallel arrangement of separators from Chapter 7 onward. Variable flow between said parallel separators, not only provides for a swing in concentrating ability from dilute to concentrated (depending on the endpoints provided by the actual separators) or vice versa, but also provides a means of responding optimally to a range of concentrating and diluting disturbances. This emphasises the model's flexibility in coping with the separate challenges of volume- and osmo-regulation, as in the sophisticated mammalian kidney.

Analogies have been drawn between the model and biological structures and/or functions of excretion throughout the process of model development, emphasising the evolutionary driving forces of volume and osmotic control, both in an exploratory bottom-up approach to modelling and in the biology the model aims to imitate. Limiting such examples here to those mirroring sophisticated excretory systems, the parallel part of the composite series-parallel structure in the fourth design of Section 7.3 in Chapter 7, followed by a series water separator, has structural similarities with the internephron heterogeneity and differential intrarenal blood supply, and collecting duct system, respectively, evident in both bird and mammalian kidneys (incidentally the only animals able to create concentrated urine [16]). In addition, the model parameters chosen as manipulated variables in the feedback control implementation of the fifth design in Chapter 8, i.e. relative flow between the branches of the parallel setup and series water reabsorption, have direct renal analogues, i.e. vascular and tubular receptors for antidiuretic hormone. The model therefore shows functional similarities with bird and mammalian kidneys as well. Interestingly, relatively few published kidney-level models (e.g. [41, 29]) take internephron heterogeneity and differential intrarenal blood supply into consideration despite "an increase in nephron heterogeneity" being "linked to an improvement in urine concentrating ability" [26] and "a growing body of literature" supporting "the hypothesis that differential regulation of blood flow to the cortex and medulla plays a mechanistic role in the regulation of salt and water excretion" [25]. The findings here suggest further investigation (both experimental and theoretical) would be of value.

A tangent of interest remained the modelling of more realistic scenarios, despite the high level of abstraction considered so far. Therefore, additional detail was added to the

model structure of the uncontrolled fourth design of Section 7.3 in Chapter 7 (and not the fifth, controlled version of Chapter 8, being more interested in innate structure and function than controller fine-tuning). The previously-lumped solute was split into two, ostensibly representing the opposing osmotic behaviours of sodium and potassium or urea. Following high-level calibration, similar trends in electrolyte imbalance and volume and osmo-dysregulation that are exhibited in the syndrome of inappropriate antidiuresis and exercise-associated-hyponatremia were achieved. In addition, a hypothesis regarding the proposed action of loop diuretics was made based on model findings; that a shunt in flow towards the diluting branch of the separator arrangement causes the same trend in volume depletion and electrolyte imbalance (i.e. potassium-losing).

Unexpectedly, an advantage of such a high-level model is the physical simplicity and achievability it has hinted at. The recycle paths within the tank-separator-recycle architecture of the series-parallel setup from the fourth design in Chapter 7 onwards, provide a means of implementing water and solute excretion so-called "passively" [1] down a concentration gradient, no matter the solute concentration in the outflow relative to the tank. The implication of this is that pressure energy from the heart provides sufficient energy to achieve similar volume and osmotic regulation as in the sophisticated mammalian kidney, simply through relative flow switching between parallel separators with differential membrane permeabilities and distal series water reabsorption. In addition, the model, relying simply on flow switching, has explanatory power without the need to invoke influence on membrane characteristics. As alluded to in the introduction, this may be considered to have contributed to evolutionary insight into efficiency of excretory function in biology. A caveat remains that many sets of model parameters can yield the same result and the findings need to be interpreted in terms of the biology they are trying to describe.

It is acknowledged and repeatedly emphasised that the high level of abstraction assumed at the start of the modelling process and the consequent assumptions (although relaxed somewhat later on) renders point prediction impossible and therefore signature trends and modes of behaviour are considered more important. Having said this, given the established model mechanism that can produce outputs that mimic those of sophisticated kidneys, a number of predictions regarding the corresponding biological mechanisms have been made and are worth following up. All are related to flow redistribution between cortical (predominantly short-looped) and juxtamedullary (predominantly long looped) nephrons, and therefore an investigation into differential intrarenal blood flow is recommended. Real-time visualisation of blood flow to cortical and medullary regions of human kidneys with non-invasive phase-contrast MRI or ultrasound is suggested. The effects of administration

of both antidiuretic hormone and a loop diuretic are of interest, the results of which would provide falsifiability for the proposed contribution of the flow redistribution mechanism.

It is appreciated that the high level of modelling and consequent inability to conduct point prediction may be self-limiting in the long-term, since the value of most Biomedical Engineering models lies in their clinical utility. It is therefore hoped that this work sparks follow-up investigation at a lower level, especially if falsifiability studies prove promising.

Much remains to be understood about solute and water excretion in living organisms. It is anticipated that the series of models developed in this thesis provide a basis to explore the alternative set of hypotheses that are physically plausible and biologically consistent. In so doing, the potential exists to explain hitherto unexplained phenomena without invoking elaborate mechanistic arguments. It is hoped that this may contribute to clinically useful insights into renal physiology.

References

[1] A. C. Guyton and J. E. Hall, *Textbook of medical physiology*. Elsevier Inc.: Philadelphia, PA, eleventh ed., 2006.

[2] R. S. Burns, *Advanced control engineering*. Butterworth-Heinemann, Oxford, 2001.

[3] R. E. MacMillen and A. K. Lee, "Water metabolism of Australian hopping mice," *Comparative Biochemistry and Physiology*, vol. 28, no. 2, pp. 493–514, 1969.

[4] P. Willmer, G. Stone, and I. Johnston, *Environmental Physiology of Animals*. Oxford, UK: Blackwell Publishing Ltd, second ed., 2005.

[5] T. L. Poulson and G. A. Bartholomew, "Salt Balance in the Savannah Sparrow," *Physiological Zoology*, vol. 35, pp. 109–119, 4 1962.

[6] H. W. Smith, "The functional and structural evolution of the vertebrate kidney," *Sigma Xi Quarterly*, vol. 21, no. 4, pp. 141–151, 1933.

[7] S. McCormick and D. Bradshaw, "Hormonal control of salt and water balance in vertebrates," *General and comparative endocrinology*, vol. 147, no. 1, pp. 3–8, 2006.

[8] "Glossary of Environment Statistics, Studies in Methods," 1997.

[9] J. P. Bentley, *Principles of Measurement Systems*. Harlow, United Kingdom: Pearson Education Limited, fourth ed., 2005.

[10] S. M. Shinners, *Modern control system theory and design*. Wiley-Interscience, second ed., 1998.

[11] K. Schmidt-Nielsen, "The salt-secreting gland of marine birds," *Circulation*, vol. 21, pp. 955–967, 5 1960.

[12] A. Keys and E. N. Willmer, ""Chloride secreting cells" in the gills of fishes, with special reference to the common eel," *The Journal of physiology*, vol. 76, pp. 368–378, 11 1932.

[13] H. W. Smith, "Water Regulation and Its Evolution in the Fishes," *The Quarterly Review of Biology*, vol. 7, no. 1, pp. 1–26, 1932.

[14] A. Krogh, "Osmotic regulation in fresh water fishes by active absorption of chloride ions," *Zeitschrift für vergleichende Physiologie*, vol. 24, no. 5, pp. 656–666, 1937.

[15] D. H. Evans, "Teleost fish osmoregulation: What have we learned since August Krogh, Homer Smith, and Ancel Keys," *American Journal of Physiology - Regulatory Integrative and Comparative Physiology*, vol. 295, no. 2, pp. 704–713, 2008.

[16] E. J. Braun, "Comparative renal function in reptiles, birds, and mammals," *Seminars in Avian and Exotic Pet Medicine*, vol. 7, no. 2, pp. 62–71, 1998.

[17] S. Thomson and R. Blantz, "Biophysical Basis of Glomerular Filtration," in *Seldin and Giebisch's The Kidney* (R. Alpern and S. Hebert, eds.), ch. 21, pp. 565–587, Amsterdam, Boston: Elsevier Academic Press, fourth ed., 2008.

[18] J. M. Sands and H. E. Layton, "Advances in understanding the urine-concentrating mechanism," *Annual Review of Physiology*, vol. 76, pp. 387–409, 2014.

[19] R. Louw, D. Rubin, D. Glasser, R. Letts, and D. Hildebrandt, "Thermodynamic considerations in renal separation processes," *Theoretical Biology and Medical Modelling*, vol. 14, no. 2, 2017.

[20] W. H. Dantzler, "Comparative physiology of the kidney," in *Handbook of physiology. Comprehensive Physiology*, ch. 11, pp. 415–474, John Wiley & Sons for American Physiological Society, 2011.

[21] R. G. Evans, G. A. Eppel, W. P. Anderson, and K. M. Denton, "Mechanisms underlying the differential control of blood flow in the renal medulla and cortex," *Journal of Hypertension*, vol. 22, no. 8, pp. 1439–1451, 2004.

[22] S. Hebert, "Nephron heterogeneity," in *Handbook of physiology. Comprehensive Physiology*, ch. 20, pp. 875–925, John Wiley & Sons for American Physiological Society, 2011.

[23] J. M. Sands and H. E. Layton, "The Urine Concentrating Mechanism and Urea Transporters," in *Seldin and Giebisch's The Kidney: physiology & pathophysiology* (R. J. Alpern and S. C. Hebert, eds.), ch. 40, pp. 1143–1178, Amsterdam; Boston: Elsevier Academic Press, fourth ed., 2008.

[24] W. Kriz and B. Kaissling, "Structural Organisation of the Mammalian Kidney," in *Seldin and Giebisch's The Kidney: physiology & pathophysiology.* (R. J. Alpern and S. C. Hebert, eds.), pp. 479–563, Amsterdam; Boston: Elsevier Academic Press, fourth ed., 2008.

[25] T. L. Pallone and C. Cao, "Renal Cortical and Medullary Microcirculations: Structure and Function," in *Seldin and Giebisch's The Kidney: physiology & pathophysiology.* (R. J. Alpern and S. C. Hebert, eds.), ch. 23, pp. 627–670, Amsterdam; Boston: Elsevier Academic Press, fourth ed., 2008.

[26] L. Bankir and C. De Rouffignac, "Urinary concentrating ability: Insights from comparative anatomy," *American Journal of Physiology - Regulatory Integrative and Comparative Physiology*, vol. 249, no. 6, pp. R643–R666, 1985.

[27] I. Sperber, "Studies on the mammalian kidney," *Zool. Bidr. Uppsula*, vol. 22, pp. 249–432, 1944.

[28] B. Schmidt-Nielsen and R. O'Dell, "Structure and concentrating mechanism in the mammalian kidney," *Am J Physiol*, vol. 200, pp. 1119–1124, 1961.

[29] R. Moss and S. R. Thomas, "Hormonal regulation of salt and water excretion: A mathematical model of whole kidney function and pressure natriuresis," *American Journal of Physiology - Renal Physiology*, vol. 306, p. F224–F248, 2014.

[30] A. M. Weinstein, "Mathematical models of renal fluid and electrolyte transport: Acknowledging our uncertainty," *American Journal of Physiology - Renal Physiology*, vol. 284, no. F871–F884, 2003.

[31] A. Edwards, "Modeling transport in the kidney: Investigating function and dysfunction," *American Journal of Physiology - Renal Physiology*, vol. 298, no. 3, p. F475–F484, 2010.

[32] A. M. Weinstein, "A mathematical model of the rat kidney: K(+)-induced natriuresis.," *American journal of physiology. Renal physiology*, vol. 312, pp. F925–F950, 6 2017.

[33] W. Kuhn and K. Ryffel, "Herstellung konzentrierter Losungen aus verdunnten durch blosse Membranwirkung: ein Modellversuch zur Funktion der Niere," *Hoppe-Seylers Z. Physiol. Chem.*, vol. 276, pp. 145–178, 1942.

[34] J. Stephenson, "Urinary concentration and dilution: models," in *Handbook of physiology. Comprehensive Physiology*, ch. 30, pp. 1349–1408, John Wiley & Sons for American Physiological Society, 2011.

[35] B. Schmidt-Nielsen, "August Krogh Lecture. The renal concentrating mechanism in insects and mammals: a new hypothesis involving hydrostatic pressures.," *The American journal of physiology*, vol. 268, pp. 1087–100, 5 1995.

[36] M. A. Knepper, G. M. Saidel, V. C. Hascall, and T. Dwyer, "Concentration of solutes in the renal inner medulla: Interstitial hyaluronan as a mechano-osmotic transducer," *American Journal of Physiology - Renal Physiology*, vol. 284, pp. F433–F446, 2003.

[37] A. C. Guyton, T. G. Coleman, and H. J. Granger, "Circulation: overall regulation," *Annual Review of Physiology*, vol. 34, pp. 13–44, 1972.

[38] N. Ikeda, F. Marumo, M. Shirataka, and T. Sato, "A model of overall regulation of body fluids.," *Annals of biomedical engineering*, vol. 7, no. 2, pp. 135–166, 1979.

[39] J. H. Bigelow, J. C. DeHaven, and M. L. Shapley, "Systems analysis of the renal function.," *Journal of theoretical biology*, vol. 41, pp. 287–322, 9 1973.

[40] W. H. Cameron, "A model framework for computer simulation of overall renal function.," *Journal of theoretical biology*, vol. 66, pp. 551–572, 6 1977.

[41] P. Chandhoke and G. Saidel, "Mathematical model of mass transport throughout the kidney: Effects of nephron heterogeneity and tubular-vascular organization," *Annals of Biomedical Engineering*, vol. 9, pp. 263–301, 7 1981.

[42] A. Garny, J. Cooper, and P. J. Hunter, "Toward a VPH/Physiome ToolKit," *Wiley interdisciplinary reviews. Systems biology and medicine*, vol. 2, no. 2, pp. 134–147, 2010.

[43] S. R. Thomas, P. Baconnier, J. Fontecave, J.-P. Françoise, F. Guillaud, P. Hannaert, A. Hernández, V. Le Rolle, P. Mazière, F. Tahi, and R. J. White, "SAPHIR: A Physiome Core Model of Body Fluid Homeostasis and Blood Pressure Regulation," *Philosophical Transactions: Mathematical, Physical and Engineering Sciences*, vol. 366, pp. 3175–3197, 4 2008.

[44] S. R. Abram, B. L. Hodnett, R. L. Summers, T. G. Coleman, and R. L. Hester, "Quantitative Circulatory Physiology: an integrative mathematical model of human physiology for medical education," *Advances in physiology education*, vol. 31, pp. 202–210, 6 2007.

[45] R. Hester, A. Brown, L. Husband, R. Iliescu, W. Pruett, R. Summers, and T. Coleman, "HumMod: A Modeling Environment for the Simulation of Integrative Human Physiology," *Frontiers in Physiology*, vol. 2, pp. 1–12, 2011.

[46] C. C. Gyenge, B. D. Bowen, R. K. Reed, and J. L. Bert, "Transport of fluid and solutes in the body I. Formulation of a mathematical model.," *The American journal of physiology*, vol. 277, pp. 1215–27, 9 1999.

[47] C. Hura and J. H. Stein, "Renal blood flow," in *Comprehensive Physiology*, vol. 51, pp. 1129–1184, Washington, DC: Wiley-Blackwell, first ed., 2011.

[48] L. Von Bertanlanffy, *General System Theory: Foundations, Development, Applications*. New York: George Braziller, 1968.

[49] D. Hitchins, *Systems Engineering: a 21st century systems methodology*. Chichester, England: John Wiley & Sons, Ltd., 2007.

[50] D. Buede and W. Miller, *The Engineering Design of Systems: Models and Methods*. Hoboken, New Jersey: John Wiley & Sons, Inc., 2016.

[51] A. Ford, *Modeling the Environment: An Introduction to System Dynamics Models of Environmental Systems*. Island Press, Washington D.C., 1999.

[52] B. Braam, "Advancement in integrated models of renal function: Closing the gap between simulation and real life," *American Journal of Physiology - Renal Physiology*, vol. 306, pp. 284–285, 2014.

[53] R. Levins, "The strategy of model building in population biology," *American Scientist*, vol. 54, pp. 421–431, 4 1966.

[54] V. Crespi, A. Galstyan, and K. Lerman, "Top-down vs bottom-up methodologies in multi-agent system design," *Autonomous Robots*, vol. 24, pp. 303–313, 2008.

[55] D. B. Kell and S. G. Oliver, "Here is the evidence, now what is the hypothesis? The complementary roles of inductive and hypothesis-driven science in the post-genomic era," *BioEssays*, vol. 26, no. 1, pp. 99–105, 2004.

[56] K. Popper, *Conjectures and Refutations: The Growth of Scientific Knowledge*. London: Routledge & Kegan Paul, fifth ed., 1992.

[57] L. Ljung, "Perspectives on System Identification," in *IFAC Proceedings Volumes*, vol. 41, pp. 7172–7184, IFAC, 2008.

[58] J. Forrester, *Industrial Dynamics*. The M.I.T. Press, 1961.

[59] T. E. Marlin, *Process control: designing processes and control systems for dynamic performance*. McGraw-Hill: New York, NY, second ed., 1995.

[60] L. Nguyen, D. Lang, N. van Gessel, A. Ostendorf geb. Beike, A. Menges, R. Reski, and A. Roth-Nebelsick, "Evolutionary Processes as Models for Exploratory Design," in *Biomimetic Research for Architecture and Building Construction: Biological Design and Integrative Structures* (J. Knippers, T. Speck, and K. Nickel, eds.), vol. 8, pp. 295–318, Springer International Publishing, 2016.

[61] B. Cheong, R. Muthupillai, M. F. Rubin, and S. D. Flamm, "Normal values for renal length and volume as measured by magnetic resonance imaging.," *Clinical journal of the American Society of Nephrology : CJASN*, vol. 2, pp. 38–45, 1 2007.

[62] K. Schmidt-Nielsen, *Animal physiology adaptation and environment*. Cambridge University Press: Cambridge, UK, 1997.

[63] L. E. N. R. B. Bird Stewart, Warren E., *Transport phenomena*. 2007.

[64] C. A. Beuchat, "Structure and concentrating ability of the mammalian kidney: Correlations with habitat," *American Journal of Physiology - Regulatory Integrative and Comparative Physiology*, vol. 271, no. 40, pp. R157–R179, 1996.

[65] L. B. Baker, "Physiology of sweat gland function: The roles of sweating and sweat composition in human health.," *Temperature (Austin, Tex.)*, vol. 6, no. 3, pp. 211–259, 2019.

[66] J. B. Rawlings and J. G. Ekerdt, *Chemical reactor analysis and design fundamentals*. Nob Hill Publishing: Madison, WI, 2002.

[67] S. Skogestad, *Chemical and Energy Process Engineering*. CRC Press, first ed., 2008.

[68] C. A. Beuchat, "Body size, medullary thickness, and urine concentrating ability in mammals.," *The American journal of physiology*, vol. 258, pp. 298–308, 2 1990.

[69] F. Sachs and M. V. Sivaselvan, "Cell volume control in three dimensions: Water movement without solute movement," *Journal of General Physiology*, vol. 145, no. 5, pp. 373–380, 2015.

[70] D. Rudman, T. J. DiFulco, J. T. Galambos, R. B. Smith 3rd, A. A. Salam, and W. D. Warren, "Maximal rates of excretion and synthesis of urea in normal and cirrhotic subjects," *The Journal of clinical investigation*, vol. 52, pp. 2241–2249, 9 1973.

[71] H. Pontzer, R. Rimbach, J. Paltan, E. L. Ivory, and C. J. Kendall, "Air temperature and diet influence body composition and water turnover in zoo-living African elephants (Loxodonta africana): Water turnover in African elephants," *Royal Society Open Science*, vol. 7, no. 11, 2020.

[72] M. A. Holliday and W. E. Segar, "The maintenance need for water in parenteral fluid therapy.," *Pediatrics*, vol. 19, pp. 823–32, 5 1957.

[73] R. S. Meyers, "Pediatric fluid and electrolyte therapy.," *The journal of pediatric pharmacology and therapeutics : JPPT : the official journal of PPAG*, vol. 14, pp. 204–11, 10 2009.

[74] B. Friis-Hansen, "Body water compartments in children: changes during growth and related changes in body composition," *Pediatrics*, vol. 28, no. August, pp. 169–81, 1961.

[75] E. Kimland and V. Odlind, "Off-label drug use in pediatric patients.," *Clinical pharmacology and therapeutics*, vol. 91, pp. 796–801, 5 2012.

[76] L. C. Ku and P. B. Smith, "Dosing in neonates: special considerations in physiology and trial design.," *Pediatric research*, vol. 77, pp. 2–9, 1 2015.

[77] D. U. De Rose, S. Cairoli, M. Dionisi, A. Santisi, L. Massenzi, B. M. Goffredo, C. Dionisi-Vici, A. Dotta, and C. Auriti, "Therapeutic Drug Monitoring Is a Feasible Tool to Personalize Drug Administration in Neonates Using New Techniques: An Overview on the Pharmacokinetics and Pharmacodynamics in Neonatal Age.," *International journal of molecular sciences*, vol. 21, 8 2020.

[78] R. L. Fournier, *Basic transport phenomena in biomedical engineering*. Taylor & Francis: Philadelphia, PA, 1999.

[79] V. H. Shoemaker and K. A. Nagy, "Osmoregulation in amphibians and reptiles," *Annual review of physiology*, vol. 39, pp. 449–471, 1977.

[80] J. M. Sands and H. E. Layton, "The Physiology of Urinary Concentration: An Update," *Seminars in Nephrology*, vol. 29, no. 3, pp. 178–195, 2009.

[81] E. J. Braun and W. H. Dantzler, "Function of mammalian-type and reptilian-type nephrons in kidney of desert quail," *The American journal of physiology*, vol. 222, pp. 617–629, 3 1972.

[82] Y. Xue, L. B. Daniels, A. S. Maisel, and N. B. T. R. M. i. B. S. Iqbal, "Cardiac Biomarkers," Elsevier, 2014.

[83] C. Jimenez, B. Melin, N. Koulmann, A. M. Allevard, J. C. Launay, and G. Savourey, "Plasma volume changes during and after acute variations of body hydration level in humans.," *European journal of applied physiology and occupational physiology*, vol. 80, pp. 1–8, 6 1999.

[84] L. Bankir, "Antidiuretic action of vasopressin: quantitative aspects and interaction between V1a and V2 receptor-mediated effects," *Cardiovasc Res*, vol. 51(3), no. 3, pp. 372–390, 2001.

[85] T. Yi, Y. Huang, M. I. Simon, and J. Doyle, "Robust perfect adaptation in bacterial chemotaxis through integral feedback control," *PNAS*, vol. 97, pp. 4649–4653, 2000.

[86] L. v. Veen, J. Morra, A. Palanica, and Y. Fossat, "Homeostasis as a proportional–integral control system," *npj Digital Medicine*, vol. 3, no. 1, p. 77, 2020.

[87] J. H. Koeslag, P. T. Saunders, and J. A. Wessels, "The chromogranins and the counter-regulatory hormones: Do they make homeostatic sense?," *Journal of Physiology*, vol. 517, no. 3, pp. 643–649, 1999.

[88] K. J. Åström and R. M. Murray, *Feedback Systems: An Introduction for Scientists and Engineers*. New Jersey: Princeton University Press, second ed., 2008.

[89] L. Desborough and R. Miller, "Increasing customer value of industrial control performance monitoring - Honeywell's experience," *AIChE Symposium Series*, vol. 98, no. 326, pp. 169–189, 2002.

[90] G. M. Steil, K. Rebrin, R. Janowski, C. Darwin, and M. F. Saad, "Modeling β-cell insulin secretion-implications for closed-loop glucose homeostasis," *Diabetes technology & therapeutics*, vol. 5, no. 6, pp. 953–964, 2003.

[91] T. H. Kwon, J. Frøkiær, and S. Nielsen, "Regulation of aquaporin-2 in the kidney: A molecular mechanism of body-water homeostasis," *Kidney Research and Clinical Practice*, vol. 32, no. 3, pp. 96–102, 2013.

[92] J. Wade, D. Stetson, and S. Lewis, "ADH action: evidence for a membrane shuttle mechanism," *Annals NY Acad Sci*, vol. 372, pp. 106–117, 1981.

[93] H. Nishimura, "Urine concentration and avian aquaporin water channels," *Pflugers Archiv European Journal of Physiology*, vol. 456, no. 4, pp. 755–768, 2008.

[94] E. J. Braun and W. H. Dantzler, "Effects of ADH on single-nephron glomerular filtration rates in the avian kidney," *American Journal of Physiology*, vol. 226(1), pp. 1–8, 1974.

[95] E. J. Braun, "Intrarenal blood flow distribution in the desert quail following salt loading," *American Journal of Physiology*, vol. 231(4), pp. 1111–1118, 1976.

[96] D. L. Goldstein, "Regulation of the avian kidney by arginine vasotocin," *General and Comparative Endocrinology*, vol. 147, no. 1, pp. 78–84, 2006.

[97] F. Park, D. L. Mattson, L. A. Roberts, and A. W. Cowley, "Evidence for the presence of smooth muscle alpha-actin within pericytes of the renal medulla," *American Journal of Physiology*, vol. 273, pp. 1742–8, 1997.

[98] K. Franchini and A. Cowley Jr, "Renal cortical and medullary blood flow responses diuring water restriction: role of vasopressin," *Am J Physiol*, vol. 270, no. 39, pp. R1257–R1264, 1996.

[99] K. Nakanishi, D. L. Mattson, V. Gross, R. J. Roman, and A. W. J. Cowley, "Control of renal medullary blood flow by vasopressin V1 and V2 receptors," *Am J Physiol*, vol. 269, pp. 193–200, 1995.

[100] B. Zimmerhackl, C. R. Robertson, and R. L. Jamison, "Effect of arginine vasopressin on renal medullary blood flow. A videomicroscopic study in the rat.," *The Journal of clinical investigation*, vol. 76, pp. 770–778, 1985.

[101] R. G. Evans, A. C. Madden, and K. M. Denton, "Diversity of responses of renal cortical and medullary blood flow to vasoconstrictors in conscious rabbits," *Acta Physiol Scand*, vol. 169(4), pp. 297–308, 2000.

[102] A. W. J. Cowley, "Control of the renal medullary circulation by vasopressin V1 and V2 receptors in the rat," *Experimental Physiology*, vol. 85, no. 85S, pp. 223S–231S, 2000.

[103] P. K. Pang, "Evolution of control of epithelial transport in vertebrates," *Journal of Experimental Biology*, vol. 106, pp. 283–299, 1983.

[104] J. A. Oliver, R. R. Sciacca, G. Le Cren, and P. J. Cannon, "Modulation by prostaglandins of the renal vascular action of arginine vasopressin," *Prostaglandins*, vol. 24, no. 5, pp. 641–656, 1982.

[105] R. L. Summers, K. R. Ward, T. Witten, V. A. Convertino, K. L. Ryan, T. G. Coleman, and R. L. Hester, "Validation of a computational platform for the analysis of the physiologic mechanisms of a human experimental model of hemorrhage," *Resuscitation*, vol. 80, pp. 1405–1410, 12 2009.

[106] W. Schwartz, W. Bennett, S. Curelop, and F. Bartter, "A syndrome of renal sodium loss and hyponatremia probably resulting from inappropriate secretion of antidiuretic hormone," *The American Journal of Medicine*, vol. 23, no. 4, pp. P529–P542, 1957.

[107] D. Ellison and T. Berl, "The Syndrome of Inappropriate Antidiuresis," *The New England Journal of Medicine*, vol. 356, no. 20, pp. 2064–2072, 2007.

[108] R. Anderson, H. Chung, R. Kluge, and R. Schrier, "Hyponatremia: A Prospective Analysis of Its Epidemiology and the Pathogenetic Role of Vasopressin," *Annals of Internal Medicine*, vol. 102, no. 2, pp. 164–168, 1985.

[109] T. Hew-Butler, M. Rosner, S. Godek, J. Dugas, M. Hoffman, D. Lewis, R. Maughan, K. Miller, S. Montain, N. Rehrer, W. Roberts, I. Rogers, A. Siegel, K. Stuempfle, J. Winger, and J. Verbalis, "Statement of the Third International Exercise-Associated Hyponatremia Consensus Development Conference, Carlsbad, California, 2015," *Clinical journal of sport medicine*, vol. 25, pp. 303–320, 7 2015.

[110] A. J. Siegel, J. G. Verbalis, S. Clement, J. H. Mendelson, N. K. Mello, M. Adner, T. Shirey, J. Glowacki, E. Lee-Lewandrowski, and K. B. Lewandrowski, "Hyponatremia in Marathon Runners due to Inappropriate Arginine Vasopressin Secretion," *American Journal of Medicine*, vol. 120, no. 5, pp. 11–17, 2007.

[111] T. Hew-Butler, V. Loi, A. Pani, and M. H. Rosner, "Exercise-Associated hyponatremia: 2017 update," *Frontiers in Medicine*, vol. 4, no. MAR, pp. 1–10, 2017.

[112] R. H. Sterns and S. M. Silver, "Hyponatremia," in *Seldin and Giebisch's The Kidney: physiology & pathophysiology* (R. J. Alpern and S. C. Hebert, eds.), ch. 41, p. 1183, Elsevier Academic Press, fourth ed., 2008.

[113] V. A. Convertino, L. E. Armstrong, E. F. Coyle, G. W. Mack, M. N. Sawka, L. C. Senay Jr, and W. M. Sherman, "American College of Sports Medicine position stand. Exercise and fluid replacement," *Medicine & Science in Sports & Exercise*, vol. 28, no. 1, pp. i–vii, 1996.

[114] T. D. Noakes, "The hyponatremia of exercise," *International Journal of Sport Nutrition*, vol. 2, pp. 205–228, 9 1992.

[115] B. R. Rose and T. Post, "Clinical use of diuretics," in *Clinical Physiology of Acid-Base and Electrolyte Disorders*, ch. 15, New York, NY: McGraw-Hill, fifth ed., 2001.

[116] T. Khan, R. Patel, and A. Siddiqui, "Furosemide," in *StatPearls [Internet]*, Treasure Island (FL): StatPearls Publishing, 2020.

[117] S. Arampatzis, G. C. Funk, A. B. Leichtle, G. M. Fiedler, C. Schwarz, H. Zimmermann, A. K. Exadaktylos, and G. Lindner, "Impact of diuretic therapy-associated electrolyte disorders present on admission to the emergency department: A cross-sectional analysis," *BMC Medicine*, vol. 11, no. 83, 2013.

[118] M. Lindinger and G. Sjøgaard, "Potassium Regulation during Exercise and Recovery," *Sports Medicine*, vol. 11, pp. 382–401, 1991.

Appendix A

Analytical solutions

Analytical solution to each design's system of ODEs in terms of volume ($V(t)$) and tank concentration ($C(t)$) follows.

A.1 General form of volume and solute balances

$$\frac{dV}{dt} = Q_{in}(t) - Q_{out}(t) \tag{A.1}$$

$$\frac{dN_s}{dt} = \frac{d(CV)}{dt} = \dot{N}_{s,in}(t) - \dot{N}_{s,out}(t) \tag{A.2}$$

A.2 Inflow to the system

Particular solutions of interest include those to pure water and pure solute impulses above steady-state (mixed input disturbances can be achieved through adding extreme input disturbances in a linear system, and are therefore not necessary to model explicitly). One means of achieving impulse disturbances is to keep the inflow rates constant (Equations A.3 and A.4) and to change the initial conditions (Equations A.5 and A.6).

$$Q_{in}(t) = Q_{ss} \tag{A.3}$$

$$\dot{N}_{s,in}(t) = \dot{N}_{s,ss} \tag{A.4}$$

$$V(0) = V_{ss} + a \tag{A.5}$$

$$N_s(0) = N_{s,ss} + b \tag{A.6}$$

It is appreciated that this only works for impulse functions, as any other shaped function would need to be implemented on the inflow rates themselves (or convolved with the system response at a later stage). An important consideration is that the system needs to be at steady-state at the start of the simulation for such an initial-condition approach to work.

A.3 Outflow from the system

Outflow from the system depends on the type of separator present.

A.3.1 No separation on outflow (Design 1 and Design 2)

$$Q_{out}(t) = Q_{ss} + m(V(t) - V_{ss}) \tag{A.7}$$

$$\dot{N}_{s,out}(t) = C(t)(Q_{ss} + m(V(t) - V_{ss})) \tag{A.8}$$

A.3.2 Solute separation (Design 3)

$$Q_{out}(t) = Q_{ss} + m(V(t) - V_{ss}) \tag{A.9}$$

$$\dot{N}_{s,out}(t) = fC(t)(Q_{ss} + m(V(t) - V_{ss})) \tag{A.10}$$

A.3.3 Water separation (Design 3)

$$Q_{out}(t) = Q_{ss} + f_w m(V(t) - V_{ss}) \tag{A.11}$$

$$\dot{N}_{s,out}(t) = C(t)\left(\frac{Q_{ss}}{f_w} + m(V(t) - V_{ss})\right) \tag{A.12}$$

A.3.4 Combined solute and water separation (Design 4)

For overall or effective f and f_w,

$$Q_{out}(t) = Q_{ss} + f_w m(V(t) - V_{ss}) \tag{A.13}$$

$$\dot{N}_{s,out}(t) = fC(t)\left(\frac{Q_{ss}}{f_w} + m(V(t) - V_{ss})\right) \tag{A.14}$$

A.3.5 Multiple solute and water separation (Application)

For solutes A and B and resultant overall or effective f_A, f_B and f_w,

$$Q_{out}(t) = Q_{ss} + f_w m(V(t) - V_{ss}) \tag{A.15}$$

$$\dot{N}_{A,out}(t) = f_A C(t)\left(\frac{Q_{ss}}{f_w} + m(V(t) - V_{ss})\right) \tag{A.16}$$

$$\dot{N}_{B,out}(t) = f_B C(t)\left(\frac{Q_{ss}}{f_w} + m(V(t) - V_{ss})\right) \tag{A.17}$$

A.4 Ordinary Differential Equations (ODEs)

The ODEs have been written in standard linear form.

A.4.1 No separation on outflow (Design 1 and Design 2)

$$\frac{dV}{dt} + mV(t) = mV_{ss} \tag{A.18}$$

$$\frac{dC}{dt} + \frac{Q_{ss}}{V_{ss} + (V_0 - V_{ss})e^{-mt}}C(t) = \frac{\dot{N}_{s,ss}}{V_{ss} + (V_0 - V_{ss})e^{-mt}} \tag{A.19}$$

A.4.2 Solute separation (Design 3)

$$\frac{dV}{dt} + mV(t) = mV_{ss} \tag{A.20}$$

$$\frac{dC}{dt} + \frac{(fQ_{ss} + (f-1)m(V_0 - V_{ss})e^{-mt})}{V_{ss} + (V_0 - V_{ss})e^{-mt}} C(t) = \frac{\dot{N}_{s,ss}}{V_{ss} + (V_0 - V_{ss})e^{-mt}} \tag{A.21}$$

A.4.3 Water separation (Design 3)

$$\frac{dV}{dt} + f_w m V(t) = f_w m V_{ss} \tag{A.22}$$

$$\frac{dC}{dt} + \frac{\left(\frac{Q_{ss}}{f_w} + (1-f_w)m(V_0 - V_{ss})e^{-f_w mt}\right)}{V_{ss} + (V_0 - V_{ss})e^{-f_w mt}} C(t) = \frac{\dot{N}_{s,ss}}{V_{ss} + (V_0 - V_{ss})e^{-f_w mt}} \tag{A.23}$$

A.4.4 Combined solute and water separation (Design 4)

For overall or effective f and f_w,

$$\frac{dV}{dt} + f_w m V(t) = f_w m V_{ss} \tag{A.24}$$

$$\frac{dC}{dt} + \frac{\left(\frac{f}{f_w} Q_{ss} + (f-f_w)m(V_0 - V_{ss})e^{-f_w mt}\right)}{V_{ss} + (V_0 - V_{ss})e^{-f_w mt}} C(t) = \frac{\dot{N}_{s,ss}}{V_{ss} + (V_0 - V_{ss})e^{-f_w mt}} \tag{A.25}$$

A.4.5 Multiple solute and water separation (Application)

For solutes A and B and resultant overall or effective f_A, f_B and f_w,

$$\frac{dV}{dt} + f_w m V(t) = f_w m V_{ss} \tag{A.26}$$

$$\frac{dC_A}{dt} + \frac{\left(\frac{f_A}{f_w} Q_{ss} + (f_A - f_w)m(V_0 - V_{ss})e^{-f_w mt}\right)}{V_{ss} + (V_0 - V_{ss})e^{-f_w mt}} C_A(t) = \frac{\dot{N}_{s,ss}}{V_{ss} + (V_0 - V_{ss})e^{-f_w mt}} \tag{A.27}$$

$$\frac{dC_B}{dt} + \frac{\left(\frac{f_B}{f_w} Q_{ss} + (f_B - f_w)m(V_0 - V_{ss})e^{-f_w mt}\right)}{V_{ss} + (V_0 - V_{ss})e^{-f_w mt}} C_A(t) = \frac{\dot{N}_{s,ss}}{V_{ss} + (V_0 - V_{ss})e^{-f_w mt}} \tag{A.28}$$

A.5 Solution to ODEs

A.5.1 No separation on outflow (Design 1, $m = 0$)

Separable volume ODE A.18 with $m = 0$ has straightforward solution

$$V(t) = V_0 \tag{A.29}$$

where V_0 is the initial tank volume. Separable concentration ODE A.19 with $m = 0$ has straightforward general solution

$$C(t) = C_{ss}\left[1 - \left(1 - \frac{C_0}{C_{ss}}\right)e^{\frac{-t}{\tau}}\right] \tag{A.30}$$

where C_0 is the initial concentration in the tank

$$C_0 = \frac{N_{s,0}}{V_0} \tag{A.31}$$

C_{ss} is the steady-state concentration entering the system

$$C_{ss} = \frac{\dot{N}_{s,ss}}{Q_{ss}} \tag{A.32}$$

and τ is the mean residence time in the tank

$$\tau = \frac{V_{ss}}{Q_{ss}} \tag{A.33}$$

Solute pulse

In response to a pure solute impulse (i.e. $V_0 - V_{ss} = a = 0$ and $N_{s,0} - N_{s,ss} = b \neq 0$), the tank volume response is

$$V(t) = V_{ss} \tag{A.34}$$

in which V_{ss} represents achieved steady-state tank volume, while the tank concentration response is

$$C(t) = C_{ss} + \frac{b}{V_{ss}}e^{\frac{-t}{\tau}} \tag{A.35}$$

where τ matches Equation A.33.

Water pulse

In response to a pure water impulse (i.e. $V_0 - V_{dss} = a \neq 0$ and $N_{s,0} - N_{s,ss} = b = 0$), the tank volume response is

$$V(t) = V_{ss} = V_{dss} + a \tag{A.36}$$

where V_{dss} represents desired (and in this case, prior to the addition of a at $t = 0$) steady-state tank volume. The tank concentration response is

$$C(t) = C_{ss}\left[1 - \left(1 - \frac{C_0}{C_{ss}}\right)e^{\frac{-t}{\tau}}\right] \tag{A.37}$$

where

$$C_0 = \frac{V_{dss}}{V_{dss} + a} C_{ss} \tag{A.38}$$

and τ matches Equation A.33, remembering V_{ss} now includes a contribution of a in Equation A.36.

A.5.2 No separation on outflow (Design 2, $m \neq 0$)

Separable volume ODE A.18 with $m \neq 0$ has straightforward general solution

$$V(t) = V_{ss} + (V_0 - V_{ss})e^{-\frac{t}{\tau_V}} \tag{A.39}$$

where

$$\tau_V = \frac{1}{m} \tag{A.40}$$

Separable concentration ODE A.19 with $m \neq 0$ has straightforward general solution

$$C(t) = C_{ss}\left[1 - \left(1 - \frac{C_0}{C_{ss}}\right)\left(\frac{V_{ss} + (V_0 - V_{ss})e^{-\frac{t}{\tau_V}}}{V_0}\right)^{-\frac{\tau_V}{\tau}} e^{\frac{-t}{\tau}}\right] \tag{A.41}$$

where

$$C_{ss} = \frac{\dot{N}_{s,ss}}{Q_{ss}} \tag{A.42}$$

$$\tau = \frac{V_{ss}}{Q_{ss}} \tag{A.43}$$

and C_0 depends on initial conditions.

Solute pulse

In response to a pure solute impulse (i.e. $V_0 - V_{ss} = a = 0$ and $N_{s,0} - N_{s,ss} = b \neq 0$), the tank volume response is

$$V(t) = V_{ss} \tag{A.44}$$

while the tank concentration response reduces to

$$C(t) = C_{ss} + \frac{b}{V_{ss}} e^{\frac{-t}{\tau}} \tag{A.45}$$

where τ matches Equation A.43. These solute pulse responses are identical to those of Design 1, Subsection A.5.1.

Water pulse

In response to a pure water impulse (i.e. $V_0 - V_{ss} = a \neq 0$ and $N_{s,0} - N_{s,ss} = b = 0$), the tank volume response is

$$V(t) = V_{ss} + ae^{-\frac{t}{\tau_V}} \tag{A.46}$$

where τ_V matches Equation A.40. The tank concentration response is

$$C(t) = C_{ss}\left[1 - \left(1 - \frac{C_0}{C_{ss}}\right)\left(\frac{V_{ss} + ae^{-\frac{t}{\tau_V}}}{V_{ss} + a}\right)^{-\frac{\tau_V}{\tau}} e^{\frac{-t}{\tau}}\right] \tag{A.47}$$

where

$$C_0 = \frac{V_{ss}}{V_{ss} + a} C_{ss} \tag{A.48}$$

τ_V matches Equation A.40 and τ matches Equation A.43.

A.5.3 Solute separation (Design 3)

Separable volume ODE A.20 has straightforward general solution

$$V(t) = V_{ss} + (V_0 - V_{ss})e^{-\frac{t}{\tau_V}} \tag{A.49}$$

where

$$\tau_V = \frac{1}{m} \tag{A.50}$$

Linear concentration ODE A.21 is less straightforward to solve, as shown in Section A.6 but it is possible to extract

$$\tau = \frac{1}{f}\frac{V_{ss}}{Q_{ss}} \tag{A.51}$$

Solute pulse

In response to a pure solute impulse (i.e. $V_0 - V_{ss} = a = 0$ and $N_{s,0} - N_{s,ss} = b \neq 0$), the tank volume response is

$$V(t) = V_{ss} \tag{A.52}$$

while the tank concentration response is

$$C(t) = C_{ss} + \frac{b}{V_{ss}}e^{\frac{-t}{\tau}} \tag{A.53}$$

where

$$C_{ss} = \frac{1}{f}\frac{\dot{N}_{s,ss}}{Q_{ss}} \tag{A.54}$$

and τ matches Equation A.51. If $f = 1$, the solution reduces to that of Design 2, as expected.

Water pulse

In response to a pure water impulse (i.e. $V_0 - V_{ss} = a \neq 0$ and $N_{s,0} - N_{s,ss} = b = 0$), the tank volume response is

$$V(t) = V_{ss} + ae^{-\frac{t}{\tau_V}} \tag{A.55}$$

where τ_V matches Equation A.50, while the tank concentration response includes the special hypergeometric function (Equation A.88 in Section A.6), where τ matches Equation A.51.

A.5.4 Water separation (Design 3)

Separable volume ODE A.22 has straightforward general solution

$$V(t) = V_{ss} + (V_0 - V_{ss})e^{-\frac{t}{\tau_V}} \tag{A.56}$$

where

$$V_{ss} = V_{dss} + \frac{Q_{ss}(1-f_w)}{f_w} \tag{A.57}$$

in which V_{ss} represents achieved steady-state while V_{dss} represents desired steady-state. In addition,

$$\tau_V = \frac{1}{f_w m} \tag{A.58}$$

Linear concentration ODE A.23 is less straightforward to solve, as shown in Section A.6 but it is possible to extract

$$\tau = f_w \frac{V_{ss}}{Q_{ss}} \tag{A.59}$$

Solute pulse

In response to a pure solute impulse (i.e. $V_0 - V_{ss} = a = 0$ and $N_{s,0} - N_{s,ss} = b \neq 0$), the tank volume response is

$$V(t) = V_{ss} \tag{A.60}$$

while the tank concentration response is

$$C(t) = C_{ss} + \frac{b}{V_{ss}} e^{\frac{-t}{\tau}} \tag{A.61}$$

where

$$C_{ss} = f_w \frac{\dot{N}_{s,ss}}{Q_{ss}} \tag{A.62}$$

and τ matches Equation A.59. If $f_w = 1$, the solution reduces to that of Design 2, as expected.

Water pulse

In response to a pure water impulse (i.e. $V_0 - V_{ss} = a \neq 0$ and $N_{s,0} - N_{s,ss} = b = 0$), the tank volume response is

$$V(t) = V_{ss} + ae^{-\frac{t}{\tau_V}} \tag{A.63}$$

where τ_V matches Equation A.58, while the tank concentration response includes the special hypergeometric function (Equation A.88 in Section A.6), where τ matches Equation A.59.

A.5.5 Combined solute and water separation (Design 4)

Separable volume ODE A.24 has straightforward general solution

$$V(t) = V_{ss} + (V_0 - V_{ss})e^{-\frac{t}{\tau_V}} \tag{A.64}$$

where

$$V_{ss} = V_{dss} + \frac{Q_{ss}(1 - f_w)}{f_w} \tag{A.65}$$

in which V_{ss} represents achieved steady-state while V_{dss} represents desired steady-state. In addition,

$$\tau_V = \frac{1}{f_w m} \tag{A.66}$$

Linear concentration ODE A.25 is less straightforward to solve, as shown for separate solute and water separation (in Section A.6), but it is possible to extract

$$\tau = \frac{f_w}{f}\frac{V_{ss}}{Q_{ss}} \tag{A.67}$$

If separation is in fact performed by multiple separators, then overall f and f_w can be used in the combined solute and water separation analysis, due to linearity of the system.

Solute pulse

In response to a pure solute impulse (i.e. $V_0 - V_{ss} = a = 0$ and $N_{s,0} - N_{s,ss} = b \neq 0$), the tank volume response is

$$V(t) = V_{ss} \tag{A.68}$$

while the tank concentration response is

$$C(t) = C_{ss} + \frac{b}{V_{ss}} e^{\frac{-t}{\tau}} \tag{A.69}$$

where

$$C_{ss} = \frac{f_w}{f} \frac{\dot{N}_{s,ss}}{Q_{ss}} \tag{A.70}$$

and τ matches Equation A.67. If $f_w = 1$ or $f = 1$, the solution reduces to that of Design 3 solute separation or water separation, respectively. If $f_w = f = 1$, the solution reduces to that of Design 2, as expected.

Water pulse

In response to a pure water impulse (i.e. $V_0 - V_{ss} = a \neq 0$ and $N_{s,0} - N_{s,ss} = b = 0$), the tank volume response is

$$V(t) = V_{ss} + ae^{-\frac{t}{\tau_V}} \tag{A.71}$$

where τ_V matches Equation A.66, while the tank concentration response includes the special hypergeometric function (of the form in Equation A.88 in Section A.6), where τ matches Equation A.67.

A.5.6 Multiple solute and water separation (Application)

Separable volume ODE A.26 has straightforward general solution

$$V(t) = V_{ss} + (V_0 - V_{ss})e^{-\frac{t}{\tau_V}} \tag{A.72}$$

where

$$V_{ss} = V_{dss} + \frac{Q_{ss}(1 - f_w)}{f_w} \tag{A.73}$$

in which V_{ss} represents achieved steady-state while V_{dss} represents desired steady-state. In addition,

$$\tau_V = \frac{1}{f_w m} \tag{A.74}$$

Linear concentration ODEs A.27 and A.28 are less straightforward to solve, as shown for separate solute and water separation (in Section A.6), but it is possible to extract

$$\tau_A = \frac{f_w}{f_A}\frac{V_{ss}}{Q_{ss}} \tag{A.75}$$

and

$$\tau_B = \frac{f_w}{f_B}\frac{V_{ss}}{Q_{ss}} \tag{A.76}$$

Solute pulse

In response to a pure solute impulse (i.e. $V_0 - V_{ss} = a = 0$ and either $N_{A,0} - N_{A,ss} = b \neq 0$ or $N_{B,0} - N_{B,ss} = b \neq 0$), the tank volume response is

$$V(t) = V_{ss} \tag{A.77}$$

while the tank concentration response is

$$C(t) = C_A(t) + C_B(t) \tag{A.78}$$

where tank component concentrations depend on initial conditions,

$$C_A(t) = C_{A,ss} + \frac{b}{V_{ss}} e^{\frac{-t}{\tau}} \tag{A.79}$$

$$C_B(t) = C_{B,ss} + \frac{b}{V_{ss}} e^{\frac{-t}{\tau}} \tag{A.80}$$

where

$$C_{A,ss} = \frac{f_w}{f_A}\frac{\dot{N}_{A,ss}}{Q_{ss}} \tag{A.81}$$

$$C_{B,ss} = \frac{f_w}{f_B}\frac{\dot{N}_{B,ss}}{Q_{ss}} \tag{A.82}$$

and τ_A matches Equation A.75 while τ_B matches Equation A.76.

Water pulse

In response to a pure water impulse (i.e. $V_0 - V_{ss} = a \neq 0$ and $N_{A,0} - N_{A,ss} = b = 0$ and $N_{B,0} - N_{B,ss} = b = 0$), the tank volume response is

$$V(t) = V_{ss} + ae^{-\frac{t}{\tau_V}} \tag{A.83}$$

where τ_V matches Equation A.74, while the tank concentration response includes the special hypergeometric function (of the form in Equation A.88 in Section A.6), where τ_A matches Equation A.75 while τ_B matches Equation A.76.

A.6 Comparison of solutions

An abstract comparison of the effect of components of the standard linear form of the governing concentration ODE provides a means of determining when the analytical solution starts to include the hypergeometric function and is no longer considered straightforward for modelling purposes.

If constant terms in Equations A.19, A.21 and A.23 are lumped together; $Q_{ss} = B$, $V_{ss} = D$, $V_0 - V_{ss} = G$, $\dot{N}_{s,ss} = R$, $fQ_{ss} = H$, $-(1-f)m(V_0 - V_{ss}) = A$, $(1-f_w)m(V_0 - V_{ss}) = J$ and $\frac{Q_{ss}}{f_w} = K$, the following abstract Equations A.84, A.85 and A.86 result, respectively, where $\tau_{V,1} = \frac{1}{m}$ and $\tau_{V,2} = \frac{1}{f_w m}$

$$\frac{dC}{dt} + \frac{B}{D + Ge^{-\frac{t}{\tau_{V,1}}}}C(t) = \frac{R}{D + Ge^{-\frac{t}{\tau_{V,1}}}} \tag{A.84}$$

$$\frac{dC}{dt} + \frac{H + Ae^{-\frac{t}{\tau_{V,1}}}}{D + Ge^{-\frac{t}{\tau_{V,1}}}}C(t) = \frac{R}{D + Ge^{-\frac{t}{\tau_{V,1}}}} \tag{A.85}$$

$$\frac{dC}{dt} + \frac{K + Je^{-\frac{t}{\tau_{V,2}}}}{D + Ge^{-\frac{t}{\tau_{V,2}}}}C(t) = \frac{R}{D + Ge^{-\frac{t}{\tau_{V,2}}}} \tag{A.86}$$

It is seen that there is a fundamental difference in form between Equation A.84 and Equations A.85 and A.86 (which can be considered to have the same form, with different constant magnitudes and values for τ_V).

First order separable ODE A.84 lacks an exponential term in the numerator of the coefficient of $C(t)$ and has a straightforward general solution (Equation A.87) with constant

of integration c_1 and $\tau = \frac{D}{B} = \frac{V_{ss}}{Q_{ss}}$.

$$C(t) = c_1(De^{\frac{t}{\tau_V}} + G)^{-\frac{\tau_V}{\tau}} + \frac{R}{B} \tag{A.87}$$

In contrast, first order linear ODEs A.85 and A.86, have an exponential term in the numerator of the coefficient of $C(t)$ and although solvable, the general solution is given in terms of the hypergeometric function ${}_2F_1(a,b;c;z)$. Equation A.88 is the solution to ODE A.85 specifically but note that if H is replaced with K, and A is replaced with J in Equation A.88, the solution to ODE A.86 follows. Here, c_1 is a constant of integration and $\frac{D}{H} = \frac{1}{f}\frac{V_{ss}}{Q_{ss}} = \tau$ or $\frac{D}{K} = f_w\frac{V_{ss}}{Q_{ss}} = \tau$, respectively.

$$C(t) = c_1 e^{\left(-\frac{(HG\tau_V - AD\tau_V)ln(De^{\frac{t}{\tau_V}}+G)+ADt}{DG}\right)} + \frac{R\tau_V e^{\frac{t}{\tau_V}}{}_2F_1\left(1, \frac{H}{D}\tau_V + 1; \frac{A}{G}\tau_V + 2; -\frac{D}{G}e^{\frac{t}{\tau_V}}\right)}{A\tau_V + G} \tag{A.88}$$

The hypergeometric function is represented by the power series in Equation A.89.

$${}_2F_1(a,b;c;z) = \sum_{n=0}^{\infty} \frac{(a)_n(b)_n}{(c)_n}\frac{z_n}{n!} = 1 + \frac{ab}{c}\frac{z}{1!} + \frac{a(a+1)b(b+1)}{c(c+1)}\frac{z^2}{2!} + ... \tag{A.89}$$

From Equation A.88, it is seen that $z = -\frac{D}{G}e^{\frac{t}{\tau_V}}$, and therefore the hypergeometric function in this case represents an infinite sum of exponential terms.

For the special case when $Ae^{-\frac{t}{\tau_{V,1}}} << H$ or $Je^{-\frac{t}{\tau_{V,2}}} << K$, the linear ODEs A.85 and A.86 simplify to separable ODEs of the form in Equation A.84 and the solution is straightforward (i.e. the form of Equation A.87).